

“ Simplicity is the ultimate sophistication. ”

- *Leonardo da Vinci*

University of Alberta

Functional characterization of urate handling by hSLC2A9 (hGLUT9)
splice variants in a heterologous expression system

by

Katarzyna Witkowska

A thesis submitted to the Faculty of Graduate Studies and Research
in partial fulfillment of the requirements for the degree of

Doctor of Philosophy

Department of Physiology

© Katarzyna Witkowska
Spring 2012
Edmonton, Alberta

Permission is hereby granted to the University of Alberta Libraries to reproduce single copies of this thesis and to lend or sell such copies for private, scholarly or scientific research purposes only. Where the thesis is converted to, or otherwise made available in digital form, the University of Alberta will advise potential users of the thesis of these terms.

The author reserves all other publication and other rights in association with the copyright in the thesis and, except as herein before provided, neither the thesis nor any substantial portion thereof may be printed or otherwise reproduced in any material form whatsoever without the author's prior written permission.

*To my parents, Barbara and Jacek, for always
encouraging me to seek more.*

Abstract

Multiple, independent Genome Wide Association Studies have uncovered a significant correlation between abnormal plasma urate levels and single nucleotide polymorphisms within the *hSLC2A9* gene. The gene product was originally characterized as a high affinity D-glucose and D-fructose transporter, which belongs to a larger family of facilitative transmembrane hexose transporters, named GLUTs. The two splice variants, *hSLC2A9a* and *hSLC2a9b*, were overexpressed in *Xenopus laevis* oocytes. A combination of radioisotope flux studies and electrophysiological analysis were employed to functionally characterize the urate-handling of these proteins.

The two human *hSLC2A9* (*hGLUT9*) isoforms mediate high capacity urate transport, which is selectively sensitive to benzbromarone. They display kinetic symmetry in their affinity and capacity to handle extracellular and intracellular urate. Surprisingly, urate uptake mediated by either isoform is not competitively inhibited by extracellular D-glucose and D-fructose over a wide range of concentrations. However, the transporters can exchange hexoses for urate, when the two substrates are placed on opposite sides of the membrane, as evidenced by *trans*-stimulation. Moreover, the two isoforms display different patterns of urate-transport

modulation in response to *trans*-hexoses and kinase activators, indicating that functional differences between the two isoforms exist.

Given that uric acid is approximately 90% dissociated under physiological pH, and exists as an organic anion (urate) in blood plasma, we investigated hSLC2A9's capacity to carry current. Indeed, hSLC2A9a- and hSLC2A9b-expressing oocytes produce positive outward current in the presence of extracellular urate. This current does not appear to be sensitive to Na⁺, and is only moderately affected by Cl⁻ depletion. Hence, we propose that the negatively charged urate is the only species contributing to the electrogenicity of hSLC2A9. Given that the membrane potential is negative inside cells, we propose that both variants act as mediators of urate efflux under physiological conditions.

Both isoforms of hSLC2A9 are expressed in opposite membrane domains of human proximal tubule epithelium. We propose a model for renal handling of urate in humans which explains how hypouricemia and hyperuricemia can be associated with the same gene product, and which may provide new treatment opportunities of gout, hypertension and metabolic syndrome.

Acknowledgements

My interest in science began in the University of Alberta lecture hall where we surveyed the diversity of invertebrates. It blossomed in a very beautiful part of Canada, at the Bamfield Marine Sciences Centre, British Columbia. I want to thank Dr. A. Richard Palmer for being one of the best professors and mentors I have ever had, and for recognizing my enthusiasm for science. He helped me with many of my “first” experiences such as field work, summer job and living in Canada.

I would not have been studying transport physiology today if not for Dr. Greg Goss. His teachings were the essential bridge which transported me from the world of an undergraduate to that of an independent thinker and researcher. His zest for life has been contagious.

I thank my graduate supervisor, Dr. Chris Cheeseman, for giving me the opportunity to work in his lab and for entrusting me with a project which keeps me excited about experiments and work day in and day out. The past six years have been an incredible journey of self discovery and perseverance. I am most grateful for all the freedom I had to explore so many avenues of academic life.

None of this work would have been possible without Debbie O’Neill. She has taught me all the laboratory techniques and ethics I know. She was the most reliable co-worker, my best friend and my “lab mom”. We have shared many laughs and cries over the years and I will miss working alongside her very much.

I want to thank all my committee members for the insightful discussions and the collaborations they offered me throughout the years. I want to thank Dr. Joe Casey for taking me under his wing during the many

conference travels. Drs. Marek Michalak and Elaine Leslie have been particularly kind in extending their helping hand to usher me into the next phase of my academic life, advising me on CV writing.

Dr. Kyla Smith has been a patient collaborator, helping my lab with the electrophysiology experiments, which have changed our understanding of how the GLUT proteins work. I would like to thank her for all the hard work she has put into this project over the years, and all her help and advice on the *Xenopus* expression system.

I have met many incredible people throughout my PhD and formed many friendships, which transformed me as a person and as a scientist. Especially, I would like to thank the following:

- Danielle Johnson, for being my great supporter, and for paving the way for me in this journey. Her thesis was an inspiration to me.
- Brendan Trayner, for being the most authentic sibling experience I will ever have, and for making sure that I fit within the modern, Western society.
- Pam Bonar, for being the most reliable and loyal person I know.
- Brittany Brown, for her positivity and eternal enthusiasm.
- Brent Martin, for his incredible intelligence. I have missed you on the seventh floor.
- Richard Kanyo, for being the social convener when things got tough.
- Barbara Roggenbeck, for being an example of strength and perseverance.
- Gonzalo Vilas, for his incredible insight into any aspect of science, and for his sober perspective on life.
- Arghya Basu, for igniting and sharing my passion for photography.

Naomi Woods and her family were the catalysts who brought me to Canada. I want to thank them for introducing me to such a beautiful part of the world.

Given that my family was far away throughout my studies, I had many people around me making sure that I never lost my sense of belonging over the years. For being my homes-away-from-home, I want to thank Nathalia Biernat, Bela Sztukowski-Papich, Kathy Malejczyk and Martha Rogalski and their families, for the warmth and the sincerity I have experienced with you.

I have many friends from many walks of life, who have yielded their relentless support over the years. They have listened, comforted, and, most importantly, shared and sparked many of my interests. Be it dark nights on the fifth floor of Zoology, “conference crazies”, opera and drama dates, crazy dance parties, laid-back popcorn feasts in the movies or challenging nature expeditions, I always had you to share the moments with.

Finally, I would have not been here if not for the love, strength and the driving force of the three most important people in my life: “Mami”, “Tati” and Mike.

Special thanks for help with thesis preparation go to: Craig Markin, Brendan Trayner, Debbie O’Neill, Pam Bonar, Jo Stanley, Danielle Johnson, Arghya Basu, Sampath Longan, Asia Jung and Dave Madole.

Chapter 1

General introduction	1
1.1 General Introduction overview.....	2
1.2 Introduction to carrier-mediated transport	2
1.2.1 Transport across semi-permeable membranes	2
1.2.2 Basic principles of carrier-mediated transport	3
1.2.3 Initial mapping of the substrate binding site	6
1.3 Family of Facilitative Glucose Transport Proteins (GLUTs).....	7
1.3.1 GLUT family characteristics and substrate specificity	7
1.3.2 GLUT structural studies.....	13
1.4 Cloning and initial functional characterization of GLUT9	
(SLC2A9).....	14
1.4.1 The human orthologue	14
1.4.2 The mouse orthologue	17
1.4.3 Examples of other GLUT splice variants	19
1.5 Molecular identity and functionality of proposed urate	
transporters in context of the kidney epithelium	21
1.5.1 The Galectin family of proteins (UAT)	21
1.5.2 Human Organic Anion Transporters (OATs)	22
1.5.3 Human urate-anion exchanger (URAT1)	25
1.5.4 Human Multidrug Resistance Proteins (ABCG2 and MRP4)	28
1.5.5 Human Sodium Phosphate transporter (NTP4)	31
1.5.6 Making sense of the urate transporter diversity	33
1.6 Physiology of urate with focus on humans	36
1.6.1 Clinical history of uric acid	36
1.6.2 The rodent model in uric acid studies.....	41
1.6.3 Fundamentals of urate handling by the human kidney	43
1.6.4 Phylogeny of purine metabolism	48
1.6.5 Pathophysiology of urate	51
1.7 Thesis objectives	53

1.8 Bibliography	54
-------------------------------	-----------

Chapter 2

Materials and Methods.....	67
----------------------------	----

2.1 Materials	68
----------------------------	-----------

2.2 Methods	68
--------------------------	-----------

2.2.1 Molecular biology.....	68
------------------------------	----

2.2.2 <i>Xenopus laevis</i> heterologous expression system	69
--	----

2.2.3 Transport assays	71
------------------------------	----

2.2.5 Measuring cell surface expression	79
---	----

2.3 Bibliography.....	94
------------------------------	-----------

Chapter 3

Functional characterization of human SLC2A9-mediated urate transport	95
--	----

3.1 Acknowledgements and contributions	96
---	-----------

3.2 Introduction	98
-------------------------------	-----------

3.3 Results	99
--------------------------	-----------

3.3.1 Human SLC2A9 is a high capacity urate transporter	99
---	----

3.3.2 Transport of urate by hSLC2A9a shows a unique sensitivity to uricosurics .	102
--	-----

3.3.3 hSLC2A9a mediates exchange of urate for D-glucose or D-fructose	106
---	-----

3.4 Discussion	112
-----------------------------	------------

3.4.1. Genetic basis for SLC2A9 as a urate carrier.....	112
---	-----

3.4.2 Functional evidence for SLC2A9 as a urate carrier	113
---	-----

3.4.3 Limitations of the study.....	116
-------------------------------------	-----

3.4.4 Conclusions	117
-------------------------	-----

3.5 Bibliography	118
-------------------------------	------------

Chapter 4

In-depth functional comparison of human hSLC2A9a and hSLC2A9b isoforms	122
4.1 Acknowledgements and contributions	123
4.2 Introduction	124
4.3 Results	127
4.3.1 Urate currents of hSLC2A9	127
4.3.2 Voltage-dependence of hSLC2A9-mediated transport	129
4.3.3 Ion-dependence of hSLC2A9-mediated transport.....	131
4.3.4 Urate influx kinetics under voltage clamp conditions	135
4.3.5 hSLC2A9 has symmetrical affinity and capacity for urate efflux	136
4.3.6 Effect of extracellular substances on hSLC2A9-mediated urate efflux.....	138
4.3.7 Effect of intracellular substances on hSLC2A9-mediated urate influx	140
4.3.8 Nucleobase transport mediated by hSLC2A9	142
4.4 Discussion.....	145
4.5 Bibliography	150

Chapter 5

Differential regulation of urate handling by human SLC2A9a and SLC2A9b isoforms in <i>Xenopus laevis</i> oocytes	155
5.1 Acknowledgements and contributions	156
5.2 Introduction	157
5.3 Results	160
5.3.1 N-terminus of hSLC2A9 isoforms confers differential responsiveness to kinases	160

5.3.2 Kinase modulators affect hSLC2A9 isoforms' catalytic properties of urate uptake.....	165
5.3.3 Kinase modulators affect hSLC2A9 isoforms' catalytic properties of urate efflux.....	171
5.3.4 Ser9 may serve as sites for modulation of hSLC2A9a urate handling by PKC.....	172
5.4 Discussion.....	176
5.5 Bibliography.....	180

Chapter 6

General discussion.....	186
6.1 Thesis' aims revisited.....	187
6.2 Physiological relevance.....	188
6.2.1 hSLC2A9 as a urate transporter and a molecular identity of plasma urate regulating mechanism.....	188
6.2.2 Electrogenic nature of hSLC2A9-mediated urate flux and the voltage-dependent urate pathways in the kidney epithelium.....	189
6.2.3 Differential regulation of hSLC2A9-mediated urate fluxes by hexoses may provide a link between hyperuricemia and metabolic syndrome.....	191
6.2.4 Differential regulation of hSLC2A9-mediated urate fluxes by cell signalling pathways may provide insight into renal control of urate secretion and reabsorption.....	194
6.2.5 Beyond the renal epithelium.....	196
6.2.6 Reconciling human and rodent systems in face of urate homeostasis.....	197
6.2.7 Validity of the simple carrier model in hSLC2A9-mediated urate transport analysis.....	198
6.3 Future directions.....	199
6.3.1 Determining phosphorylation state of hSLC2A9 in the expression system...	199
6.3.2 Alternative hSLC2A9 isoform targeting in the human tissue.....	200
6.3.3 Mammalian expression system for studies of urate flux.....	200

6.3.4 Mechanism of benzbromarone action	201
6.3.5 Structure-function studies of hSLC2A9	202
6.3 Bibliography	206

Appendix 1

<i>cis</i> -Stimulation and dual label experiments.....	210
A1.1 <i>cis</i>-Stimulation experiment.....	210
A1.1.1 Experimental design	210
A1.1.2. Results commentary	210
A1.2 Dual-label experiment	215
A1.2.1 Experimental design	215
A1.2.2 Results commentary	215

Appendix 2

hSLC2A9 and multiple urate binding sites.....	218
A2.1 Fitting kinetic data with Hill equation	219
A2.1.1 Experimental design	219
A2.1.2. Results commentary	220

List of tables

Chapter 1

Table 1.1	8
------------------------	----------

Tissue distribution and substrate specificity of GLUTs

Chapter 2

Table 2.1	83
------------------------	-----------

Reagents

Table 2.2	85
------------------------	-----------

DNA modifying enzymes and DNA kits

Table 2.3	86
------------------------	-----------

Constructs and primers

Table 2.4	87
------------------------	-----------

Antibodies and protein work

Table 2.5	88
------------------------	-----------

Equipment

Table 2.6	88
------------------------	-----------

Software

Table 2.7	89
Barth's Medium composition	
Table 2.8	89
Phosphate Buffer composition	
Table 2.9	90
Sodium transport buffer composition	
Table 2.10	90
Phosphate-buffered saline (PBS) composition	
Table 2.11	91
Cell-surface biotinylation buffers' composition	
Table 2.12	92
Western Blotting buffers' composition	

List of figures

Chapter 1

Figure 1.1	5
Four-step simple carrier kinetic model	
Figure 1.2	9
Unrooted dendrogram of human facilitative glucose transporter gene family	
Figure 1.3	11
General topology model of the GLUT protein family	
Figure 1.4	16
Predicted topology models for hGLUT1 and hGLUT9	
Figure 1.5	38
Summary of molecular identities of putative urate transporters in human proximal convoluted tubule epithelium	
Figure 1.6	46
Summary of putative transport processes involved in renal urate handling in the human proximal convoluted epithelium	
Figure 1.7	50
Phylogeny of purine catabolism	

Chapter 2

Figure 2.1.....72

Representative time course of ^{14}C -urate uptake into SLC2A9a- and SLC2A9b-expressing *Xenopus* oocytes

Figure 2.2.....76

Proof-of-principle of the *trans*-stimulation technique: hGLUT1-mediated ^3H 3-O-Methyl-D-glucoside (3OMG) efflux from *Xenopus* oocytes

Figure 2.3.....81

Representative staining of *Xenopus* oocytes expressing hSLC2A9

Chapter 3

Figure 3.1.....100

Representative time course for hSLC2A9a-mediated ^{14}C -urate uptake into *Xenopus* oocytes

Figure 3.2.....101

Michaelis-Menten kinetics for hSLC2A9a-mediated ^{14}C -urate uptake into *Xenopus* oocytes

Figure 3.3.....	103
 Representative ¹⁴C-urate uptake into hGLUT-expressing <i>Xenopus</i> oocytes	
Figure 3.4.....	104
 Drug panel testing their effects on hSLC2A9a-mediated ¹⁴C-urate uptake into <i>Xenopus</i> oocytes	
Figure 3.5.....	105
 Effect of the uricosuric benzbromarone on hSLC2A9a-mediated ¹⁴C-urate uptake into <i>Xenopus</i> oocytes	
Figure 3.6.....	107
 Interaction between hSLC2A9a and its substrates I: Effect of extracellular urate on ¹⁴C-hexose uptake into <i>Xenopus</i> oocytes	
Figure 3.7.....	109
 Interaction between hSLC2A9a and its substrates II: Effect of extracellular D-glucose on urate transport in <i>Xenopus</i> oocytes	
Figure 3.8.....	110
 Representative experiment: hSLC2A9a exchanges intracellular ¹⁴C-urate for extracellular hexoses in <i>Xenopus</i> oocytes	
Figure 3.9.....	111
 Representative experiment: hSLC2A9a mediates exchange of intracellular ¹⁴C-urate for extracellular hexoses and urate in <i>Xenopus</i> oocytes	

Chapter 4

Figure 4.1	128
Steady-state currents of hSLC2A9	
Figure 4.2	130
Voltage-dependence of hSLC2A9-mediated transport of urate	
Figure 4.3	132
Effect of extracellular ions on the transport activity of hSLC2A9	
Figure 4.4	134
Urate influx kinetics of hSLC2A9	
Figure 4.5	137
Urate efflux kinetics of hSLC2A9	
Figure 4.6	139
Effect of extracellular substances on hSLC2A9-mediated urate efflux	
Figure 4.7	141
Effect of intracellular substances on hSLC2A9-mediated urate influx	
Figure 4.8	144
Nucleobase transport mediated by hSLC2A9	

Chapter 5

Figure 5.1	161
Predicted topology models for hSLC2A9a and hSLC2A9b	
Figure 5.2	163
hSLC2A9a- and hSLC2A9b-expressing <i>Xenopus</i> oocytes show different ¹⁴C-urate uptake profiles in response to PKA and PKC modulation	
Figure 5.3	164
Effect of inhibitors on hSLC2A9a- and hSLC2A9b-mediated ¹⁴C-urate uptake in <i>Xenopus</i> oocytes	
Figure 5.4	166
hSLC2A9a- and hSLC2A9b-expressing <i>Xenopus</i> oocytes show different ¹⁴C-urate uptake profiles in response to PKA and PKC modulation	
Figure 5.5	168
Cell-surface biotinylation of hSLC2A9a-expressing <i>Xenopus</i> oocytes	
Figure 5.6	169
Representative Michaelis-Menten fits of hSLC2A9a- and hSLC2A9b-mediated ¹⁴C-urate uptake into <i>Xenopus</i> oocytes in presence of kinase modulators	

Figure 5.7	170
Mean values of kinetic constants for hSLC2A9a- and hSLC2A9b-mediated ¹⁴C-urate uptake into <i>Xenopus</i> oocytes in presence of kinase modulators	
Figure 5.8	173
hSLC2A9a- and hSLC2A9b-expressing <i>Xenopus</i> oocytes show different ¹⁴C-urate efflux profiles in response to PKA and PKC modulation	
Figure 5.9	175
Serine 9 may be involved in modulating hSLC2A9a ¹⁴C-urate transport in <i>Xenopus</i> oocytes	

Chapter 6

Figure 6.1	191
Proposed model for urate reabsorptive and secretory mechanisms in the human proximal convoluted tubule of the kidney	
Figure 6.2	204
Predicted topology models for hGLUT1 and hGLUT9	
Figure 6.3	205
hURAT1 and hSLC2A9a sequence alignment	

Appendix 1

Figure A1.1	213
Effects of <i>cis</i> hexoses on hSLC2A9-mediated ¹⁴C-urate uptake in <i>Xenopus</i> oocytes	
Figure A1.2	214
Effects of <i>cis</i> hexoses on hSLC2A9-mediated ¹⁴C-urate uptake in <i>Xenopus</i> oocytes: time-course	
Figure A1.3	216
Measuring the stoichiometry of urate – hexose exchange in hSLC2A9-expression <i>Xenopus</i> oocytes: dual label experiment	

Appendix 2

Figure A2.1	221
Reanalysis of kinetics of hSLC2A9-mediated ¹⁴C-urate uptake in <i>Xenopus</i> oocytes using allosteric sigmoidal curve fit	
Figure A2.2	222
Mean Hill coefficients from alternative kinetic analysis of hSLC2A9a- and hSLC2A9b-mediated ¹⁴C-urate uptake in response to PKA and PKC modulating drugs	

List of symbols

[X] – concentration of X

μM – micromolar

2DOG – 2-deoxy-D-glucose

6CF – 6-Carboxyfluorescein

ABC – ATP-binding cassette

ABCG2 – Breast Cancer Resistance Protein (BCRP)

AIRC – Atherosclerosis Risk in Communities

ATP – adenosine triphosphate

BBMV – brush border membrane vesicles

BCRP – Breast Cancer Resistance Protein

BIS – Bisindolylmaleimide dichloride, Protein Kinase C inhibitor

cAMP – cyclic adenosine monophosphate

CB – Cytochalacin B

cDNA – complementary deoxyribonucleic acid

Cl⁻ - chloride anion

COOH (C-) – carboxy terminus

COS 7 – CV-1 in Origin with a version of the SV40 genome (cell line derived from kidney cells of the African green monkey), form 7

cRNA – complementary ribonucleic acid

DHA – dehydroascorbic acid

DNA – deoxyribonucleic acid

EGF – epithelial growth factor

ER – endoplasmic reticulum

ES – estrone sulphate

EST – expressed sequence tag

FDG – ¹⁸F-Fludeoxyglucose

GlpT – glycerol-3-phosphate transporter

GLUT X – Facilitative Glucose Transporters, X denotes isoform number

GLUT9ΔN – GLUT9 delta N

GSH – glutathione

GWAS – genome-wide association scans

h – human, referring to protein homologue

H89 – H89 dichloride, Protein Kinase A inhibitor

HCO₃⁻ - bicarbonate anion

HEK 293 – human embryonic kidney cell line

HepG2 – human liver carcinoma cell line

HMIT – proton-coupled myo-inositol transporter

IBMX – 3-isobutyl-1-methylxanthine, phosphodiesterase inhibitor

IL-1β – interleukin 1β

iv – intravenous

K⁺ - potassium cation

kDa – kiloDaltons

K_m – Michaelis-Menten kinetic constant representing half-maximal saturation of a carrier by a substrate, also referred to as apparent affinity of substrate for a given carrier

K_{mi/o} – as above, denoting intracellular and extracellular constants, respectively

KO – knock-out

LacY – proton-coupled lactose transporter

m – mouse, referring to protein homologue

MCT – proton-coupled monocarboxylate transporter

MDCK – Madin Darby canine kidney cell line

MFS – Major Facilitative Superfamily

mM – millimolar

mRNA – messenger ribonucleic acid

MRP – Multidrug Resistance Protein

MRP4 – multiresistance protein transporter 4 (ABCC4)

n – Hill coefficient

Na⁺ - sodium cation

NH₂ (N-) – amino terminus

NHERF-1 – sodium-proton exchanger regulatory factor 1

NO – nitric oxide

OA⁻ - organic anion

OAT X - organic anion transporter, X denotes isoform number

OH⁻ - hydroxide anion

ORF – open reading frame

PAH – *para*-aminohippurate

PCR – polymerase chain reaction

PCT – proximal convoluted tubule

PDZ – protein acronym: PDS-95, DLG1, ZO-1

PDZK1 – PDZ-domain binding protein 1

pH – measure of acidity or basicity of an aqueous solution

PKA – Protein Kinase A

PKC – Protein Kinase C

PMA – Phorbol 12-myristate 13-acetate, Protein Kinase C activator

PZA – pyrazinamide

S.E.M – standard error of mean

Sf9 – *Spodoptera frugiperda* insect cells

SLC – Solute Carrier Proteins

SLC17A3 – sodium-phosphate cotransporter 4 (NPT4)

SLC22A12 – gene name URAT1

SLC2A – gene name for GLUT

SMCT1 – sodium-dependent monocarboxylate transporter

SNP – single nucleotide polymorphism

SSSF – Sodium/Solute Symporter Family

TLC – thin layer chromatography

TM – transmembrane

TMVC – two microelectrode voltage clamping

TNF- α – tumour necrosis factor α

UTR – untranslated region

V_{max} – Michaelis-Menten kinetic constant representing maximal rate of carrier-mediated transport, also referred to as a carrier's capacity to transport a substrate

V_{max*i*/o} – as above, denoting intracellular and extracellular constants, respectively

WT – wildtype

α KG – α Ketoglutarate

Chapter

1

General introduction*

* A version of this chapter has been published.

Andrei R. Manolescu, Kate Witkowska, Adam Kinnaird, Tara Cessford and Chris Cheeseman. (2007) Facilitated hexose transporters: New perspectives on form and function. *Physiology*. **22**: 234 – 240.

1.1 **G**eneral Introduction overview

This section aims to introduce the following topics: the solute carrier family of GLUTs, with the focus on the members' substrate specificities; The cloning of mouse and human GLUT9 homologues, and the functional studies pertaining to all known GLUT isoforms; the molecular identity of all proposed urate carriers, discussing the plausibility of each as a physiological urate carrier in human; the physiology of urate homeostasis, outlining key experiments and discussing important metabolic differences between man and the animal model systems available. Also throughout this section, I will aim to address inconsistencies within the fields of research at hand, hinting at key considerations and experiments which need to be addressed in order to move the studies forward.

1.2 **I**ntroduction to carrier-mediated transport

1.2.1 Transport across semi-permeable membranes

Hexoses are a major metabolic fuel for numerous cell types. Specialized, integral membrane protein transporters are required to confer the selective permeability of biological membranes to hexoses. These belong to one of two protein super families, the Sodium / Solute Symporter Family (SSSF) (1), and the Major Facilitative Superfamily (MFS) (2), which are expressed in numerous phyla. As with all solute transport, energy is required to move molecules

across membranes. In the case of hexoses, they either employ the potential energy stored in the sodium gradient to drive their net movement across the selective barrier, concentrating the sugar (secondary active transport, former transporter family), or they move molecules passively down their concentration gradient, until they reach transmembrane equilibrium (facilitated diffusion, latter transporter family). In humans, facilitated transport of hexoses is mediated by MFS transporters, the GLUT proteins, which belong to the gene family SLC2A. These were among the very first facilitated transporters to be studied systematically. Their detailed kinetic analysis led to the development of a number of key concepts as to how carrier proteins might work.

1.2.2 Basic principles of carrier-mediated transport

In 1952, Widdas (3) documented the '*Inability of diffusion to account for placental glucose transfer in the sheep and consideration of the kinetics of a possible carrier transfer*'. A year later, the first meaningful application of Michaelis-Menten equation to model glucose movement across the wall of the rat intestine (4) revolutionized the field of solute transport. Further study of red blood cells, sheep placenta and rat intestine, led to development of the 'simple carrier' theory, which predicted that two related, but separate, processes must occur during transport.

The first step is binding, or adsorption, of the substrate to a recognition site on the protein. This interaction is considered to be much like that between an enzyme and its substrate, but unlike an enzyme, no chemical change occurs to the substrate during the subsequent step, the translocation. This, in turn, involves a conformational change within the protein, leading to reorientation of the substrate-carrier complex. The

result is the presentation of the binding site to the other side of the membrane and subsequent release of the substrate. To complete the cycle, the binding site needs to reorient, to face the side of the membrane where the initial binding process started. In case of facilitated transporters, where net movement of substrate results from solute concentration gradient across the membrane, this implies possible molecule movement in either 'forward' or 'reverse' direction, with respect to the starting concentration gradient. As such, when referring to facilitated diffusion, the vectorial sum of a given solute's movement, or its net movement, should be considered (**Figure 1.1**).

Given the bi-directional nature of transport, it became quickly appreciated that the carrier's affinity for a substrate may not be the same on opposite sides of the membrane. To fulfill thermodynamic laws, this must mean that the maximal rate of transport in one direction would also have to be greater. This could be satisfied if the ratio of the half-maximal saturation constant (K_M) to the maximal rate of transport (V_{max}) was the same for movement in both directions:

$$\frac{K_{mi}}{V_{maxi}} = \frac{K_{mo}}{V_{maxo}}$$

Moreover, it was postulated that the rate-limiting step for transport is the reorientation of the empty carrier, a concept supported by *trans*-acceleration experiments. These experiments showed that if transport of solute in one direction is measured in the presence or absence of a transportable solute on the opposite (*trans*) side, it will be faster than when the substrate is initially present only on one side of the membrane (*zero-trans* conditions). This can be explained by acceleration of the

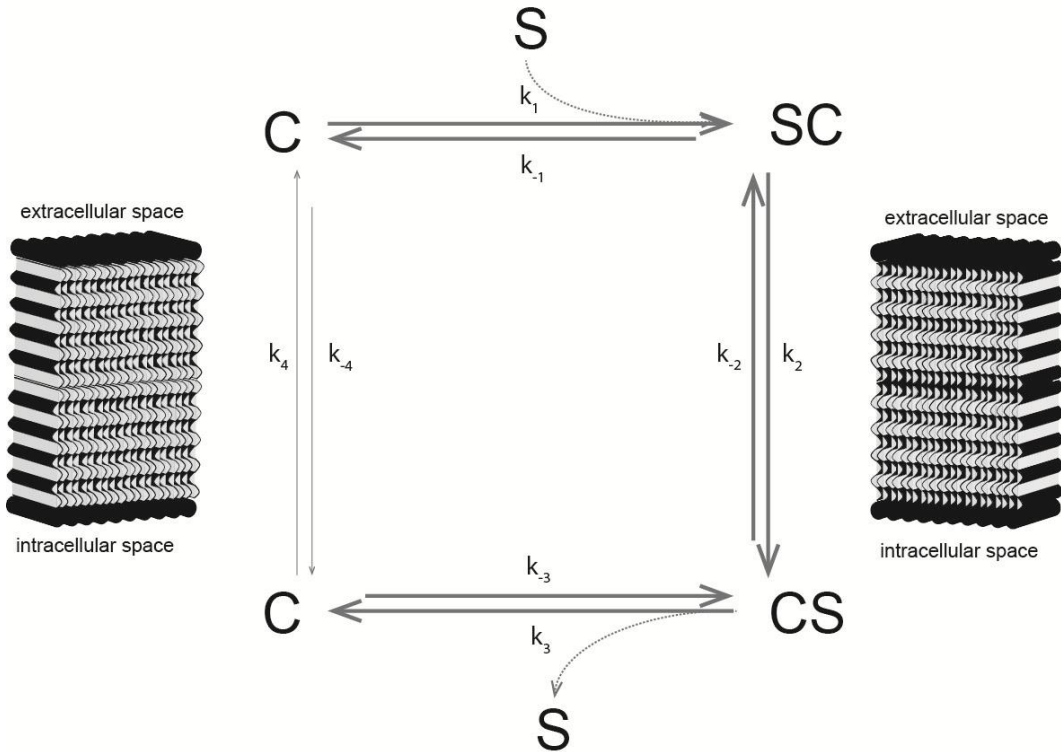


Figure 1.1. Four-step simple carrier kinetic model. Model for carrier-mediated transport of solutes modeled on Michaelis-Menten enzyme kinetics. A facilitative carrier (C) undergoes a series of four basic reorientation steps, while binding and releasing a specific substrate (S). The direction of each step is determined by the sum of two unique kinetic constants representing reversible reactions (eg. k_1 and k_{-1}). The rate limiting step in the cycle is thought to be the reorientation of the empty carrier, depicted by thin arrows (k_4 / k_{-4}). *Trans*-stimulation experiments are thought to take advantage of the reversibility of the transport steps and to circumvent the empty-carrier cycling.

reorientation step, which is thermodynamically favoured when the binding site is occupied. Similarly, if kinetic constants for transport are measured when the solute concentration is the same on both sides of the membrane (equilibrium conditions), the V_{\max} is greater than when measured under *zero-trans* conditions (5).

1.2.3 Initial mapping of the substrate binding site

The determination of the architecture of D-glucose interaction with a putative binding site of the carrier resulted from a series of elegant experiments measuring the accumulation of different hexose analogs in the everted hamster and rat intestinal preparations, and later on the human erythrocyte (6, 7). This work suggested that hydrogen bonds are formed between specific hydroxyl groups on the hexoses and the side chains of certain hydrophilic amino acids lining an aqueous cleft or vestibule. Also, it appeared that these bonds were modified as the protein went through its conformational change so that the binding site facing the exofacial side was partially or completely different from that facing the endofacial side. However, it also reinforced the notion that the specificity of the red cell hexose transporter would be defined by which sugars could interact with the binding sites as they faced either the exofacial or endofacial environment. Finally, it needs to be appreciated that a structural difference between the two binding sites may not be reflected by kinetic asymmetry since, at least for GLUT1, influx and efflux appear to be nearly the same when measured at 37°C (8). Similar analyses have not been made for other GLUT isoforms.

1.3 Family of Facilitative Glucose Transport Proteins (GLUTs)

1.3.1 GLUT family characteristics and substrate specificity

In 1985, the first GLUT protein was cloned and found to be a 492-amino acid single protein constitutively expressed in almost all cell types (9). However, differing kinetic parameters and substrate specificities in some tissues suggested the existence of several additional discrete entities responsible for moving hexoses. Subsequent expression cloning confirmed this hypothesis with the rapid expansion of the hGLUT family to five members. This small number of hexose transporters appeared to satisfy most physiological metabolic processes, with only two members showing any ability to promote fructose movement. However, recent sequencing of the human and other genomes has transformed this landscape. There are now 14 members of the hSLC2A gene family, and many of the newly described members have discrete tissue expression and function (10) (see **Table 1.1** for comprehensive description).

Primary sequence and tertiary structure similarities allowed these 14 transmembrane (TM) proteins to be clustered into three families, or subclasses, numbered I, II, and III (**Figure 1.2**). The majority of the originally identified members belong to class I, along with the new GLUT14, which appears to have resulted from a gene duplication of GLUT3 (11). GLUT5 has been placed in class II along with GLUTs 7, 9, and 11, all of which appear to be high affinity D-glucose and D-fructose transporters, with GLUT5 being the exception (12–15).

Table 1.1 Tissue distribution and substrate specificity of GLUTs.

GLUT	K_m /mM (oocyte)	Tissue	Special feature	Substrate specificity
GLUT1	5	RBC; ubiquitous	tissue-specific <i>trans</i> -stimulation	glucose, galactose, DHA
GLUT3 (GLUT14)	1	neurons	---	glucose, galactose, DHA
GLUT4	5	fat, skeletal and cardiac muscle	insulin-regulated membrane trafficking	glucose, DHA
GLUT2	11	intestine, kidney, liver, β cell	glucose sensor	glucose, galactose, fructose, glucosamine
GLUT5	6	intestine, sperm	predominant in fructose- metabolizing tissues	fructose, some glucose
GLUT7	0.3	intestine	present in ileum where [hexose] is low	glucose, fructose
GLUT9 (a&b)	0.3	kidney, liver, placenta	alternate trafficking of splice variants; electrogenic	urate, some glucose and fructose
GLUT11	0.2	skeletal and cardiac muscle, fat, placenta, pancreas	alternate trafficking of splice variants; no rodent orthologue	glucose, fructose
GLUT6 (GLUT9)	high K_m	brain, spleen	gene duplicon	glucose?
GLUT8	2.4	testis, brain, fat, liver, spleen	[DE]XXXL[LI] N- terminal motif; intracellular	glucose, some fructose
GLUT10	0.3	heart, lung	---	glucose, galactose
GLUT12	~5	insulin sensitive tissues	[DE]XXXL[LI] N- terminal motif; intracellular	glucose, galactose, fructose
HMIT (GLUT13)	0.1	brain	proton-coupled	<i>myo</i> -inositol

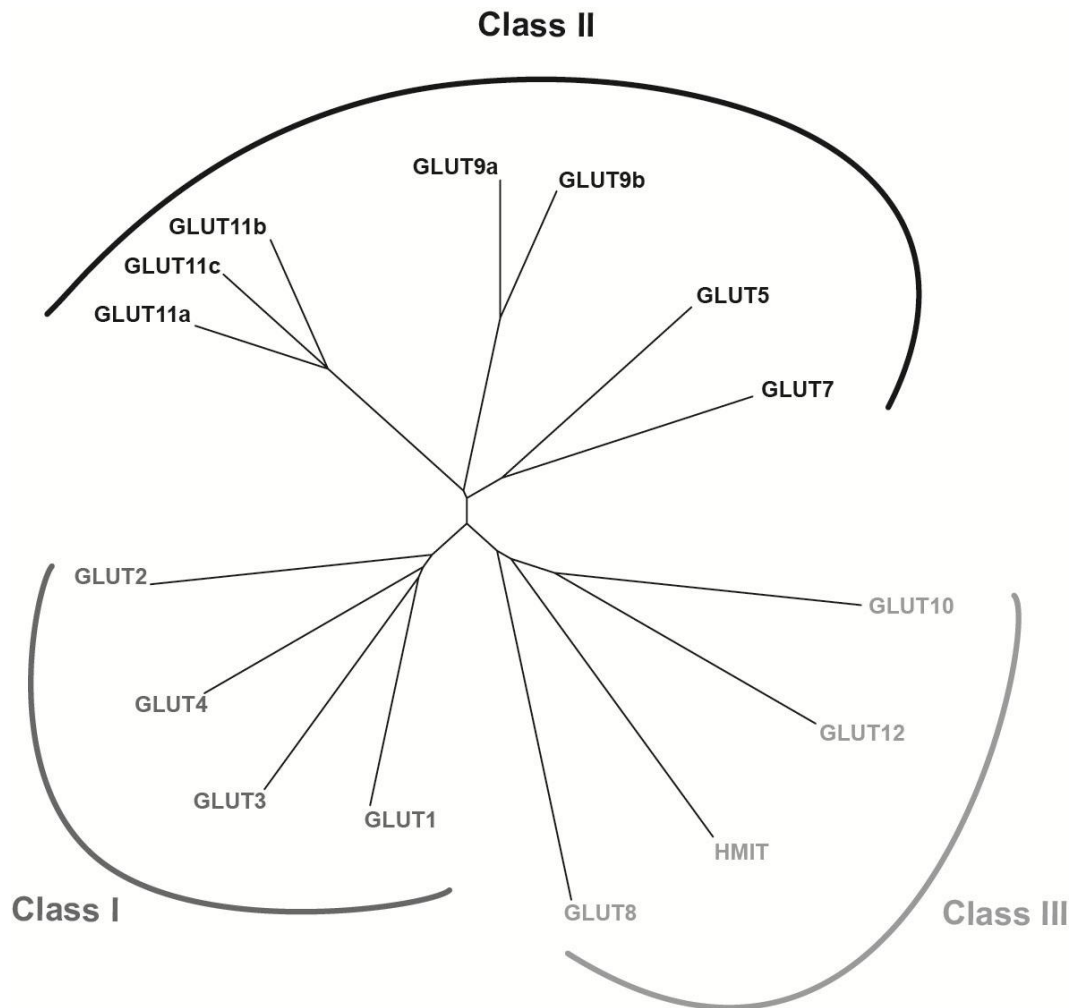
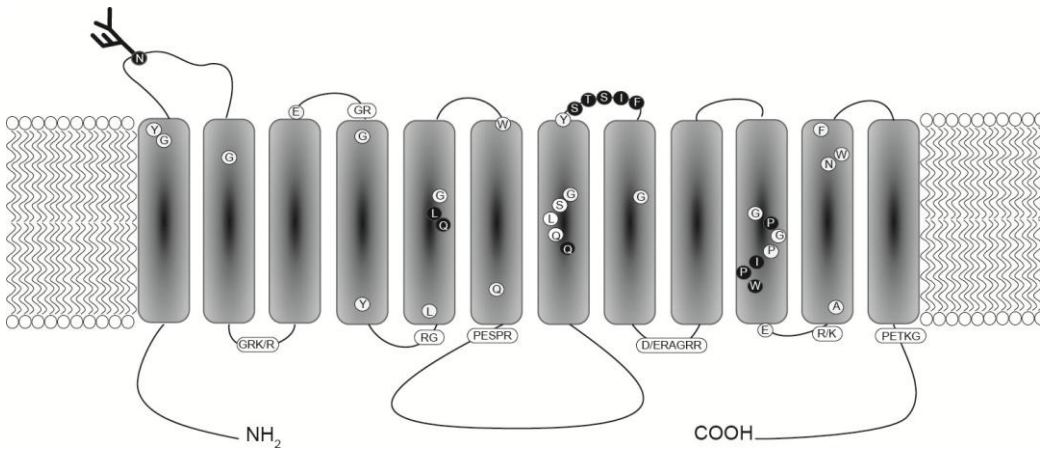


Figure 1.2. Unrooted dendrogram of human facilitative glucose transporter gene family. Amino acid sequences corresponding to SLC2A genes were aligned using ClustalW (<http://www.ebi.ac.uk/Tools/msa/clustalw2/>). Phylogenetic relationships were established using Clustal W software (<http://align.genome.jp/>). The length of each branch represents relative evolutionary distance. Subfamilies or classes of this protein family, representing genetic, structural and functional similarities, are indicated by the semi-circles.

Furthermore, these class members are capable of little or no galactose or 2-deoxy- glucose (2DOG) transport, although GLUT9 was initially functionally characterized using 2DOG ((16) see later discussion). Subfamilies I and II are also unified by a common topology with twelve TM domains, cytoplasmic N- and C- termini, putative N-glycosylation on first extracellular loop (between TM 1 – 2), and a long intracellular loop between TMs 6 – 7 (**Figure 1.3**). Finally, GLUT9 (16) and GLUT11 (17) possess alternative splice variants, which have been reported to confer alternative tissue distribution, but, to date, have not been well studied. As discussed below, GLUT9, unlike GLUT11 (15), has a rodent orthologue. However, its functional study in the model system is limited due to physiological differences between the two organisms, as discussed later. The following chapters will shed more light on the functionality of GLUT9 splice variants.

The structure of the class III GLUTs, on the other hand, preserves the above mentioned twelve helix arrangement, but the N-glycosylation site appears to be located on the fifth extracellular loop (between TM 9 – 10; **Figure 1.3**). Much less is known about the functional activity of these GLUTs, but most have the capacity to transport hexoses. Furthermore, these transporters contain one or more complex retention motifs (N- or C-terminal), which may be confining them to intracellular compartments under steady-state conditions (18). GLUT8 is mainly expressed in testis and brain and is localized in the endoplasmic reticulum (ER), late endosome and lysosome compartments. It has shown insulin responsiveness in mouse blastocysts, but failed to respond to the stimulus in any other cell line (19). GLUT12, expressed in heart, skeletal muscle, small intestine and prostate, shares an expression, which resembles that of GLUT4 (20). Recent evidence suggests that the extended targeting motifs confer specific transporter-adaptor protein interactions within GLUT8 and GLUT12, which regulate the sorting mechanism (19). GLUT10

Class I



Class III

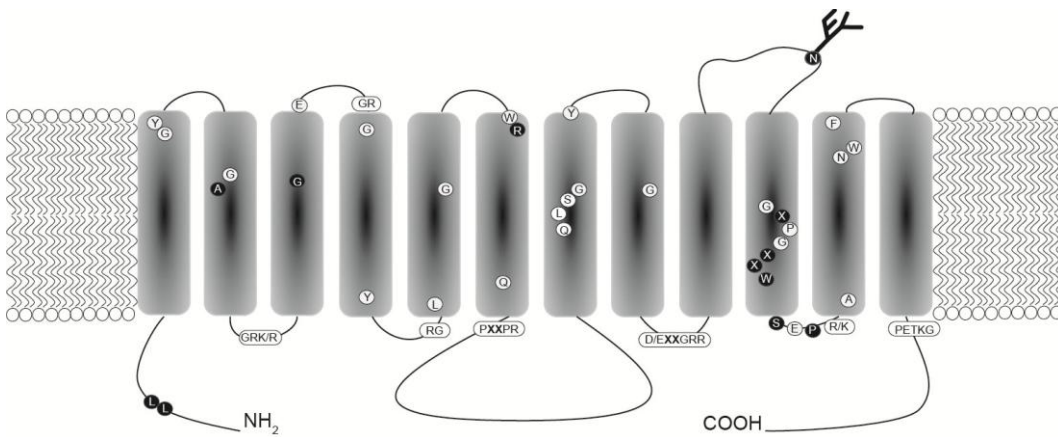


Figure 1.3. General topology model of the GLUT protein family. Class I and Class II GLUT subfamilies share identical topology which differs from that of Class III, especially with respect to the glycosylation site. Residues highlighted on a white background represent amino acids which are conserved throughout the GLUT family. Residues highlighted on a black background indicate amino acids which distinguish Class I from Class III GLUTs. Adapted from Joost and Thorens, 2001 (22).

is widely detected in human tissues, with predominant Golgi expression as well as plasma membrane presence. It contains a similar N-terminal LL-motif (21). Insulin can induce GLUT12 plasma-membrane intracellular stores, possibly due to the presence of an additional C-terminal internalization motif (23). GLUT13 (HMIT) is a proton-coupled *myo*-inositol transporter, prior to this study, making it the first GLUT with a non-hexose physiological substrate, and the only GLUT to use a proton gradient for substrate translocation (24). It is tempting to speculate that GLUT13 represents an ancient hexose transporter because of its high sequence conservation across phyla and its H⁺-coupling transport mechanism (25).

With new functional studies of GLUTs emerging, it is becoming clear that not all of them facilitate exclusive movement of hexoses across the cellular membranes. In fact, GLUTs 1,3 and 4 have been identified as dehydroascorbic (DHA) acid transporters (26), GLUT2 is capable of glucosamine transport (27), and GLUT13 contributes to phospholipid homeostasis in the brain (24). In this thesis, alternative substrate specificity of GLUT9 will be discussed. It is becoming clear, that comparative primary sequence analysis combined with the conserved tertiary fold of the protein, do not suffice in predicting the substrate selectivity of these transporters. On the contrary, they point out that substrate-carrier interactions are far more complex than those proposed in the simple carrier model. Also, given an abundance of non-hexose substrates identified for many of the GLUT members, a question of what is the ancestral permeant for this protein family should be revisited.

1.3.2 GLUT structural studies

The original hydrophathy analysis of GLUT1 indicated that the protein was arranged into 12 TM helices that combined to form a central aqueous pore or channel through which the substrate crossed the lipid bilayer (9). A comprehensive series of studies using cysteine scanning mutagenesis supports such a model with up to 8 of the 12 helices contributing to parts of the surface lining of the pore (28). X-ray crystal structure analysis of two related bacterial proteins, which are also members of the MFS (the proton coupled lactose transporter LacY (29), and the glycerol-3-phosphate transporter GlpT (30)), indicates a barrel structure in which two clusters of six transmembrane helices surround the aqueous pore in the centre. The alternating tilting of these two clusters appears to close the channel on one side and simultaneously open it on the other, forming the outward or inward facing clefts. The substrate binding site for both proteins was identified as being at the center of the aqueous pore, such that the alternating tilting sequentially exposed bound substrate to one side of the membrane or the other (31). Computer analysis of the structure of GLUT1, using the coordinates for GlpT, has generated a very similar structure, verifying much of the findings identified by the cysteine scanning studies, as well as emphasizing the considerable flexibility of the arrangement, imparted by the long intracellular loop between helices 6 and 7.

1.4 Cloning and initial functional characterization of GLUT9 (SLC2A9)

1.4.1 The human orthologue

Fifteen years after cloning of GLUT1, and subsequent GLUT2 through GLUT5 isoforms, it became apparent that “novel” GLUTs must exist. For example, knock-out (KO) GLUT4 mice still maintain normal glucose homeostasis, and thyroid carcinoma cells still display ^{18}F -Fludeoxyglucose (FDG) uptake, despite lack of expression of GLUTs 1 through 5.

In year 2000 Phay *et al.*, 2000 cloned the first of the “novel” GLUTs, which along with GLUT5 and GLUT11, ultimately became the class II subfamily of GLUTs (32). GLUT9 (later termed full length, or isoform a) mRNA displayed a specific tissue distribution, being most abundant in the human kidney tissue, from which the clone was obtained, followed by liver, placenta, lung and blood leukocytes. All transcript-expressing tissues contained three mRNA transcripts: 1.9 kb (major transcript containing full length sequence), 3.1 kb and 5.0 kb, presumably as a result of different 3' untranslated regions (UTRs). The gene contains 12 exons and is mapped to chromosome 4p15.3 – p16. The open reading frame (ORF) encodes a 540 amino acid protein of approximately 58.7 kDa, which displays 44% and 39% identity with GLUT5 and GLUT1, respectively. It contains two signature sugar transporter motifs (**Figure 1.4**) and distinguishes itself with the longest N-terminus among all family members. As discussed in this thesis, this N-terminus may play an important functional role in modulating transport activity of this protein. Finally, six polymorphisms of GLUT9 were

identified, with three of them resulting in amino acid changes. These include: R25G, V282I and P350L mutants. Interestingly, all three of these polymorphisms are associated with elevated plasma urate levels in human populations (Caulfield, private communication).

Expressed sequence tags (EST) screen of the human kidney cDNA library revealed an alternative splice variant of GLUT9 (16). In contrast to the original GLUT9 full length clone, this variant's (termed GLUT9 Δ N, or isoform b) mRNA was organized into 13 exons, which in turn encoded for a 28-amino acid shorter protein (512 amino acids), due to transcriptional regulation by different promoters. The differences between full length and Δ N coincide within the N-terminal region of the transporter, preserving the TMs', loop and C-terminal's region sequence. GLUT9 Δ N displays a much more restricted human tissue expression, with mRNA being detected in the kidney and placenta only. Immunostaining with a general antibody raised towards the C-terminal region of GLUT9, revealed that GLUT9 is expressed in the proximal convoluted tubule (PCT) region of the kidney. Stable expression of the two isoforms in MDCK polarized cells revealed alternative targeting of GLUT9 full length and GLUT9 Δ N to the basolateral and apical membranes, respectively (16). It is important to note, however, that human kidney tissue immunohistochemistry did not corroborate the cell line study, with GLUT9 being detected only in the basolateral membrane of the epithelial cells. To date, the targeting motif of GLUT9 remains unknown. Transport assays in *Xenopus* oocytes revealed that GLUT9 transports 25 μ M 2DOG, a commonly used non-metabolizable glucose analog, the capacity of which was half of that observed for GLUT4 under the same set of conditions. This transport was not inhibited by 100 μ M Cytochalacin B (CB), due to its lack of binding to the transporter. Only the full length isoform was functionally tested in this study. In another study, full length GLUT9 expressed in the *Xenopus* oocytes was shown to

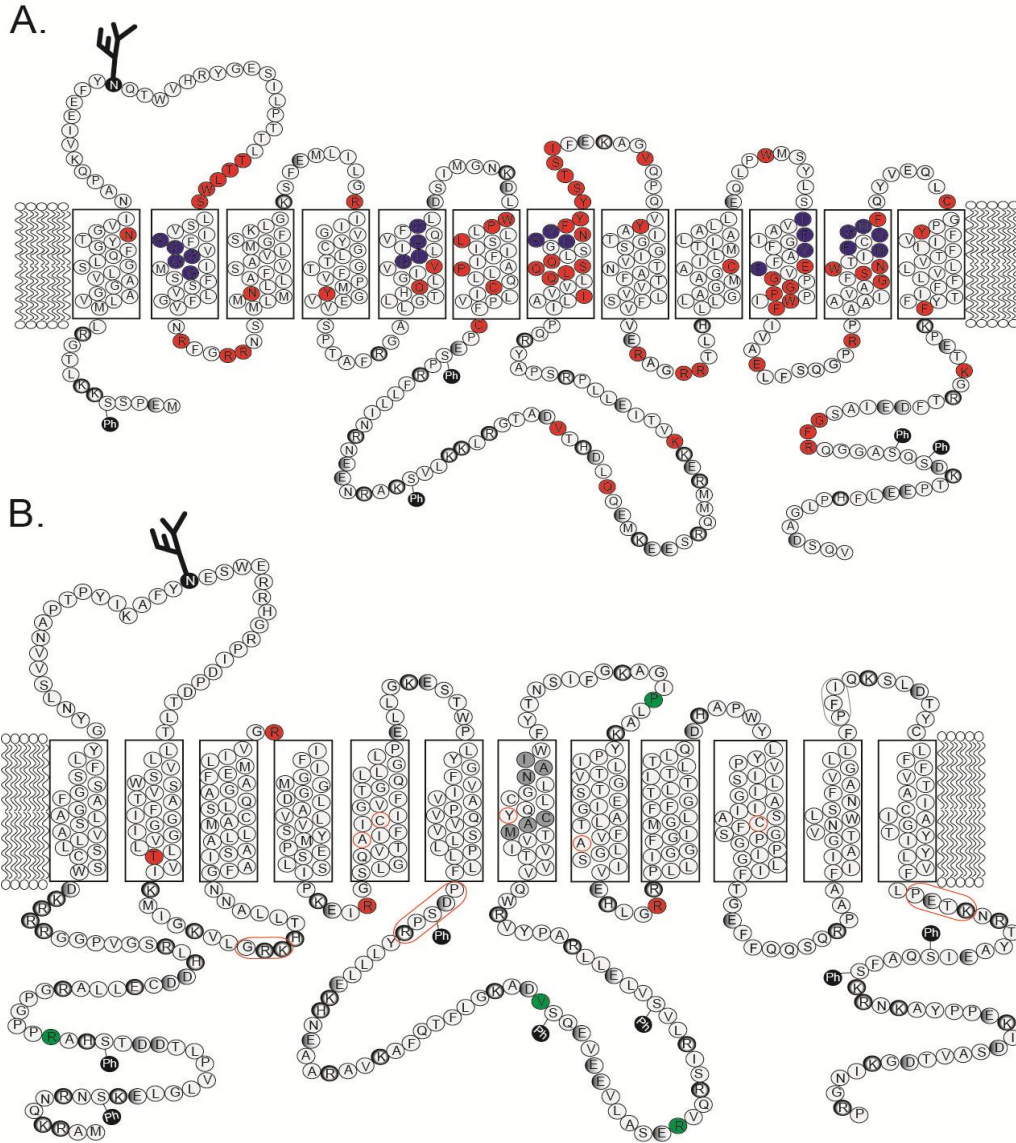


Figure 1.4. Predicted topology models for hGLUT1 (panel A) and hGLUT9 (panel B). Circled letters represent amino acids. (●) – amino acids identified to have functional importance via cysteine-scanning mutagenesis or GWAS; (●) – solvent-accessible residues; (●) – naturally occurring SNPs; (○ and ○) – positive and negative residues, respectively; (Ph) – putative phosphorylation sites with prediction scores $P > 0.5$ (www.cbs.dtu.dk/services/NetPhos/); (○) – residues implicated in GLUT1 – D-glucose interaction which are not conserved in GLUT9; (●) – motif residues thought to play a role in substrate selectivity; (○ and ○) – sugar transporter and class II GLUT motifs, respectively.

transport D-glucose and D-fructose with comparable capacities under a comparable set of transport conditions (14). The apparent affinity of the transport protein for the two substrates was reported at 0.61 ± 0.16 mM and 0.42 ± 0.09 mM, respectively, although it is possible that the constants have been overestimated due to relatively low levels of mediated transport. Finally, GLUT9, along with GLUT5, GLUT7 and GLUT11, contains an isoleucine in a characteristic motif within TM 7 (NAV / NAI), which is thought to confer, at least in part, the protein's specificity for D-fructose. As a result of this study, until recently, GLUT9 was believed to be a high affinity D-glucose and D-fructose transporter, with a dubious physiological role.

Given today's knowledge of GLUT9's substrate specificity, discussed at length in this thesis, it is interesting that Augustin *et al.*, 2004 noted in their study the absence of conservation of key residues between GLUT9 and GLUT1 (16). These residues were deemed important in conferring D-glucose transport and CB binding based on a series of cysteine scanning mutagenesis studies with GLUT1 (33). Finally, the TM 7 motifs QLS and QQLS, important in conferring specificity for glucose in most class I GLUTs, are absent from GLUT9 (**Figure 1.4**).

1.4.2 The mouse orthologue

The mouse orthologue was originally cloned from a mouse 7 – d embryo cDNA library (34). PCR of the open reading frame (ORF) resulted in two cDNA fragments. The first, encoded a 539 amino acid protein with 12 TMs, termed mGLUT9a. The second, encoded a 432 amino acid protein, with only 10 TMs (TM 6 and TM 7 of mGLUT9a deleted), named mGLUT9a_(Δ 209–316). A third isoform was mined from the database, and

coded for the 10 TM protein with a slightly altered N – terminus (mGLUT9b_(NH2b/Δ209-316)). All mouse isoforms possess the same primary and secondary sequence characteristics of the human GLUT9 orthologues discussed above. mGLUT9a and mGLUT9a_(Δ209-316) mRNA was detected in the following adult mouse tissues: liver (most), kidney, and heart (least). However, no reports of protein expression were provided in the corresponding tissues. Furthermore, the two short isoforms, mGLUT9a_(Δ209-316) and mGLUT9b_(NH2b/Δ209-316), were expressed at both mRNA and protein levels, displaying differential cellular protein localization at different developmental stages. Finally, both mGLUT9a and mGLUT9a_(Δ209-316) had the capacity to handle 2DOG. In fact, the deletion isoform, with TMs 6 and 7 missing, displayed a 30% higher transport of 2DOG, compared to mGLUT9a. It is a surprising finding, given TM7's central role in substrate specificity and translocation. The authors postulated that the 10 TM isoforms found in the embryo may be involved in transport of lactate and pyruvate, given their structural similarity with the proton-coupled monocarboxylate transporters (MCTs) and the embryo's preference for those substrates in pre-blastocyst stages of development.

In another study, adult mouse GLUT9 isoforms were revisited (35). A fourth mouse isoform was cloned from the mouse liver cDNA library, encoding a 523 amino acid protein, named mGLUT9b. This protein differs from mGLUT9a in the amino terminal region of the protein, just like the human ΔN and the mouse embryonic NH2b/Δ209-316 isoforms differ from their counterparts. Expression of both isoforms (a and b) was detected in adult mouse tissues on both the mRNA and the protein level. Just like with the human isoforms, mGLUT9a showed a much wider pattern of tissue distribution while mGLUT9b was more restricted. In fact, mGLUT9a was identified in a wider array of tissues including: liver, kidney, brain, lung, and heart muscle, while mGLUT9b was present in liver, kidney and heart.

At the protein level, both isoforms co-localized with GLUT2 expression in the liver, indicating basolateral membrane targeting. In contrast, no co-localization of the two GLUTs, or of mGLUT9 isoforms with loop of Henle's and collecting duct markers, was observed in the kidney tissue, suggesting that mGLUT9 must be expressed in the distal tubules of the kidney. Lack of alternative targeting of the two isoforms was confirmed with polarized MDCK cells. As with the human orthologue, both isoforms transport 2DOG. The authors proposed that mGLUT9 is important in mediating glucose efflux from mouse hepatocytes.

To this day, the physiological function of mGLUT9 still remains unclear. However, the predominance of both isoforms in adult mouse liver, and not kidney, is in marked contrast with the human counterparts, suggests either important metabolic differences between the two organisms, or distinct functions for these two orthologues. Also, the systematic presence of two splice variants in mouse embryo, in adult mouse and in human, indicates that the N-terminus may play an important role in modulation of GLUT9 function at all stages of development. As will be discussed in this thesis, this seems to be the case for the human isoforms, as observed in the *Xenopus* oocyte expression system.

1.4.3 Examples of other GLUT splice variants

To date, two other GLUTs have been reported to undergo transcriptional regulation. These include GLUT11 (15), which results in three hGLUT11 isoforms: GLUT11A, GLUT11B and GLUT11C, and the product of GLUT3 gene duplication, GLUT14 (11), which generates two putative isoforms. All human adult GLUT splice variants seem to undergo alternative splicing within exon1 and exon2 regions, yielding

transmembrane proteins which differ in composition and length of the cytoplasmic N-termini only, thereby maintaining the identity of the remaining TMs, loops and the C-terminus intact.

Careful examination of the 5' flanking regions of GLUT11 exons A – C revealed varied promoter activity in these regions, with promoter 1C displaying the highest expression, as measured by luciferase gene activity (15). All three isoforms were targeted to the membrane when overexpressed in COS-7 (CV-1 in Origin and carrying SV-40 material) cells, and all had comparable capacity to transport D-glucose and D-fructose when expressed in *Xenopus* oocytes. In general, GLUT11 shows a wide pattern of human tissue distribution, however, isoform expression is tissue selective. Curiously, most tissues express two isoforms at the mRNA level, for example kidney and placenta express GLUT11A and GLUT11B. Pancreatic tissue is the only one to express GLUT11C mRNA exclusively. However, no immunohistochemistry exists for native tissue protein distribution of GLUT11 isoforms. It would be interesting to see which region of the kidney expresses GLUT11, and if present in polarized cells, whether the two isoforms target to different membranes. It is not clear what purpose would be served by expression of two isoforms with seemingly identical substrate selectivity within the same membrane. Based on single-concentration transport assays, it has been postulated that the three isoforms handle hexoses identically. Given its substrate specificity and the lack of a rodent orthologue, the proposed physiological function of GLUT11 is its potential compensatory role for loss of pancreatic GLUT2 function in the Fanconi-Bickel syndrome. However, this theory has not been tested.

Both human GLUT14 splice variants have been reported to be exclusively expressed in the testis. Like GLUT11, GLUT14 does not have

a mouse orthologue. No functional studies have investigated the potential function of this gene duplication product (11).

1.5 Molecular identity and functionality of proposed urate transporters in context of the kidney epithelium

1.5.1 The Galectin family of proteins (UAT)

Cloning and functional characterization - By the early 1990's it was well established that the kidney is involved in urate transport. Porcine anti-uricase antibody was used to localize and isolate a protein from a rat kidney brush border membrane (BBM), which was capable of voltage-sensitive urate transport (36). This protein was shown to be expressed in the PCT of the renal cortex. Molecular cloning of cDNA, termed UAT, revealed no linear homology with uricase, but significant homology with a family of soluble proteins called Galectins (37), known to be involved in cell-cell communication, adhesion, apoptosis and immunity. Functional reconstitution of the rat urate transporter in a lipid bilayer system, and subsequently of the human orthologue (38), showed that the protein is capable of electrogenic urate transport with high specificity for the organic anion. Furthermore, detailed analysis confirmed its insertion into the membrane, making it a likely membrane transporter of urate (38). Tissue mRNA expression profile of both human and rat orthologues indicated that they are widely expressed in a variety of organs, with highest transcript levels along the gastrointestinal tract, liver and spleen (37, 38). This

expression pattern, although functionally incomplete, suggests that UAT may not be involved significantly in regulation of plasma urate levels, but rather, that it may serve as a ubiquitous urate efflux protein, which rids the cell of the purine metabolism end-product. Furthermore, it may play a significant role in urate secretion throughout the gastrointestinal tract, where it is highly expressed. However, this process has not been investigated to date. Interestingly, human UAT-mediated urate flux was shown to be stimulated by sugars, like lactose or glucose, possibly revealing a novel mechanism for channel regulation, through sugar-gating (39). Finally, UAT was reported to exist in multiple isoforms, due to alternative splicing (39). Few functional studies followed since 2004, perhaps due to the fact that no genetic variations could be correlated between abnormal plasma urate levels and the gene encoding UAT.

1.5.2 Human Organic Anion Transporters (OATs)

Cloning and functional characterization of hOAT1 - Given that urate is an organic anion under physiological conditions, and the wealth of human and animal studies identifying the existence of a urate – anion exchanger in the kidney's epithelium, efforts were undertaken to search for a molecular identity of a transporter that displays a *para*-aminohippurate (PAH) transport profile in the proximal tubule of the kidney. Given that the rat orthologue, among others, has already been identified (40), its full length DNA was used to screen the human kidney library. This resulted in cloning of cDNA encoding a 563 (41) or 550 (42) amino acid, twelve TM protein, displaying 86% homology with the rat orthologue, which was termed Organic Anion Transporter (OAT1). The discrepancy in the ORF of the product sizes may be a result of multiple isoforms of OAT1 in the

kidney, most likely due to alternative splicing of the transporter gene (43). Northern and Western blotting confirmed OAT1's unique expression in the kidney (41, 42) and human tissue staining localized it to the basolateral membrane of the PCT epithelium (41). Functionally, OAT1 exhibited saturable PAH uptake consistent with Michaelis-Menten transport model, which was insensitive to extracellular Na^+ but sensitive to removal of Cl^- . Furthermore, in both studies, varying degrees of *cis*-inhibition were observed with the uricosuric probenecid, the diuretic furosamide and α -ketoglutarate (α KG). Finally, extracellular urate was also tested as a potential competitive inhibitor of PAH uptake, and as such, a potential hOAT1 substrate. Hosoyamada *et al.*, 1999 reported competitive inhibition at 1mM urate (41), while no effect was observed at a more physiological urate concentration of 100 μ M by Race *et al.*, 1999 (42). Disregarding the fact that at millimolar concentrations of urate slowly precipitate out of solution under physiological pH, many groups begun studying hOAT1 as a urate transporter, overexpressing it in mouse S2 segment cell lines (44), and modelling it as a potential basolateral urate – dicarboxylate exchanger in the PCT epithelium (45–49). Although still not confirmed, basolateral multispecific hOAT1 is thought to be involved in moving urate from the kidney interstitium into the proximal tubule epithelium for possible secretion into the urine. As evident from the discussion in the next section, hOAT1 is of secondary importance in regulating plasma urate levels in humans.

Cloning and functional characterization of hOAT3 – Two groups attempted cloning of hOAT3 (42, 50), however only Cha *et al.*, 2000 succeeded in isolating a functional DNA fragment. hOAT3 proved to mediate saturable transport of a conjugated steroid, esterone sulphate (ES), and display specificity of substrates with bulky side chains, not transported by hOAT1. Its strong mRNA expression in the kidney,

basolateral immunostaining in human kidney slices, and an ES uptake inhibition profile by probencid and furosamide, lead to a conclusion that hOAT3 may be a urate transporter candidate. However, expression of hOAT3 in *Xenopus* oocytes, and direct uptake studies with 10 μ M ¹⁴C urate, revealed 0.8 pmol/ oocyte/ hr net uptake rate, which is roughly 30 times lower than that for 50 μ M ES, and approximately 300 times lower than that for 50nM Methotrexate (50). These direct uptake findings suggest that hOAT3 is an unlikely mediator of urate transport, and a likely key player in pharmacokinetics of anionic drugs.

Cloning and functional characterization of hOAT4 – Human OAT4 was identified to be predominantly expressed in the placenta and the kidneys. Functional study revealed its ES transport capacity and its affinity for hydrophobic side chains, making it a likely candidate for hormone precursor exchange between fetus and mother. Its ES transport was not inhibited by substrates of OAT1 (glutaric acid) and OAT2 (salicylate), or OAT3 inhibitor (penicillin G), giving it a unique substrate profile among OATs (51), and more importantly, excluding it as a likely candidate as a urate carrier. Immunohistochemistry localized its expression to the apical membrane of PCT epithelium (52).

However, the transport mechanism of hOAT4 was postulated to differ from that of hOAT1 and hOAT3, and its tandem gene expression with URAT1, which was shown to impart functional similarities on the gene products (53), reopened the investigation of hOAT4's function as a potential low-affinity urate exchanger mechanism in the kidney. In 2007, Hagos *et al.* (54), carried out a series of experiments expressing hOAT4 in *Xenopus* oocytes, and, in HEK293 cells, proposing that the apical hOAT4 operates as an asymmetric urate transporter. They used two substrates for inhibition screens: ES, a high affinity, naturally occurring substrate ($K_m \sim 1\mu$ M) and 6-Carboxyfluorescein (6CF), a low affinity substrate ($K_m \sim$

100 μ M). In short, their cell transport assays showed 40% *cis*-inhibition of 6CF uptake, at a relatively high urate concentration of 500 μ M, and a direct uptake of 50 μ M urate which was 1.4 fold higher than the non-transfected control. Their oocyte assays, at 400 μ M urate concentration, showed a net uptake of 1.9 pmol/ oocyte/ 60 min, as compared with approximately 20 pmol/ oocyte/ 20 min of 100 μ M urate uptake for hGLUT9a (see Chapter 3). Furthermore, the hOAT4-mediated urate uptake was reported as two times greater than that mediated by URAT1. However, these observations were made after prolonged uptake periods (1 hr), at concentrations close to the reported K_m for URAT1 (~ 371 μ M) (55), making equilibrium-exchange as well as protein expression differences impossible to rule out. In general, most of the reported observations provided weak evidence for hOAT4 being a low-affinity urate resorption mechanism in the proximal tubule of the kidney. Finally, OAT4 is able to transport PAH, while human apical urate transport was shown to be PAH-independent (56).

1.5.3 Human urate-anion exchanger (URAT1)

Cloning and functional characterization - In 2002, based on OAT4 homology, Enomoto *et al.*, identified a new gene SLC22A12 and cloned URAT1 cDNA from human kidney (55), where it is uniquely expressed. Very thorough substrate specificity screen performed in *Xenopus* oocytes revealed that URAT1 was highly selective for urate, not sensitive to PAH, which is a representative substrate for OATs, and was sensitive to uricosuric drugs such as benzbromarone or probenecid. This description made it a likely candidate for a *bona fide* urate transporter. It also provided a molecular identity for functional observations on urate handling capacity of human kidney epithelium made earlier, as discussed in the next section.

Lactate, among other organic anion metabolites, was shown to be a strong competitive inhibitor of urate uptake in frog oocytes, leading the authors to propose a counter-transport mechanism for hURAT1. As such, intracellular accumulation of metabolites would allow for exchange with extracellular urate, allowing urate movement against its electrochemical gradient, thus allowing for effective urate reabsorption in the kidney. The original study has also identified and functionally characterized two homozygous mutations within SLC22A12 gene, which are associated with renal hypouricemia. Since then, a number of URAT1 mutations have been identified, the most common being W258X mutation, which significantly decreases the transporter's function without affecting its expression (57).

URAT1 and PDZ domains - Furthermore, there exists a substantial body of work pointing to the importance of scaffold proteins in regulating proximal tubule transport (58, 59). These are thought to involve a large group of proteins, all of which contain a type of binding domain known as PDZ domain (named based on three proteins: PDS-95, DLG1, and ZO-1), present across eukaryotic, prokaryotic and plant phyla. These motifs aid in building complex protein-protein interactions which allow for protein modulation and cell-membrane communication. The 'classical' binding mode dictates that PDZ domains bind to the most C-terminal residues of a given target protein. Many factors can influence the specificity of those interactions (60). Human and mouse URAT1 orthologues have been shown to possess the tripeptide motif **(S/T)(X)(Φ)**, where X is any amino acid and Φ is a hydrophobic amino acid, and have been functionally assessed to interact with proximal tubule scaffold counterparts (61, 62). A yeast two-hybrid method was used to detect putative, reactive PDZ 2, 3, and 4 domains with the transporter, the presence of which was traced to PDZK1, which also contains PDZ1 and is expressed in human kidney. Mutation of any of the three most C-terminal amino acids, abolished

URAT1-PDZ interactions, indicating that this motif was functionally necessary. Transport and expression analysis showed that co-expression of hURAT1 and PDZK1 in HEK293 cells increased urate uptake, through an increase in V_{\max} , which corresponded with comparable surface expression augmentation of the transporter, suggesting that this protein-protein interaction modulates hURAT1 function by influencing stability of its expression in the cell membrane. Relevance of these findings to the human tissue was confirmed by co-immunostaining (61).

Presence of other PDZ-containing scaffolders in the proximal tubule epithelium (for example, NHERF-1) combined with multiple transporters possessing functional PDZ-binding motifs begs the question of whether these may aid in formation of transportosomes, fostering localized concentration gradients, and ultimately promoting greater transport efficiency of solutes in question. Studies of the mURAT1 revealed that *in vivo* knockout of PDZ-containing scaffold which interacts with the urate transporter, NHERF-1, leads to a decrease in urate and PAH uptake in primary mouse kidney cell culture (62). Given that PAH is not a substrate for URAT1 (55), this finding suggests NHERF-1 interacts with other organic anion transporters in the kidney. Furthermore, the multidomain nature of PDZ domains suggests that these proteins are designed to form multimeric complexes with a broad range of proteins, as well as with themselves (60). NHERF-1 and PDZK-1 have been shown to form heterodimers, thus having the potential to link functionally different membrane proteins (58). Using the same line of reasoning, Anzai *et al.*, 2007 proposed an attractive model for PCT epithelium transportosome, where apically expressed hURAT1 would be linked to SMCT1 (Sodium - Monocarboxylate Transporter 1, gene name SLC5A8) via PDZK1 interactions (47). Given that URAT1 mediates electroneutral exchange of urate for lactate, and that SMCT1 mediates electroneutral import of

sodium and lactate into the cell, this close proximity association of the two carriers, could lead to sub-membrane lactate concentration gradient, which would favour urate resorption, increasing URAT1's efficiency. Both transporters contain PDZ-binding motifs, making their physical association likely. Furthermore, single nucleotide polymorphisms (SNPs) within URAT1 (57) and PDZK1 (63, 64) have been correlated with imbalance in plasma urate levels in humans, while no such associations were found for SMCT1. Regardless of the validity of the above model, renal urate transport activity modulation in the kidney through scaffold proteins is an important avenue to explore from a perspective of membrane expression, stability and localization, transcriptional regulation, transporter phosphorylation, and overall intracellular messenger communication. As will be evident from the following discussion, tertiary dependence of apical urate transport is well corroborated in human BBMV studies (65).

1.5.4 Human Multidrug Resistance Proteins (ABCG2 and MRP4)

Cloning and functional characterization of ABCG2 (BCRP) – Breast Cancer Resistance Protein (BCRP) was cloned from the human breast cancer cell line MCF7/AdrVp (66). It displayed a high degree of homology with the ABC family of transport proteins and appeared to be a widely expressed in human tissues, with predominant expression in the placenta, followed by brain, prostate, liver, intestine and testis. Initially, no detectable levels of expression were reported in the human kidney. Overexpression of BCRP in MCF7 cell line demonstrated that the transporter mediates ATP-dependent efflux of xenobiotics. Given its topology characteristics, namely a single Walker motif, it was proposed

that BCRP must dimerize in order to satisfy the general Multidrug Resistance Protein (MRP) topology (NH₂-[ATP binding1]-[TM]-[ATP binding2]-[TM]-COOH). Ten years later, Huls *et al.* detected mRNA levels of BCRP (ABCG2) in healthy, human kidney samples, which were confirmed in proximal but not distal tubule primary culture monolayers (67). Use of more specific MRP antibodies allowed detection of moderate ABCG2 protein levels in PCT, with precise localization within the BBM. Given its relatively low levels of functional expression, in comparison with the rodent model system, and its high degree of regulation by growth factors such as EGF, IL-1 β , and TNF- α , the authors postulated that ABCG2 plays a regulatory role in xenobiotic homeostasis.

ABCG2 as a urate efflux protein – Multiple Genome Wide Association Scan (GWAS) studies have identified SNPs within the ABCG2 gene, which correlated with elevated plasma urate levels in human populations (63, 68–70). Woodward *et al.* has provided a *direct* demonstration that ABCG2, when expressed in *Xenopus* oocytes, acts as a urate efflux mediator, reducing urate accumulation in comparison to the water-injected oocytes not expressing the protein (71). Furthermore, this effect was abolished with a specific inhibitor of ABCG2 (5 μ M FTC) and when a non-functional mutant S187T of ABCG2 was expressed. The rate of ABCG2-mediated urate efflux was dependent on both intracellular and extracellular urate concentrations, with 500 μ M external urate being inhibitory. Finally, the authors provided a functional link between ABCG2 and hyperuricemia. SNP rs2231442 identified in Atherosclerosis Risk in Communities (AIRC) Study encodes Q141K variant of ABCG2, which when expressed in the oocytes, displayed loss of ABCG2's secretory function, resulting in 50% higher urate accumulation compared to the WT-expressing oocytes. It is believed that 10% of gout cases may be attributed to this mutation.

MRP4 as a urate efflux protein – MRP4 (ABCC4) was initially directly implicated in conferring resistance to nucleoside monophosphate analogs and thus thought to confer resistance to a whole family of nucleoside-based antiviral drugs (72). Further cloning and functional studies showed that MRP4 is capable of cyclic AMP (cAMP) transport, which is both glutathione (GSH)- and ATP- dependent in HepG2 cells stably transfected with MRP4 (73), and later on in Sf9 *Spodoptera frugiperda* insect cells' vesicles (74). Furthermore, MRP4 protein expression has been confirmed in PCT cells in healthy human tissues, and through strong co-localization with monoclonal MRP2 staining, has been localized to the BBM. Its expression pattern and its high affinity for cytosolic cAMP and cGMP suggests that MRP4 may be involved in cyclic nucleotide signalling pathways in the proximal parts of the kidney (74). Lack of a clear molecular identity of a urate secreting protein, combined with an ATP-dependent urate transporter documented in human erythrocytes (75), lead the researchers to test MRP4 involvement in urate efflux. Using Sf9 cell vesicles overexpressing MRP4, the authors demonstrated that MRP4 mediates ATP-dependent urate transport over a range of urate concentrations. Interestingly, the transport profile did not fit simple Michaelis-Menten kinetics, but rather it fit the Hill equation with the Hill coefficient of $n=1.7$, suggesting positive allostery of urate with MRP4. Utilizing the other two known substrates of MRP4, cAMP and cGMP, the authors observed that presence of *cis* urate does not competitively inhibit the transport of either cyclic nucleotides, and, more importantly, that the presence of urate and cGMP on the same side of the membrane, shifted cGMP interaction with the transporter from multiple to single binding (Hill coefficient shift from $n>1$ to $n=1$). This suggests that urate is able to displace cGMP from its binding site, implicating two independent binding pockets for the two substrates. Finally, the authors showed diminished

accumulation of urate due to MRP4 in a mammalian system, by stably transfecting HEK293 cells with the transporter's DNA (76).

In conclusion, this study identified a urate efflux mechanism with kinetic parameters comparable to those observed in red blood cells. However, when MRP4 and ABCG2 are expressed in the same expression system, such as *Xenopus* oocytes, ABCG2 is responsible for efflux of approximately 70% of intracellular urate as compared with 30% of that mediated by MRP4 over 120 minute time frame (71), suggesting lower affinity of the latter transporter for the substrate. Furthermore, standardized gene expression levels in human kidney tissue for the two transporters are 6.9 ± 0.7 (ABCG2) and 4.9 ± 0.4 (MRP4) (67). Assuming that the two proteins have similar basal levels of protein expression in the native tissue, and that no intracellular microdomains of urate concentration exist, ABCG2 seems the more likely physiological candidate for an ATP-dependent apical secretory pathway in PCT epithelium under basal conditions.

1.5.5 Human Sodium Phosphate transporter (NPT4)

The GWAS study by Dehghan *et al.*, 2008 identified three genetic loci associated with elevated plasma urate levels and gout: SLC2A9 (discussed in the following sections of the thesis), ABCG2 (discussed above), and SLC17A3 (NPT4), the latter two being novel associations. Of these, NPT4 showed the weakest association with the phenotype. Furthermore, SNPs within a gene encoding SLC17A1 (NPT1) were also found to be associated with hyperuricemia, leading the authors to postulate that there may be more causal genetic variants downstream of SLC17A3 (63).

Further study of SLC17A3 revealed that there are two isoforms of the transporter, long (L) and short (S), and that their mRNAs are co-expressed in human liver and kidney (77). When expressed in *Xenopus* oocytes the S isoform was found to be not functional. Furthermore, NPT4 protein was shown to be localized to the apical membrane of the PCT epithelium. Together with the genetic studies, these observations made NPT4 an elegant candidate for a urate secretory component in the kidney epithelium. The authors demonstrated that NPT4 could handle a variety of organic anions, with PAH, estradiol-17- β -glucuronide, prostaglandin E₂, and esterone sulphate being some of the substrates directly tested for uptake. The transporter was shown to mediate both uptake and efflux of PAH over a range of extracellular and intracellular substrate concentrations, respectively. Also, both modes of transport were affected by membrane depolarization when Na⁺ was replaced with equimolar K⁺, and uptake of PAH was shown to increase with increasing membrane potential by two microelectrode voltage clamping (TMVC). PAH uptake was used to screen other potential substrates of NTP4. Only a very high concentration of urate (5mM) produced a moderate 30% inhibition of PAH uptake, in comparison to many other substances which effectively abolished this substrate's uptake. Despite these findings, the authors concluded that urate is a substrate for NTP4, and proceeded to measure its transport in NTP4 expressing oocytes. 50 μ M net urate uptake was reported at 0.5 pmol/ oocyte/ hour in contrast to 10 μ M net PAH uptake which was approximately 1pmol/ oocyte/ hour in normal Na⁺ conditions. Furthermore. urate efflux reached only 30% of total initial internal radioactivity after 90 minutes, while PAH was 50% cleared from the oocytes just after 30 minutes. However, direct comparison of transport efficacy could not be made because initial internal concentrations were not specified. Membrane potential dependence was observed when Na⁺ was replaced with K⁺ and when the membrane was voltage-clamped with

electrodes, although these findings were difficult to interpret, given that oocytes were clamped at 20mV and different PAH (5mM) and urate (4mM) concentrations were perfused. Both resulted in increased NPT4-mediated substrate flux, with PAH producing higher responses than urate, regardless of the conditions. Finally, one expressing mutant of NPT4, drawn from a patient population with hyperuricemia, was shown to display reduced urate uptake by 5% as compared to WT. The mutation affected N68, which is a putative glycosylation site.

Given the above observations, the authors concluded that NPT4 is the missing step in the PCT's secretory pathway for urate, arguing that urate from an evolutionary standpoint should be treated as a xenobiotic, validating the existence of multiple, low specificity transporters for its excretion, in contrast to the reabsorptive route composed of highly specific carriers of urate (URAT1 and SLC2A9a). This argument was further substantiated by the group's publication testing five documented nonsynonymous SNPs of NPT4 (78). Only one mutation (V257F) reduced urate uptake by 5% of the WT, under normal ionic conditions. Two other mutations affected urate uptake in high K⁺ medium, however this finding does not seem physiologically relevant. Finally, NPT4 is capable of PAH transport, while apical urate transport in the human PCT appears to be PAH-independent (see discussion below).

1.5.6 Making sense of the urate transporter diversity

Given the well established link between hyperuricemia and gout, and the power of GWAS in identifying putative genetic loci associated with a phenotype, it appears that almost any transporter expressed in the human epithelium of the PCT is capable of urate transport. As discussed

above, many transport proteins have been implicated in this role, with varying degrees of credibility. In order to elucidate the contribution of each of these carriers in a physiological context, one has to consider the following:

1. substrate specificity
2. human tissue expression
3. direct urate fluxes
4. genetic evidence linking gene product to transport function

Based on these criteria, only three of the six transporters discussed above appear to be the likely candidates: URAT1, ABCG2 and MRP4. All of these are expressed within the BBM (apical) of the PCT's polarized epithelium. Based on their functionality, URAT1 is a *bona fide* reabsorptive mechanism, taking up urate from the glomerular filtrate into the epithelial cell. On the other hand, ABCG2 and MRP4 are two likely candidates for urate's secretory route. In order to discriminate between them, the following key questions should be answered:

1. relative affinities of the two transporters for intracellular urate, assessed in the same mammalian system
2. relative levels of protein expression in the native tissue
3. regulatory mechanisms governing surface expression of these two proteins
4. physiological contribution of ATP-dependent mechanism in human urate secretion

Unfortunately, most of these questions, to date, remain unanswered.

Furthermore, one has to consider the complete physiological process of renal urate regulation, which involves a balance of urate reabsorption and secretion in order to maintain constant plasma urate

levels (discussed below). As will become evident from the data presented in this thesis, facilitative transporters may be implicated in the process of basolateral urate reabsorption and, possibly, in apical urate secretion. Electrochemical gradient-driven transport poses additional queries that need to be considered in assessing a transporter's physiological relevance. These include:

1. urate concentration on either side of the membrane (and possible effects of urate microdomains)
2. contribution of the electrical gradient (inside-negative membrane potential) in face of negative charge movement
3. possible modulation of a transport process by way of multiple-substrate interactions

Some of the above aspects will be discussed in light of the novel substrate specificity of hGLUT9. Finally, it is important to remember that urate flux is not limited to the kidney alone. In fact, every cell in our body must rid of purines by breaking them down and exporting them into the bloodstream. Presumably, the more “promiscuous” transporters, like MRPs or OATs, may facilitate this process ubiquitously throughout the tissues. Furthermore, some of the aforementioned transporters are also known to transport signalling molecules. For example, MRP4, as well as other OATs, have been demonstrated to mediate movement of cyclic nucleotides, like cAMP and cGMP across cell membranes (76, 79). As discussed in this thesis, some of these second messengers may modulate urate transport in the kidney epithelium. As such, changes in handling of second messengers or their precursors may indirectly influence urate homeostasis. For a summary of putative molecular identities of urate-handling carriers in PCT, please see **Figure 1.5**

1.6 Physiology of urate with focus on humans

1.6.1 Clinical history of uric acid

Uric acid crystals were first isolated from urinary calculi and reported by Sheele (1779). Its chemical formula was discerned over 50 years later by Whöler and Liebig (80), who investigated its decomposition process. They reported its conversion to allantoin, but believed that the more complete, and thus physiologically relevant, route of elimination involved urea and oxalic acid end products.

As reviewed by Folin *et al.*, 1924 (81), clinical study of uric acid took off with development of the compound's detection methods of amonical silver precipitation, allowing its determination in urine (82). The late 1800's and beginning of the twentieth century saw an explosion of research concerning uric acid's metabolic origin and fate. It was believed that two pools of uric acid exist, endogenous and exogenous, the latter being of special interest after observation of increased levels of uric acid in urine post ingestion of sweetmeats. Many feeding experiments followed, accompanied by laborious determination of purine content in foods. Several observations were consistent: lack of uric acid detection in feces, its indestructibility by pancreatic and gastric juices, and its constantly low excretion recorded at 5 -10% of total amount filtered. Much of the subcutaneous, intramuscular and intravenous uric acid injection experiments failed because of highly toxic effects of the injections, which used piperazine as a solvent.

Studies of uric acid metabolism in dog revealed that it differed dramatically from that of man, and that the kidneys had great capacity to “abstract” the substance from blood while the “bulky tissues” (muscle) were impermeable to it. Interestingly, even among dogs’ species, differences with respect to urate handling were observed, with Dalmatians displaying 3 – 4 fold higher uric acid excretion than all other dogs. Birds and reptiles were noted for their extraordinary concentrative power of the kidney, and were distinguished in their uric acid metabolism from mammals. Improved protocol of uric acid administration using sterilized lithium urate, allowed for better studies of uric acid metabolism in man (81). Through a series of experiments with “normal” and gouty subjects the following observations were made:

1. Uric acid excretion is not directly linked to its concentration in the plasma.
2. Uric acid load lingers in humans for a long time and maximal 50% to 60% clearance is observed up to four days after the substance’s administration.
3. Protein- or Na⁺-rich diets promote faster uric acid elimination in healthy and gouty individuals.
4. No allantoin is present in human urine.
5. Human plasma contains ten to twenty fold higher levels of circulating plasma urate than other animals (excluding apes).
6. Most of the uric acid exists free in solution under physiological conditions.

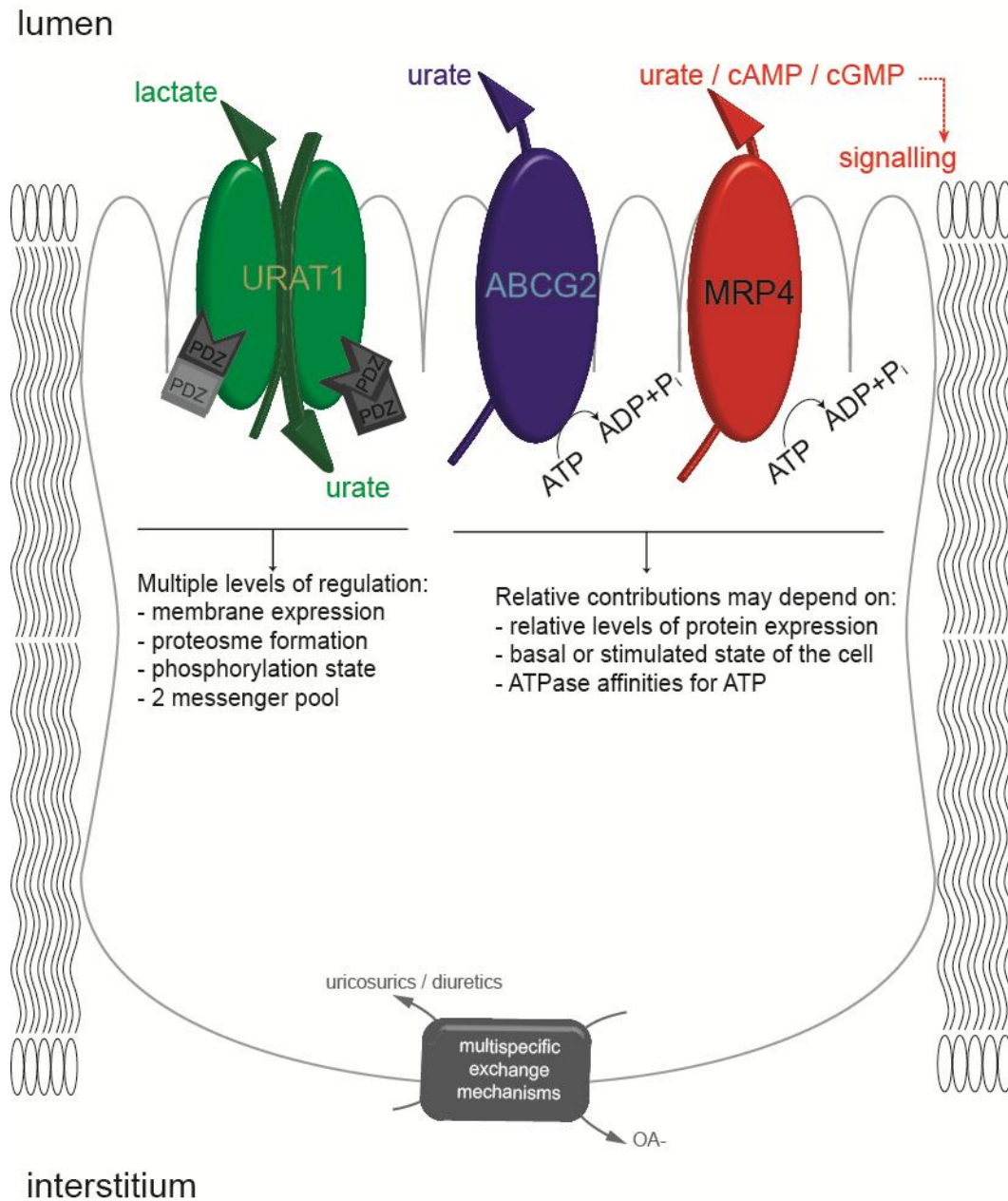


Figure 1.5. Summary of molecular identities of putative urate transporters in human proximal convoluted tubule epithelium.

Furthermore, some fundamental observations of gout were made. The disease is characterized by abnormal circulating plasma uric acid levels, deposition of crystals in select tissues (joints, bone, some connective tissue) and uniform distribution of the acid between blood and joint fluid, regardless of the uric acid load. The final conclusion of the study pointed to the inefficiency of the kidney in dealing with the increased uric acid load, but no suggestions as to the reason for the heightened uric acid levels were given.

By 1950 it was well established that urate excretion in man involved glomerular filtration and some form of active tubular reabsorption process. Moreover, the filtered uric acid load was unable to saturate the human kidney's capacity to recycle urate back into the system. Thus the final 10% urate excretion observed in man for decades was not a consequence of inefficient reabsorption (83). A few observations from clinical studies including: dissociation between filtered uric acid load and final excretion product in gouty patients (large variations already noted by Folin *et al.*, 1924), suppression of uric acid secretion by lactate, and the salicylate "paradox", suggested that excretion of this metabolite may be more complex. A drug, C-28315, shown to block uric acid reabsorption was administered in normal and gouty patients by continuous *iv* infusion. All subjects showed a ratio of excreted urate to filtered urate which was greater than 1, suggesting that excreted uric acid is delivered largely thru secretion. Given that reabsorption block achieved by the drug was probably incomplete, these values represent an underestimate (84).

1980, Levinson and Sorensen performed the reverse experiment, using "pyrazinamide (PZA) suppression test", now inhibiting tubular uric acid secretion. On its own, PZA administration results in almost urate-free

urine (0.7% of the filtered load) and benzbromarone-only administration induces uricosuria. Pre-treatment with PZA prior to benzbromarone administration abolished the latter drug's uricosuric effect. Taken together the authors proposed a four compartment model of tubular urate handling, which involved the following steps: glomerular filtration (100%), proximal reabsorption (99.3%), secretion (50%), distal reabsorption (40%), resulting in 10 – 12% of filtered urate secreted. The authors argued that this model fit micropuncture experiments performed in rats, which displayed a distal reabsorption component (85).

1.6.2 The rodent model in uric acid studies

Given that both humans and rats have been classified as net reabsorbers of uric acid (ie. the ratio of net secreted urate to net filtered urate is less than 1), much research was devoted to the study of the rat model. Particularly useful for these purposes was the ability to perform micropuncture and microperfusion studies of the rat kidney, and thus the ability to measure real-time, localized responses to uric acid loads and to drugs. A summary of this research is presented by Khan and Weinman 1985 (86). As already hinted in the early uric acid literature, significant species differences exist between rodents and humans, making data obtained from the former organism difficult to interpret in the context of man. However, if analyzed with caution, they can provide a useful guide for human studies. The following general statements obtained from the rodent model have furthered our understanding of uric acid handling, and can be applied to humans:

1. Net urate excretion is a result of absorptive and secretory mechanisms, even in urate reabsorbers.
2. Distal nephrons have low permeability to uric acid.
3. Urate transport systems are saturable, can be inhibited by drugs and alternative substrates, and are insensitive to Na^+ .

Our ability to isolate membranes from the rat nephron allowed for direct study of brush border membrane and basolateral membrane transport processes. The collection of these experiments led to a proposed model of urate handling in the rodent kidney. Generally accepted was the existence of *trans*-cellular mechanisms which allowed urate to move from the lumen of the kidney tubule into the tissues, against its electrochemical gradient. These were most likely exchange

mechanisms, one of which could exchange urate for OH^- or HCO_3^- ions, and the other for organic anions (PAH-sensitive). The latter was proposed to function as a tertiary active transporter, where the organic anions could be concentrated inside the cell *via* the power of the Na^+ gradient, in turn to be exchanged for uric acid.

Basolateral transport processes proved more difficult to discern. However, exit of uric acid from the cytoplasm into the interstitium was postulated to occur *via* facilitated diffusion, constitutively driven by the inside-negative membrane potential. Finally, the complexity of the substrate's transport system was recognized, outlining the following reasons for the scientific lag in this field of study:

1. balance of reabsorption and secretion determines net urate excretion
2. multiple exchange mechanisms are involved
3. indirect influence of urate movement by ions like Na^+ , and therefore the possible linkage with salt and water homeostasis
4. "paradoxical effect" of drugs, like salicylates, which can up- or down- regulate urate exchange processes depending on the dosage

Today, much focus is still placed on the rodent model for understanding human urate homeostasis. Recently, URAT1 (SLC22A12) global knock-out (KO) mouse was established (87) and a liver-specific SLC2A9 KO mouse, displaying elevated plasma urate levels similar to those of man, was proposed to serve as an adequate model for urate handling by the kidney (86). However, much higher circulating levels of urate are but one of the main differences in uric acid metabolism between man and rodent. As already noted by Folin *et al.*, 1924 (see above), human urine does not contain allantoin. In contrast, rodents, as well as

most other mammals, convert urate into a more soluble molecule, allantoin, as catalyzed by a liver-residing enzyme called uricase (89). This physiological difference has two implications: rodent kidneys are not “designed” to handle urate as an excretory product, and, presumably, it is the liver which is the “hot-spot” for regulation of plasma urate. The significance of these differences will be discussed below. Needless to say, they impede the use of animal models, slowing down progress in the field of uric acid regulation.

1.6.3 Fundamentals of urate handling by the human kidney

Given the lack of an acceptable animal model and the difficulty of conducting experiments on higher primates, most of the research on urate handling in humans is anecdotal. To my knowledge, only three papers providing direct evidence of renal urate handling in humans exist. These have employed the use of brush border membrane vesicles (BBMVs) from superficial cortex of human kidneys, removed from cancer patients (tissue used was tumour-free, as assessed by morphology) and enriched 17-fold with respect to the basolateral membrane. Rapid-filtration method was used to assess the transport properties of the epithelium at 25°C, under non-equilibrating conditions (15 sec uptakes) (65, 90, 91).

In the first study, Roch-Ramel *et al.*, 1994 (90) showed the existence of a urate / anion exchange mechanism in the human kidney epithelium, a “hallmark” feature of urate reabsorbers. Using an outward-directed Cl⁻ gradient ($[Cl^-]_{intra-vesicle} = 40mM$) they demonstrated more than two fold increase in urate uptake by BBMVs, as compared with the control, suggesting the presence of a Cl⁻-dependent exchange mechanism. Voltage-clamping the vesicles with valinomycin in presence of

extravesicular Cl^- depressed the plateau of the curve, suggesting presence of another, voltage-sensitive pathway for apical movement of urate. This was confirmed by conducting experiments in presence of 100mM K^+ and its ionophore (valinomycin) in absence of Cl^- , which resulted in a significant increase in the vesicles' rate and capacity to take up urate. Through *trans*-stimulation and *cis*-inhibition experiments using different putative substrates and drugs, the authors were able to demonstrate that the Cl^- -and the voltage- dependent pathways are both saturable, and are likely mediated by distinct transport proteins. Finally, in contrast to the rat experiments under voltage-clamped conditions, no urate / OH^- exchange and no PAH sensitivity was observed in the human kidney epithelium, further strengthening the argument that rodent and human epithelia, although both adapted for reabsorbing plasma urate, do so in very different ways¹.

In the following study, using the high affinity substrates for urate exchangers (PZA and nicotinate), Roch-Ramel *et al.*, 1996 were able to discern two apical urate / anion exchange mechanisms in the human kidney BBMV: the low affinity urate / Cl^- exchanger and the high affinity organic anion (OA^-) / urate exchanger (65). Carefully examining physiologic availability of anions, the former exchanger was modelled to efflux urate out of the vesicles / cell while the latter was proposed to take up urate into the vesicle / cell. Although, as mentioned before, no sodium-coupled urate transporters have been reported, the high affinity OA^- / urate exchanger is thought to be functionally coupled to a Na^+ -cotransporter with overlapping substrate specificity for the said OA^- . This was evident when *cis* extravesicular nicotinate and Na^+ were able to upregulate urate uptake, with μM intravesicular concentrations of nicotinate being sufficient to

¹ Apical PAH transport is diverse when comparing renal epithelia of different animal species. However, PAH basolateral counterpart is much more conserved with respect to the transport profile (65).

produce the response. PZA behaved in a similar fashion, although much higher concentrations inside the vesicle were necessary to elicit the response. Under control experimental conditions lactate did not have any effects on urate uptake into BBMVs. However, preloading of the vesicles with 5mM lactate produced trans-stimulation of urate uptake, suggesting that this is a substrate of the low-affinity urate / OA⁻ exchanger system. Furthermore, another level of complexity was added from the observation that extraventricular *cis* Na⁺ and αKG can up-regulate PAH uptake. In turn, αKG is an overlapping substrate for the Na⁺-PZA/nicotinate cotransport. All in all, this study demonstrated the immense complexity of urate handling by the apical membrane of the PCT's epithelium, which is illustrated in **Figure 1.6**. This multiplicity of substrates' influences on urate handling provides room for physiological regulation as well as pathophysiological deregulation.

Further complexity of the human renal urate-handling system arises from the urate carriers' interactions with different classes of drugs, such as uricosurics, hypertensives and diuretics. Careful control of experimental conditions allowed the authors to isolate the four possible urate handling pathways and examine their responsiveness to all drug classes (91). Based on the drugs' affinities for the different urate transport components it was proposed that urate / Cl⁻ and the low affinity urate / lactate (OA⁻) transport are likely mediated by the same carrier. The low affinity urate exchanger was the best target for all uricosurics tested, while the voltage-dependent route of apical urate flux proved least sensitive to the drugs tested. One exception was benzbromarone, which inhibited the voltage-dependent urate uptake into BBMVs by 90% at a relatively low concentration of 100μM. Moreover, under physiological conditions, the long lasting uricosuric effects of benzbromarone were likely due to

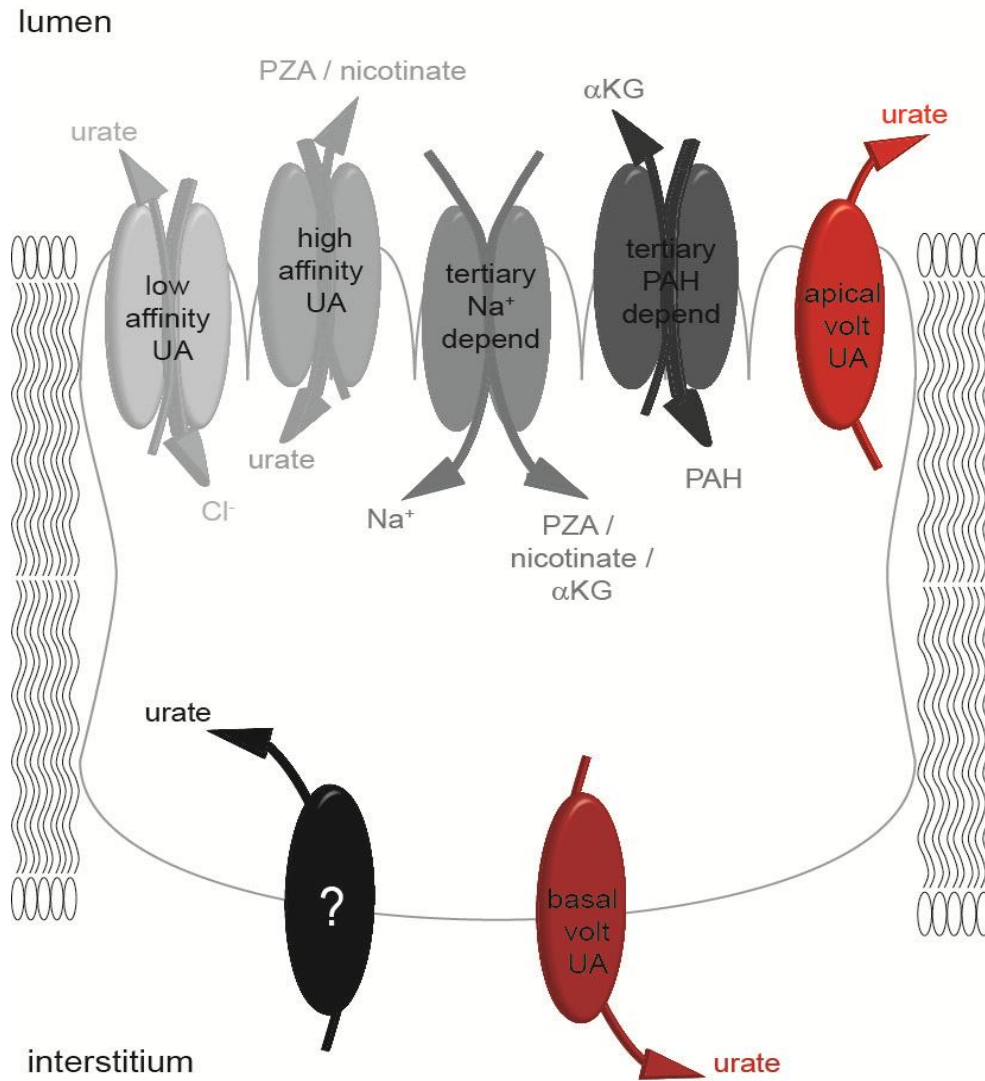


Figure 1.6. Summary of putative transport processes involved in renal urate handling in the human proximal convoluted epithelium.

Review of human kidney BBM vesicle experiments (65, 90, 91). (**low affinity UA**) – exchange process with low affinity for urate; (**high affinity UA**) - exchange process with high affinity for urate; These two were later deemed the same route (91); (**tertiary Na⁺ depend**) – putative process explaining tertiary dependence of urate transport on Na⁺ gradient; (**tertiary PAH depend**) – putative process explaining tertiary dependence of urate transport on PAH gradient; (**apical volt UA**) – apical, voltage-dependent urate transport mechanism with unique sensitivity for benzbromarone; (**basal volt UA**) – basolateral, voltage-dependent urate transport mechanism; (?) – unknown mechanism for tissue – epithelium urate transport.

allosteric binding of either of its metabolites, M1 or M2, rather than the native compound itself. Circulating concentrations in the range of 2 - 4 μ M suffice to produce the enhanced urate excretion, presumably by targeting the exchanger system. Furthermore, the mechanism of “paradoxical effect” of uricosurics was elucidated. As mentioned before, many drugs used to manage plasma urate can produce a biphasic response, with lower concentrations eliciting anti-uricosuria. The authors argued that this is a consequence of relatively high affinity of these agents for plasma binding proteins, which effectively lower the drugs’ active concentrations. As such, it is possible that interstitial drug concentrations exceed those found in the tubule’s lumen. Basolateral entry of the drug into the cell down its concentration gradient, followed by apical exchange of the drug for luminal urate, would result in urate reabsorption. Together with the data suggesting that uricosurics show relatively low affinity for the voltage-dependent secretory route, the likely mechanism for drug-induced anti-uricosuria is a consequence of increased urate reabsorption rather than decreased secretion, as proposed previously. Finally, this distinctive drug selectivity of the voltage-dependent pathway may allow for development of new drugs, which can promote more successful treatment of diseases associated with urate imbalance.

In light of these studies, the four compartment model (85) for urate handling in the human kidney described in the previous section does not hold much ground. Rather, urate fluxes appear to comprise of three steps, all taking place in the PCT:

1. Glomerular filtration
2. Reabsorption of filtered urate
3. Secretion

The PZA effects attributed to inhibition of post-secondary reabsorption are, most likely, a result of *trans*-acceleration of urate reabsorption by PZA's metabolite, pyrazinoate, which enters the cell in a Na⁺-dependent manner (56). Please see **Figure 1.6** for a summary of these processes.

1.6.4 Phylogeny of purine metabolism

Purines, adenine and cytosine, are an integral part of the deoxynucleic acid (DNA) structure. As such, they need to be degraded after the events of cell death. Their catabolism serves two purposes: rendering the relatively insoluble purines more hydrophilic, and salvaging precious carbons for energy (92). Throughout evolution, purine metabolism within living systems has undergone many changes, to meet the energetic demands of organisms, as well as to adapt them to changing habitats. During the journey from simple aquatic organisms, through amphibians and reptiles, to higher-order apes, three enzymes in this catabolic pathway have been lost. Enzyme silencing meant that the relative contribution of the different branches of nitrogenous waste catabolism was altered. Two emerging patterns can be associated with these changes: shift from ammonia to urea renders nitrogenous waste less toxic, while shift from urea to uric acid renders excretions less water-soluble, and thus more efficient at ridding excess nitrogen while conserving body fluids, of special importance in adaptation to terrestrial habitats (92).

Of particular importance is the loss of function of uric oxidase (uricase) enzyme, which converts uric acid to the more soluble allantoin, that has occurred multiple times within the higher vertebrate evolution: once in higher reptiles and birds (92), and at least twice within the

hominoid evolution (93) (**Figure 1.7**). According to Wu *et al.*, 1992 two independent genetic loss-of-function events occurred; One, a deletion resulting in no uricase activity in gibbons and the other, a non-sense mutation in uricase gene of humans, chimpanzees and orangutans. With uric acid being the final breakdown product of purine metabolism in these species, their circulating plasma levels are tenfold higher compared to other mammals with functional uricase (93). The significance of this phenomenon is still debated.

Humans maintain near-saturation levels of urate in the plasma which, along with ascorbate, are meant to provide the extraordinary anti-oxidant power of the blood, thus reducing cancer incidence and contributing to longevity (94, 95). Specifically, these two agents are thought to react with reactive oxygen species (hydrogen peroxide or organic peroxides), which arise as a consequence of tissue metabolism and haemoglobin auto-oxidation. If allowed to persist as free radicals, they can trigger a cascade of erythrocyte lipid peroxidation, accelerating the cells' aging process and / or causing their malfunction. In an elegant study by Ames *et al.*, 1981 (96), circulating urate and ascorbate were shown to have similar capacity in quenching most reactive oxygen species tested. However, due to urate's excess in relation to ascorbate (5mg / 100mL vs. <0.5mg / 100mL, respectively) it is thought to be the predominant anti-oxidant in the bloodstream.

On a whole-body scale, urate anti-oxidative power is demonstrated through the following observations: its gender-specific differences (higher plasma urate levels in males vs. females), its elevation during heavy exercise, and its high concentration in saliva where it is thought to quench reactive nitrosilates over a much wider pH range than ascorbate. Interestingly, urate levels in the cerebrospinal fluid are much lower than those in the plasma, suggesting that this scavenger is not responsible in

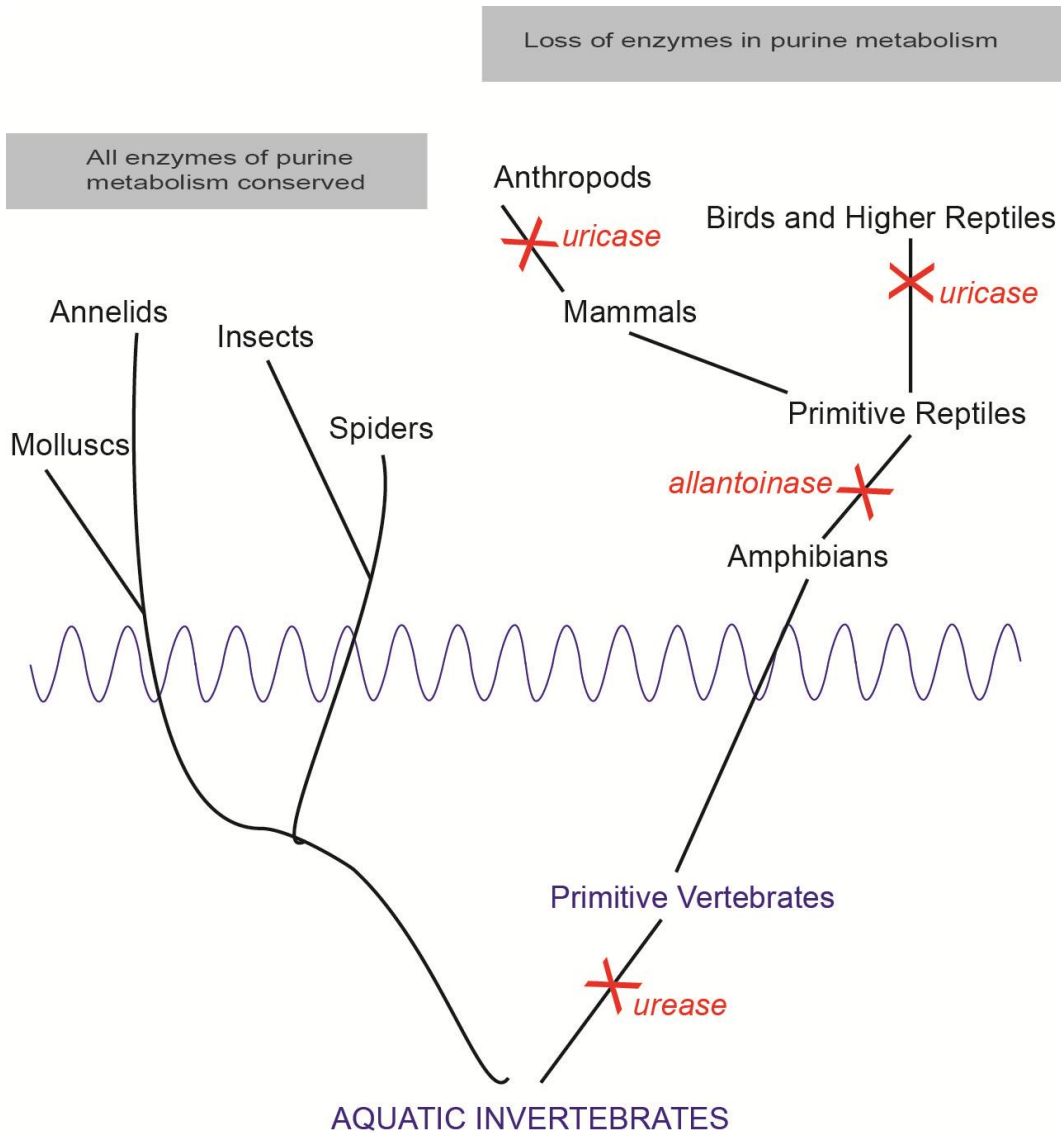


Figure 1.7. Phylogeny of purine catabolism. Loss of function of enzymes involved in purine breakdown is thought to be, at least in part, associated with increase in cellular and systemic complexity and transition from aquatic to terrestrial environments. **X** indicates loss of enzyme function indicated in red. Adapted from Balinsky, 1972 (92).

regulating the oxidative power of the brain (96). As evident from the next section, this near-saturation of blood plasma with urate can have detrimental effects on human health, placing uric acid at the centre of the “oxidant-antioxidant paradox” (97).

1.6.5 Pathophysiology of urate

As recognized in the vast literature dealing with urate metabolism, tightly controlled plasma urate concentrations (reported levels range from 250 μ M - 370 μ M) are of utmost importance for proper function of the human body (45–47, 49, 56, 94, 95, 98–100). Many factors contribute to natural variations of these levels within the human population, and these include: age, gender, and race (68). On another side of the spectrum are environmental factors such as: diet, exercise, and drug use (70, 101). A striking feature of uric acid homeostasis is the tight regulation of urate circulating levels’ set-point; 10% change in the set-point may result in pathology. Hypouricemia (decreased plasma urate levels) and hyperuricemia (increased plasma urate levels) are thought to be a result of altered renal handling of this substrate (101), but diet may also play a role in causing an imbalance (102). Hypouricemia is thought to be relatively asymptomatic, in some cases manifested by nephrolithiasis and acute renal failure, as well as exercise-induced nausea and fainting particularly in Asian populations (103). Hyperuricemia has been studied for centuries, as the causative agent of gout (104). However, hyperuricemia is also associated with other disorders such as hypertension, cardiovascular disease, hyperfructosemia, and the many manifestations of metabolic syndrome (105).

With the explosion of GWAS, which are a powerful tool in relating genetic defects to studied phenotypes, much debate exists around the coincidence of hyperuricemia with hypertension. Few studies have managed to identify hyperuricemia as an independent factor of hypertension (106, 107), while others fail to find statistically significant correlation between the two variables (108). Interestingly, strong correlations have been observed between elevated plasma urate levels and drug-induced hypertension (109) and preeclampsia (110). The mechanism of uric acid pathogenesis is thought to involve water-Na⁺ imbalance, endothelial dysfunction, vascular damage and disruption in nitric oxide (NO) signalling (105).

Another area of interest is the correlation of abnormal plasma urate levels associated with metabolic syndrome, which comprises of disorders such as: glucose intolerance, insulin resistance, obesity, dislipidemia, and hypertension. Majority of these have been correlated with hyperuricemia (111). One proposed underlying mechanism of the syndrome involves direct influence of insulin on renal handling of urate, thus decreasing plasma urate clearance. Another, involves increased consumption of D-fructose in the Western diet, which results in hyperfructosemia, and in turn, coincides with hyperuricemia. Metabolic shunt through the glucose-6-phosphate pathway, a common avenue for fructose and purine metabolism, has been implicated.

In summary, uric acid balance seems to be essential in human health, as evident from scientific literature. However, renal handling of the molecule is still a puzzle, since no agreement exists on the molecular identity and relative contributions of the membrane transport proteins involved in its regulation. Discerning the human renal epithelium model of urate handling is key to understanding the disease mechanisms of gout, cardiovascular disorders and metabolic syndrome. Finally, turning our

attention to the mechanisms contributing to the endogenous pool of urate will complete the picture.

1.7 Thesis objectives

This thesis aims to investigate the novel function of human facilitative hexose transporter, isoform 9 as a urate transporter using the *Xenopus* oocyte heterologous expression system. First, genome-wide association scans' findings are corroborated by functional data demonstrating that hGLUT9 is a high capacity urate transporter, capable of D-glucose and D-fructose exchange for urate, and demonstrating sensitivity to uricosuric drugs. Second, electrogenic properties of hGLUT9-mediated urate transport are characterized, establishing the transporter as a mediator of urate efflux under physiological conditions. Finally, the two splice variants of hGLUT9 are functionally assessed and important differences in their responsiveness to monosaccharides and kinase activators are revealed. Ultimately, these findings further our understanding of the molecular nature of urate transport and regulation, which is critical in effective management of human plasma urate levels, and thus in improving drug targeting of multifactorial diseases such as gout, diabetes and metabolic syndrome. Given the substrate specificity profile of the transporter, throughout the remainder of this work, I will refer to hGLUT9 as hSLC2A9.

1.8 Bibliography

1. Reizer, J., Reizer, A., and Saier, M. H. (1994) A functional superfamily of sodium/solute symporters., *Biochimica et biophysica acta* 1197, 133-66.
2. Marger, M. D., and Saier, M. H. (1993) A major superfamily of transmembrane facilitators that catalyse uniport, symport and antiport., *Trends in biochemical sciences* 18, 13-20.
3. Widdas, W. F. (1952) Inability of diffusion to account for placental glucose transfer in the sheep and consideration of the kinetics of a possible carrier transfer, *Journal of Physiology* 118, 23-39.
4. Fisher, R. B., and Parsons, D. S. (1953) Glucose movements across the wall of the rat small intestine, *Journal of Physiology* 119, 210 - 223.
5. Neame, K. D., and Richards, T. G. (1972) Elementary kinetics of membrane carrier transport 1st ed. Blackwell Scientific Publications, Oxford, England.
6. Barnett, J., Holman, G. D., and Munday, K. A. (1973) An explanation of the asymmetric binding of sugars to the human erythrocyte sugar-transport systems, *The Biochemical Journal* 135, 539-541.
7. Barnett, J. E., Holman, G. D., Chalkley, R. A., and Munday, K. A. (1975) Evidence for two asymmetric conformational states in the human erythrocyte sugar-transport system., *The Biochemical journal* 145, 417-29.
8. Brahm, J. (1983) Kinetics of glucose transport in human erythrocytes., *The Journal of physiology* 339, 339-54.
9. Mueckler, M., Caruso, C., Baldwin, S. A., Panico, M., Blench, I., Morris, H. R., Allard, W. J., Lienhard, G. E., and Lodish, H. F. (1985) Sequence and Structure of a Human Glucose Transporter, *Science* 229, 941-945.
10. Joost, H.-G., Bell, G. I., Best, J. D., Birnbaum, M. J., Charron, M. J., Chen, Y. T., Doege, H., James, D. E., Lodish, H. F., Moley, K. H.,

- Moley, J. F., Mueckler, M., Rogers, S., Schürmann, A., Seino, S., and Thorens, B. (2002) Nomenclature of the GLUT/SLC2A family of sugar/polyol transport facilitators., *American journal of physiology. Endocrinology and metabolism* 282, E974-6.
11. Wu, X., and Freeze, H. H. (2002) GLUT14, a duplicon of GLUT3, is specifically expressed in testis as alternative splice forms., *Genomics* 80, 553-7.
 12. Kane, S., Seatter, M. J., and Gould, G. W. (1997) Functional studies of human GLUT5: effect of pH on substrate selection and an analysis of substrate interactions., *Biochemical and biophysical research communications* 238, 503-5.
 13. Manolescu, A., Salas-Burgos, A. M., Fischbarg, J., and Cheeseman, C. I. (2005) Identification of a hydrophobic residue as a key determinant of fructose transport by the facilitative hexose transporter SLC2A7 (GLUT7)., *The Journal of biological chemistry* 280, 42978-83.
 14. Manolescu, A. R., Augustin, R., Moley, K., and Cheeseman, C. (2007) A highly conserved hydrophobic motif in the exofacial vestibule of fructose transporting SLC2A proteins acts as a critical determinant of their substrate selectivity., *Molecular membrane biology* 24, 455-63.
 15. Scheepers, A., Schmidt, S., Manolescu, A., Cheeseman, C. I., Bell, A., Zahn, C., Joost, H., and Schürmann, A. (2005) Characterization of the human SLC2A11 (GLUT11) gene: alternative promoter usage, function, expression, and subcellular distribution of three isoforms, and lack of mouse orthologue., *Molecular membrane biology* 22, 339-51.
 16. Augustin, R., Carayannopoulos, M. O., Dowd, L. O., Phay, J. E., Moley, J. F., and Moley, K. H. (2004) Identification and characterization of human glucose transporter-like protein-9 (GLUT9): alternative splicing alters trafficking., *The Journal of biological chemistry* 279, 16229-36.
 17. Doedje, H., Bocianski, A., Scheepers, A., Axer, H., Eckel, J., Joost, H., and Schurmann, A. (2001) Characterization of human glucose transporter (GLUT) 11 (encoded by SLC2A11), a novel sugar-transport facilitator specifically expressed in heart and skeletal muscle, *Biochemistry Journal* 359, 443-449.

18. Augustin, R. (2010) The protein family of glucose transport facilitators: It's not only about glucose after all., *IUBMB life* 62, 315-33.
19. Aerni-Flessner, L. B., Otu, M. C., and Moley, K. H. (2011) The amino acids upstream of NH(2)-terminal dileucine motif play a role in regulating the intracellular sorting of the Class III transporters GLUT8 and GLUT12., *Molecular membrane biology* 28, 30-41.
20. Stuart, C. A., Howell, M. E., Zhang, Y., and Yin, D. (2009) Insulin-stimulated translocation of glucose transporter (GLUT) 12 parallels that of GLUT4 in normal muscle, *Journal of Clinical Endocrinology and Metabolism* 94, 3535 - 3542.
21. Flessner, L. B., and Moley, K. H. (2009) Similar [DE]XXXL[LI] motifs differentially target GLUT8 and GLUT12 in Chinese hamster ovary cells., *Traffic (Copenhagen, Denmark)* 10, 324-33.
22. Crouke, P. J., Willaert, A., Wessels, M. W., Callewaert, B., Zoppi, N., Backer, J. De, Fox, J. E., Mancini, G. M., Kambouris, M., Gardella, R., Facchetti, F., J. W. P., R, F., Deitz, H. C., Barlati, S., Colombi, M., Loeys, B., and Paepe, A. De. (2006) Mutations in facilitative hexose transporter GLUT10 alter angiogenesis and cause arterial tortuosity syndrome, *Nature Genetics* 38, 452 - 457.
23. Joost, H. G., and Thorens, B. (2001) The extended GLUT-family of sugar/polyol transport facilitators: nomenclature, sequence characteristics, and potential function of its novel members (review), *Molecular membrane biology* 18, 247-56.
24. Uldry, M., Ibberson, M., and Horisberger, J.-D. (2001) Identification of a mammalian H + myo-inositol symporter expressed predominantly in the brain, *EMBO Journal* 20, 4467-4477.
25. Ibberson, M., Uldry, M., and Thorens, B. (2000) GLUTX1, a novel mammalian glucose transporter expressed in the central nervous system and insulin-sensitive tissues., *The Journal of biological chemistry* 275, 4607-12.
26. Corti, A., Casini, A. F., and Pompella, A. (2010) Cellular pathways for transport and efflux of ascorbate and dehydroascorbate., *Archives of biochemistry and biophysics*. Elsevier Inc. 500, 107-15.

27. Uldry, M., Ibberson, M., Hosokawa, M., and Thorens, B. (2002) GLUT2 is a high affinity glucosamine transporter., *FEBS letters* 524, 199-203.
28. Hruz, P. W., and Mueckler, M. M. (2001) Structural analysis of the GLUT1 facilitative glucose transporter (review)., *Molecular membrane biology* 18, 183-93.
29. Abramson, J., Smirnova, I., Kasho, V., Verner, G., Iwata, S., and Kaback, H. R. (2003) The lactose permease of Escherichia coli: overall structure, the sugar-binding site and the alternating access model for transport., *FEBS letters* 555, 96-101.
30. Huang, Y., Lemieux, M. J., Song, J., Auer, M., and Wang, D.-N. (2003) Structure and mechanism of the glycerol-3-phosphate transporter from Escherichia coli., *Science (New York, N.Y.)* 301, 616-20.
31. Abramson, J., Kaback, H. R., and Iwata, S. (2004) Structural comparison of lactose permease and the glycerol-3-phosphate antiporter: members of the major facilitator superfamily., *Current opinion in structural biology* 14, 413-9.
32. Phay, J. E., Hussain, H. B., and Moley, J. F. (2000) Cloning and expression analysis of a novel member of the facilitative glucose transporter family, SLC2A9 (GLUT9)., *Genomics* 66, 217-20.
33. Mueckler, M., and Makepeace, C. (2009) Model of the exofacial substrate-binding site and helical folding of the human Glut1 glucose transporter based on scanning mutagenesis., *Biochemistry* 48, 5934-42.
34. Carayannopoulos, M. O., Schlein, A., Wyman, A., Chi, M., Keembiyehetty, C., and Moley, K. H. (2004) GLUT9 is differentially expressed and targeted in the preimplantation embryo., *Endocrinology* 145, 1435-43.
35. Keembiyehetty, C., Augustin, R., Carayannopoulos, M. O., Steer, S., Manolescu, A., Cheeseman, C. I., and Moley, K. H. (2006) Mouse glucose transporter 9 splice variants are expressed in adult liver and kidney and are up-regulated in diabetes., *Molecular endocrinology (Baltimore, Md.)* 20, 686-97.

36. Knorr, B. A., Lipkowitz, M. S., Potter, B. J., Masur, S. K., and Abramson, R. G. (1994) Isolation and immunolocalization of a rat renal cortical membrane urate transporter., *The Journal of biological chemistry* 269, 6759-64.
37. Leal-Pinto, E., Tao, W., Rappaport, J., Richardson, M., Knorr, B. A., and Abramson, R. G. (1997) Molecular cloning and functional reconstitution of a urate transporter/channel., *The Journal of biological chemistry* 272, 617-25.
38. Lipkowitz, M. S., Leal-Pinto, E., Rappoport, J. Z., Najfeld, V., and Abramson, R. G. (2001) Functional reconstitution, membrane targeting, genomic structure, and chromosomal localization of a human urate transporter., *The Journal of clinical investigation* 107, 1103-15.
39. Lipkowitz, M. S., Leal-Pinto, E., Cohen, B. E., and Abramson, R. G. (2004) Galectin 9 is the sugar-regulated urate transporter/channel UAT., *Glycoconjugate journal* 19, 491-8.
40. Sekine, T., Watanabe, N., Hosoyamada, M., Kanai, Y., and Endou, H. (1997) Expression cloning and characterization of a novel multispecific organic anion transporter., *The Journal of biological chemistry* 272, 18526-9.
41. Hosoyamada, M., Sekine, T., Kanai, Y., and Endou, H. (1999) Molecular cloning and functional expression of a multispecific organic anion transporter from human kidney., *The American journal of physiology* 276, F122-8.
42. Race, J. E., Grassl, S. M., Williams, W. J., and Holtzman, E. J. (1999) Molecular cloning and characterization of two novel human renal organic anion transporters (hOAT1 and hOAT3)., *Biochemical and biophysical research communications* 255, 508-14.
43. Bahn, A., Ebbinghaus, C., Ebbinghaus, D., Ponimaskin, E. G., Fuzesi, L., Burckhardt, G., and Hagos, Y. (2004) Expression studies and functional characterization of renal human organic anion transporter 1 isoforms., *Drug metabolism and disposition: the biological fate of chemicals* 32, 424-30.
44. Ichida, K., Hosoyamada, M., Kimura, H., Takeda, M., Utsunomiya, Y., Hosoya, T., and Endou, H. (2003) Urate transport via human

- PAH transporter hOAT1 and its gene structure., *Kidney international* 63, 143-55.
45. Rafey, M. A., Lipkowitz, M. S., Leal-Pinto, E., and Abramson, R. G. (2003) Uric acid transport., *Current opinion in nephrology and hypertension* 12, 511-6.
 46. Hediger, M. A., Johnson, R. J., Miyazaki, H., and Endou, H. (2005) Molecular physiology of urate transport., *Physiology (Bethesda, Md.)* 20, 125-33.
 47. Anzai, N., Kanai, Y., and Endou, H. (2007) New insights into renal transport of urate., *Current opinion in rheumatology* 19, 151-7.
 48. Endou, H., and Anzai, N. (2008) Urate transport across the apical membrane of renal proximal tubules., *Nucleosides, nucleotides & nucleic acids* 27, 578-84.
 49. So, A., and Thorens, B. (2010) Uric acid transport and disease., *The Journal of clinical investigation* 120, 1791-9.
 50. Cha, S. H., Sekine, T., Fukushima, J. I., Kanai, Y., Kobayashi, Y., Goya, T., and Endou, H. (2001) Identification and characterization of human organic anion transporter 3 expressing predominantly in the kidney., *Molecular pharmacology* 59, 1277-86.
 51. Cha, S. H., Sekine, T., Kusuhara, H., Yu, E., Kim, J. Y., Kim, D. K., Sugiyama, Y., Kanai, Y., and Endou, H. (2000) Molecular cloning and characterization of multispecific organic anion transporter 4 expressed in the placenta., *The Journal of biological chemistry* 275, 4507-12.
 52. Ekaratanawong, S., Anzai, N., Jutabha, P., Miyazaki, H., Noshiro, R., Takeda, M., Kanai, Y., Sophasan, S., and Endou, H. (2004) Human organic anion transporter 4 is a renal apical organic anion/dicarboxylate exchanger in the proximal tubules., *Journal of pharmacological sciences* 94, 297-304.
 53. Eraly, S. A., Hamilton, B. A., and Nigam, S. K. (2003) Organic anion and cation transporters occur in pairs of similar and similarly expressed genes., *Biochemical and biophysical research communications* 300, 333-42.

54. Hagos, Y., Stein, D., Ugele, B., Burckhardt, G., and Bahn, A. (2007) Human renal organic anion transporter 4 operates as an asymmetric urate transporter., *Journal of the American Society of Nephrology : JASN* 18, 430-9.
55. Enomoto, A., Kimura, H., Chairoungdua, A., Shigeta, Y., Jutabha, P., Cha, S. H., Hosoyamada, M., Takeda, M., Sekine, T., Igarashi, T., Matsuo, H., Kikuchi, Y., Oda, T., Ichida, K., Hosoya, T., Shimokata, K., Niwa, T., Kanai, Y., and Endou, H. (2002) Molecular identification of a renal urate anion exchanger that regulates blood urate levels., *Nature* 417, 447-52.
56. Komatsuda, A., Iwamoto, K., Wakui, H., Sawada, K.-I., and Yamaguchi, A. (2006) Analysis of Mutations in the Urate Transporter 1 (URAT1) Gene of Japanese Patients with Hypouricemia in Northern Japan and Review of the Literature, *Renal Failure* 28, 223-227.
57. Gisler, S. M., Pribanic, S., Bacic, D., Forrer, P., Gantenbein, A., Sabourin, L. A., Tsuji, A., Zhao, Z.-S., Manser, E., Biber, J., and Murer, H. (2003) PDZK1: I. a major scaffold in brush borders of proximal tubular cells., *Kidney international* 64, 1733-45.
58. Cunningham, R., Biswas, R., Steplock, D., Shenolikar, S., and Weinman, E. (2010) Role of NHERF and scaffolding proteins in proximal tubule transport., *Urological research* 38, 257-62.
59. Wang, C. K., Pan, L., Chen, J., and Zhang, M. (2010) Extensions of PDZ domains as important structural and functional elements., *Protein & cell* 1, 737-51.
60. Anzai, N., Miyazaki, H., Noshiro, R., Khamdang, S., Chairoungdua, A., Shin, H.-J., Enomoto, A., Sakamoto, S., Hirata, T., Tomita, K., Kanai, Y., and Endou, H. (2004) The multivalent PDZ domain-containing protein PDZK1 regulates transport activity of renal urate-anion exchanger URAT1 via its C terminus., *The Journal of biological chemistry* 279, 45942-50.
61. Cunningham, R., Brazie, M., Kanumuru, S., Xiaofei, E., Biswas, R., Wang, F., Steplock, D., Wade, J. B., Anzai, N., Endou, H., Shenolikar, S., and Weinman, E. J. (2007) Sodium-hydrogen exchanger regulatory factor-1 interacts with mouse urate transporter 1 to regulate renal proximal tubule uric acid transport., *Journal of the American Society of Nephrology : JASN* 18, 1419-25.

62. Dehghan, A., Köttgen, A., Yang, Q., Hwang, S.-J., Kao, W. L., Rivadeneira, F., Boerwinkle, E., Levy, D., Hofman, A., Astor, B. C., Benjamin, E. J., Duijn, C. M. van, Witteman, J. C., Coresh, J., and Fox, C. S. (2008) Association of three genetic loci with uric acid concentration and risk of gout: a genome-wide association study., *Lancet* 372, 1953-61.
63. Yang, Q., Köttgen, A., Dehghan, A., Smith, A. V., Glazer, N. L., Chen, M.-H., Chasman, D. I., Aspelund, T., Eiriksdottir, G., Harris, T. B., Launer, L., Nalls, M., Hernandez, D., Arking, D. E., Boerwinkle, E., Grove, M. L., Li, M., Linda Kao, W. H., Chonchol, M., Haritunians, T., Li, G., Lumley, T., Psaty, B. M., Shlipak, M., Hwang, S.-J., Larson, M. G., O'Donnell, C. J., Upadhyay, A., Duijn, C. M. van, Hofman, A., Rivadeneira, F., Stricker, B., Uitterlinden, A. G., Paré, G., Parker, A. N., Ridker, P. M., Siscovick, D. S., Gudnason, V., Witteman, J. C., Fox, C. S., and Coresh, J. (2010) Multiple genetic loci influence serum urate levels and their relationship with gout and cardiovascular disease risk factors., *Circulation. Cardiovascular genetics* 3, 523-30.
64. Doyle, L. A., Yang, W., Abruzzo, L. V., Krogmann, T., Gao, Y., Rishi, A. K., and Ross, D. D. (1998) A multidrug resistance transporter from human MCF-7 breast cancer cells., *Proceedings of the National Academy of Sciences of the United States of America* 95, 15665-70.
65. Huls, M., Brown, C. D. a, Windass, a S., Sayer, R., Heuvel, J. J. M. W. van den, Heemskerk, S., Russel, F. G. M., and Masereeuw, R. (2008) The breast cancer resistance protein transporter ABCG2 is expressed in the human kidney proximal tubule apical membrane., *Kidney international* 73, 220-5.
66. Kolz, M., Johnson, T., Sanna, S., Teumer, A., Vitart, V., Perola, M., Mangino, M., Albrecht, E., Wallace, C., Farrall, M., Johansson, A., Nyholt, D. R., Aulchenko, Y., Beckmann, J. S., Bergmann, S., Bochud, M., Brown, M., Campbell, H., Connell, J., Dominiczak, A., Homuth, G., Lamina, C., McCarthy, M. I., Meitinger, T., Mooser, V., Munroe, P., Nauck, M., Peden, J., Prokisch, H., Salo, P., Salomaa, V., Samani, N. J., Schlessinger, D., Uda, M., Völker, U., Waeber, G., Waterworth, D., Wang-Sattler, R., Wright, A. F., Adamski, J., Whitfield, J. B., Gyllenstein, U., Wilson, J. F., Rudan, I., Pramstaller, P., Watkins, H., Doering, A., Wichmann, H.-E., Spector, T. D., Peltonen, L., Völzke, H., Nagaraja, R., Vollenweider, P., Caulfield, M., Illig, T., and Gieger, C. (2009) Meta-analysis of 28,141

individuals identifies common variants within five new loci that influence uric acid concentrations., *PLoS genetics* 5, e1000504.

67. Choi, H. K., Zhu, Y., and Mount, D. B. (2010) Genetics of gout., *Current opinion in rheumatology* 22, 144-51.
68. Merriman, T. R., and Dalbeth, N. (2011) The genetic basis of hyperuricaemia and gout., *Joint, bone, spine : revue du rhumatisme*. Elsevier Masson SAS 78, 35-40.
69. Woodward, O. M., Köttgen, A., Coresh, J., Boerwinkle, E., Guggino, W. B., and Köttgen, M. (2009) Identification of a urate transporter, ABCG2, with a common functional polymorphism causing gout., *Proceedings of the National Academy of Sciences of the United States of America* 106, 10338-42.
70. Schuetz, J. D., Connelly, M. C., Sun, D., Paibir, S. G., Flynn, P. M., Srinivas, R. V., Kumar, A., and Fridland, A. (1999) MRP4: A previously unidentified factor in resistance to nucleoside-based antiviral drugs., *Nature medicine* 5, 1048-51.
71. Lai, L., and Tan, T. M. C. (2002) Role of glutathione in the multidrug resistance protein 4 (MRP4/ABCC4)-mediated efflux of cAMP and resistance to purine analogues., *The Biochemical journal* 361, 497-503.
72. Aubel, R. A. M. H. van, Smeets, P. H. E., Peters, J. G. P., Bindels, R. J. M., and Russel, F. G. M. (2002) The MRP4/ABCC4 gene encodes a novel apical organic anion transporter in human kidney proximal tubules: putative efflux pump for urinary cAMP and cGMP., *Journal of the American Society of Nephrology : JASN* 13, 595-603.
73. Lucas-Heron, B., and Fontenaille, C. (1979) Urate transport in human red blood cells. Activation by ATP., *Biochimica et biophysica acta* 553, 284-94.
74. Aubel, R. A. M. H. Van, Smeets, P. H. E., Heuvel, J. J. M. W. van den, and Russel, F. G. M. (2005) Human organic anion transporter MRP4 (ABCC4) is an efflux pump for the purine end metabolite urate with multiple allosteric substrate binding sites., *American journal of physiology. Renal physiology* 288, F327-33.
75. Jutabha, P., Anzai, N., Kitamura, K., Taniguchi, A., Kaneko, S., Yan, K., Yamada, H., Shimada, H., Kimura, T., Katada, T., Fukutomi, T.,

- Tomita, K., Urano, W., Yamanaka, H., Seki, G., Fujita, T., Moriyama, Y., Yamada, A., Uchida, S., Wempe, M. F., Endou, H., and Sakurai, H. (2010) Human sodium phosphate transporter 4 (hNPT4/SLC17A3) as a common renal secretory pathway for drugs and urate., *The Journal of biological chemistry* 285, 35123-32.
76. Jutabha, P., Anzai, N., Kimura, T., Taniguchi, A., Urano, W., Yamanaka, H., Endou, H., and Sakurai, H. (2011) Functional analysis of human sodium-phosphate transporter 4 (NPT4/SLC17A3) polymorphisms., *Journal of pharmacological sciences* 115, 249-53.
77. Ahn, S.-young, and Nigam, S. K. (2009) Toward a Systems Level Understanding of Organic Anion and Other Multispecific Drug Transporters: A Remote Sensing and Signaling Hypothesis, *Molecular Pharmacology* 76, 481-490.
78. Wöhler, F., and Liebig, J. (1838) Untersuchungen über die Natur der Harnsäure, *Annalen der Pharmacie* 26, 241-336.
79. Folin, O., Berglund, H., and Derick, C. (1924) The uric acid problem. An experimental study on animals and man, including gouty subjects., *Journal of Biological Chemistry* 60, 361 - 471.
80. Salkowski, E. (1871) Untersuchungen über die Ausscheidung der Alkalisalze, *Archiv für Pathologische Anatomie und Physiologie und für Klinische Medizin* 53, 209-234.
81. Berlinger, R. W., Hilton, J. G., Yu, T. F., and Kennedy, T. J. (1950) The renal mechanism for urate excretion in man., *The Journal of clinical investigation* 29, 396-401.
82. Gutman, A. B., Yu, T. F., and Berger, L. (1959) Tubular secretion of urate in man., *The Journal of clinical investigation* 38, 1778-81.
83. Levinson, D. J., and Sorensen, L. B. (1980) Renal handling of uric acid in normal and gouty subject: evidence for a 4-component system., *Annals of the Rheumatic Diseases* 39, 173-179.
84. Kahn, A. M., and Weinman, E. J. (1985) Urate transport in the proximal tubule: in vivo and vesicle studies., *The American journal of physiology* 249, F789-98.

85. Hosoyamada, M., Takiue, Y., Morisaki, H., Cheng, J., Ikawa, M., Okabe, M., Morisaki, T., Ichida, K., Hosoya, T., and Shibasaki, T. (2010) Establishment and analysis of SLC22A12 (URAT1) knockout mouse., *Nucleosides, nucleotides & nucleic acids* 29, 314-20.
86. Preitner, F., Bonny, O., Laverrière, A., Rotman, S., Firsov, D., Costa, A. Da, Metref, S., and Thorens, B. (2009) Glut9 is a major regulator of urate homeostasis and its genetic inactivation induces hyperuricosuria and urate nephropathy., *Proceedings of the National Academy of Sciences of the United States of America* 106, 15501-6.
87. Terzuoli, L., Porcelli, B., Ponticelli, F., and Marinello, E. (2009) Purine nucleotide catabolism in rat liver. Certain preliminary aspects of uricase reaction., *Nucleosides, nucleotides & nucleic acids* 28, 193-203.
88. Roch-Ramel, F., Werner, D., and Guisan, B. (1994) Urate transport in brush-border membrane of human kidney., *The American journal of physiology* 266, F797-805.
89. Roch-Ramel, F., Guisan, B., and Schild, L. (1996) Indirect coupling of urate and p-aminohippurate transport to sodium in human brush-border membrane vesicles., *The American journal of physiology* 270, F61-8.
90. Roch-Ramel, F., Guisan, B., and Diezi, J. (1997) Effects of uricosuric and antiuricosuric agents on urate transport in human brush-border membrane vesicles., *The Journal of pharmacology and experimental therapeutics* 280, 839-45.
91. Roch-Ramel, F., and Guisan, B. (1999) Renal Transport of Urate in Humans., *News in physiological sciences : an international journal of physiology produced jointly by the International Union of Physiological Sciences and the American Physiological Society* 14, 80-84.
92. Balinsky, J. B. (1972) Phylogenetic aspects of purine metabolism., *South African Medical Journal* 46, 993-7.
93. Wu, X. W., Muzny, D. M., Lee, C. C., and Caskey, C. T. (1992) Two independent mutational events in the loss of urate oxidase during hominoid evolution., *Journal of molecular evolution* 34, 78-84.
94. Hediger, M. A. (2002) Gateway to a long life ?, *Nature* 417.

95. Sautin, Y. Y., and Johnson, R. J. (2008) Uric acid: the oxidant-antioxidant paradox., *Nucleosides, nucleotides & nucleic acids* 27, 608-19.
96. Ames, B. N., Cathcart, R., Schwiers, E., and Hochstein, P. (1981) Uric acid provides an antioxidant defense in humans against oxidant- and radical-caused aging and cancer: a hypothesis., *Proceedings of the National Academy of Sciences of the United States of America* 78, 6858-62.
97. Sautin, Y. Y., and Johnson, R. J. (2008) Uric acid: the oxidant-antioxidant paradox., *Nucleosides, nucleotides & nucleic acids* 27, 608-19.
98. Mount, D. B., Kwon, C. Y., and Zandi-Nejad, K. (2006) Renal urate transport., *Rheumatic diseases clinics of North America* 32, 313-31, vi.
99. Johnson, R. J., Sautin, Y. Y., Oliver, W. J., Roncal, C., Mu, W., Gabriela Sanchez-Lozada, L., Rodriguez-Iturbe, B., Nakagawa, T., and Benner, S. A. (2009) Lessons from comparative physiology: could uric acid represent a physiologic alarm signal gone awry in western society?, *Journal of comparative physiology. B, Biochemical, systemic, and environmental physiology* 179, 67-76.
100. Wright, A. F., Rudan, I., Hastie, N. D., and Campbell, H. (2010) A "complexity" of urate transporters., *Kidney international* 78, 446-52.
101. Marangella, M. (2005) Uric acid elimination in the urine. Pathophysiological implications., *Contributions to nephrology* 147, 132-48.
102. Miller, A., and Adeli, K. (2008) Dietary fructose and the metabolic syndrome., *Current opinion in gastroenterology* 24, 204-9.
103. Esparza Martín, N., and García Nieto, V. (2011) Hypouricemia and tubular transport of uric acid., *Nefrología: publicación oficial de la Sociedad Española Nefrología* 31, 44-50.
104. Doherty, M. (2009) New insights into the epidemiology of gout., *Rheumatology (Oxford, England)* 48 Suppl 2, ii2-ii8.
105. Lippi, G., Montagnana, M., Franchini, M., Favaloro, E. J., and Targher, G. (2008) The paradoxical relationship between serum uric

acid and cardiovascular disease., *Clinica chimica acta; international journal of clinical chemistry* 392, 1-7.

106. Panoulas, V. F., Douglas, K. M. J., Milionis, H. J., Nightingale, P., Kita, M. D., Klocke, R., Metsios, G. S., Stavropoulos-Kalinoglou, a, Elisaf, M. S., and Kitas, G. D. (2008) Serum uric acid is independently associated with hypertension in patients with rheumatoid arthritis., *Journal of human hypertension* 22, 177-82.
107. Fang, J. (2000) Serum Uric Acid and Cardiovascular Mortality: The NHANES I Epidemiologic Follow-up Study, 1971-1992, *JAMA: The Journal of the American Medical Association* 283, 2404-2410.
108. Caulfield, M. J., Munroe, P. B., O'Neill, D., Witkowska, K., Charchar, F. J., Doblado, M., Evans, S., Eyheramendy, S., Onipinla, A., Howard, P., Shaw-Hawkins, S., Dobson, R. J., Wallace, C., Newhouse, S. J., Brown, M., Connell, J. M., Dominiczak, A., Farrall, M., Lathrop, G. M., Samani, N. J., Kumari, M., Marmot, M., Brunner, E., Chambers, J., Elliott, P., Kooner, J., Laan, M., Org, E., Veldre, G., Viigimaa, M., Cappuccio, F. P., Ji, C., Iacone, R., Strazzullo, P., Moley, K. H., and Cheeseman, C. (2008) SLC2A9 is a high-capacity urate transporter in humans., *PLoS medicine* 5, e197.
109. Curtis, J. J., Luke, R. G., Jones, P., and Diethelm, A. G. (1988) Hypertension in cyclosporine-treated renal transplant recipients is sodium dependent., *The American journal of medicine* 85, 134-8.
110. Schackis, R. C. (2004) Hyperuricaemia and preeclampsia: is there a pathogenic link?, *Medical hypotheses* 63, 239-44.
111. Soleimani, M. (2011) Dietary fructose, salt absorption and hypertension in metabolic syndrome: towards a new paradigm., *Acta physiologica (Oxford, England)* 201, 55-62.

Chapter 2

Materials and Methods

2.1 Materials

Standard reagents for this work were ordered from Sigma Aldrich Canada (Oakville, Canada) or Fisher Scientific (Ontario, Canada). For all other materials used, please see the following: less common reagents (**Table 2.1**), DNA modifying enzymes and DNA kits (**Table 2.2**), list of constructs and primers used for mutagenesis (**Table 2.3**), and antibodies and reagents used for protein work (**Table 2.4**). Finally, the equipment and software used are listed in **Table 2.5** and **Table 2.6**, respectively.

2.2 Methods

2.2.1 Molecular biology

Constructs – hSLC2A9a and hSLC2A9b clones, and their mutants, were expressed in the pGEM-HE vector (1), which contains 5' and 3' untranslated regions of the *Xenopus* β -globin gene, for enhanced expression of non-native proteins in the oocytes.

In vitro transcription – hSLC2A9 constructs were linearized at a unique restriction site using *NheI* endonuclease (1 hour incubation, 37°C). The reaction was then purified by phenol-chloroform extraction method. Resulting pure, linear cDNA was *in vitro* transcribed (T7 polymerase, 1 hour incubation, 37°C) using a commercially available kit (see **Table 2.2**).

Resulting synthetic cRNA was diluted with ultrapure, RNA-se free water to a concentration of ~200ng/μl, tested on an agarose gel, and injected into *Xenopus* oocytes (see 2.2.2).

Site-directed mutagenesis – Appropriate SLC2A9 constructs were used as template for oligotide-directed mutagenesis using a commercially available kit (see **Table 2.2**). For a list of primers, please refer to **Table 2.3**. Resulting PCR products were sequenced (Macrogen, Maryland, USA). Correct constructs were transcribed and expressed in oocytes, as mentioned above.

2.2.2 *Xenopus laevis* heterologous expression system

Advantages of the system – *X. laevis* oocytes were essential in cloning of the GLUT proteins (2). It is a well developed and widely-used system for expression and functional characterisation of mammalian membrane proteins, such as channels and facilitative transporters (1, 3, 4). It is relatively easy and inexpensive to manipulate oocytes, as they do not require a sterile environment, expensive transfection reagents and culture media to sustain them. Furthermore, large number of mutants can be tested functionally using both radiolabelled tracer uptake as well as electrophysiological approaches. Finally, oocytes can be microinjected with substrates and inert substances, allowing the study of *trans*-membrane transport from both the extracellular and the intracellular compartments, a particularly useful approach when dealing with efflux transporters (5, 6).

Potential limitations of the system – Given that an oocyte is a living system, it is important to acknowledge the potential influence of a cell's

metabolism on exogenous protein expression and function, as well as the potential consequences of expressing mammalian proteins in an amphibian system.

It has been shown that expression of certain proteins can deregulate the expression levels of oocytes' native proteins, often confounding the observations (7). Furthermore, one has to consider the potential metabolism of substrates in question. In particular, metabolic modification of a substrate can be desirable when investigating mediated uptake, as it enhances the signal-to-noise ratio. On the other hand, the same process may render the system inadequate when studying mediated efflux.

Oocyte architecture should also be considered in expression and transport assays. It has been shown that the oocyte membrane is highly folded (surface area 18 – 20mm²) thus resembling the brush border apical membrane of polarized, epithelial cells (8). Furthermore, the yolk of the oocyte occupies a significant portion of the cell volume, thus reducing the volume of the aqueous cytoplasm space. These two facts may contribute to unstirred layer and microdomain formation, affecting measurement of substrates' movement properties across the membrane.

Finally, it is widely accepted that transport proteins are not isolated entities within the membrane, but rather, that they are highly regulated through interaction with other membrane components and / or with cytoskeleton proteins *via* their intracellular moieties (9). Furthermore, these effects are known to be species and cell-type specific. As such, these suggest, that oocyte transport data should be interpreted with caution, keeping in mind that the aforementioned complex regulatory mechanisms may be different in the amphibian cell.

X. laevis oocyte isolation and preparation – The protocol for oocyte preparation and cRNA injection has been described extensively (4). In brief, two-year old female *Xenopus laevis* frogs (Biological Sciences Vivarium, University of Alberta and Nasco, Fort Atkinson, Wisconsin, USA) were anaesthetized by immersion in 0.3 % (w/v) tricaine methanesulphonate (pH 7.4). Stage V-VI oocytes from ovarian lobes were isolated by collagenase treatment (6 mg/ml, 1 hour 20 minutes, dissolved in Barth's Medium, see Table 2.7). The remaining follicular layers were removed by phosphate treatment (see **Table 2.8**) and manual defolliculation. Oocytes were injected with 10 – 20 nl of cRNA transcript (200 ng/nl) or 20 nl of water alone (control). Injected oocytes were then incubated for 4 days at 18 °C in Barth's Medium (see **Table 2.7**). Media were changed daily and eggs were sorted to increase viability of expressing cells.

2.2.3 Transport assays

Radiolabelled uptake studies - Uptake assays were performed, as described previously (4). Batches of 10 – 12 oocytes, either injected with hSLC2A9 isoform or water, were equilibrated to room temperature (20°C) before each experiment. All uptake experiments, unless otherwise stated, were performed at 100µM substrate dissolved in Barth's Medium (**Table 2.7**). In order to observe zero-*trans* conditions for substrate uptake, a 20 minute uptake time was chosen for all hSLC2A9 experiments, as determined from initial time course data (**Figure 2.1**). Radiolabelled

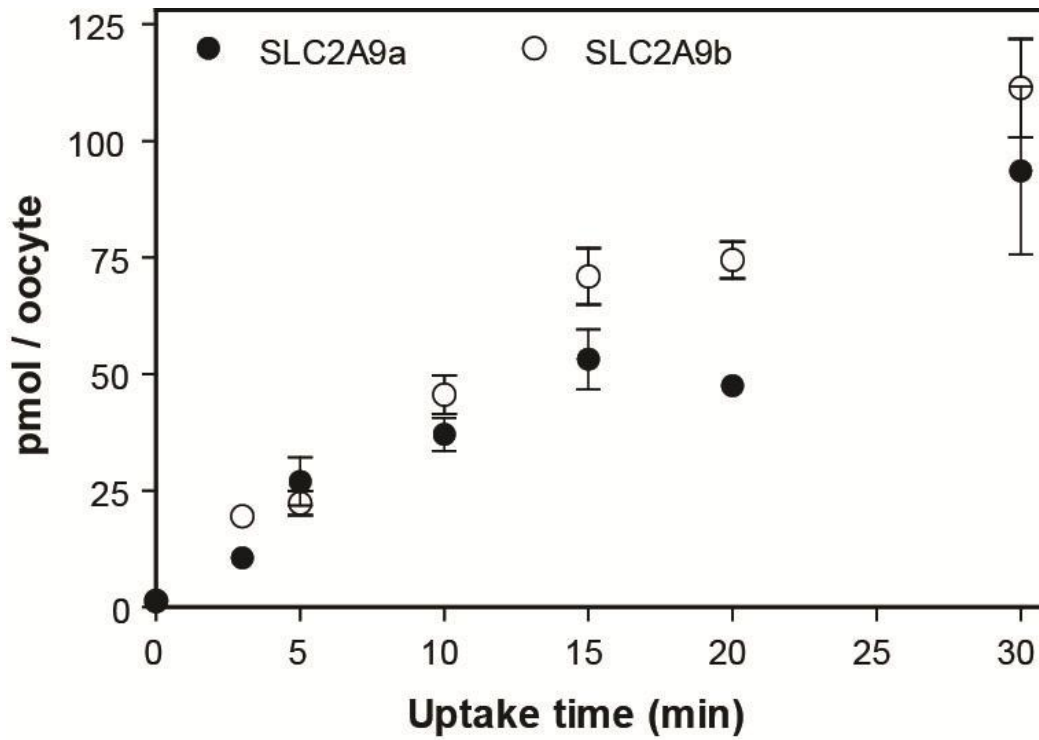


Figure 2.1. Representative time course of ¹⁴C-urate uptake into hSLC2A9a- and hSLC2A9b-expressing *Xenopus* oocytes. (● and ○) represent net ¹⁴C-urate uptake, corrected for water-injected oocytes, into hSLC2A9a- and hSLC2A9b- expressing oocytes, respectively. Vertical lines represent S.E.M.

permeant was used at a concentration of 2 μ Ci/ml. At the end of the incubation period the uptake reaction was stopped by five rapid washes with ice-cold Barth's medium. Individual oocytes were dissolved in 5% (w/v) SDS, and the radioactivity associated with each oocyte was quantified using Beckman scintillation counter (see **Table 2.5**).

Radiolabelled efflux studies - Facilitative transporters move substrates down their concentration gradient across selective cellular membranes (10). This implies that these carriers can function in either 'forward' or 'reverse' mode, bringing substrates into or out of the cell, respectively. In order to study the 'reverse' mode of facilitative hexose transporters, such as hSLC2A9, the permeant in question has to be effectively introduced into the cytoplasm of the cell.

In this study, we developed a protocol where radiolabelled urate was microinjected into carrier-expressing oocytes. As a result, we were able to minimize non-specific binding of the isotope to oocytes' surface and to conserve the radiolabelled substance. Prior to the experiments, we have ascertained that the ^{14}C recorded from the effluent corresponds to ^{14}C urate and not its labeled metabolite. As published previously (11), first, we ran a thin layer chromatography (TLC) plate eluted with a 80 : 15 : 5 *n*-propanol : ammonium hydroxide (25%) : water solution. We loaded 100 μ l of the efflux media from hSLC2A9-expressing oocytes, prepared as described below, alongside urate and allantoin standards. Vanillin spray was used as a general stain to visualize the distance travelled from the water front. ^{14}C sample from the protein-expressing oocytes and the urate standard ran at $R_f^1 \sim 0.01\text{cm}$. Second, we have tested total protein obtained from water-injected oocytes for presence of fructokinase, which can phosphorylate exogenous fructose into fructose-1-phosphate, a

¹ R_f is the retardation factor defined as defined as the ratio of the distance traveled by the center of a spot to the distance traveled by the solvent front.

precursor for *de novo* uric acid synthesis. 1:500 dilution of the human fructokinase antibody (see **Table 2.4**) did not detect a band at 75kDa mark, suggesting that the kinase is not present in the oocytes (data not shown). Finally, other groups have demonstrated that total RNA isolated from the oocytes contains no uricase RNA (12).

Details of the efflux methodology have been previously published (11), while other groups developed similar approaches independently (5). In summary, efflux assays were performed on groups of 20 oocytes² for each experimental and control condition. hSLC2A9a- or hSLC2A9b-expressing, or water-injected control oocytes, were injected with ¹⁴C-urate (see **Table 2.1**). The volume of urate injected varied between 5nl and 50nl, which is defined by the lower and upper limit of injectable volume, and depended on the experiment performed. In general, the oocytes were stored in cold Barth's Medium (4°C), in order to minimize efflux of injected substrate prior to the start of an experiment. To minimize background radioactivity, oocytes were transferred to clean glass tubes and excess cold Barth's Medium was removed and replaced with 1ml³ of room temperature (22°C) Barth's Medium, unless otherwise stated. Simultaneously, 20 µl of medium was sampled to obtain the zero time point. The incubation volume was kept constant by sequential addition of Barth's Medium volume equivalent after removal of each sample. Sampling was carried out over a period of 14 minutes, during which efflux was linear (see Chapter 4). Following the last time point, incubation medium was removed from the tubes and the oocytes were dissolved in 1 ml of 5 % (w/v) SDS. The lysate (50 µl) was sampled in triplicates to obtain the total amount of radioactivity remaining within the cells. The counts obtained from the sampled medium were corrected for background and

² Increased batch size, with respect to uptake assays, was necessary to improve the signal : noise ratio, thus increasing accuracy of measurements.

³ Large volume minimized the probability of formation of 'unstirred layers'.

dilution, and expressed as the percentage of total ^{14}C -urate remaining within oocytes at a given time. These were plotted against time and fitted with a straight line $y = ax + b$, where a represents the slope of the straight line and b represents the y -intercept (Prism GraphPad), where the magnitude of the slope (in % urate efflux.min $^{-1}$) represents the initial rate of efflux for a given concentration. Starting intracellular concentrations of injected ^{14}C -urate (specific activity 58.1 mCi/mmol) were calculated from the total amounts of radioactivity in each batch of 20 cells, assuming a water content of 0.5 μl /oocyte (24). Where different conditions were compared, intracellular ^{14}C urate concentrations were normalized against each other, for accurate comparison of hexose or drug effects on hSLC2A9 mediated efflux.

Trans-stimulation experiments – Initially, these were designed to ascertain that urate flux observed in hSLC2A9-expressing oocytes is indeed facilitated by the carrier in question and not another endogenous transporter upregulated during protein expression. We have made the assumption that hSLC2A9 obeys the simple carrier kinetics (see **Figure 1.1**) and that placing two substrates on opposite sides of the cell membrane (*trans*-) will eliminate the rate-limiting step of the transport cycle, resulting in perceived increase of radiolabelled substrate's uptake or efflux. The non-labeled (cold) substrate, or the inert substance osmotic control counterpart (L-glucose or PEG), is placed in ten fold excess to prevent rapid equilibration of the species. Proof of principle of this technique is demonstrated using the well-characterized GLUT isoform hGLUT1 expressed in oocytes injected with ^3H 3-O-Methyl-D-glucoside (3OMG), a non-metabolizable analog of D-glucose in presence of a variety of hexoses (5mM extracellular concentration; **Figure 2.2**).

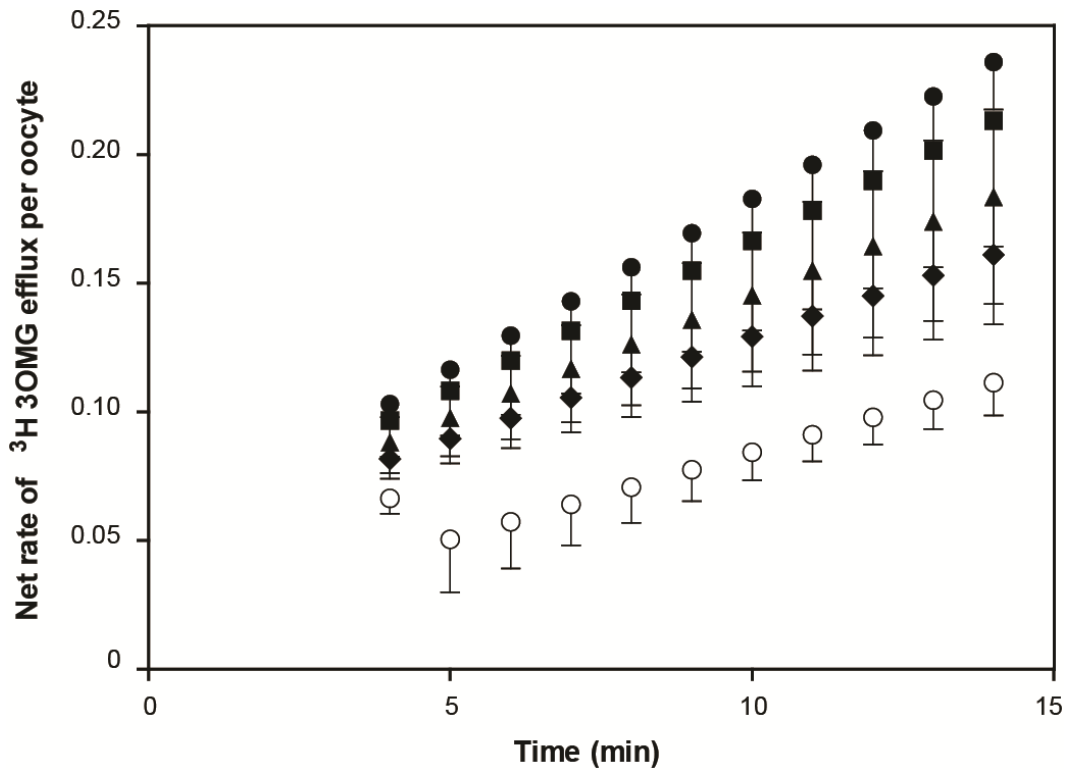


Figure 2.2. Proof-of-principle of the *trans*-stimulation technique: hGLUT1-mediated ^3H 3-O-Methyl-D-glucoside (3OMG) efflux from *Xenopus* oocytes. Oocytes were injected with hGLUT1 cRNA 4 days prior to efflux experiments, which were carried out at room temperature (22°C). Immediately prior to the experiment oocytes were injected with ~50nl of ^3H -3OMG. Ten intact oocytes were placed in a perfusion chamber (500 μl total volume) and perfused (1ml/min) with Barth's solution containing 5mM supplement. The symbols indicate net ^3H 3OMG efflux (corrected for matched water-injected oocytes) for the following perfusates: (●) – 5mM D-glucose; (■) – 5mM D-fructose; (▲) – 5mM 4,6 ethyldine- α -D-glucose⁴; (◆) – 5mM 3OMG; (○) – 5mM L-glucose, osmotic control; Samples of perfusate were taken every minute for a duration of 15 minutes; Vertical bars represent SEM. n = 3.

⁴ This substance has been shown to be an inhibitor of glucose exit. However at concentrations <1 mM it can promote endofacial CB binding (14) . It is possible that perfusion rates did not allow for sufficient intracellular accumulation of 4,6 ethyldine- α -D-glucose to allow its inhibitory effect to take place.

Two microelectrode voltage clamp studies – Given that under physiologic conditions uric acid is present in its dissociated, anionic state, urate-evoked membrane currents were measured in hSLC2A9a- or hSLC2A9b-producing oocytes at room temperature (20 °C) using a GeneClamp 500B oocyte clamp (**Table 2.6**) in the two-electrode, voltage-clamp mode. The GeneClamp 500B was interfaced to an IBM-compatible PC via a Digidata 1322A A/D converter and controlled by pCLAMP software (Table 2.6). The microelectrodes were filled with 3 M KCl and had resistances that ranged from 0.5 - 2.5 MΩ. Oocytes were penetrated with the microelectrodes and their membrane potentials were monitored for periods of 10 - 15 min. Oocytes were discarded when membrane potentials were unstable, or more positive than -30 mV. Current signals were filtered at 20Hz (four-pole Bessel filter) and sampled at a sampling interval of 20ms. Current-voltage (I-V) curves were determined from differences between steady-state currents generated in the presence and absence of permeant during 250ms voltage pulses to potentials between -100 and +60mV (10 mV increments). I-V curves were measured before and 30 s after the addition of permeant. For I-V relations, the voltage rise time of the clamp was adjusted by use of an oscilloscope such that it varied between 200 and 500μs. Currents were filtered at 2kHz (four-pole Bessel filter) and sampled at a rate of 200μs/point (corresponding to a sampling frequency of 5kHz).

Transport media – All uptake and efflux assays were performed in Barth's Medium (**Table 2.7**). All test substances used for competition and *trans*-stimulation experiments were also dissolved in Barth's medium. Electrophysiology studies were performed in Na⁺-containing transport medium (**Table 2.9**). Where Na⁺-dependence of urate transport was examined, Na⁺ in the transport medium was replaced by equimolar choline chloride, to maintain isomolarity. To examine the effect of Cl⁻ on hSLC2A9 mediated uptake, Cl⁻ ions in the transport medium were replaced with

gluconate salt, to achieve the following Cl^- test concentration range: 2mM - 100mM, either under voltage-clamp or non-clamp conditions.

Kinetic parameters – All uptake measurements were expressed as net uptake, where total radiolabelled uptake from water-injected oocytes was subtracted from that of SLC2A9-expressing oocytes. Each experiment was repeated at least three times. The results were expressed as either pmols / oocyte.20 min⁻¹ or were normalized to the appropriate controls, and expressed as a percentage of control.

In experiments determining intracellular K_m , initial rates of efflux (v_0) were converted to pmol/oocyte.min⁻¹, plotted against individual values of S , and analyzed by least squares fits to the Michaelis-Menten equation (Sigmaplot 11, Table 2.6) to estimate values (\pm S.E.) for V_{max} , the maximal rate of efflux, and K_m , the SLC2A9's internal apparent affinity for urate.

Urate kinetic parameters (K_m , apparent affinity for urate, and I_{max} , predicted current maximum) calculated from electrophysiology experiments were determined by current measurements at different urate concentrations (0 - 5 mM) and analyzed by least squares fits to the Michaelis-Menten equation (Sigmaplot 11, **Table 2.6**). The K_m for urate was determined from fits to data averaged from individual oocytes normalized to the I_{max} value obtained for that oocyte, and is presented as the mean \pm S.E. of 7 or more cells.

Drug application – All drugs used to test the involvement of kinases in hSLC2A9-mediated urate uptake were prepared according to manufacturer's specifications (see **Table 2.1**). Stocks of 3-Isobutyl-1-methylxanthine (IBMX), forskolin and Phorbol 12-myristate 13-acetate (PMA) were dissolved in 100% ethanol while those of H89 dichloride and bisindolylmaleimide IV (BIS) were dissolved in dimethyl sulphoxide (DMSO). Final concentrations of ethanol and DMSO in the experimental

solutions were 1%⁵ and 0.1%, respectively, and all experiments were matched with solvent controls to test for non-specific effects of solvent on oocytes' membrane permeability. Drug concentrations used in the experiments presented in this thesis were within the lower range of the suggested effective concentrations, and matched the recommended *in vivo* concentrations. Given that responses were observed under the conditions used, no higher concentrations were tested, to minimize non-specific effects of the drugs.

Statistical analysis – Student's t-test or one-way ANOVA were performed where appropriate, to determine whether differences between treatments were statistically significant. P-value of 0.05 or lower was used as criterion. Prism software was used (see Table 2.6).

2.2.5 Measuring cell surface expression

Immunohistochemistry - In order to determine whether the protein is targeted to the membrane of the oocyte, whole oocytes can be fixed and probed with specific antibodies for presence of protein. All solutions are prepared in phosphate-buffered saline (PBS; **Table 2.10**) and kept ice-cold throughout the procedure. In brief, GLUT-expressing oocytes, are washed with PBS and fixed in 3% perfluoroalkoxy (PFA; 15 minutes). Excess polymer is removed by washing with 50mM ammonium chloride solution. The oocytes are then permeabilized with 0.1% Triton X (4 minutes) and washed thereafter. 2% BSA blocking solution is applied for 30 minutes, followed by 1^o antibody, at an appropriate dilution (1 hr at RT

⁵ Although 1% ethanol can affect integrity of oocytes' membrane, it was the lowest possible concentration of solvent that could be used, given the maximum solubility of drug used. Appropriate measures were taken to control for possible side effects of ethanol.

or overnight at 4°C). 2^o antibody (1:200 dilution, Alexa 488) is applied for 30 minutes at RT. Stained oocytes are individually mounted in Vectashield on glass slides with secure-seal spacers (1X13mm) and stored until visualized under confocal microscope. For a list of specific reagents see **Table 2.4** and **Table 2.5** for microscope specifications. **Figure 2.3** shows representative immunohistochemistry staining for hSLC2A9-expressing oocytes.

Cell-surface biotinylation – 50 – 100 hSLC2A9-expressing or water-injected oocytes were used per condition for this cell-surface expression assay. All steps were performed at 4°C, with biotin incubation performed in the dark. The protocol has been described previously (13). In brief, oocytes were washed with cold PBS three times, prior to 30 minute incubation, with gentle agitation, in biotin buffer (**Table 2.11**). To quench the binding reaction, and to remove excess biotin, oocytes were washed three times with cold quenching buffer (**Table 2.11**). Subsequently, oocytes were lysed in lysis buffer supplemented with protease inhibitors, using a syringe fitted with 21- followed by 26- gauge needle. Resulting slurry was then centrifuged for 15 min at 2000rpm. Supernatants were collected and two more centrifugation steps were performed at 4000rpm and 6000rpm respectively. The final supernatant was ultracentrifuged at 40 000rpm for 60min. Obtained pellets were resuspended in 500µl RIPA buffer (**Table 2.11**). Half of the aliquot was frozen down to control for cytosolic protein. The remaining half (250µl) was transferred into a clean microfuge tube and 100µl of streptavidin resin (**Table 2.4**) was added. The suspension was incubated overnight, with gentle agitation. The reaction was then spun for 5 min at 8000rpm to precipitate the bound, biotinylated protein. An aliquot of the resultant supernatant (250µl) was kept to test for unlabelled, unbound protein. The pellet was washed five times with RIPA buffer, and denatured at 95°C (3 min) with 125µl NuPage sample buffer

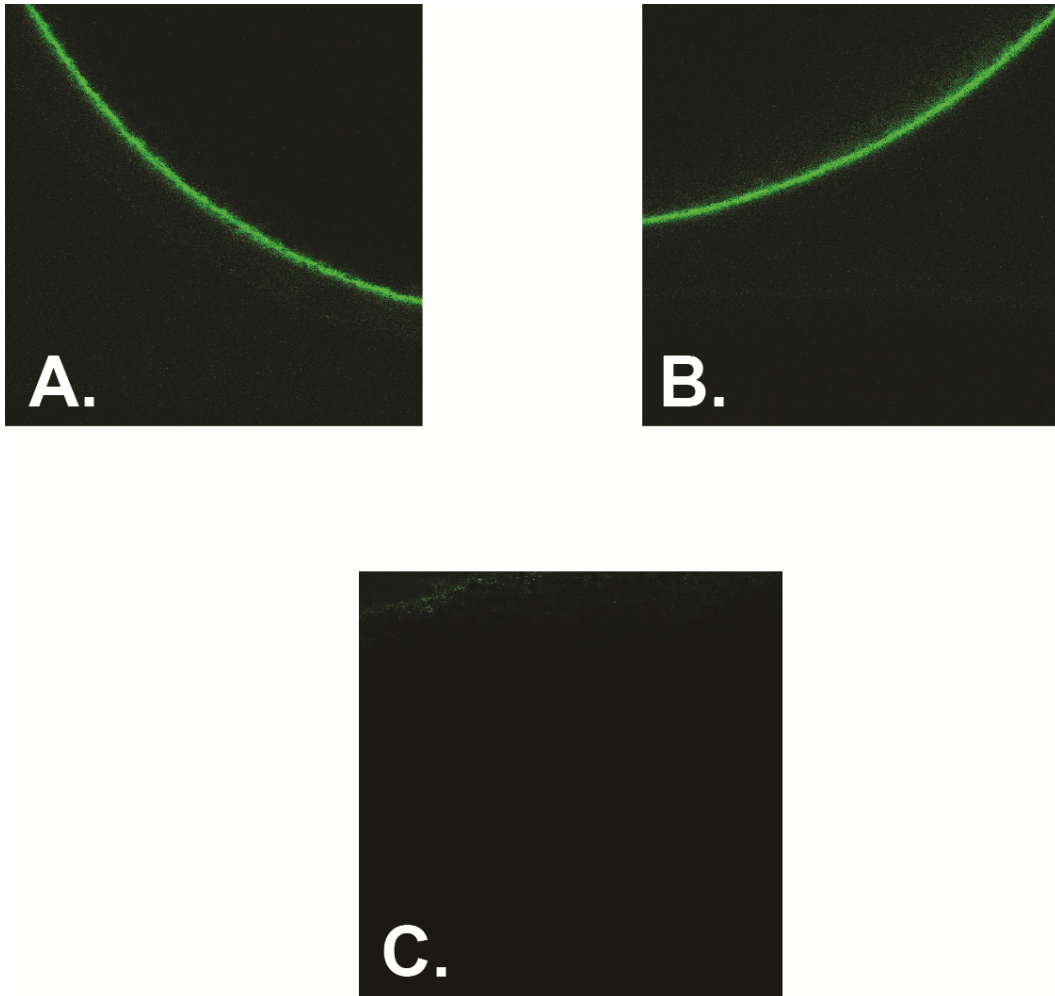


Figure 2.3. Representative staining of *Xenopus* oocytes expressing hSLC2A9. Oocytes were injected with hSLC2A9a or hSLC2A9b cRNA 4 days prior to immunostaining. C-terminus-directed hSLC2A9 antibody was used in the procedure, which recognizes both isoforms. **A.** hSLC2A9a-expressing oocyte; **B.** hSLC2A9b-expressing oocyte; **C.** Water-injected oocyte.

(**Table 2.4**). The final supernatant (8000 rpm, 5 min) was collected. Western blots were run using three protein preparations per conditions. These included: total biotinylated protein, unbound protein and bound protein.

Western Blot Analysis – Western blots were prepared as described before (4), with minor optimization for GLUT-protein preparation. For a list of chemicals, buffers and equipment used, see **Table 2.1**, **Table 2.4**, **Table 2.5**, and **Table 2.12**. 10% separating polyacrylamide gel in combination with 4% stacking gel was used, and the gel mixtures were degassed under vacuum before being poured. Protein samples were thawed out on bench top, mixed with Nu PAGE® LDS Sample Buffer, and incubated at room temperature for 15 – 20 minutes. For all biotinylation assays, samples were loaded by volume (maximum of 20µl per well). Gels were ran at 100V for an hour. Transfer onto nitrocellulose membrane was performed on ice, at 200V for 1.5 hours. The membrane was blocked for non-specific antibody binding in a series of four washes for a total of 1 hour. Primary antibody was applied overnight at 4°C at dilutions ranging from 1:500 – 1:1000. The membrane was then rinsed in a series of three 15 minute washes using the blocking solution, and secondary antibody (1:1000) was applied for 1 hour at room temperature. Chemiluminescence reactions were carried out according to manufacturer’s kit instructions and membranes were exposed to the film for a duration of time ranging from 3 – 15 minutes.

Table 2.1: Reagents

Name	Source
Animals and oocyte isolation	
Tricaine methanesulphonate	ARGENT Chemical Laboratories, USA
Collagenase	WORTHINGTON, Lakewood, NJ, USA
Antibiotics	
Ampicillin	SIGMA Aldrich, Canada
Gentamycin sulphate	SIGMA Aldrich, Canada
Penicillin	SIGMA Aldrich, Canada
Streptomycin	SIGMA Aldrich, Canada / Gibco
Radiolabelled isotopes	
³ H Adenine	Moravek, USA
³ H Cytosine	Moravek, USA
¹⁴ C D-glucose	Amersham, UK
³ H Guanine	Moravek, USA
³ H Hypoxanthine	Moravek, USA
³ H Thymine	Moravek, USA
³ H 3-O-methyl-D-glucoside	Moravek, USA
³ H Uridine	Moravek, USA
¹⁴ C uric acid	Moravek, USA
³ H Xanthine	Moravek, USA
Detergents and gels	
Agarose	Invitrogen
30% Acrylamide/Bis	Bio-Rad Laboratories, Inc.
Sodium-dodecyl sulphate (SDS)	Bio-Rad Laboratories, Inc.
Phenylmethylsulfonyl fluoride (PMFS)	SIGMA Aldrich, Canada
Deoxycholic acid (DOC)	SIGMA Aldrich, Canada

Triton-X-100	SIGMA Aldrich, Canada
TEMED	SIGMA Aldrich, Canada
Ammonium Persulfate (10%)	SIGMA Aldrich, Canada
1.5M Tris-HCl, pH 8.8	Bio-Rad Laboratories, Inc.
0.5M Tris-HCl, pH 6.8	Bio-Rad Laboratories, Inc.
Miscellaneous	
Triethanolamine	SIGMA Aldrich, Canada
Express™ PLUS bottle-top vacuum filters (0.22µm)	Millipore
MF™ membrane filters (0.025µm) VSWP	Millipore
Gene Pulser® Cuvette	Bio-Rad Laboratories, Inc.
ImMedia™ Amp Agar	Invitrogen
DH5α electrocompetent cells	Invitrogen
1Kb Plus DNA Ladder	Invitrogen
Kinase modulators	
3-Isobutyl-1-methylxanthine (IBMX)	SIGMA Aldrich, Canada
Forskolin	SIGMA Aldrich, Canada
H89 dichloride	Cell Signaling TECHNOLOGY
Phorbol 12-myristate 13-acetate (PMA)	SIGMA Aldrich, Canada
Bisindolylmaleimide IV	SIGMA Aldrich, Canada

Table 2.2: DNA modifying enzymes and DNA kits

Name	Source
Enzymes	
Calf intestinal alkaline phosphatase (CIP)	Invitrogen
Platinum <i>Pfx</i> DNA polymerase	Invitrogen
Restriction endonucleases	New England BioLabs
T4 DNA ligase	Invitrogen
mMESSAGE mMACHINE™	Ambion
QuickChange® Site-Directed Mutagenesis Kit	Stratagene
DNA kits	
QIAprep® Spin Miniprep Kit	QIAGEN
QIAEX® II Gel Extraction Kit	QIAGEN

Table 2.3: Constructs and primers

cDNAs and vectors		
Name	Source	Accession number
human GLUT9a	Dr. Kelle Moley	BC110414
human GLUT9b	Dr. Kelle Moley	BC018897
pGEM-HE	Dr. James Young	N/A
Primers		
Name	Sequence	
hGLUT9a S9A Fwd	5'gcaaggaaacaaaataggaatgccaaggaactgggcctagttc3'	
hGLUT9a S9A Rev	5' gaactaggcccagttccttggcattcctattttgttccttgc 3'	
hGLUT9a S22A Fwd	5' ctacagatgacaccgcacacgccgggcctcca 3'	
hGLUT9a S22A Rev	5' tggaggcccggcgtgtgcggtgtcatctgtgag 3'	

Table 2.4: Antibodies and protein work

Antibodies		
Name	Source	Catalogue number
hGLUT9-C terminus	Dr. Kelle Moley	N/A
hGLUT9-N terminus	Dr. Kelle Moley	N/A
ECL Anti-Rabbit IgG Antibody	GE Healthcare, UK Ltd.	NA 934V
Anti-Ketohexokinase	SIGMA Prestige Antibodies	HPA 007040
Reagents		
Name		Source
EZ-Link Sulfo-NHS-LC Biotin		Thermo SCIENTIFIC (Fisher, Canada)
Nu PAGE® LDS Sample Buffer		Invitrogen
Protease inhibitor cocktail		SIGMA Aldrich, Canada
Streptavidin agarose resin		Thermo SCIENTIFIC (Fisher, Canada)
Amersham ECL™ Advance Western Blotting Detection Kit		GE Healthcare, Canada
Kodak BioMax Light Chemiluminescence Film		SIGMA Aldrich, Canada
Bio-Rad Precision Plus™ Protein dual color standards ladder		Bio-Rad Laboratories, Inc.

Table 2.5: Equipment

Function	Model name and number
DH5 α electroporator	Electroporator 2510, eppendorf
RNA injection system	PLI-100 Pico injector (HARVARD Aparatus, USA)
β Scintillation counter	LS 6500 Beckman, USA
Two microelectrode voltage clamp (TMVC)	GeneClamp 500B (Molecular Devices Corp.) Digidata 1322A A/D converter
Spectrophotometer	Ultraspec 2000, Pharmacia Biotech (Fisher Scientific)
Thermocycler	MyCycler thermal cycler (Bio-Rad)
Confocal microscope	ZEISS LSM 510
PowerPac™ Basic power supply	Bio-Rad Laboratories, Inc.
MiniTrans-Blot® Electrophoretic Transfer Cell Apparatus	Bio-Rad Laboratories, Inc.

Table 2.6: Software

Purpose	Name
TMVC control	pCLAMP (Molecular Devices Corp.)
Data entry and calculation	Excel (Microsoft Office)
Data plotting and statistical analysis	GraphPad Prism v.5 (Graphpad Software Inc., CA, USA) Sigmaplot 11 (Systat Software Inc., IL, USA)
Confocal image visualization and quantification	ImageJ (NIH resources)

Table 2.7: Barth's Medium composition

Salts	
Component	Concentration (mM)
NaCl	90
KCl	3.0
MgSO ₄	0.82
HEPES	5.0
CaCl ₂	0.40
Ca(NO ₃) ₂	0.33
Sodium pyruvate	2.50
Antibiotics	
Component	Concentration (mg/ml)
penicillin	0.1
streptomycin	0.1
kanamycin	0.1
pH 7.6	

Table 2.8: Phosphate Buffer composition

Component	Concentration (mM)
K ₂ PO ₄	100
pH 6.5	

Table 2.9: Sodium transport buffer composition

Component	Concentration (mM)
NaCl	100
KCl	2.0
CaCl ₂	1.0
MgCl ₂	1.0
Hepes	10
pH 7.5	

Table 2.10: Phosphate-buffered saline (PBS) composition

Component	Concentration (mM)
NaCl	135
KCl	1.3
Na ₂ HPO ₄	3.2
KH ₂ PO ₄	0.5
pH 7.4	

Table 2.11: Cell-surface biotinylation buffers' composition

Component	Concentration (mM)
Biotinylation buffer	
NaCl	150
CaCl ₂	2
Triethanolamine	10
EZ-Link Sulfo-NHS-SS-Biotin	2
pH 9.5	
Quenching buffer	
PBS	Table 2.10
Glycine	192
Tris-HCl	25
pH 7.5	
Homogenizing buffer	
Sucrose	250
Tris-HCl	5
EDTA	0.5
Protease inhibitor cocktail	0.1% (v/v)
pH 7.5	
RIPA buffer	
NaCl	150
Triton-X-100	1% (v/v)
Deoxycholic acid (DOC)	0.5% (w/v)
Sodium dodecyl sulphate (SDS)	0.1% (w/v)
Phenylmethylsulfonyl fluoride (PMSF)	1.0
pH 8.5	

Table 2.12: Western Blotting buffers' composition

Component	Concentration (mM)
1X Running Buffer	
Tris Base	24.8
Glycine	192
SDS	3.5
pH = 8.3	
1 X Transfer Buffer	
Tris Base	50
Glycine	384
Methanol	20% (v/w)
pH = 8.1 – 8.4, do not adjust pH with acid/base	
Blocking solution	
Dried Milk Powder	15g
Tween 20	0.05% (v/w)
PBS	500ml total volume

2.3 Bibliography

1. Liman, E. R., Tytgat, J., and Hess, P. (1992) Subunit stoichiometry of a mammalian K⁺ channel determined by construction of multimeric cDNAs., *Neuron* 9, 861-71.
2. Mueckler, M., Caruso, C., Baldwin, S. A., Panico, M., Blench, I., Morris, H. R., Allard, W. J., Lienhard, G. E., and Lodish, H. F. (1985) Sequence and Structure of a Human Glucose Transporter, *Science* 229, 941-945.
3. Hediger, M. A. (1994) Structure, function and evolution of solute transporters in prokaryotes and eukaryotes., *The Journal of experimental biology* 196, 15-49.
4. Yao SYM, Cass, C.E., and Young, J. . (2000) The *Xenopus* oocyte expression system for the cDNA cloning and characterization of plasma membrane transport proteins, in *Membrane Transport: A Practical Approach* Baldwin SA., pp 47 - 78. Oxford and New York: Oxford University Press.
5. Chernova, M. N., Jiang, L., Crest, M., Hand, M., Vandorpe, D. H., Strange, K., and Alper, S. L. (1997) Electrogenic sulfate/chloride exchange in *Xenopus* oocytes mediated by murine AE1 E699Q., *The Journal of general physiology* 109, 345-60.
6. Augustin, R. (2010) The protein family of glucose transport facilitators: It's not only about glucose after all., *IUBMB life* 62, 315-33.
7. Sobczak, K., Bangel-Ruland, N., Leier, G., and Weber, W.-M. (2010) Endogenous transport systems in the *Xenopus laevis* oocyte plasma membrane., *Methods (San Diego, Calif.)*. Elsevier Inc. 51, 183-9.
8. Orsini, F., Santacroce, M., Arosio, P., and Sacchi, V. F. (2010) Observing *Xenopus laevis* oocyte plasma membrane by Atomic Force Microscopy., *Methods (San Diego, Calif.)* 51, 106-13.

9. Neumann, A. K., Itano, M. S., and Jacobson, K. (2010) Understanding lipid rafts and other related membrane domains., *F1000 biology reports* 2, 31.
10. Neame, K. ., and Richards, T. . (1972) Elementary kinetics of membrane carrier transport 1st ed. Blackwell Scientific Publications, Oxford, England.
11. Caulfield, M. J., Munroe, P. B., O'Neill, D., Witkowska, K., Charchar, F. J., Doblado, M., Evans, S., Eyheramendy, S., Onipinla, A., Howard, P., Shaw-Hawkins, S., Dobson, R. J., Wallace, C., Newhouse, S. J., Brown, M., Connell, J. M., Dominiczak, A., Farrall, M., Lathrop, G. M., Samani, N. J., Kumari, M., Marmot, M., Brunner, E., Chambers, J., Elliott, P., Kooner, J., Laan, M., Org, E., Veldre, G., Viigimaa, M., Cappuccio, F. P., Ji, C., Iacone, R., Strazzullo, P., Moley, K. H., and Cheeseman, C. (2008) SLC2A9 is a high-capacity urate transporter in humans., *PLoS medicine* 5, e197.
12. Woodward, O. M., Köttgen, A., Coresh, J., Boerwinkle, E., Guggino, W. B., and Köttgen, M. (2009) Identification of a urate transporter, ABCG2, with a common functional polymorphism causing gout., *Proceedings of the National Academy of Sciences of the United States of America* 106, 10338-42.
13. Avella, M., Borgese, F., and Ehrenfeld, J. (2011) Characterization of the L683P mutation of SLC26A9 in *Xenopus* oocytes., *Biochimica et biophysica acta*. Elsevier B.V. 1810, 277-83.
14. Barnett, J., Holman, G. D., and Munday, K. A. (1973) An explanation of the asymmetric binding of sugars to the human erythrocyte sugar-transport systems, *The Biochemical Journal* 135, 539-541.

Functional characterization of human SLC2A9-mediated urate transport *

* A version of this chapter has been published.

Mark J. Caulfield, Patricia B. Munroe, Deb O'Neill, Kate Witkowska, Fadi J. Charchar, Manuel Doblado, Sarah Evans, Susana Eyheramendy, Abiodun Onipinla, Philip Howard, Sue Shaw-Hawkins, Richard J. Dobson, Chris Wallace, Stephen J. Newhouse, Morris Brown, John M. Connell, Anna Dominiczak, Martin Farrall, G. Mark Lathrop, Nilesh J. Samani, Meena Kumari, Michael Marmot, Eric Brunner, John Chambers, Paul Elliott, Jaspal Kooner, Maris Laan, Elin Org, Gudrun Veldre, Margus Viigimaa, Francesco P. Cappuccio, Chen Ji, Roberto Iacone, Pasquale Strazzullo, Kelle H. Moley, Chris Cheeseman. (2008) SLC2A9 is a high-capacity urate transporter in humans. *PLoS Medicine*. **5** (10): e197.

3.1 Acknowledgements and contributions

Contributors: M.J. Caulfield, P.B. Munroe, F.J. Charchar, K.H. Moley, and C. Cheeseman contributed to study design, execution, planning, analysis, and writing of the manuscript, and were the principal investigators in the study. I contributed by designing the protocol for testing carrier-mediated urate efflux in the frog oocyte system, and performing the efflux experiments. Debiie O'Neil, the technician in my lab, executed the remaining functional characterization in the oocyte system. M. Doblado, S. Evans, P. Howard, S. Newhouse, A. Onipinla, S. Shaw-Hawkins, R. Dobson, C. Wallace, M. Brown, J. Connell, A. Dominiczak, G.M. Lathrop, N.J. Samani, M. Marmot, E. Brunner, J. Chambers, P. Elliott, J. Kooner, M. Laan, E. Org, G. Veldre, and M. Viigimaa contributed to design and execution of the study. S. Eyheramendy, M. Farrall, M. Kumari, F. Cappuccio, C. Ji, R. Iacone, and P. Strazzullo contributed to design, execution, and analysis.

Funding: The BRIGHT study and current work are supported by the Medical Research Council (MRC) of Great Britain (grant no.G9521010D) and the British Heart Foundation (grant no. PG02/128). K.H. Moley is supported by an American Diabetes Association Research Grant. S. Evans is funded by National Institutes of Health (NIH) grant no. NIH-NIDDK T32-DK07120. C. Cheeseman is funded by the Canadian Breast Cancer Foundation. The Wellcome Trust Case Control Consortium was funded by the Wellcome Trust (grant number 076113/B/04/Z). The Barts and The London Charity funded the Barts and The London Genome Centre. A. Dominiczak and N.J. Samani are British Heart Foundation

Chair holders. C. Wallace is funded by the British Heart Foundation (grant no. FS/05/061/19501). The LOLIPOP Study was funded by the British Heart Foundation. The HYPEST sample collection was financed by Wellcome Trust International Senior Research Fellowship to M. Laan (grant no. 070191/Z/03/Z) in Biomedical Science in Central Europe and by Estonian Ministry of Education and Science core grant no. 0182721s06. M. Marmot is supported by an MRC Research Professor-ship. The Whitehall II study has been supported by grants from the UK: MRC; Economic and Social Research Council; British Heart Foundation; Health and Safety Executive; Department of Health; National Heart Lung and Blood Institute (grant no. HL36310); and from the US: NIH, National Institute on Aging (NIA; grant no. AG13196); NIH, Agency for Health Care Policy Research (grant no. HS06516); and the John D. and Catherine T. MacArthur Foundation Research Networks on Successful Midlife Development and Socio- economic Status and Health. Samples from the English Longitudinal Study of Ageing (ELSA) DNA Repository (EDNAR), received support under a grant (AG1764406S1) awarded by the NIA. ELSA was developed by a team of researchers based at the National Centre for Social Research, University College London and the Institute of Fiscal Studies.

3.2 Introduction

Elevated serum urate levels are associated with important common disorders, such as gout, metabolic syndrome, diabetes, hypertension, and cardiovascular morbidity and mortality (1–4). Uric acid is principally derived from the breakdown of dietary and cellular purines. Humans and Great Apes are exposed to higher urate levels than other mammalian species due to inactivation of hepatic uricase (5). In man the kidney has a pivotal role in urate handling with secretory mechanisms balanced against efficient reabsorption resulting in only 10% of the filtered load actually being excreted in the urine (5). The established urate transporter systems in the proximal nephron includes; the urate anion transporter (URAT1), which is a target of uricosuric drugs, multiple organic anion transporters (OATs 1-4), the urate transporter (UAT), and a voltage dependent organic anion transporter (OATv1) (5).

It is possible that genetic variation in either enzymatic breakdown of purines or renal transporters of uric acid might elevate serum levels and account for epidemiological associations of this trait with inflammatory crystal arthropathy, blood pressure and common cardiovascular phenotypes (1–5). Recently, two separate genomewide association scans identified and replicated association of serum urate level with common variants within the glucose transporter *hSLC2A9* (GLUT9) gene region on chromosome 4 (6, 7). Interestingly, this member of the facilitative glucose transporter family has two splice variants most strongly expressed in the apical and basolateral membranes of the proximal tubular epithelial cells of the kidney. Although *hSLC2A9* is not as efficient a glucose transporter as GLUT 1 and 4 there were no data suggesting it is a functional urate

transporter in the proximal nephron (8, 9). Here we set out to test whether hSLC2A9 a and b splice variants act as a urate transporter, and used the Olivetti Heart Study and three hypertension case : control resources to investigate if there is a relationship of *SLC2A9* gene variants with urate, blood pressure and hypertension.

3.3 Results

3.3.1 Human SLC2A9 is a high capacity urate transporter

To test whether *SLC2A9* splice variants act as urate transporters we separately microinjected synthetic human SLC2A9a and SLC2A9b messenger RNA transcripts into *Xenopus laevis* oocytes and measured uptake or efflux of radiolabelled urate. We found that human hSLC2A9a mediated very rapid urate fluxes, which necessitated incubation for only 20 minutes in subsequent kinetic and inhibition experiments (**Figure 3.1** and **Figure 2.1**). In contrast, uptake of urate into non-injected eggs was very slow indicating negligible endogenous transport activity for this substrate. Transport was then measured over a range of urate concentrations which bracketed the normal human physiological plasma concentrations (200 – 500 μM). Both human SLC2A9a and SLC2A9b mediated urate fluxes showed saturation and were identical so data for the two splice variants were combined for kinetic analysis. **Figure 3.2** shows the averaged data from six such experiments and non-linear regression analysis was used to fit a Michaelis-Menten function with a K_m of 981 μM and a V_{max} of 304 pmoles/ oocyte/ 20 min.

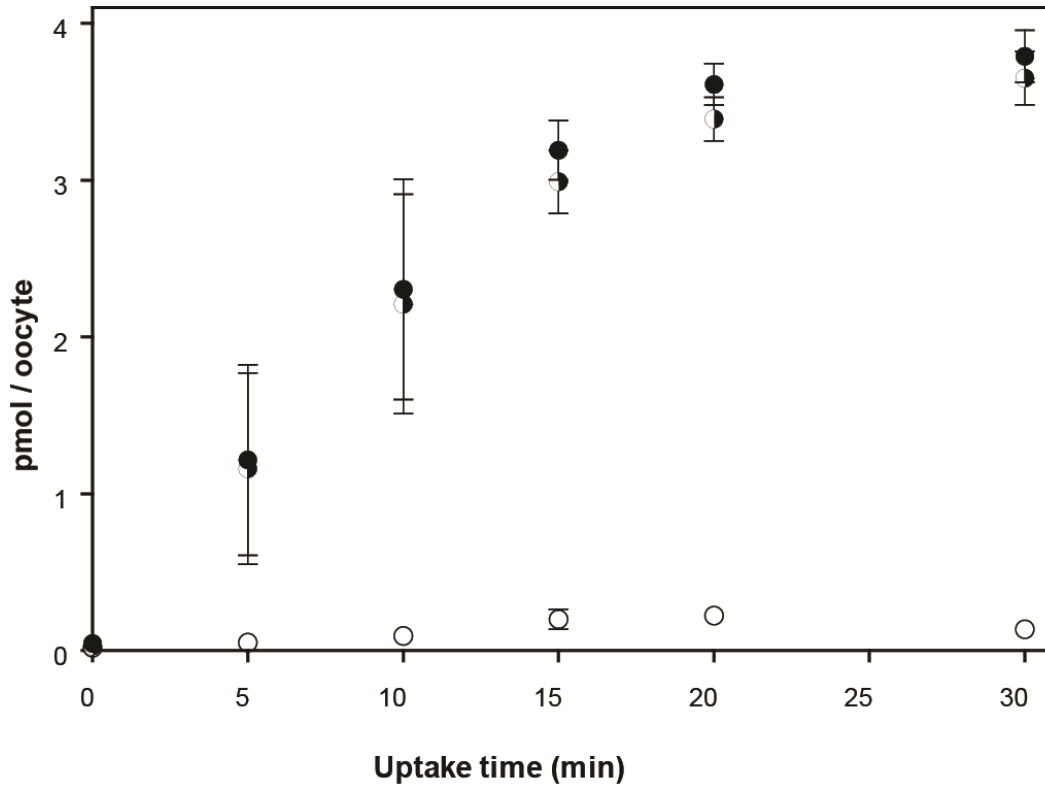


Figure 3.1. Representative time course for hSLC2A9a-mediated ¹⁴C-urate uptake into *Xenopus* oocytes. Oocytes were injected with hSLC2A9a cRNA 4 days prior to uptake experiments, which were carried out at room temperature (22°C). (●) – total 10μM ¹⁴C urate uptake into hSLC2A9a-expressing oocytes, averaged for 10 oocytes; (◐) – net 10μM ¹⁴C urate uptake into hSLC2A9a-expressing oocytes corrected for water-injected oocytes and averaged for 10 oocytes; (○) - total 10μM ¹⁴C urate uptake into water-injected control oocytes, averaged for 10 oocytes; Vertical bars represent ± S.E.M. n = 2.

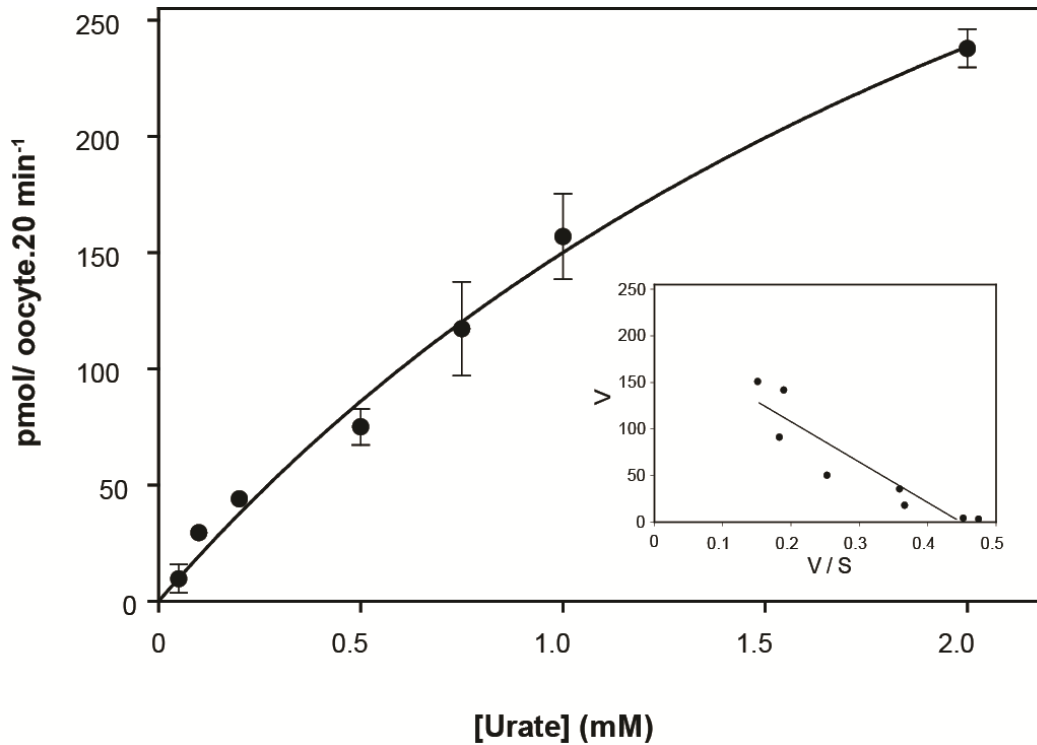


Figure 3.2. Michaelis-Menten kinetics for hSLC2A9a-mediated ¹⁴C-urate uptake into *Xenopus* oocytes. Oocytes were injected with hSLC2A9a cRNA 4 days prior to uptake experiments, which were carried out at room temperature (22°C). (●) – mean net ¹⁴C urate uptake into hSLC2A9a-expressing oocytes, averaged for 10 oocytes per concentration. The curve was fitted by non-linear regression analysis. The $K_m = 981 \mu\text{M}$ and $V_{max} = 304 \text{ pmoles / oocyte.20 min}^{-1}$. Insert shows an Eadie plot of the same data. Vertical bars represent \pm S.E.M. $n = 3$.

The insert shows the Eadie plot for the same data. It is important to mention that the two forms of analysis produce slightly different estimates of the K_m value. A variety of reasons may be responsible for this disparity. First, due to low solubility of urate, we are unable to obtain saturating urate concentrations, influencing the fit of the Michaelis-Menten curve. Secondly, the loose fit of the data points with the curve suggests that there may be more than one substrate binding site within the carrier, making this analysis inadequate for the transport process in question. Please refer to Appendix 2 for further analysis.

To test the specificity of urate transport for isoform 9 of the SLC2A protein family, we tested urate flux in other GLUT members. We were unable to detect any urate flux (100 μM) mediated by either human GLUT1 or GLUT2, both class I facilitative glucose transporters (**Figure 3.3**).

3.3.2 Transport of urate by hSLC2A9a shows a unique sensitivity to uricosurics

A number of compounds known to promote urate loss in the urine *via* their interaction with other renal urate transporters, such as URAT1 (10), were tested to determine if they reduced hSLC2A9-mediated urate transport. Probenecid, at a concentration of 1 mM, had minimal effect on urate uptake (**Figure 3.4**), whereas benzbromarone showed a dose responsive inhibition with 10 μM reducing urate uptake by 17% and 100 μM by 80% (**Figure 3.5**). In contrast, furosemide had no effect at 100 μM , and neither did any of the short chain fatty acids like lactate, pyruvate, butyrate or acetate, at a concentration of 1 mM (**Figure 3.4**). Finally, the class I hexose transporter inhibitor phloretin had only a minimal effect on

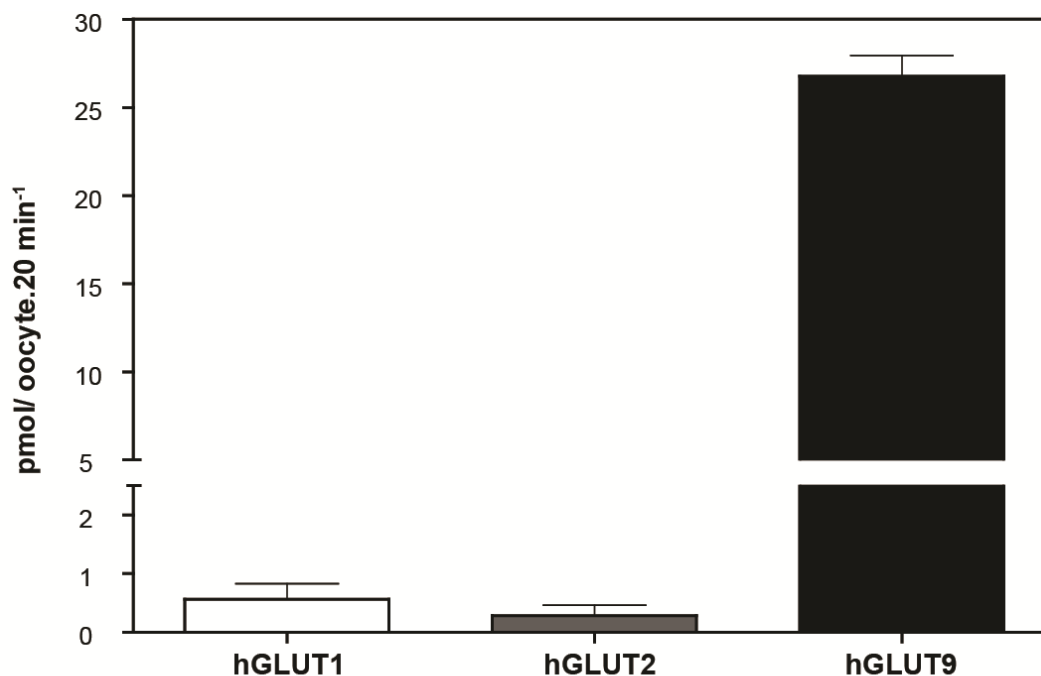


Figure 3.3. Representative ¹⁴C-urate uptake into hGLUT-expressing *Xenopus* oocytes. Oocytes were injected with corresponding cRNA 4 days prior to uptake experiments, which were carried out at room temperature (22°C). (□) – net 10μM ¹⁴C urate uptake into hGLUT1-expressing oocytes, averaged for 10 oocytes; (▒) – net 10μM ¹⁴C urate uptake into hGLUT2-expressing oocytes, averaged for 10 oocytes; (■) – net 10μM ¹⁴C urate uptake into hGLUT9-expressing oocytes, averaged for 10 oocytes; Vertical bars represent ± S.E.M. n = 3.

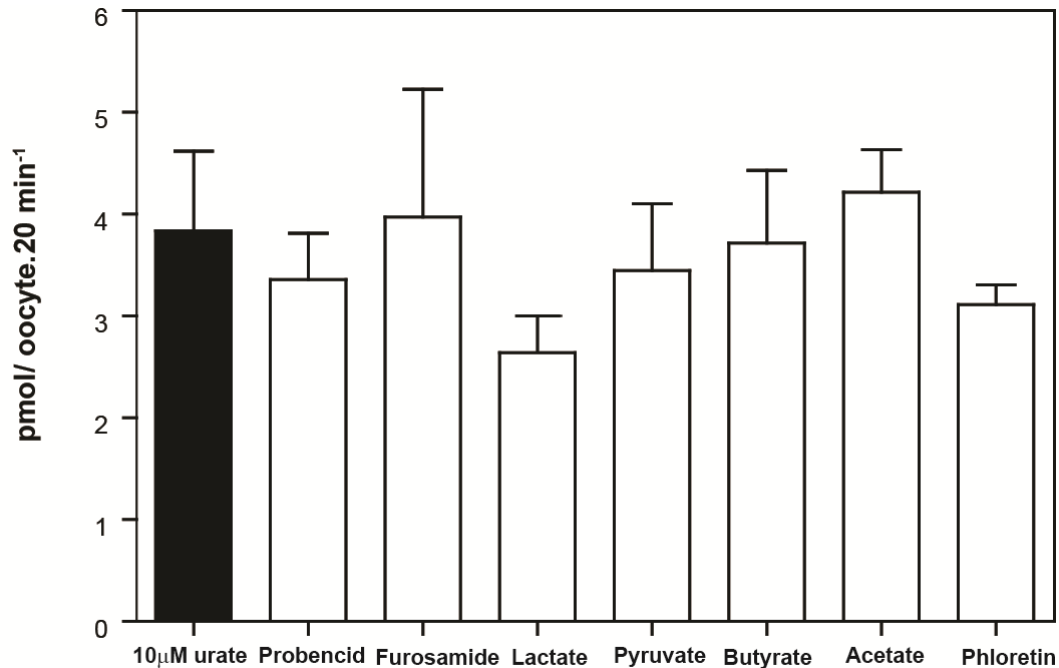


Figure 3.4. Drug panel testing their effects on hSLC2A9a-mediated ¹⁴C-urate uptake into *Xenopus* oocytes. Oocytes were injected with hSLC2A9a cRNA 4 days prior to uptake experiments, which were carried out at room temperature (22°C). (■) – control condition: net 10µM ¹⁴C urate uptake into hSLC2A9a-expressing oocytes, corrected for water-injected oocytes, no reagent in the extracellular medium. Averaged for 10 oocytes; (□) – experimental conditions showing net 10µM ¹⁴C-urate uptake into hSLC2A9a-expressing oocytes, corrected for water-injected oocytes. Averaged for 10 oocytes. Following reagents were placed in extracellular medium (left to right): 1mM probenecid, 100 µM furosamide, 1mM lactate, 1mM pyruvate, 1mM butyrate, 1mM acetate, 1mM phloretin. Vertical bars represent ± S.E.M. n = 3.

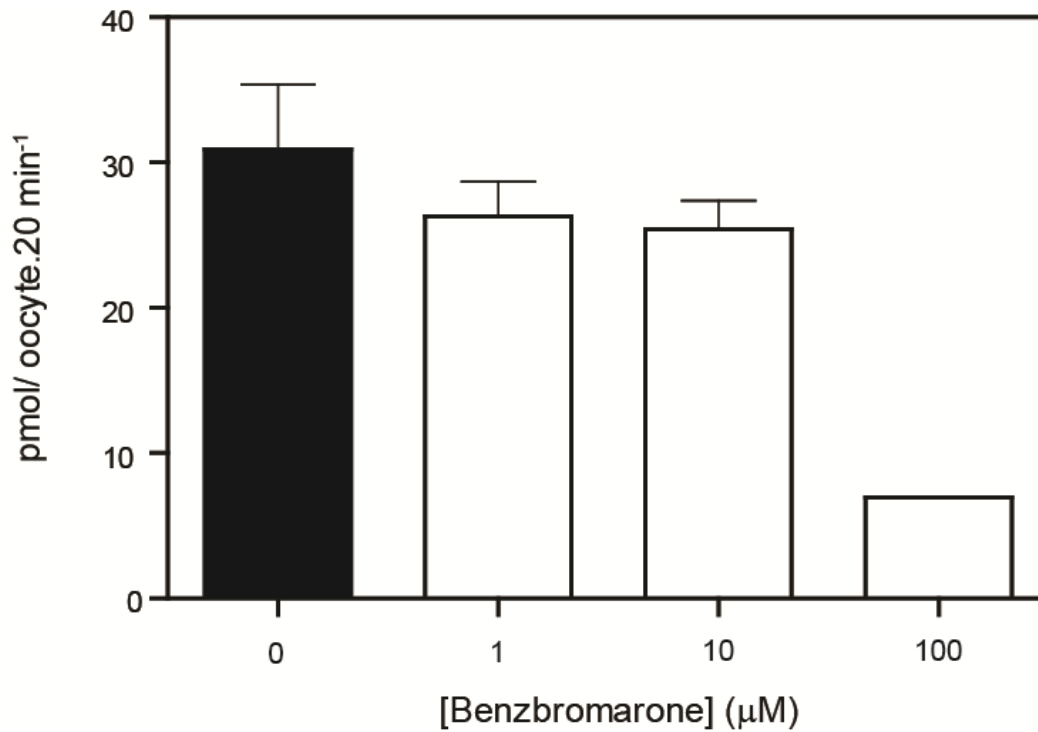


Figure 3.5. Effect of the uricosuric benzbromarone on hSLC2A9a-mediated ¹⁴C-urate uptake into *Xenopus* oocytes. Oocytes were injected with hSLC2A9a cRNA 4 days prior to uptake experiments, which were carried out at room temperature (22°C). (■) – mean net 10µM ¹⁴C-urate uptake into hSLC2A9a-expressing oocytes, averaged for 10 oocytes; (□) – mean net 10µM ¹⁴C-urate uptake into hSLC2A9a-expressing oocytes in presence of corresponding extracellular benzbromarone concentrations, averaged for 10 oocytes. Vertical bars represent ± S.E.M.

urate transport (< 10% inhibition) when applied at a concentration of 1 mM (**Figure 3.4**).

3.3.3 hSLC2A9a mediates exchange of urate for D-glucose or D-fructose

As hSLC2A9a and hSLC2A9b have been characterized previously as high affinity, low capacity glucose and fructose transporters (8), we tested the ability of these two hexoses to inhibit urate fluxes and, conversely, for urate to inhibit hexose uptake. Surprisingly, concentrations of D-glucose up to 1 mM had no effect on the transport of 5 μ M urate while only a slight inhibition (approximately 15%) of urate uptake was observed by D-fructose (data not shown; See Chapter 5 for further discussion). Moreover, urate concentrations of up to 2mM had no effect on 50 μ M D-glucose and 50 μ M D-fructose uptake (**Figure 3.6**). Note that the rates of urate transport were significantly greater than those for D-glucose. Urate fluxes were measured at 5 μ M or 10 μ M substrate concentration for 20 minutes, whereas D-glucose rates were determined using 50 μ M substrate for 30 minutes. Thus, converting flux rates to the same time period and equivalent concentrations suggest that urate is transported by hSLC2A9a at rates 45 – 60 fold faster. The failure to find significant competition between the hexoses and urate suggests that urate binds to a site on hSLC2A9a which is different from the binding site for the hexoses. As such, the widely accepted simple carrier model is not adequate to describe the transport processes mediated by hSLC2A9.

However, it could be argued that the injection of hSLC2A9a mRNA was inducing expression of an endogenous protein which could

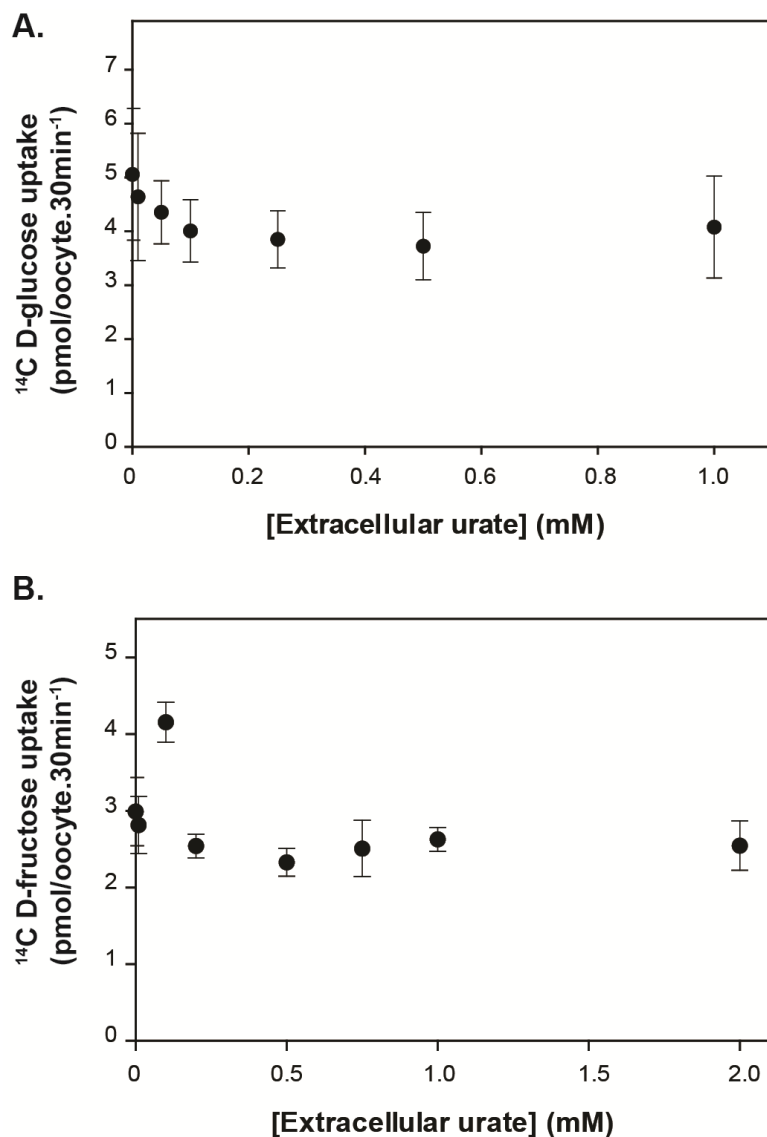


Figure 3.6. Interaction between hSLC2A9a and its substrates I: Effect of extracellular urate on ¹⁴C-hexose uptake into *Xenopus* oocytes.

Oocytes were injected with hSLC2A9a cRNA 4 days prior to uptake experiments, which were carried out at room temperature (22°C). **A.** (●) – mean net 50μM ¹⁴C-D-glucose uptake into hSLC2A9a-expressing oocytes in presence of increasing extracellular concentrations of urate; **B.** (●) – mean net 50μM ¹⁴C-D-fructose uptake into hSLC2A9a-expressing oocytes in presence of increasing extracellular concentrations of urate. All means averaged for ten oocytes. Vertical bars represent ± S.E.M.

separately mediate urate uptake. Therefore, we attempted to determine whether hSLC2A9a could exchange hexoses for urate, providing further support for a single pathway mechanism. Since D-glucose and D-fructose are both phosphorylated upon entry into the oocyte, and no urate metabolism has been detected in the oocytes (see Chapter 2 for discussion), only urate efflux could be used to give a meaningful estimate of exchange rates. First, the exchange of urate for D-glucose was confirmed by preloading the oocytes with 2 mM cold urate for one hour and then, after washing to remove extracellular urate, measuring ^{14}C -D-glucose uptake. The influx of hot glucose was increased two-fold by intracellular urate in hSLC2A9a-expressing eggs (**Figure 3.7B**). These data indicate that hSLC2A9a can exchange extracellular glucose for intracellular urate. Conversely, we performed the reverse experiment where oocytes were injected with radiolabelled urate and the ^{14}C -urate efflux determined in presence of 5 mM extracellular D-glucose, D-fructose, L-glucose or 2 mM urate. Urate efflux could be described by a single exponential curve over a period of up to 20 minutes and the presence of extracellular D-glucose greatly accelerated urate movement, while D-fructose did so to a lesser degree (7 fold vs 3 fold respectively; **Figure 3.8**). These observations represent mediated transport since leakage of radiolabeled L-glucose or urate was minimal from water injected oocytes. Moreover, extracellular cold urate also accelerated efflux of hot urate, pointing to the presence of a facilitative carrier (**Figure 3.9**).

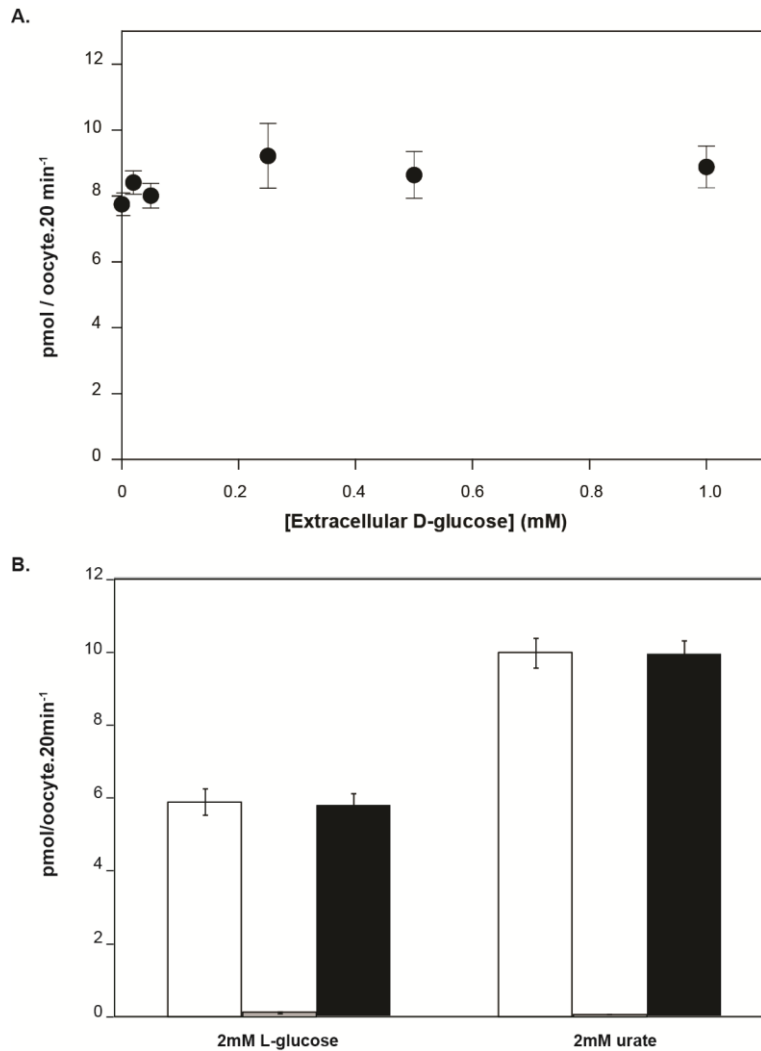


Figure 3.7. Interaction between hSLC2A9a and its substrates II: Effect of extracellular D-glucose on urate transport in *Xenopus* oocytes.

Oocytes were injected with hSLC2A9a cRNA 4 days prior to uptake experiments, which were carried out at room temperature (22°C). **A.** (●) – mean net 5µM ^{14}C urate uptake into hSLC2A9a-expressing oocytes in presence of increasing extracellular concentrations of D-glucose; **B.** hSLC2A9a-expressing oocytes were pre-incubated with 2mM L-glucose or urate for 1 hour at 22°C and then 10µM ^{14}C D-glucose uptake was measured over 30 minutes. (□) – total ^{14}C D-glucose uptake into hSLC2A9a-expressing oocytes; (▤) – total ^{14}C D-glucose uptake into water-injected oocytes; (■) – net ^{14}C D-glucose uptake into hSLC2A9a-expressing oocytes. All means averaged for ten oocytes. Vertical bars represent \pm S.E.M.

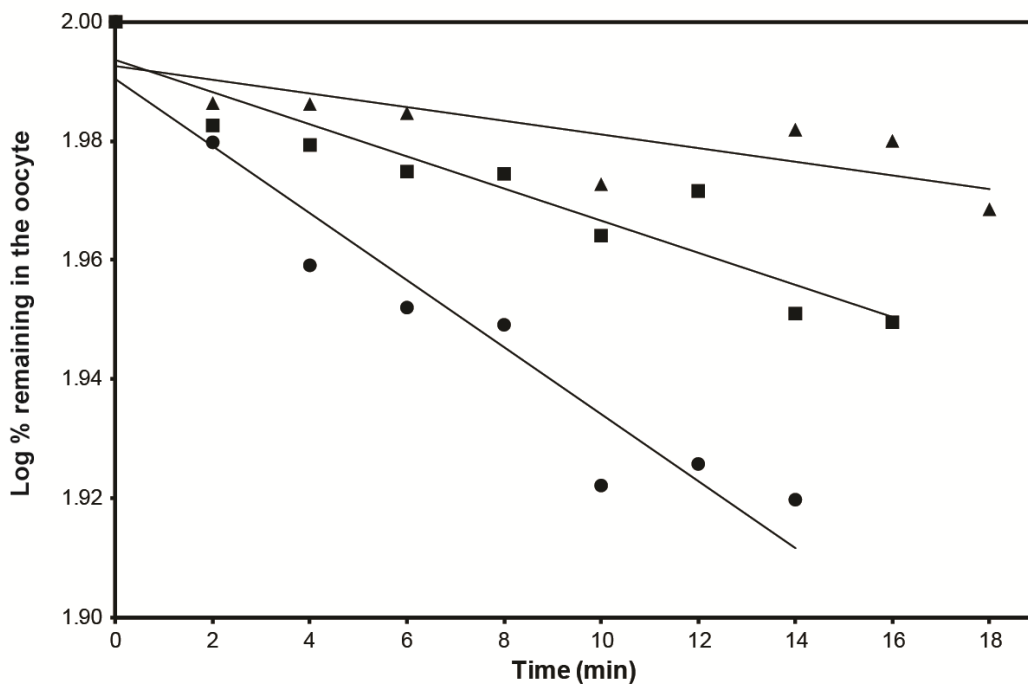


Figure 3.8. Representative experiment: hSLC2A9a exchanges intracellular ^{14}C -urate for extracellular hexoses in *Xenopus* oocytes.

Oocytes were injected with corresponding cRNA 4 days prior to uptake experiments, which were carried out at room temperature (22°C). Immediately prior to the experiment oocytes were injected with $\sim 50\text{nl}$ of ^{14}C -urate to achieve an intracellular [urate] $\sim 200\mu\text{M}$. 20nl of extracellular media was sampled and replaced per time point over 16 – 20min efflux period. All traces represent hSLC2A9a-mediated ^{14}C -urate efflux into the following extracellular solutions: (●) – 5mM D-glucose; (■) – 5mM D-fructose; (▲) – 5mM L-glucose. Slopes of the fitted straight lines represent the rates of ^{14}C -urate efflux from oocytes.

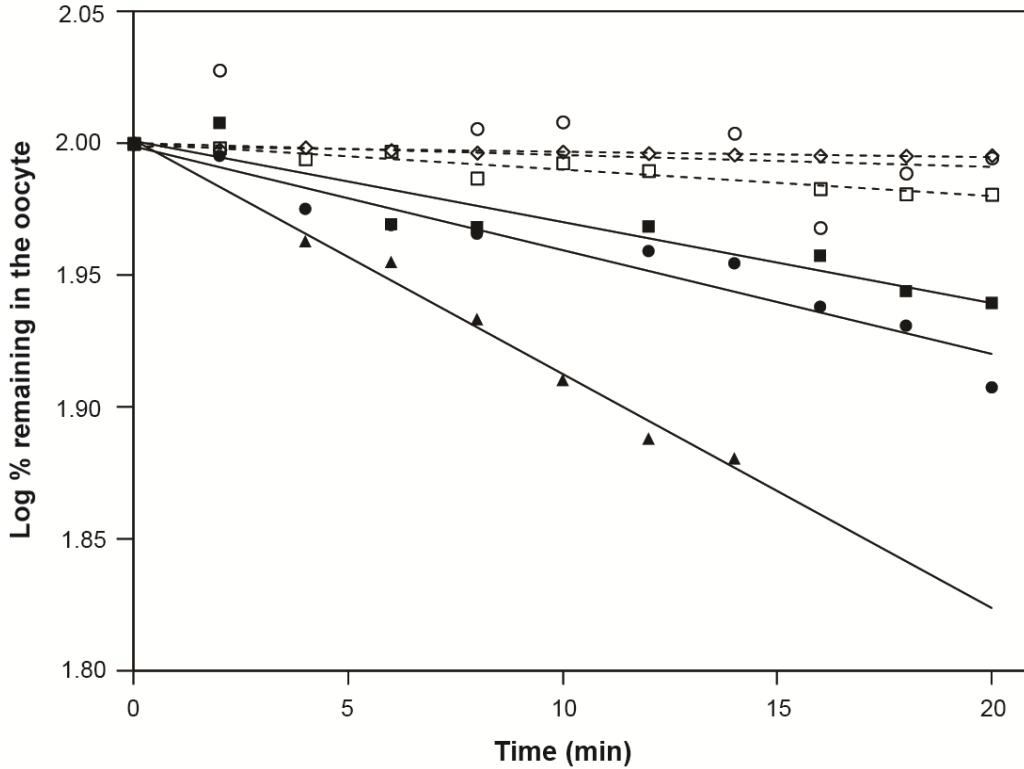


Figure 3.9. Representative experiment: hSLC2A9a mediates exchange of intracellular ^{14}C -urate for extracellular hexoses and urate in *Xenopus* oocytes. Oocytes were injected with corresponding cRNA 4 days prior to uptake experiments, which were carried out at room temperature (22°C). Immediately prior to the experiment oocytes were injected with $\sim 50\text{nl}$ of ^{14}C -urate to achieve an intracellular [urate] $\sim 200\mu\text{L}$. 20nl of extracellular media was sampled and replaced per time point over 16 – 20min efflux period. All solid lines represent hSLC2A9a-mediated ^{14}C -urate efflux while the dashed lines represent rate of leakage of ^{14}C -material from water-injected oocytes. The symbols indicate intracellular / extracellular substance combinations: (\blacktriangle) – ^{14}C -urate / 2mM urate, hSLC2A9a oocytes; (\bullet) – ^{14}C -urate / 5mM D-glucose, hSLC2A9a oocytes; (\blacksquare) – ^{14}C urate / 5mM L-glucose, hSLC2A9a oocytes; (\circ) – ^{14}C -urate / 5mM D-glucose, water oocytes; (\square) – ^{14}C -urate / 5mM L-glucose; (\diamond) – ^{14}C L-glucose / L-glucose. Slopes of the fitted straight lines represent the rates of ^{14}C -material efflux from oocytes.

3.4 Discussion

The functional study of hSLC2A9 as a urate transporter was initiated by the results of GWAS study which identified SNPs within *hSLC2A9* gene which corresponded with abnormal plasma urate levels. Another group involved in this study furthered the functional analysis of hSLC2A9's urate-handling capacity by overexpressing, and knocking-down with siRNA, SLC2A9 in mouse insulinoma MIN6 cell line. For full description of the findings, please refer to Caulfield *et al.*, 2008 (11). Parts of the discussion that follows, offer insight into the aforementioned manuscript.

3.4.1. Genetic basis for hSLC2A9 as a urate carrier

The Olivetti Heart Study has previously published a strong longitudinal relationship of serum urate levels with blood pressure (11). Interestingly, they also reported correlation of urate with reduced fractional clearance of lithium as an index of Na⁺ reabsorption in the proximal nephron. This could reflect Na⁺ retention and offer a mechanism for reported associations of urate and blood pressure (12). The two SNPs genotyped in the Olivetti cohort validate association of the *SLC2A9* locus with serum urate and demonstrate association of both SNPs with reduced urinary urate excretion at two time points, 6 years apart. This provides additional support for our hypothesis that *SLC2A9* variants reduce urinary urate loss. In this study we further explored relationship of *SLC2A9* SNPs with blood pressure and found significant association of one SNP with systolic blood pressure, diastolic blood pressure and hypertension at the

1994/1995 time-point only. This association was not confirmed in the 2002 - 2004 data from Olivetti, or in two independent case : control resources, but there was weak association with hypertension in one cohort. These data taken together with negative unpublished findings from *circa* 16,000 subjects with *SLC2A9* variants and blood pressure suggest that this locus may not have major genetic influence on blood pressure (personal communication, Patricia Munroe and Mark Caulfield). Indeed, there is also no association of *SLC2A9* gene variants in meta-analysis of GWAS for coronary artery disease (13). It remains possible that the link between uric acid and blood pressure might be explained by other genes influencing serum urate, or a very small effect size of *SLC2A9*. In the context of life course a single time-point effect size of a risk factor may underestimate the true longitudinal impact of genetic influence. In addition, as our studied populations were middle-aged or older, it also is possible that any effect of urate on blood pressure may be more prominent in early life and diminish once hypertension is established.

3.4.2 Functional evidence for hSLC2A9 as a urate carrier

Recent genome-wide association scans identified and replicated association between SNPs at the *hSLC2A9* gene locus and serum urate (6, 7). In this study we have shown that both human *SLC2A9* splice variants, a and b, can mediate urate fluxes at a very high rate and significantly faster than their facilitated transport of either D-glucose or D-fructose. The kinetics indicate that the transporter's apparent affinity for substrate, or K_m value (~ 1 mM), is above the basal, physiologic plasma concentrations of urate. Moreover, the V_{max} value indicates a high capacity transporter. All of these data suggest that this membrane protein plays a

significant role in the handling of urate in the proximal nephron which completely fits with the findings from genome-wide scans of common allelic variation elevating urate by 20 μ mol/l per allele (7). In the context of everyday clinical practice, this genetic influence on urate is equivalent to 10% of the normal range of serum urate (180 μ mol/l to 420 μ mol/l) per allele, which is not trivial.

Current models of urate handling in the kidney's PCT indicate that several types of transporters are involved in the fluxes of urate across both the apical and the basolateral membranes of the epithelial cells. In the apical membrane these include: URAT1, a urate/lactate exchanger which mediates urate movement from urine to epithelium (14), also OATv1 (15), a putative voltage-dependent organic anion transporter, MRP4 an ATP-driven pump (16), and a postulated urate channel, UAT (17). At the other pole of the cells, two of the organic anion exchangers, OAT1 & OAT2, present in the basolateral membrane, are thought to be able to handle urate, but their physiological role remains to be confirmed (18, 19). Therefore, at present there is a well defined absorptive route across the apical membrane via URAT1 and a secretory route via MRP4, while the means by which urate can either leave the renal epithelium and enter the blood, or move in the opposite direction across the basolateral membrane, remains to be confirmed.

Recently, it has been proposed that both hSLC2A9 proteins are high affinity D-glucose / D-fructose transporters. However, when compared with the principal members of the *SLC2A* gene family, their transport capacity (V_{max}) is very low (8, 9, 20). We now have evidence that urate is a preferred substrate for both human SLC2A9 variants and for the mouse orthologue. The ability of SLC2A9 to exchange urate with glucose, in the absence of competition between these two substrates when present on the same side of the membrane, indicates that the

protein has separate binding sites for the two classes of substrate. This is not a unique phenomenon in exchange proteins. The glycerol-6-phosphate transporter, for which the atomic structure was recently solved, exchanges glucose-6-phosphate for inorganic phosphate (21)

This ability of hSLC2A9 to exchange D-glucose, and to a lesser degree D-fructose, for urate has potentially significant physiological significance. The renal proximal nephron plays a major role in the reabsorption of D-glucose from urine using a combination of Na⁺-coupled hexose transporters, SGLT1 and SGLT2 and members of the SLC2A family, GLUT2, GLUT5, and possibly GLUT9 (22–25). Furthermore, the PCT epithelium is a significant site of gluconeogenesis, converting pyruvate to D-glucose, which is then released across the basolateral membrane into the blood (26, 27). Our data showing that hSLC2A9a can exchange D-glucose for urate suggest that this protein might play a role in the secretion of urate from the blood into the urine. D-glucose in the epithelial cells resulting from both reabsorption and neogenesis could exchange for plasma urate promoting the accumulation of urate in the cells. This could then either be secreted into the lumen via MRP4 or, again, in exchange for luminal glucose, *via* SLC2A9b in the apical membrane. Our findings, in combination with epidemiologic data showing correlation of elevated serum urate with diabetes, metabolic syndrome, obesity and hyperinsulinemia provide a potential mechanism for these associations which warrants further investigation (28–30). In this context, it is of particular interest that recent data from the Health and Nutrition Survey shows correlation between consumption of sugar-based soft drinks and serum urate levels, as well as gout, which might be partly explained by D-glucose-facilitated uptake of urate by hSLC2A9 isoforms (31).

Probenecid and benzbromarone are uricosuric drugs that inhibit renal uptake of urate via URAT1 on the apical proximal nephron

membrane (5). We found that probenecid had a minimal effect on urate uptake into hSLC2A9a-expressing oocytes whereas benzbromarone showed a dose dependent inhibition. The significant inhibition of urate transport by 10 and 100 μ M benzbromarone implies that there must be some common features in the binding sites for urate in both URAT1 and hSLC2A9a. Benzbromarone promotes the loss of urate in the urine and this is believed to be a consequence of an inhibition of uptake across the apical membrane mediated by URAT1 (2). However, we have also found that this drug can inhibit urate transport by hSLC2A9a, which we propose plays a role in urate secretion, which would then also be reduced by this compound. At present, the K_i of benzbromarone for these two transporters is not known and its relative effect at the luminal and interstitial surfaces requires further study, to understand its regulation of hSLC2A9-mediated urate fluxes.

3.4.3 Limitations of the study

We have not defined precisely the causative variant of *SLC2A9* responsible for elevated serum urate and reduced urinary urate clearance. There are several known SNPs within the gene region that might influence function of the SLC2A9 protein. Such studies will be facilitated by detailed re-sequencing of the *SLC2A9* locus to establish a comprehensive inventory of genetic variation across this gene locus. In addition to dietary and metabolic influences on uric acid levels, there will be other, as yet unidentified, genetic influences on serum urate level that may contribute to epidemiologic correlations with metabolic syndrome, diabetes, gout and cardiovascular disease. Elucidation of these other influences combined

with genotyping in larger numbers may allow us to detect small effect sizes not attainable in this study.

3.4.4 Conclusions

This chapter has translated genetic association of the *hSLC2A9* locus with serum urate derived from genome-wide scanning into functional confirmation that hSLC2A9 splice variants acts as a high affinity urate transporter which can be facilitated by exchange with hexoses, inhibited by high concentrations of some uricosurics, and by siRNA technology (see manuscript (32) for detailed description). These findings offer potential novel pathogenic mechanisms and new drug targets for diseases, such as, gout, diabetes and cardiovascular disease.

3.5 Bibliography

1. Cannon, P. J., Stason, W. B., Demartini, F. E., Sommers, S. C., and Laragh, J. H. (1966) Hyperuricemia in primary and renal hypertension., *The New England journal of medicine* 275, 457-64.
2. Sundström, J., Sullivan, L., D'Agostino, R. B., Levy, D., Kannel, W. B., and Vasan, R. S. (2005) Relations of serum uric acid to longitudinal blood pressure tracking and hypertension incidence., *Hypertension* 45, 28-33.
3. Fang, J. (2000) Serum Uric Acid and Cardiovascular Mortality: The NHANES I Epidemiologic Follow-up Study, 1971-1992, *JAMA: The Journal of the American Medical Association* 283, 2404-2410.
4. Nakanishi, N., Okamoto, M., Yoshida, H., Matsuo, Y., Suzuki, K., and Tatara, K. (2003) Serum uric acid and risk for development of hypertension and impaired fasting glucose or Type II diabetes in Japanese male office workers., *European journal of epidemiology* 18, 523-30.
5. Anzai, N., Kanai, Y., and Endou, H. (2007) New insights into renal transport of urate., *Current opinion in rheumatology* 19, 151-7.
6. Li, S., Sanna, S., Maschio, A., Busonero, F., Usala, G., Mulas, A., Lai, S., Dei, M., Orrù, M., Albai, G., Bandinelli, S., Schlessinger, D., Lakatta, E., Scuteri, A., Najjar, S. S., Guralnik, J., Naitza, S., Crisponi, L., Cao, A., Abecasis, G., Ferrucci, L., Uda, M., Chen, W.-M., and Nagaraja, R. (2007) The GLUT9 gene is associated with serum uric acid levels in Sardinia and Chianti cohorts., *PLoS genetics* 3, e194.
7. Wallace, C., Newhouse, S. J., Braund, P., Zhang, F., Tobin, M., Falchi, M., Ahmadi, K., Dobson, R. J., Marçano, A. C. B., Hajat, C., Burton, P., Deloukas, P., Brown, M., Connell, J. M., Dominiczak, A., Lathrop, G. M., Webster, J., Farrall, M., Spector, T., Samani, N. J., Caulfield, M. J., and Munroe, P. B. (2008) Genome-wide association study identifies genes for biomarkers of cardiovascular disease: serum urate and dyslipidemia., *American journal of human genetics* 82, 139-49.

8. Augustin, R., Carayannopoulos, M. O., Dowd, L. O., Phay, J. E., Moley, J. F., and Moley, K. H. (2004) Identification and characterization of human glucose transporter-like protein-9 (GLUT9): alternative splicing alters trafficking., *The Journal of biological chemistry* 279, 16229-36.
9. Keembiyehetty, C., Augustin, R., Carayannopoulos, M. O., Steer, S., Manolescu, A., Cheeseman, C. I., and Moley, K. H. (2006) Mouse glucose transporter 9 splice variants are expressed in adult liver and kidney and are up-regulated in diabetes., *Molecular endocrinology (Baltimore, Md.)* 20, 686-97.
10. Hediger, M. A., Johnson, R. J., Miyazaki, H., and Endou, H. (2005) Molecular physiology of urate transport., *Physiology (Bethesda, Md.)* 20, 125-33.
11. Jossa, F., Farinaro, E., Panico, S., Krogh, V., Celentano, E., Galasso, R., Mancini, M., and Trevisan, M. (1994) Serum uric acid and hypertension: the Olivetti heart study., *Journal of human hypertension* 8, 677-81.
12. Cappuccio, F. P., Strazzullo, P., Farinaro, E., and Trevisan, M. (1993) Uric acid metabolism and tubular sodium handling. Results from a population-based study., *JAMA : the journal of the American Medical Association* 270, 354-9.
13. Samani, N. J., Erdmann, J., Hall, A. S., Hengstenberg, C., Mangino, M., Mayer, B., Dixon, R. J., Meitinger, T., Braund, P., Wichmann, H.-E., Barrett, J. H., König, I. R., Stevens, S. E., Szymczak, S., Tregouet, D.-A., Iles, M. M., Pahlke, F., Pollard, H., Lieb, W., Cambien, F., Fischer, M., Ouwehand, W., Blankenberg, S., Balmforth, A. J., Baessler, A., Ball, S. G., Strom, T. M., Braenne, I., Gieger, C., Deloukas, P., Tobin, M. D., Ziegler, A., Thompson, J. R., and Schunkert, H. (2007) Genomewide association analysis of coronary artery disease., *The New England journal of medicine* 357, 443-53.
14. Enomoto, A., Kimura, H., Chairoungdua, A., Shigeta, Y., Jutabha, P., Cha, S. H., Hosoyamada, M., Takeda, M., Sekine, T., Igarashi, T., Matsuo, H., Kikuchi, Y., Oda, T., Ichida, K., Hosoya, T., Shimokata, K., Niwa, T., Kanai, Y., and Endou, H. (2002) Molecular identification of a renal urate anion exchanger that regulates blood urate levels., *Nature* 417, 447-52.

15. Hediger, M. A. (2004) [Physiology and biochemistry of uric acid]., *Therapeutische Umschau. Revue thérapeutique* 61, 541-5.
16. Aubel, R. A. M. H. Van, Smeets, P. H. E., Heuvel, J. J. M. W. van den, and Russel, F. G. M. (2005) Human organic anion transporter MRP4 (ABCC4) is an efflux pump for the purine end metabolite urate with multiple allosteric substrate binding sites., *American journal of physiology. Renal physiology* 288, F327-33.
17. Lipkowitz, M. S., Leal-Pinto, E., Cohen, B. E., and Abramson, R. G. (2004) Galectin 9 is the sugar-regulated urate transporter/channel UAT., *Glycoconjugate journal* 19, 491-8.
18. Bakhiya, A., Bahn, A., Burckhardt, G., and Wolff, N. (2003) Human organic anion transporter 3 (hOAT3) can operate as an exchanger and mediate secretory urate flux., *Cellular physiology and biochemistry: international journal of experimental cellular physiology, biochemistry, and pharmacology* 13, 249-56.
19. Ichida, K., Hosoyamada, M., Kimura, H., Takeda, M., Utsunomiya, Y., Hosoya, T., and Endou, H. (2003) Urate transport via human PAH transporter hOAT1 and its gene structure., *Kidney international* 63, 143-55.
20. Manolescu, A. R., Augustin, R., Moley, K., and Cheeseman, C. (2007) A highly conserved hydrophobic motif in the exofacial vestibule of fructose transporting SLC2A proteins acts as a critical determinant of their substrate selectivity., *Molecular membrane biology* 24, 455-63.
21. Lemieux, M. J., Huang, Y., and Wang, D.-N. (2004) Glycerol-3-phosphate transporter of Escherichia coli: structure, function and regulation., *Research in microbiology* 155, 623-9.
22. Dominguez, J. H., Camp, K., Maianu, L., and Garvey, W. T. (1992) Glucose transporters of rat proximal tubule: differential expression and subcellular distribution., *The American journal of physiology* 262, F807-12.
23. Thorens, B., Lodish, H. F., and Brown, D. (1990) Differential localization of two glucose transporter isoforms in rat kidney., *The American journal of physiology* 259, C286-94.

24. Sugawara-Yokoo, M., Suzuki, T., Matsuzaki, T., Naruse, T., and Takata, K. (1999) Presence of fructose transporter GLUT5 in the S3 proximal tubules in the rat kidney., *Kidney international* 56, 1022-8.
25. Wright, E. M. (2001) Renal Na(+)-glucose cotransporters., *American journal of physiology. Renal physiology* 280, F10-8.
26. Conjard, A., Martin, M., Guitton, J., Baverel, G., and Ferrier, B. (2001) Gluconeogenesis from glutamine and lactate in the isolated human renal proximal tubule: longitudinal heterogeneity and lack of response to adrenaline., *The Biochemical Journal* 360, 371-7.
27. Mithieux, G., Gautier-Stein, A., Rajas, F., and Zitoun, C. (2006) Contribution of intestine and kidney to glucose fluxes in different nutritional states in rat., *Comparative biochemistry and physiology. Part B, Biochemistry & molecular biology* 143, 195-200.
28. Baker, J. F., Krishnan, E., Chen, L., and Schumacher, H. R. (2005) Serum uric acid and cardiovascular disease: recent developments, and where do they leave us?, *The American journal of medicine* 118, 816-26.
29. Chien, K.-L., Chen, M.-F., Hsu, H.-C., Chang, W.-T., Su, T.-C., Lee, Y.-T., and Hu, F. B. (2008) Plasma uric acid and the risk of type 2 diabetes in a Chinese community., *Clinical chemistry* 54, 310-6.
30. Krishnan, E., Kwoh, C. K., Schumacher, H. R., and Kuller, L. (2007) Hyperuricemia and incidence of hypertension among men without metabolic syndrome., *Hypertension* 49, 298-303.
31. Choi, J. W. J., Ford, E. S., Gao, X., and Choi, H. K. (2008) Sugar-sweetened soft drinks, diet soft drinks, and serum uric acid level: the Third National Health and Nutrition Examination Survey., *Arthritis and rheumatism* 59, 109-16.
32. Caulfield, M. J., Munroe, P. B., O'Neill, D., Witkowska, K., Charchar, F. J., Doblado, M., Evans, S., Eyheramendy, S., Onipinla, A., Howard, P., Shaw-Hawkins, S., Dobson, R. J., Wallace, C., Newhouse, S. J., Brown, M., Connell, J. M., Dominiczak, A., Farrall, M., Lathrop, G. M., Samani, N. J., Kumari, M., Marmot, M., Brunner, E., Chambers, J., Elliott, P., Kooner, J., Laan, M., Org, E., Veldre, G., Viigimaa, M., Cappuccio, F. P., Ji, C., Iacone, R., Strazzullo, P., Moley, K. H., and Cheeseman, C. (2008) SLC2A9 is a high-capacity urate transporter in humans., *PLoS medicine* 5, e197.

Chapter

4

In-depth functional comparison of human hSLC2A9a and hSLC2A9b isoforms *

* A version of this chapter has been submitted for publication.

Witkowska, K., Smith, K.M., Yao, S.Y.M., Ng A.M.L., O'Neill, D., Karpinski, E., Young, J.D., and Cheeseman, C.I. (2011) Human SLC2A9a and SLC2A9b isoforms mediate electrogenic transport of urate with different characteristics in presence of hexoses. *Am. J. Physiol.*

4.1 Acknowledgements and contributions

All radiolabelled flux and efflux analysis of hSLC2A9 isoforms was performed by myself. Dr. Kyla Smith performed all the electrophysiological studies, while Dr. Sylvia Yao and Mrs. Amy Ng contributed the nucleoside panels. Mrs. Debbie O'Neill helped with oocyte isolation and preparation. hSLC2A9a and hSLC2A9b cDNA was a generous gift from Dr. Kelle Moley.

Funding: This work was supported by the Canadian Institutes of Health Research. I was funded by a Queen Elizabeth II PhD Scholarship and an Alberta Diabetes Institute Studentship. Dr. James Young holds the title of Senior Investigator of the Alberta Heritage Foundation for Medical Research.

4.2 Introduction

Urate is an organic anion and the physiologically predominant form of uric acid, the end product of purine metabolism in humans and higher primates. Due to the loss of hepatic uricase activity, humans and higher primates maintain high levels of urate in the blood (180 - 420 μM) compared to the majority of mammals (30 - 120 μM), which do express uricase (1). The role for elevated urate in human plasma has not been explained, although one suggestion is that it may function as an antioxidant (2). Human plasma urate levels are regulated within closely defined limits and even small increases above normal show significant correlation with the incidence of gout, metabolic disease, diabetes, cardiovascular morbidity and mortality, and hypertension (3–8).

The high circulating levels of plasma urate result from a balance between intake from the diet and production in the liver and muscle, and loss in the urine. About 70 % of daily urate production enters the renal filtrate, and 10 % is finally excreted in the urine (9). The kidney epithelium is therefore the main regulatory site of plasma urate, where this metabolite's reabsorption and secretion occur. However, the molecular basis for urate handling in the human kidney has not been fully determined because of differences between species and the multitude of urate transport systems involved. The proposed urate transport systems in the human proximal nephron include the electroneutral urate/anion exchanger SLC22A12 (URAT1) (10), the organic anion transporters SLC22A6/8 (OAT1/3) (11, 12), the multidrug resistance protein ABCC4 (MRP4) (13, 14), the breast cancer resistance protein ABCG2 (BCRP) (15) and the sodium/phosphate transporter SLC17A3 (NPT4) (16). Genetic loci of the

latter three transporters contain SNPs which have been correlated with urate imbalance, although their function in urate regulation still needs to be elucidated. SLC22A12 (URAT1), however, appears to be the only transporter whose role in urate reabsorption has been confirmed, with loss-of-function mutations in the URAT1 gene being associated with renal hypouricemia (10). Furthermore, mutations in hSLC2A9 (GLUT9) have also been correlated with decreased plasma urate levels in the Dalmatian dog model (17) and in humans (18–20), although the mechanisms underlying this phenotype are still not fully elucidated. Two putative electrogenic urate transporters have also been identified. Transport of PAH by the voltage-driven organic anion transporter OAT_v1 cloned from pig kidney is electrogenic, and uptake is competitively inhibited by urate (12, 21). There is, however, no evidence that OAT_v1 is expressed in human kidney. Cloned initially from rat kidney, the urate transporter UAT displays voltage-sensitive channel activity that is highly urate-specific (22). Human UAT (also known as Galectin 9 (9), however, is expressed ubiquitously in numerous tissues, undermining claims that it mediates urate secretion specifically in the kidney.

Genome-wide association scans have linked SNPs in the gene encoding the facilitative hexose transporter isoform hSLC2A9 with abnormal plasma urate concentrations in human population cohorts (17, 18, 21, 23–27). hSLC2A9 is a member of the facilitative glucose transporter gene family (GLUTs), but is now primarily described as a novel high-capacity urate transporter, which can exchange both glucose and fructose for urate (24, 27). hSLC2A9 has two splice variants, hSLC2A9a (full length) and hSLC2A9b (or Δ N), both of which are present in human kidney (28). The two splice variants differ in their N-terminal sequence and are expressed differentially in polarized cells: hSLC2A9b (512 amino

acids) is localized apically, while hSLC2A9a (540 amino acids) is expressed on the basolateral membrane. Current evidence suggests that the two isoforms are functionally identical in terms of hexose and urate transport kinetics (24, 28).

We have postulated that negatively-charged urate transport by human SLC2A9 is electrogenic. In support of this, Anzai *et al.* (21) have provided indirect evidence that human SLC2A9 urate transport in *Xenopus* oocytes is influenced by membrane potential. Depolarizing the oocyte membrane through elevation of extracellular K⁺ resulted in stimulation of radiolabelled urate uptake. They did not, however, directly measure currents generated in hSLC2A9-producing oocytes in response to urate exposure. The predominant basolateral localization and voltage-dependence of hSLC2A9 led to the conclusion that this protein is mainly involved in urate reabsorption, in concert with apically expressed SLC22A12 (URAT1). Even more, recent findings by Bibert *et al.* (29) suggest that urate uptake mediated by mouse SLC2A9 induced an outward current when produced in oocytes.

In the present study, we have undertaken a combined electrophysiological and radiotracer flux analysis of recombinant human SLC2A9 isoforms produced in *Xenopus* oocytes. Using the two-electrode voltage-clamp technique, the electrogenic nature of urate transport mediated by hSLC2A9a and hSLC2A9b was investigated by examining the effect of membrane potential and ion concentrations on membrane currents. We also measured the K_m for urate influx under voltage-clamp conditions. Using radiotracer fluxes, we investigated the effect of intracellular hexoses on urate uptake, showing key functional differences in the two isoforms of the transporter. We also demonstrate that extracellular urate accelerates efflux of urate from the oocytes, suggesting

that hSLC2A9 acts as a non-obligatory urate-urate exchanger. The permeant selectivity of hSLC2A9 was examined by testing its ability to transport other radiolabelled purine and pyrimidine nucleobases. Finally, we report kinetic studies of urate efflux, supporting the concept that the direction of urate flux is determined primarily by the electrochemical gradient.

4.3 Results

4.3.1 Urate currents of hSLC2A9

Since urate is predominately a weak acid at pH 7.5 ($pK_a = 5.75$) (1), we examined the electrogenic nature of hSLC2A9-mediated transport of urate in *Xenopus* oocytes using the two-electrode voltage-clamp technique. In the representative experiment shown in **Figure 4.1A**, an oocyte producing hSLC2A9a was voltage-clamped at -30 mV and a transient outward current was generated when the extracellular medium (100 mM NaCl, pH 7.5) was changed to one containing 1 mM urate. This current decayed to a new steady-state and, upon removal of extracellular urate, a corresponding inward transient current, which returned to baseline, developed. A similar response was observed with hSLC2A9b-producing oocytes voltage clamped under the same conditions (**Figure 4.1B**). Current magnitudes observed with hSLC2A9a were consistently less than those seen with hSLC2A9b. In contrast, these the addition of 1 mM urate to water-injected oocytes, small inward currents,

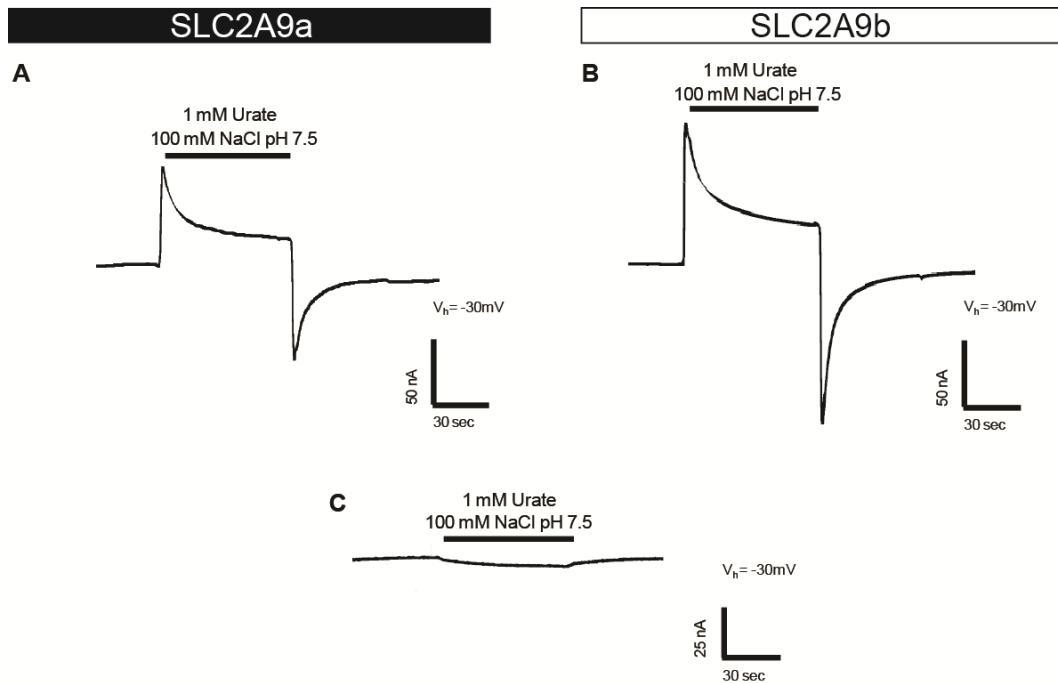


Figure 4.1. Steady-state currents of hSLC2A9. **A.** A representative current trace in a single hSLC2A9a-producing oocyte clamped at -30 mV in Na^+ -containing transport medium (100 mM NaCl, pH 7.5). The bar denotes addition of urate (1 mM) to the bath. The same experiment was performed on a hSLC2A9b-producing oocyte (**B**) and a representative control water-injected oocyte (**C**).

which slowly increased in amplitude were currents were not observed in control water-injected oocytes (**Figure 4.1C**). Following the addition of 1mM urate to water-injected oocytes, small inward currents, which slowly increased in amplitude were observed, possibly due to interactions of urate with endogenous oocyte transporters and channels (30). The much larger currents in hSLC2A9- producing oocytes are consistent with the movement of negatively charged urate through the transporter, the large outward spike in the current record observed following the addition of urate decaying to a new steady-state as the inwardly directed urate gradient is reduced. Upon removal of extracellular urate, transient inward currents are observed as a result of the efflux of cytoplasmic urate. These transient currents also decay as urate gradient is once again depleted. The current record is biphasic, likely due to the bidirectional movement of urate mediated by hSLC2A9. hSLC2A9 therefore mediates the electrogenic transport of urate.

4.3.2 Voltage-dependence of hSLC2A9-mediated transport

To obtain the current magnitudes in response to the addition of urate, two methods were used. In the first, current was calculated as the difference between baseline current and the transient spike observed following urate addition. In the second method, the steady-state urate current that followed the transient spike was calculated by integrating the area under the current record from baseline using fixed time points. The two methods showed similar voltage-dependence (data not shown), and in voltage-dependence and subsequent experiments reported here, current was calculated as the difference from baseline to transient spike. To

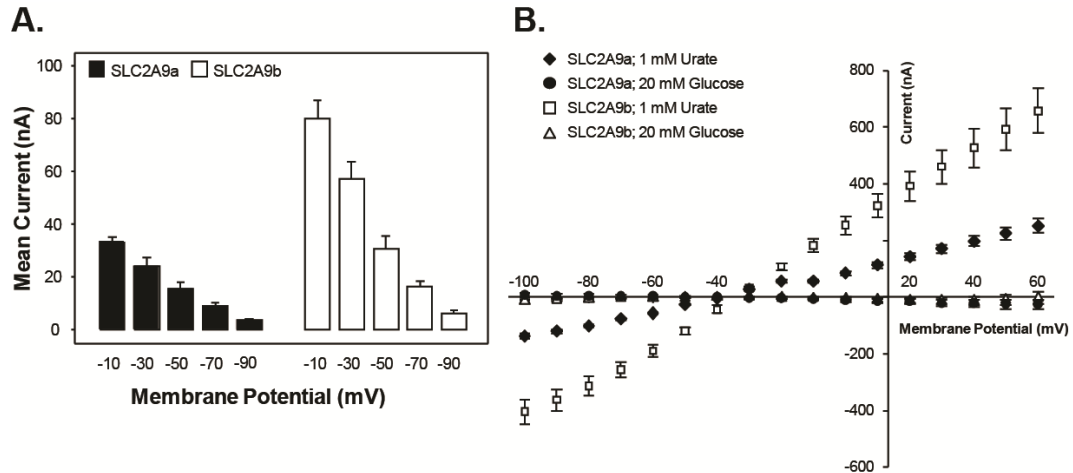


Figure 4.2. Voltage-dependence of hSLC2A9-mediated transport of urate. **A.** hSLC2A9a- (■) or hSLC2A9b- (□) producing oocytes were voltage clamped sequentially at 5 different holding potentials (-90, -70, -50, -30 and -10 mV) and the maximum current generated in response to the addition of 1 mM urate (100 mM NaCl, pH 7.5) was measured at each potential. Currents are the means \pm S.E.M. of 4 different oocytes from the same batch of cells used on the same day. **B.** The current-voltage (I-V) curves for hSLC2A9a (black symbols) and hSLC2A9b (open symbols) were generated from the difference between steady-state currents recorded in the presence and absence of 1 mM urate (◆ and □, respectively) or in the presence and absence of 20 mM glucose (● and △, respectively) in Na⁺-containing medium (100 mM NaCl, pH 7.5) upon voltage pulses from V_h of -30 mV to final potentials ranging between -100 and +60 mV, in 10 mV steps. Urate- and D-glucose-induced I-V curves were measured in the same hSLC2A9-producing oocytes, and data are averaged from 3 cells.

examine the voltage-dependence of transport mediated by hSLC2A9, steady-state currents were measured sequentially at five different holding potentials (-10, -30, -50, -70 and -90 mV) in response to the addition of urate (1 mM urate; 100 mM NaCl, pH 7.5) (**Figure 4.2A**). Additionally, the current-voltage (I-V) relation of the two isoforms of hSLC2A9 mediated urate transport was compared to that of glucose (**Figure 4.2B**). Currents evoked by urate (1 mM; 100 mM NaCl, pH 7.5) at potentials between -100 and +60 mV were voltage-dependent, with the magnitude of the outward current increasing as the membrane potential became more positive. The I-V curves observed with urate showed a similar voltage-dependence as those observed by Bibert *et al.* (29) for mouse GLUT9a. Measured in the same oocyte, glucose-induced currents (20 mM; 100 mM NaCl, pH 7.5) were minor compared to those of urate, and exhibited a slight voltage-dependence (**Figure 4.2B**). Since glucose is electrically neutral and transport of glucose mediated by hSLC2A9a or hSLC2A9b is not coupled to the movement of ions (3), the currents observed in the I-V relation may be the result of glucose transport mediated by endogenous sodium glucose transporters (38, 39). Although D-glucose and D-fructose are high affinity permeants of hSLC2A9a, neither inhibit ¹⁴C-urate uptake (24). Consistent with this, hSLC2A9a and hSLC2A9b currents were unaffected by high concentrations (5 - 20 mM) of extracellular D-glucose.

4.3.3 Ion-dependence of hSLC2A9-mediated transport

The dependence of hSLC2A9-mediated transport of urate on the presence of extracellular Na⁺ was examined at a holding potential of -30 mV (**Figure 4.3A**). Currents in response to the addition of 1 mM urate

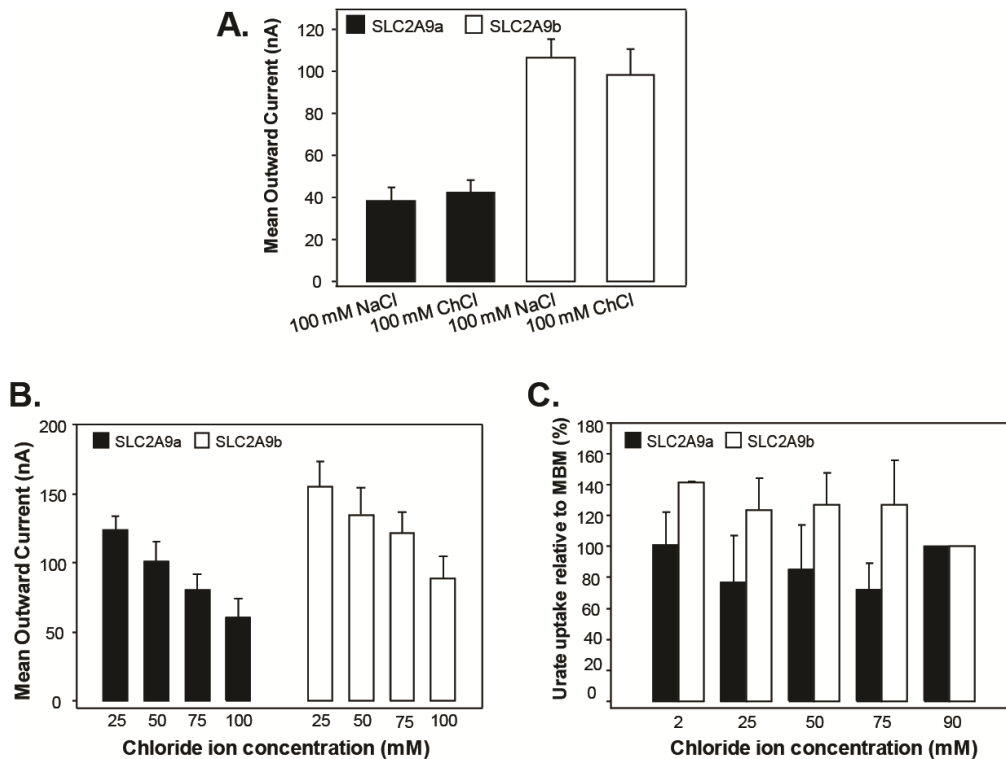


Figure 4.3. Effect of extracellular ions on the transport activity of hSLC2A9. **A.** Mean urate-induced currents in oocytes producing hSLC2A9a (■) or hSLC2A9b (□) were measured in transport media containing Na⁺ (100 mM NaCl, pH 7.5) or choline (100 mM ChCl, pH 7.5) at a membrane potential of -30 mV. Currents are the means ± S.E.M. of 3 different oocytes from the same batch of cells used on the same day. **B.** Mean urate-induced currents in oocytes producing hSLC2A9a (■) and hSLC2A9b (□) were measured in transport media containing a range of Cl⁻ concentrations (25, 50, 75 and 100 mM Cl⁻, pH 7.5). Cl⁻ was replaced with Na⁺ gluconate to maintain osmotic conditions. Membrane potential was held at -30 mV. Currents are the means ± S.E.M. of 4 different oocytes from the same batch of cells used on the same day. The currents were not corrected for those in control water-injected cells. **C.** Uptake of 100 μM radiolabelled urate was measured in oocytes producing hSLC2A9a (■) and hSLC2A9b; (□) in the presence of varying concentrations of Cl⁻ (2, 25, 50, 75 and 90 mM Cl⁻). Uptake at each Cl⁻ concentration was measured in 12 oocytes and the experiments repeated in 3 different batches of cells. The data were averaged and presented as the % uptake relative to that in normal MBM. Values were corrected for basal non-mediated uptake in control water-injected oocytes.

were measured in oocytes producing hSLC2A9a or hSLC2A9b, in the presence (100 mM NaCl, pH 7.5) and absence (100 mM ChCl, pH 7.5) of extracellular Na⁺. Urate-induced currents were not significantly different in the presence and absence of Na⁺, demonstrating that the transport of urate by hSLC2A9 was not Na⁺-dependent.

The effect of extracellular Cl⁻ on hSLC2A9-mediated transport of urate was also examined at a holding potential of -30 mV (**Figure 4.3B**). Currents were measured in hSLC2A9a- or hSLC2A9b-producing oocytes in the presence of a high extracellular Cl⁻ concentration (100 mM NaCl, pH 7.5), intermediate Cl⁻ concentrations (75 mM NaCl + 25 mM Na⁺ gluconate and 50 mM NaCl + 50 mM Na⁺ gluconate, pH 7.5), and with the extracellular Cl⁻ concentration reduced by 75 % (25 mM NaCl + 75 mM Na⁺ gluconate, pH 7.5). Decreasing the external Cl⁻ concentration significantly increased the magnitude of the outward currents associated with urate uptake, in both isoforms of hSLC2A9, demonstrating that hSLC2A9-mediated transport is affected by the extracellular concentration of Cl⁻. In contrast, Anzai *et al.* (21) and Bibert *et al.* (29) found no effect of lowering the external Cl⁻ concentration on the transport of radiolabelled urate by hSLC2A9a or its mouse homologue, although uptake was measured over an extended period and, unlike the present electrophysiological study, was not performed under voltage clamp conditions. Our ¹⁴C-urate influx studies, performed on hSLC2A9a and hSLC2A9b under initial rate conditions, also found no difference in hSLC2A9-mediated uptake of urate as the extracellular concentration of Cl⁻ was varied between 2 and 90 mM (**Figure 4.3C**). Anzai *et al.* (21) and Bibert *et al.* (29) concluded that SLC2A9 does not have an exchange mechanism for inorganic Cl⁻. Our observations support the conclusion that Cl⁻ is not required for hSLC2A9-mediated urate transport, and instead

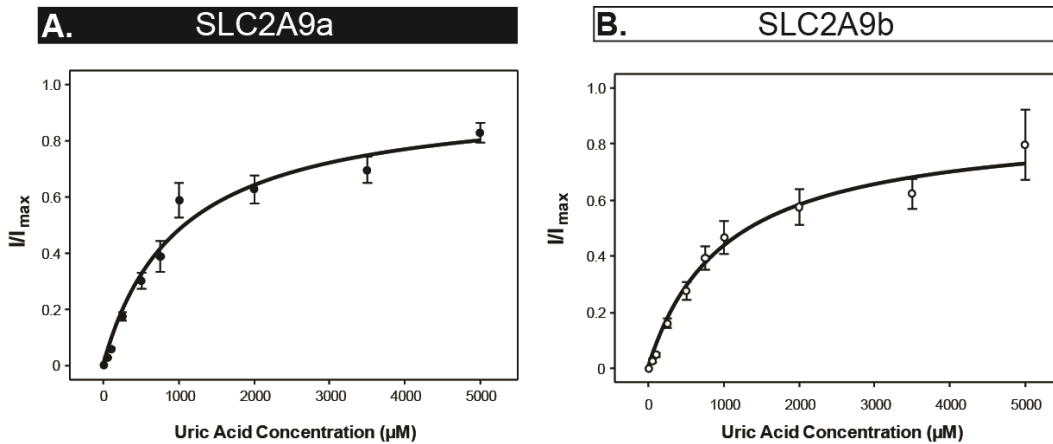


Figure 4.4. Urate influx kinetics of hSLC2A9. The dependence of hSLC2A9a- and hSLC2A9b- mediated currents on the external concentration of urate (0 - 5 mM) was measured at a membrane potential of -30 mV (100 mM NaCl, pH 7.5). hSLC2A9a and hSLC2A9b currents are averaged from concentration dependence relationships for 7 different oocytes, where currents at each urate concentration were normalized to the fitted I_{max} value for that oocyte. The currents were not corrected for those in control water-injected cells. **A.** SLC2A9a-producing oocytes: $K_m = 1.0 \pm 0.15$ mM. **B.** hSLC2A9b-producing oocytes: $K_m = 1.0 \pm 0.20$ mM. Individual I_{max} values were in the range 150 - 200 nA for hSLC2A9a-producing oocytes, and 175 - 250 nA for hSLC2A9b- producing oocytes.

suggest that Cl^- is inhibitory, possibly through negative-charge competition with urate for binding to the transporter. The lack of effect of Cl^- observed with ^{14}C -urate influx *versus* the inhibition seen with electrophysiology studies is due to differences in the experimental techniques. In voltage-clamped oocytes, urate-induced currents decrease when the membrane potential is hyperpolarized (**Figure 4.2A**). In ^{14}C -urate influx experiments, the membrane potential is hyperpolarized as ^{14}C -urate enters the cell (data not shown). The effect of Cl^- on ^{14}C -urate uptake is therefore the combination of both an increased influx of urate due to decreased Cl^- concentration and a decreased influx of urate due to membrane hyperpolarization. As a result, decreasing the external Cl^- concentration (**Figure 4.3C**) shows no net effect on extracellular ^{14}C -urate uptake.

4.3.4 Urate influx kinetics under voltage clamp conditions

Figure 4.4 shows the dependence of hSLC2A9-mediated currents on the concentration of extracellular urate (0 - 5 mM; 100 mM NaCl, pH 7.5). Oocytes producing hSLC2A9a (**Figure 4.4A**) or hSLC2A9b (**Figure 4.4B**) were voltage clamped at a holding potential of -30 mV and the currents generated in response to increasing urate concentrations were measured. For both isoforms, currents were saturable and consistent with simple Michaelis-Menten kinetics. For hSLC2A9a, the apparent K_m value was 1.0 ± 0.15 mM (**Figure 4.4A**), while for hSLC2A9b the apparent K_m value was 1.0 ± 0.20 mM (**Figure 4.4B**). At 5 mM urate, the corresponding small inward current in control water-injected oocytes was < 25 nA. These K_m values are similar to those determined by radiotracer flux experiments in unclamped oocytes (~ 1 mM for both isoforms) ((12), data not shown).

The large I_{\max} observed for both isoforms (150 - 200 nA for hSLC2A9a and 175 - 250 nA for SLC2A9b), confirms by electrophysiology that hSLC2A9 is a high capacity urate transporter.

4.3.5 hSLC2A9 has symmetrical affinity and capacity for urate efflux

In order to determine if hSLC2A9-mediated fluxes of urate are symmetrical or vectorial in nature, we compared the kinetics for ^{14}C -urate efflux to those of influx. Since the apparent affinity ($K_m \sim 1 \text{ mM}$) and capacity ($V_{\max} \sim 15 \text{ pmol/oocyte.min}^{-1}$) of the transporter for ^{14}C -urate influx has previously been established (24), we determined the corresponding kinetics of urate efflux. Following injection of oocytes with varying amounts of ^{14}C -urate, individual concentrations of intracellular urate at time zero ranged between 17 - 624 μM for hSLC2A9a and 39 - 495 μM for hSLC2A9b. The low solubility of urate and maximum injectable volume set an upper limit to the intracellular concentrations of urate that could be achieved. As shown for hSLC2A9a in **Figure 4.5A**, efflux at each urate concentration was plotted against time and fitted with a straight line to determine the initial rate of efflux. The experiments were also performed in control water-injected oocytes (**Figure 4.5A**). **Figure 4.5B** shows the Michaelis-Menten fit for the initial rates of hSLC2A9a-mediated urate efflux plotted against the starting intracellular urate concentration, and **Figure 4.5C** shows the corresponding data for hSLC2A9b. Efflux rates for the two isoforms are similar and appear to be saturable. Projected apparent K_m values were outside the concentration studied, but were

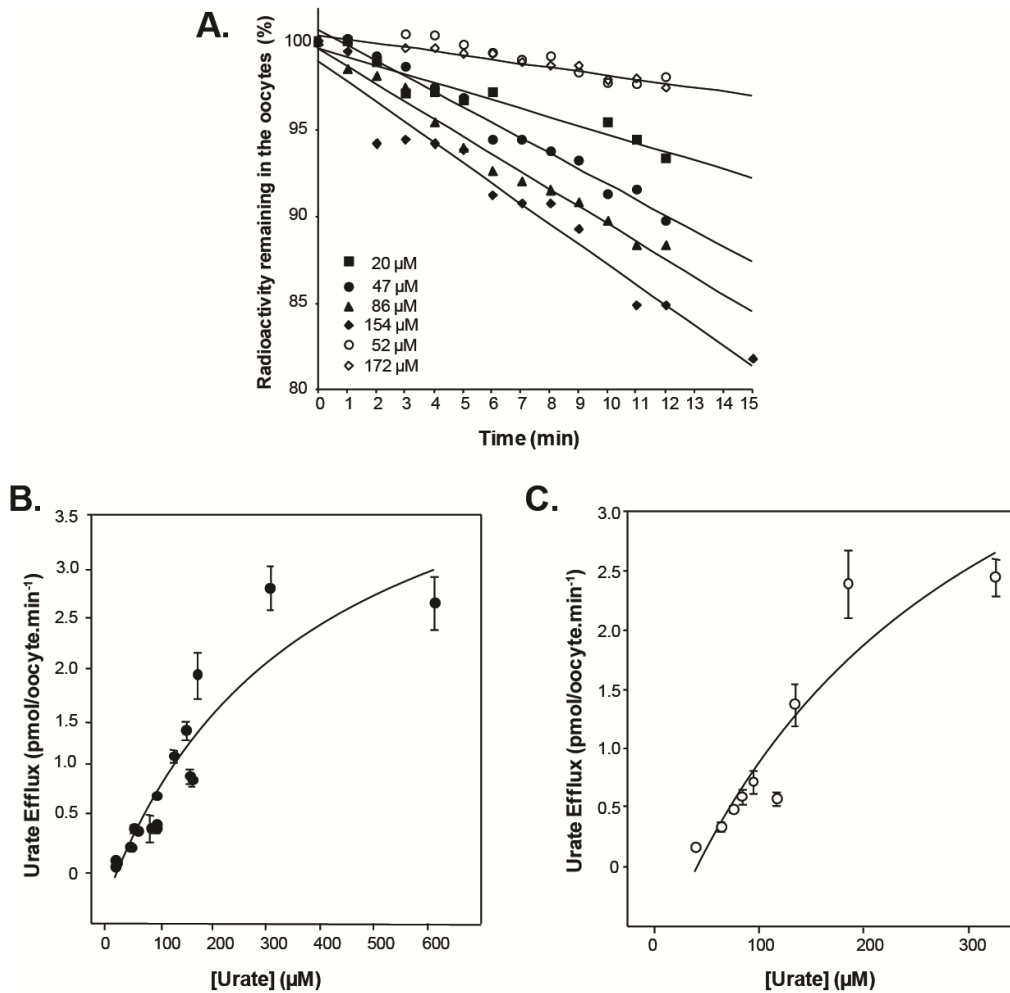


Figure 4.5. Urate efflux kinetics of hSLC2A9. **A.** Representative results demonstrating ¹⁴C-urate efflux from ¹⁴C-urate preloaded hSLC2A9-producing oocytes (*solid symbols*) and from water-injected oocytes (*open symbols*). Magnitudes of the slopes of the lines (\pm S.E.), indicating the rates of intracellular urate efflux (% efflux/min) for each concentration were: water-injected oocytes, 0.26 ± 0.06 (52 μ M) and 0.21 ± 0.06 (172 μ M); hSLC2A9a-producing oocytes, 0.46 ± 0.06 (20 μ M), 0.89 ± 0.06 (47 μ M), 0.92 ± 0.06 (86 μ M), and 1.10 ± 0.06 (154 μ M). Only low and high intracellular urate concentrations for water-injected oocytes are shown for clarity. **B.** Initial rates of ¹⁴C-urate efflux for hSLC2A9a-producing oocytes in units of pmol/oocyte.min⁻¹ are plotted against the starting internal urate concentration. **C.** Corresponding data for ¹⁴C-urate efflux in hSLC2A9b-producing oocytes. Fitted apparent K_m values were ~ 1 mM for both transporter isoforms.

~1mM for both transporter isoforms and of the same magnitude as those seen for hSLC2A9a and hSLC2A9b urate influx measured either electrophysiologically (**Figure 4.4**) or using ^{14}C -urate ((24), data not shown). Efflux of ^{14}C -urate from control water-injected oocytes was minimal, suggesting that endogenous transporters did not contribute to urate efflux.

4.3.6 Effect of extracellular substances on hSLC2A9-mediated urate efflux

We have demonstrated previously that both D-glucose and D-fructose, which have been shown to be high affinity permeants for hSLC2A9a (31), are not competitive inhibitors of urate uptake. However, both of these hexoses can accelerate urate efflux mediated by hSLC2A9a when placed in the extracellular medium, suggesting that facilitated movement of both urate and hexoses is likely mediated by the same carrier (24). In the present study, we extended this experiment to include the effects of extracellular hexoses on both hSLC2A9a- and hSLC2A9b-mediated efflux in order to compare the two isoforms, as well as tested the effect of extracellular urate on urate efflux mediated by the two isoforms. The next section also presents complementary new findings for the *trans* effects of urate and sugars on ^{14}C -urate influx.

For each condition, hSLC2A9a- or hSLC2A9b-producing oocytes were preloaded with ^{14}C -urate to achieve final, intracellular permeant concentrations in the μM range. Urate efflux was measured over 14 minutes, at 2 minute time intervals. Initial rates of urate efflux obtained

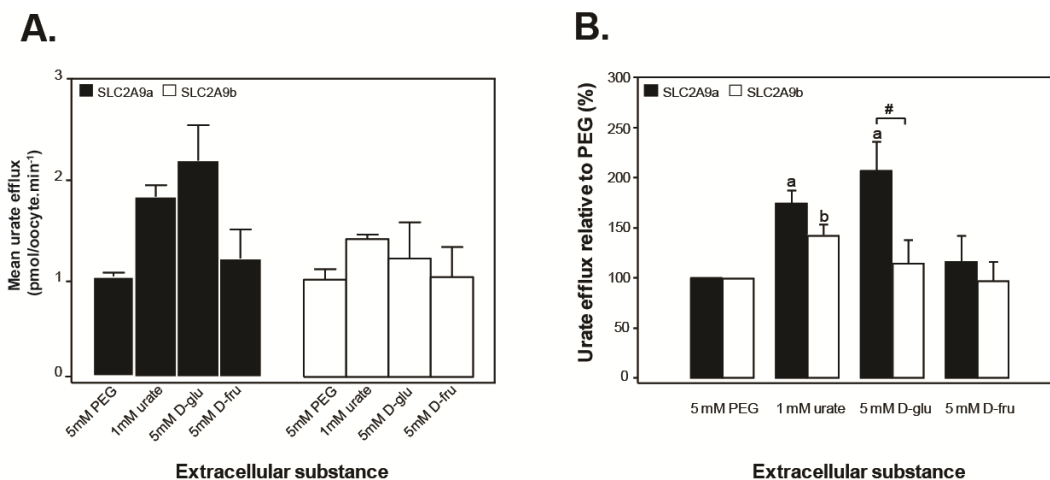


Figure 4.6. Effect of extracellular substances on hSLC2A9-mediated urate efflux. hSLC2A9a- (■) and hSLC2A9b- (□) producing oocytes were preloaded with ¹⁴C-urate and the rate of urate efflux was measured in presence of different substances added to MBM. Vertical bars represent mean urate efflux \pm S.E.M. of 20 oocytes per condition from 3 - 6 batches of cells used on the same day. Efflux rates were corrected for variations in intracellular ¹⁴C-urate concentrations. **A.** Represents rates of ¹⁴C-urate efflux in pmol/oocyte.min⁻¹ averaged for 3 – 6 experiments. **B.** Represents mean ¹⁴C-urate efflux rates expressed as % of efflux compared to osmotic control (5 mM PEG). “a” and “b” symbols above the bars denote statistically significant urate efflux values from the control (5 mM PEG) for hSLC2A9a- and hSLC2A9b-producing oocytes, respectively ($p \leq 0.01$). # denotes statistical significance ($p \leq 0.05$) between hSLC2A9a and hSLC2A9b isoforms in response to extracellular 5 mM D-glucose.

from the linear fits of efflux data were corrected for variations in intracellular urate concentrations and normalized to urate efflux under osmotic control conditions (5 mM PEG). hSLC2A9a-mediated urate efflux (**Figure 4.6**) was significantly accelerated in presence of excess extracellular urate (1 mM) and D-glucose (5 mM), while D-fructose produced small, but insignificant acceleration. These results are consistent with the effect of extracellular hexoses previously reported by our group (9). hSLC2A9b-mediated urate efflux (**Figure 4.6**), on the other hand, was significantly accelerated only in presence of 1 mM extracellular urate. Although hSLC2A9b repeatedly showed decreased acceleration of urate efflux in presence of excess *trans* urate, as compared with hSLC2A9a, this difference did not reach statistical significance. Both hSLC2A9 isoforms therefore function as non-obligatory urate-urate exchangers, hSLC2A9a, but not hSLC2A9b, also exhibiting *trans*-acceleration by physiological levels of extracellular D-glucose.

4.3.7 Effect of intracellular substances on hSLC2A9-mediated urate influx

In order to further investigate the possible effects of permeant hexoses on hSLC2A9-mediated urate uptake, we preloaded hSLC2A9a- or hSLC2A9b-producing oocytes with various substances at a final intracellular concentration of 5 mM (unless otherwise stated), and measured ¹⁴C-urate influx (**Figure 4.7**). Uptake data were normalized to the osmotic control (5 mM PEG) for each experiment. All substrates tested produced a significant increase of urate uptake in the case of hSLC2A9a-producing oocytes. hSLC2A9b-producing oocytes showed similar

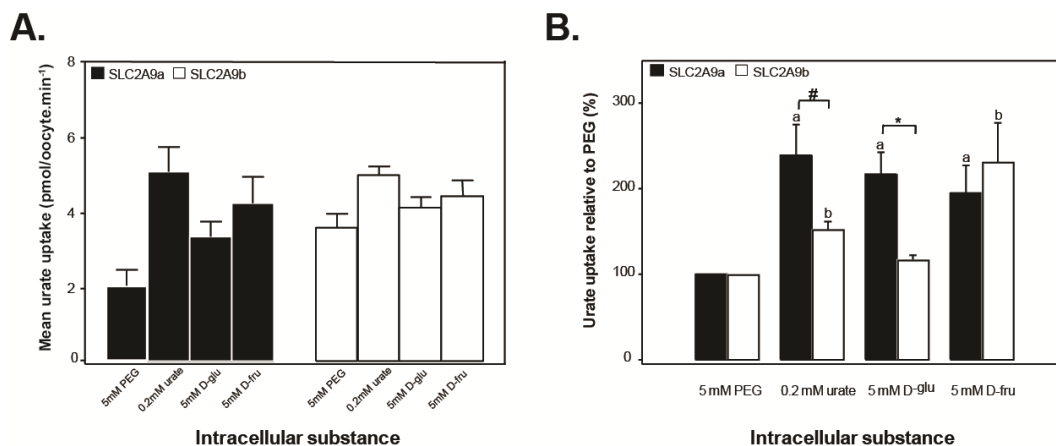


Figure 4.7. Effect of intracellular substances on hSLC2A9-mediated urate influx. hSLC2A9a- (■) and hSLC2A9b- (□) producing oocytes were preloaded with different cold substances, at a final intracellular concentration of 5 mM, unless otherwise stated and $100\mu\text{M}$ ^{14}C -urate uptake was measured. Vertical bars represent mean urate influx \pm S.E.M. of 10 oocytes per condition from 3 - 6 batches of cells used on the same day. **A.** Represents ^{14}C -urate uptake rates in $\text{pmol/oocyte}\cdot\text{min}^{-1}$ averaged for 3 – 6 experiments. **B.** Represents mean ^{14}C -urate uptake expressed as % of urate uptake compared to osmotic control (5 mM PEG). “a” and “b” symbols above the bars denote statistically significant urate influx values from the control (5 mM PEG) for hSLC2A9a- and hSLC2A9b-producing oocytes, respectively ($p \leq 0.01$). # denotes statistical significance ($p \leq 0.05$) between hSLC2A9a and hSLC2A9b isoforms in response to intracellular urate and * denotes statistical significance ($p \leq 0.01$) between the two isoforms in response to intracellular D-glucose.

responses except that intracellular D-glucose produced no effect with respect to control. In other experiments, the non-metabolized D-glucose analogues 2DOG and 3OMG increased urate uptake into oocytes producing hSLC2A9a but not hSLC2A9b (data not shown). Significant differences between the two isoforms were also observed in response to intracellular urate and D-glucose, with hSLC2A9a's response to these intracellular substances being significantly greater than that of hSLC2A9b. The results also reveal interesting differences in permeant specificity between the exofacial and endofacial binding sites for hexoses. Specifically, while extracellular D-fructose was a poor accelerator of urate efflux in both hSLC2A9a- and hSLC2A9b-producing oocytes (**Figure 4.6**), it significantly increased urate uptake by both hSLC2A9 isoforms when placed inside the cell (**Figure 4.7**).

4.3.8 Nucleobase transport mediated by hSLC2A9

The pathways for nucleobase transport in mammalian cells have not been fully characterized and no human transporter specific for nucleobases has been cloned. Since hSLC2A9 has been shown to be a high capacity urate transporter (24), and since urate is a negatively charged purine nucleobase, we have tested the hypothesis that hSLC2A9 may also transport other nucleobases. In the cross-inhibition experiment in *Xenopus* oocytes shown in **Figure 4.8A**, hSLC2A9a-mediated urate transport (20 μ M; 100 mM NaCl, pH 7.5; 20 min flux) was measured in the absence (control) or presence of excess (0.2 - 5 mM) pyrimidine (uracil, thymine and cytosine) or purine (adenine, guanine, hypoxanthine and xanthine) nucleobases or the pyrimidine nucleoside uridine (5 mM).

Mediated transport of urate (uptake in RNA transcript-injected oocytes *minus* uptake in water-injected oocytes) was inhibited 55 % by excess (5 mM) unlabelled adenine, but was unaffected by any other nucleobases tested, or by uridine. The finding that hSLC2A9a-mediated urate transport was inhibited by adenine suggests that adenine may be an hSLC2A9 permeant¹.

Transport inhibition can occur in the absence of translocation of the inhibiting substance, and low-affinity permeants may not cause detectable cross-inhibition. The ability of hSLC2A9a or hSLC2A9b to transport nucleobases and uridine was therefore also measured directly with a panel of radiolabelled nucleobases and uridine. **Figure 4.8B** shows the uptake of nucleobases (20 μ M) and uridine (20 μ M) compared with urate in hSLC2A9a-producing oocytes and in control water-injected cells. hSLC2A9a transported urate at high levels and, consistent with the inhibition profile shown in **Figure 4.8A**, there was also a small, but significant amount of adenine transport (mediated fluxes of 0.71 ± 0.11 and 0.051 ± 0.010 pmol/oocyte.min⁻¹ for urate and adenine, respectively). No uptake was observed with any other nucleobases tested, or with uridine. Corresponding data for adenine, uridine and cytosine transport by hSLC2A9b in **Figure 4.8B** (*inset*) showed a similar pattern. Therefore, both hSLC2A9 isoforms are not entirely specific for urate, and mediate a small, but significant amount of adenine uptake. SLC2A9 does not, however, transport other purine (or pyrimidine) nucleobases. Functioning as a high capacity urate transporter, hSLC2A9 is not a major route for the entry of other nucleobases into cells.

¹ Alternatively, slight inhibition of SLC2A9-mediated urate transport by adenine may hint at a potential interaction of this transporter with xanthine-based drugs and / or cAMP. See Chapter 5 for further discussion.

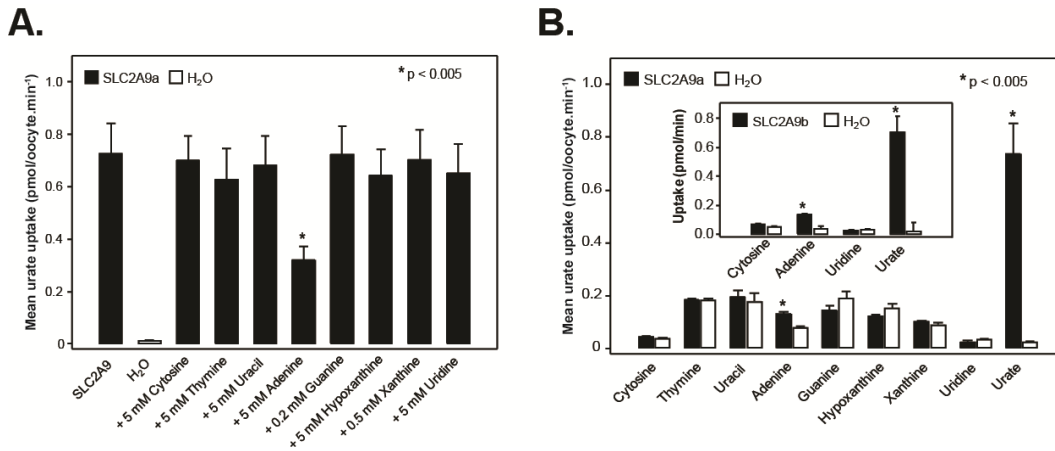


Figure 4.8. Nucleobase transport mediated by hSLC2A9. A. Inhibition of hSLC2A9a-mediated urate influx by pyrimidine and purine nucleobases and the pyrimidine nucleoside uridine. Urate (20 μ M; 100 mM NaCl, pH 7.5) influx was measured in hSLC2A9a-producing oocytes in the absence (control) or presence of excess nonradioactive nucleobases or uridine. Because of their low solubility, guanine and xanthine were added at concentrations of 0.2 mM and 0.5 mM, respectively. Other nucleobases and uridine were tested at a concentration of 5 mM. Values were corrected for basal non-mediated uptake in control water-injected oocytes and are means \pm S.E.M. of 10 - 12 oocytes. H₂O, water-injected oocytes. **B.** Uptake of 20 μ M radiolabelled pyrimidine and purine nucleobases (20 μ M) and the pyrimidine nucleoside uridine (20 μ M) were measured in oocytes producing SLC2A9a (■) or in control water-injected oocytes (□) and compared to the uptake of urate (20 μ M). Values are means \pm S.E.M. of 10 - 12 oocytes. The *inset* shows the same experiment repeated in oocytes producing hSLC2A9b.

4.4 Discussion

In this paper we have examined the membrane currents associated with urate fluxes mediated by human SLC2A9a and SLC2A9b produced in *Xenopus* oocytes. The uptake of the organic anion urate generated a membrane potential-sensitive outward current, the simplest interpretation of which is that urate enters the cell in its charged form with no coupled cation or anion movement, which confirms previous observations of mouse SLC2A9 full length being an electrogenic uniporter of urate (29, 32). In corresponding radiotracer flux studies under non-voltage clamped conditions, we have also found that the apparent K_m for urate efflux is equal or greater than that for uptake (~ 1 mM). Rates of urate influx and efflux are also similar, which suggests that the driving force of the membrane potential would favour urate efflux over influx under physiological conditions. Uptake of urate mediated by hSLC2A9 appears to be affected by the extracellular chloride concentration, but there is no evidence for the transporter to be exchanging these two anions. The ability for this transporter to also mediate the uptake of adenine suggests that this may provide an additional route of uptake for this nucleobase. hSLC2A9 does not, however, function as a generalized nucleobase transporter, and the fluxes of adenine relative to urate are small. hSLC2A9a is expressed in the basolateral membrane of hepatocytes, where the majority of urate is generated, and in the basolateral membrane of the kidney proximal convoluted tubule. In both sites, the membrane potential would promote the efflux of the organic anion into the plasma, helping to maintain the high circulating levels of this metabolite and providing a plausible mechanism for the contribution of hSLC2A9 SNPs to

hyperuricemia. However, the ultimate direction of flux facilitated by basolateral hSLC2A9 in both of the aforementioned organs will be determined by local electrochemical gradients of urate across the cell membranes in question, which to date have not been elucidated in the physiological setting. Given present information, it is still difficult to reconcile the curious phenotype of the Dalmatian dog, which displays hyperuricemia despite hyperuricosuria, expresses high levels of the basolateral (N) isoform and low levels of the apical (O) isoform of hSLC2A9 on the mRNA level, and has an amino acid substitution in TM5 not present in other breeds of dog, which differ in overall urate phenotype (17). It is unknown whether this C188F substitution renders the transporter inactive, but given the breed's inability to reabsorb urate in the kidney (uricosuria), it suggests that renal hSLC2A9-mediated urate efflux may be indeed compromised, strengthening the transporter's role in renal urate reabsorption. Furthermore, the Dalmatian model does not preclude hSLC2A9's role as a urate efflux pump in the liver, although it suggests that other transporters may be preferentially involved (eg. ABCC4 / MRP4). Also, it suggests that mechanisms other than SLC2A9 may be involved in urate uptake into hepatocytes (eg. SLCO1B3 / OATP1B3 (33), capable of organic anion transport), which may not be expressed in Dalmatians, explaining dog's inability to degrade plasma urate despite a functional liver uricase.

In contrast, the renal secretory route for urate is still under debate. Recently, a sodium-phosphate transporter 4 (SLC17A3/NTP4) has been implicated in urate secretion. According to Jutabha *et al.* (16), two missense mutations of this protein decreased urate transport in oocytes and were identified to cause hyperuricemia in Japanese patients. They have demonstrated SLC17A3 to be voltage-dependent and capable of

mediating urate movement across the membrane, along with many other organic anions. Moreover, a number of diuretics, which have been shown to cause hyperuricemia, were shown to interact with SLC17A3 by inhibiting PAH uptake. Given the above observations, the authors proposed that the urate secretory route is defined by a host of multispecific and drug-sensitive transporters, where apical SLC17A3 is thought to be one of the key players. They did not discuss the potential contribution of hSLC2A9b (ΔN), which is suggested to be expressed in the apical membrane of human proximal convoluted tubule epithelium (28), has high specificity for urate, is driven by membrane potential and, as such, is the likely apical component of the urate secretory route. In this case, the Dalmatian model does not offer any arguments for or against our model of apical hSLC2A9 isoform as a renal secretory route for urate. It is difficult to reconcile the low levels of apical SLC2A9 ((O) isoform) and the presence of an amino acid substitution (17), which may affect both isoforms' transport function, with the unusual urate-handling phenotype.

Thorough comparison of hSLC2A9a and hSLC2A9b in the present study has revealed that although both isoforms act as functionally symmetric uniporters of urate, where the membrane potential drives urate efflux across both poles of the cell, there are fundamental differences in the way these two splice variants respond to intracellular and extracellular monosaccharides. The effect of physiological levels of D-glucose on urate efflux seems to be more pronounced than that of D-fructose, which may explain the frequently observed association between hyperuricemia, hyperfructosemia and metabolic syndrome (34). Interestingly, there are also marked differences in hSLC2A9's isoform sensitivity to extracellular D-glucose, with the effect of *trans*-stimulation of urate efflux by D-glucose being lost in hSLC2A9b, the apical isoform. This observation has two

implications. First, this differential response, combined with uniform presence of extracellular D-glucose in the lumen and in the bloodstream, suggests that functional symmetry of the two isoforms is lost, favouring the basolateral efflux of urate *via* hSLC2A9a. Secondly, these results point to the potential, novel role of the N-terminus of hSLC2A9 in modulating the handling of urate and/or hexoses. How the presence or absence of the first 28 amino acids of the protein confers this difference is unclear, however, Ser9 on hSLC2A9a has been identified as a high probability residue for phosphorylation by PKA ((35), unpublished observation). Whether kinase activity at this site changes the hexose binding profile of the transporter or its interaction with other intracellular binding proteins is yet to be determined. D-fructose also produced a differential response in urate handling, stimulating urate uptake when placed inside the cell, and failing to significantly affect urate efflux when placed outside of the cell. In this case, both isoforms behaved in a similar manner, suggesting that there is asymmetry in permeant interaction between the exofacial and endofacial binding sites of the transporter, which is independent of the N-terminus. Finally, these subtle changes in hSLC2A9 isoform-specific responses to hexoses may be cell specific and may involve transporter's interaction with other accessory proteins. For example, hSLC2A9/GLUT9 KO mice do not display any abnormalities in glucose or fructose metabolism perhaps because of the distal expression of the transporter in the mouse renal tubule epithelium, in contrast to the more proximal distribution in humans. Moreover hyperuricemia has also been correlated with SNPs in PDZK1, a scaffold protein capable of direct and indirect interaction with membrane proteins. Although hSLC2A9 does not possess PDZ binding motifs (unpublished observation), it may interact with transcription factors or signaling messengers, which are modulated by PDZK1.

In summary, the unique expression pattern of hSLC2A9 in the human kidney proximal convoluted tubule and its electrogenic transport of urate strongly suggest that this transporter plays a key role in the maintenance of elevated plasma urate levels in humans, and is therefore a potentially important transport protein when investigating diseases associated with hyperuricemia and hypouricemia. Given the novel finding, that the two isoforms of hSLC2A9 display differential urate handling profiles in response to hexoses, the study of potential mechanisms of urate transport in the human kidney epithelium may yield possible new avenues for drug targeting for treatment of hyperuricemia and hypouricemia.

4.5 Bibliography

1. Hediger, M. A., Johnson, R. J., Miyazaki, H., and Endou, H. (2005) Molecular physiology of urate transport., *Physiology (Bethesda, Md.)* 20, 125-33.
2. Sautin, Y. Y., and Johnson, R. J. (2008) Uric acid: the oxidant-antioxidant paradox., *Nucleosides, nucleotides & nucleic acids* 27, 608-19.
3. Bo, S., Cavallo-Perin, P., Gentile, L., Repetti, E., and Pagano, G. (2001) Hypouricemia and hyperuricemia in type 2 diabetes: two different phenotypes., *European journal of clinical investigation* 31, 318-21.
4. Feig, D. I., Kang, D.-H., Nakagawa, T., Mazzali, M., and Johnson, R. J. (2006) Uric acid and hypertension., *Current hypertension reports* 8, 111-5.
5. Hjortnaes, J., Algra, A., Olijhoek, J., Huisman, M., Jacobs, J., Graaf, Y. van der, and Visseren, F. (2007) Serum uric acid levels and risk for vascular diseases in patients with metabolic syndrome., *The Journal of rheumatology* 34, 1882-7.
6. Onat, A., Uyarel, H., Hergenç, G., Karabulut, A., Albayrak, S., Sari, I., Yazici, M., and Keleş, I. (2006) Serum uric acid is a determinant of metabolic syndrome in a population-based study., *American journal of hypertension* 19, 1055-62.
7. Panoulas, V. F., Douglas, K. M. J., Milionis, H. J., Nightingale, P., Kita, M. D., Klocke, R., Metsios, G. S., Stavropoulos-Kalinoglou, a, Elisaf, M. S., and Kitas, G. D. (2008) Serum uric acid is independently associated with hypertension in patients with rheumatoid arthritis., *Journal of human hypertension* 22, 177-82.
8. Rathmann, W., Haastert, B., Icks, A., Giani, G., and Roseman, J. M. (2007) Ten-year change in serum uric acid and its relation to changes in other metabolic risk factors in young black and white

adults: the CARDIA study., *European journal of epidemiology* 22, 439-45.

9. Marangella, M. (2005) Uric acid elimination in the urine. Pathophysiological implications., *Contributions to nephrology* 147, 132-48.
10. Enomoto, A., Kimura, H., Chairoungdua, A., Shigeta, Y., Jutabha, P., Cha, S. H., Hosoyamada, M., Takeda, M., Sekine, T., Igarashi, T., Matsuo, H., Kikuchi, Y., Oda, T., Ichida, K., Hosoya, T., Shimokata, K., Niwa, T., Kanai, Y., and Endou, H. (2002) Molecular identification of a renal urate anion exchanger that regulates blood urate levels., *Nature* 417, 447-52.
11. Anzai, N., Kanai, Y., and Endou, H. (2007) New insights into renal transport of urate., *Current opinion in rheumatology* 19, 151-7.
12. Jutabha, P., Kanai, Y., Hosoyamada, M., Chairoungdua, A., Kim, D. K., Iribe, Y., Babu, E., Kim, J. Y., Anzai, N., Chatsudthipong, V., and Endou, H. (2003) Identification of a novel voltage-driven organic anion transporter present at apical membrane of renal proximal tubule., *The Journal of biological chemistry* 278, 27930-8.
13. Aubel, R. A. M. H. Van, Smeets, P. H. E., Heuvel, J. J. M. W. van den, and Russel, F. G. M. (2005) Human organic anion transporter MRP4 (ABCC4) is an efflux pump for the purine end metabolite urate with multiple allosteric substrate binding sites., *American journal of physiology. Renal physiology* 288, F327-33.
14. Yu, X.-Q., Xue, C. C., Wang, G., and Zhou, S.-F. (2007) Multidrug resistance associated proteins as determining factors of pharmacokinetics and pharmacodynamics of drugs., *Current drug metabolism* 8, 787-802.
15. Woodward, O. M., Köttgen, A., Coresh, J., Boerwinkle, E., Guggino, W. B., and Köttgen, M. (2009) Identification of a urate transporter, ABCG2, with a common functional polymorphism causing gout., *Proceedings of the National Academy of Sciences of the United States of America* 106, 10338-42.
16. Jutabha, P., Anzai, N., Kimura, T., Taniguchi, A., Urano, W., Yamanaka, H., Endou, H., and Sakurai, H. (2011) Functional Analysis of Human Sodium-Phosphate Transporter 4

(NPT4/SLC17A3) Polymorphisms, *Journal of Pharmacological Sciences* 115, 249-253.

17. Bannasch, D., Safra, N., Young, A., Karmi, N., Schaible, R. S., and Ling, G. V. (2008) Mutations in the SLC2A9 gene cause hyperuricosuria and hyperuricemia in the dog., *PLoS genetics* 4, e1000246.
18. Matsuo, H., Chiba, T., Nagamori, S., Nakayama, A., Domoto, H., Phetdee, K., Wiriyasermkul, P., Kikuchi, Y., Oda, T., Nishiyama, J., Nakamura, T., Morimoto, Y., Kamakura, K., Sakurai, Y., Nonoyama, S., Kanai, Y., and Shinomiya, N. (2008) Mutations in glucose transporter 9 gene SLC2A9 cause renal hypouricemia., *American journal of human genetics* 83, 744-51.
19. Dinour, D., Gray, N. K., Campbell, S., Shu, X., Sawyer, L., Richardson, W., Rechavi, G., Amariglio, N., Ganon, L., Sela, B.-A., Bahat, H., Goldman, M., Weissgarten, J., Millar, M. R., Wright, A. F., and Holtzman, E. J. (2010) Homozygous SLC2A9 mutations cause severe renal hypouricemia., *Journal of the American Society of Nephrology: JASN* 21, 64-72.
20. Stiburkova, B., Ichida, K., and Sebesta, I. (2011) Novel homozygous insertion in SLC2A9 gene caused renal hypouricemia., *Molecular genetics and metabolism* 102, 430-5.
21. Anzai, N., Ichida, K., Jutabha, P., Kimura, T., Babu, E., Jin, C. J., Srivastava, S., Kitamura, K., Hisatome, I., Endou, H., and Sakurai, H. (2008) Plasma urate level is directly regulated by a voltage-driven urate efflux transporter URATv1 (SLC2A9) in humans., *The Journal of biological chemistry* 283, 26834-8.
22. Leal-Pinto, E., Tao, W., Rappaport, J., Richardson, M., Knorr, B. A., and Abramson, R. G. (1997) Molecular cloning and functional reconstitution of a urate transporter/channel., *The Journal of biological chemistry* 272, 617-25.
23. Brandstätter, A., Kiechl, S., Kollerits, B., Hunt, S. C., Heid, I. M., Coassin, S., Willeit, J., Adams, T. D., Illig, T., Hopkins, P. N., and Kronenberg, F. (2008) Sex-specific association of the putative fructose transporter SLC2A9 variants with uric acid levels is modified by BMI., *Diabetes care* 31, 1662-7.

24. Caulfield, M. J., Munroe, P. B., O'Neill, D., Witkowska, K., Charchar, F. J., Doblado, M., Evans, S., Eyheramendy, S., Onipinla, A., Howard, P., Shaw-Hawkins, S., Dobson, R. J., Wallace, C., Newhouse, S. J., Brown, M., Connell, J. M., Dominiczak, A., Farrall, M., Lathrop, G. M., Samani, N. J., Kumari, M., Marmot, M., Brunner, E., Chambers, J., Elliott, P., Kooner, J., Laan, M., Org, E., Veldre, G., Viigimaa, M., Cappuccio, F. P., Ji, C., Iacone, R., Strazzullo, P., Moley, K. H., and Cheeseman, C. (2008) SLC2A9 is a high-capacity urate transporter in humans., *PLoS medicine* 5, e197.
25. Dehghan, A., Köttgen, A., Yang, Q., Hwang, S.-J., Kao, W. L., Rivadeneira, F., Boerwinkle, E., Levy, D., Hofman, A., Astor, B. C., Benjamin, E. J., Duijn, C. M. van, Witteman, J. C., Coresh, J., and Fox, C. S. (2008) Association of three genetic loci with uric acid concentration and risk of gout: a genome-wide association study., *Lancet* 372, 1953-61.
26. Stark, K., Reinhard, W., Neureuther, K., Wiedmann, S., Sedlacek, K., Baessler, A., Fischer, M., Weber, S., Kaess, B., Erdmann, J., Schunkert, H., and Hengstenberg, C. (2008) Association of common polymorphisms in GLUT9 gene with gout but not with coronary artery disease in a large case-control study., *PloS one* 3, e1948.
27. Vitart, V., Rudan, I., Hayward, C., Gray, N. K., Floyd, J., Palmer, C. N. a, Knott, S. a, Kolcic, I., Polasek, O., Graessler, J., Wilson, J. F., Marinaki, A., Riches, P. L., Shu, X., Janicijevic, B., Smolej-Narancic, N., Gorgoni, B., Morgan, J., Campbell, S., Biloglav, Z., Barac-Lauc, L., Pericic, M., Klaric, I. M., Zgaga, L., Skaric-Juric, T., Wild, S. H., Richardson, W. a, Hohenstein, P., Kimber, C. H., Tenesa, A., Donnelly, L. A., Fairbanks, L. D., Aringer, M., McKeigue, P. M., Ralston, S. H., Morris, A. D., Rudan, P., Hastie, N. D., Campbell, H., and Wright, A. F. (2008) SLC2A9 is a newly identified urate transporter influencing serum urate concentration, urate excretion and gout., *Nature genetics* 40, 437-42.
28. Augustin, R., Carayannopoulos, M. O., Dowd, L. O., Phay, J. E., Moley, J. F., and Moley, K. H. (2004) Identification and characterization of human glucose transporter-like protein-9 (GLUT9): alternative splicing alters trafficking., *The Journal of biological chemistry* 279, 16229-36.
29. Bibert, S., Hess, S. K., Firsov, D., Thorens, B., Geering, K., Horisberger, J.-D., and Bonny, O. (2009) Mouse GLUT9: evidences

for a urate uniporter., *American journal of physiology. Renal physiology* 297, F612-9.

30. Shayeghi, M., Akerman, R., and Jarvis, S. M. (1999) Nucleobase transport in opossum kidney epithelial cells and *Xenopus laevis* oocytes: the characterisation, structure-activity relationship of uracil analogues and oocyte expression studies of sodium-dependent and -independent hypoxanthine uptake., *Biochimica et biophysica acta* 1416, 109-18.
31. Doblado, M., and Moley, K. H. (2009) Facilitative glucose transporter 9, a unique hexose and urate transporter., *American journal of physiology. Endocrinology and metabolism* 297, E831-5.
32. Preitner, F., Bonny, O., Laverrière, A., Rotman, S., Firsov, D., Costa, A. Da, Metref, S., and Thorens, B. (2009) Glut9 is a major regulator of urate homeostasis and its genetic inactivation induces hyperuricosuria and urate nephropathy., *Proceedings of the National Academy of Sciences of the United States of America* 106, 15501-6.
33. Le, M. T., Shafiu, M., Mu, W., and Johnson, R. J. (2008) SLC2A9--a fructose transporter identified as a novel uric acid transporter., *Nephrology, dialysis, transplantation: official publication of the European Dialysis and Transplant Association - European Renal Association* 23, 2746-9.
34. Miller, A., and Adeli, K. (2008) Dietary fructose and the metabolic syndrome., *Current opinion in gastroenterology* 24, 204-9.
35. Blom, N., Gammeltoft, S., and Brunak, S. (1999) Sequence and structure-based prediction of eukaryotic protein phosphorylation sites., *Journal of molecular biology* 294, 1351-62.

Chapter

5

Differential regulation of urate
handling by human SLC2A9a and
SLC2A9b isoforms in *Xenopus laevis*
oocytes

5.1 Acknowledgements and contributions

All the experiments presented in this chapter were performed by Kate Witkowska. Special thanks are extended to Debbie O'Neill in the Cheeseman laboratory who helped with oocyte isolation and manipulation. The hSLC2A9 antibodies were a gracious gift from Dr. Kelle Moley, Washington University.

Funding for this project was provided by Canadian Institutes of Health Research (CIHR).

5.2 Introduction

Three years ago many GWAS studies independently recognized the link between the *hSLC2A9* gene and abnormal urate levels (1–7). It is now well established that the facilitative hexose transporter isoform 9 (GLUT9), originally characterized as a high affinity D-glucose / D-fructose transporter (8, 9), is in fact a high capacity urate transporter under physiological conditions. To date, four mutations within *hSLC2A9* have been functionally described. These give rise to amino acid substitutions that affect the urate handling capacity of the transporter, and which are associated with hypouricemia (10, 11). Furthermore, four naturally occurring SNPs have been identified by Phay *et al.*, 2000 during the initial cloning of hGLUT9 (12). Given the wealth of literature linking this gene's SNPs with plasma urate imbalance, hypertension, cardiovascular disease and metabolic syndrome, some of these may play a role as contributing factors (13–16). However, the causal relationship between genetic defects in *hSLC2A9* and aforementioned morbidity is not always apparent concluding that urate imbalance may not be a direct causative factor, and, as anticipated, that these diseases are multifactorial in nature.

Despite avid interest in uric acid in man since the beginning of the 1800's (17) and the impact urate imbalance has on human health, we still have much to learn about the molecular identities and the regulatory mechanisms that control urate homeostasis in humans going beyond its division into glomerular filtration (100%), proximal reabsorption (99.3%), secretion (50%), distal reabsorption (40%), thus resulting in 10 – 12% of filtered urate excreted (18). Purines derived from endogenous (cellular

degradation) and exogenous (diet) sources undergo a series of enzymatic catabolic steps. In human, genetic silencing of the uricase gene has made uric acid the final breakdown product of purine metabolism, eliminating excretion of the more soluble allantoin (19). Resultant tenfold elevation of plasma urate levels in man, compared with lower mammals, is thought to have anti-oxidant properties, contributing to extraordinary longevity of man (16, 20). However, even 10 μ M changes in plasma urate level set-point, which is also influenced by factors such as age, gender and race (7, 14, 21), can lead to disease states. Tightly controlled processes of renal reabsorption and secretion are probably at play in urate homeostasis maintenance.

Three key papers by Roch-Ramel *et al.*, used human BBMVs prepared from superficial cortex of human kidneys to study different modes of urate transport in human epithelium (22–24). Of most importance was the identification of two distinct apical routes for urate movement: high affinity urate / anion exchange mechanisms and a voltage-dependent urate efflux pump, with a complex affinity profile for uricosurics and diuretics. Today, many molecular identities of putative urate transporters have been elucidated (for review see Chapter 1.5 or (13, 14, 25)). hURAT1 (SLC22A11) was the first urate-specific transporter cloned (26). Its high affinity for urate ($K_m = 371 \pm 28 \mu\text{M}$), its ability to exchange it with Cl⁻, lactate, PZA and nicotinate, and its apical expression in PCT fits with the high affinity exchange urate route proposed by Roch-Ramel *et al.*, 1994 (22) and revisited in 1999 (27). Furthermore, its lack of sensitivity to PAH fits the description of the human urate transport pathways, which, in marked contrast with the rodent model, are PAH-independent. In addition, the proposed link with SMCT (28), although not

tested functionally, would explain the existence of the tertiary Na^+ -dependent urate transport reported by Roch-Ramel *et al.*, 1996 (23).

Another apical urate pathway discerned in the BBMV studies was voltage-dependent with distinct specificity for benzbromarone. To date, only three molecular identities of urate-specific apical transporters have been discerned: MRP4 (ABCC4) (29), ABCG2 (30) and the apically targeted isoform b of SLC2A9 ((9), Chapter 3). Of these only SLC2A9b shows a specific benzbromarone inhibition (Chapter 3), and could have contributed to the voltage-dependent urate fluxes under the particular prep conditions (Chapter 4).

Less can be postulated about urate permeation pathways on the basolateral membrane of the kidney PCT epithelium, as no studies with human PCT basolateral membrane vesicles have been done. Presumably, another voltage-dependent efflux pump exists completing the transcellular urate reabsorption process (27). The most likely candidate for that is hSLC2A9a, as it is the most specific voltage-dependent urate transporter, which under physiologic conditions acts as an efflux pump, and is expressed basolaterally in the PCT epithelium (Chapter 4)

As discussed at length in Chapter 4 of this thesis, the two isoforms of SLC2A9, despite their similar kinetic profile of urate-handling, display differential hexose-carrier-urate interactions with respect to intracellular and extracellular hexoses. In this chapter, the potential mechanisms underlying those differences will be explored.

5.3 Results

5.3.1 N-terminus of hSLC2A9 isoforms confers differential responsiveness of carrier to kinases

Since the two isoforms of hSLC2A9 differ only in their N-terminal region (9), we have examined these sequences more closely in search of clues explaining the differences in hSLC2A9a and hSLC2A9b urate handling in response to *trans*-hexoses. As shown in **Figure 5.1**, the two proteins appear to be true splice variants, with N-terminal amino acid residue differences, which lead to alternative putative phosphorylation sites. Since only Serine residues (Ser, S) displayed different patterns of modification, we have focused on Ser phosphorylation sites for the remainder of this study. Thus, we have investigated the responsiveness of the two transporter splice variants to elevated levels of intracellular 2^o messenger cAMP and to a general Protein Kinase C (PKC) activator, since these two kinases are predicted to phosphorylate the amino terminus in a varied manner. In order to elevate intracellular cAMP concentrations 200µM forskolin (adenylate cyclase activator), 200µM 3-isobutyl-1-methylxanthine (IBMX, nonselective phosphodiesterase inhibitor) or a mixture of 200µM IBMX and 200µM forskolin were applied to the extracellular medium for 20 minutes at room temperature, while 100µM ¹⁴C-urate uptake into *Xenopus* oocytes was measured. As shown in **Figure 5.2A**, either of the drugs alone had no effect on hSLC2A9a- or

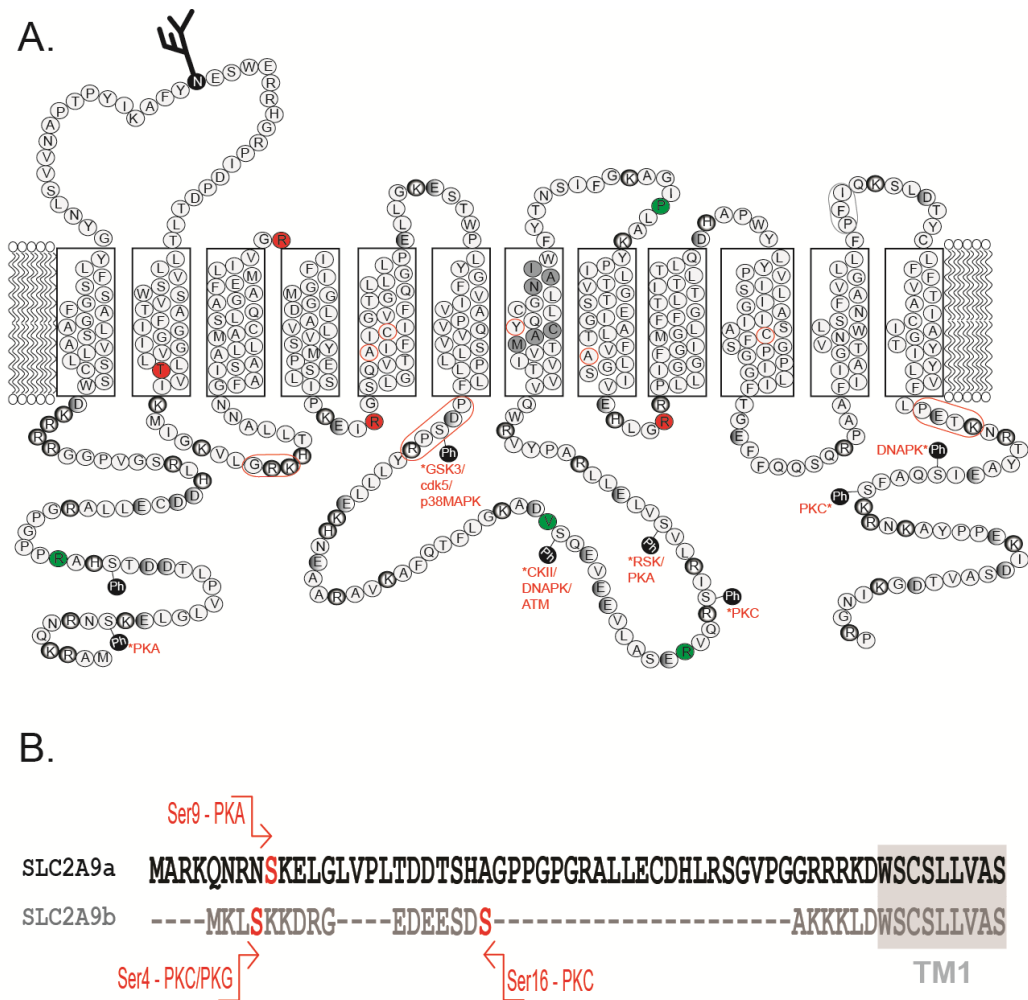


Figure 5.1. Comparing sequence alignments of the N terminus of hSLC2A9a and hSLC2A9b isoforms. A. Topology model for hSLC2A9a isoform. Circled letters represent amino acids. (●) – amino acids identified to have functional importance via GWAS; (●) – naturally occurring SNPs; (○ and ●) – positive and negative residues, respectively; (○) – residues implicated in hGLUT1 – D-glucose interaction which are not conserved in hSLC2A9; (●) – motif residues thought to play a role in substrate selectivity; (○ and ○) – sugar transporter and class II GLUT motifs, respectively; (Ph) – putative phosphorylation sites with prediction scores $P > 0.5$ (www.cbs.dtu.dk/services/NetPhos/); (*) – putative kinases targeting the marked sites with prediction scores $P > 0.5$ (<http://www.cbs.dtu.dk/services/NetPhosK/>). **B.** Sequence alignment comparing the N terminal region of the two hSLC2A9 isoforms. Serine residues (S) represent high probability of phosphorylation by indicated kinases, as predicted *in silico*.

hSLC2A9b-mediated 100 μ M urate uptake into *Xenopus* oocytes, however when applied in combination, the two drugs significantly decreased hSLC2A9b-mediated urate uptake into the cells with respect to the solvent control. This observation that single drug administration produced no changes in urate transport ruled out the possible non-specific interaction of methyl xanthines (eg. IBMX) with the SLC2A9 transport protein, and was strengthened by the isoform-specific responses observed with the drug combination. To test the possible involvement of PKC, or its downstream targets, we have applied an activator of PKC, phorbol 12-myristate 13-acetate (PMA), at a concentration of 0.2 μ M in the same manner as the cAMP-augmenting drugs. **Figure 5.2B** shows that PMA significantly increased 100 μ M 14 C-urate uptake into the oocytes expressing hSLC2A9a, but not hSLC2A9b, as compared with the solvent control. As such, we have established drug administration conditions which elicit a measurable response while, presumably being brief enough, not to elicit protein transcription and translation effects. Given that only the combination of IBMX and Forskolin produced a response, we have used this treatment for the remainder of experiments presented here.

Finally, to verify that the observed response was specific to the kinase activity in question, we have used potent, specific inhibitors H89 dichloride and Bisindolylmaleimide IV of PKA and PKC, respectively. The drugs were dissolved in DMSO, and oocytes were preincubated with the inhibitors (0.5 μ M final concentration) prior to the start of uptake for 40 minutes, as well as during the duration of uptake, for a total of 1 hour of incubation with inhibitor. cAMP elevating drugs (IBMX + Forskolin) or PKC activator (PMA) were used in the same manner as before, added to the uptake medium for 20 minutes only. **Figure 5.3** shows the effect of this

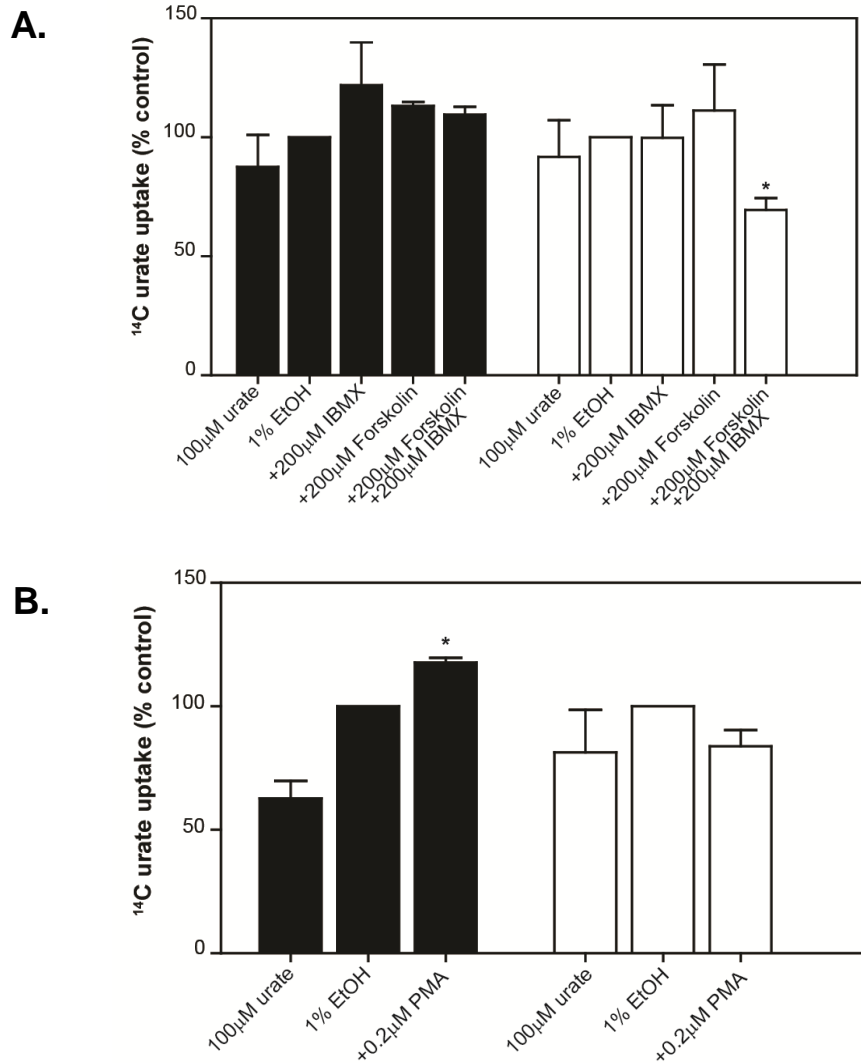


Figure 5.2. hSLC2A9a- and hSLC2A9b-expressing *Xenopus* oocytes show different ¹⁴C-urate uptake profiles in response to PKA and PKC modulation. Oocytes were injected with corresponding cRNA 4 days prior to uptake experiments, which were carried out at room temperature (22°C). Drugs were applied only for the duration of uptake (20 min). Bars represent net 100 μM ¹⁴C-urate uptake into hSLC2A9a-expressing oocytes (■) or hSLC2A9b-expressing oocytes (□), corrected for solvent control; **A.** Responses to elevated intracellular cAMP; **B.** Responses to PKC activator; Averaged for 10 - 12 oocytes; Vertical bars represent ± S.E.M. n = 3. (*) – P ≤ 0.05, significance from solvent control.

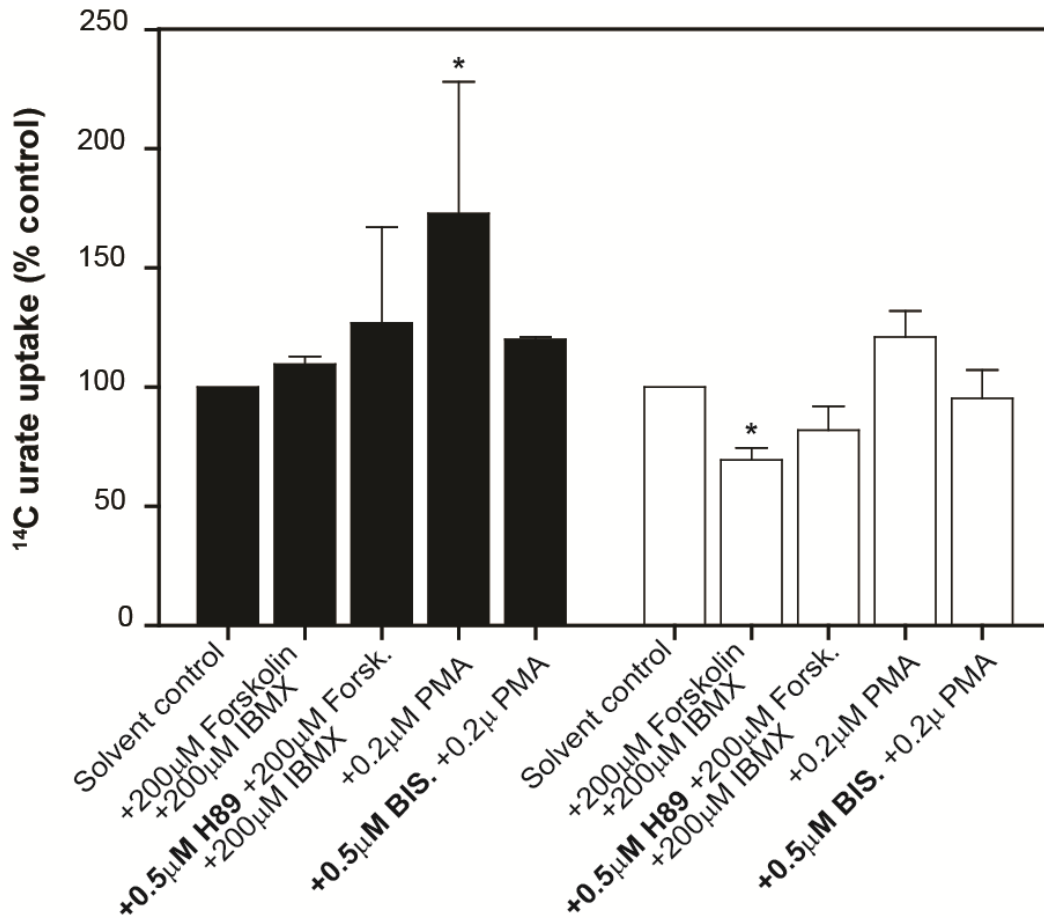


Figure 5.3. Effect of inhibitors on hSLC2A9a- and hSLC2A9b-mediated ^{14}C -urate uptake in *Xenopus* oocytes. Oocytes were injected with corresponding cRNA 4 days prior to uptake experiments, which were carried out at room temperature (22°C). Activators were applied only for the duration of uptake (20 min) while inhibitors were applied for a total of 1 hour (40 min preincubation + 20 min uptake). Bars represent net $100\mu\text{M}$ ^{14}C -urate uptake into hSLC2A9a-expressing oocytes (■) or hSLC2A9b-expressing oocytes (□) corrected for solvent control; Averaged for 10 - 12 oocytes; Vertical bars represent \pm S.E.M. $n = 2 - 4$. (*) – $P \leq 0.05$, significance from control.

manipulation on both hSLC2A9a- and hSLC2A9b- mediated urate uptake at a concentration of 100 μ M. Consistent with previous observations, cAMP and PKC stimulation affected hSLC2A9b and hSLC2A9a isoforms, respectively. 0.5 μ M concentrations of both inhibitors abolished these responses, indicating that differential modulation of the two isoforms by the different kinases, their downstream effects, or the kinases' complex interplay is possible.

5.3.2 Kinase modulators affect hSLC2A9 isoforms' catalytic properties of urate uptake

Having established drug application conditions, we sought to investigate whether the applied kinase modulators affect membrane protein expression and / or its catalytic activity. Hence, we have performed an uptake experiment using urate concentrations closer to the K_m value determined for SLC2A9a and SLC2A9b (~1mM, see Chapter 3). In contrast to the 100 μ M 14 C-urate concentration tested in **Figure 5.2**, 500 μ M 14 C-urate uptake revealed differences in the isoforms' responses to elevated intracellular cAMP levels (IBMX + forskolin treatment). First, hSLC2A9b's decrease in urate uptake at 100 μ M was not observed when 500 μ M urate was used (**Figure 5.4**). Also, at 500 μ M urate concentration, 200 μ M equimolar mixture of forskolin and IBMX produced a significant decrease in hSLC2A9a-mediated 14 C-urate uptake, which was not seen at the lower substrate concentration. The PKC activator, 0.2 μ M PMA, produced a response observed with hSLC2A9a- but not hSLC2A9b-expressing oocytes when 14 C-urate uptake was measured at both 100 μ M

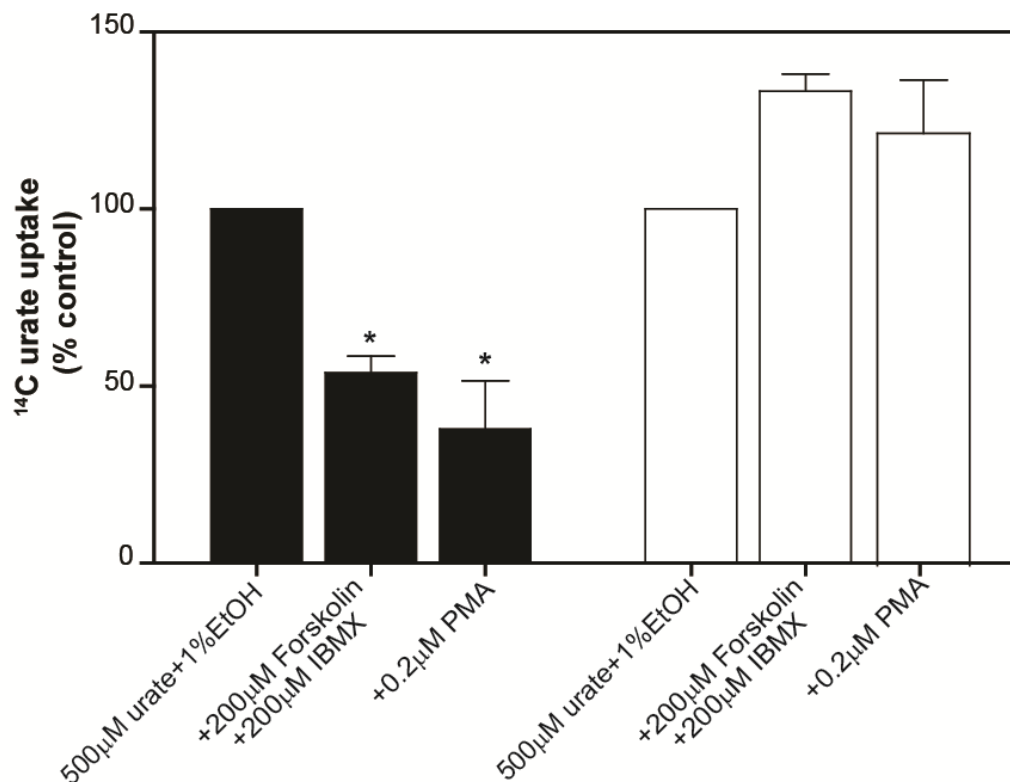


Figure 5.4. hSLC2A9a- and hSLC2A9b-expressing *Xenopus* oocytes show different ¹⁴C-urate uptake profiles in response to PKA and PKC modulation. Oocytes were injected with corresponding cRNA 4 days prior to uptake experiments, which were carried out at room temperature (22°C). Drugs were applied only for the duration of uptake (20 min). Bars represent net 500µM ¹⁴C-urate uptake into hSLC2A9a-expressing oocytes (■) or hSLC2A9b-expressing oocytes (□) expressed as % of solvent control; Averaged for 10 - 12 oocytes; Vertical bars represent ± S.E.M. n = 3. (*) – P ≤ 0.05, significance from control.

and 500 μ M, although when tested at lower substrate concentrations the drug upregulated hSLC2A9a-mediated urate uptake, while at higher concentrations, the drug decreased 14 C-urate accumulation (**Figure 5.4**). Cell-surface biotinylation performed in conjunction with the 500 μ M urate uptake experiments suggests that the amount of hSLC2A9a protein expressed in the oocyte membrane was the same under the control and the PMA-treated conditions (**Figure 5.5**).

To address the discrepancy observed in hSLC2A9 isoforms' response to drug treatments when single urate concentrations were used, we performed kinetic experiments to further investigate the effects that elevated cAMP and activated PKC may have on urate handling ability of the two carrier isoforms. **Figure 5.6** shows representative curves for kinetic experiments, which were performed in triplicate. All conditions were tested on the same day to assure comparable levels of protein expression in the oocytes.

When the individual kinetic constants, K_m and V_{max} , were averaged, application of 0.2 μ M PMA produced a statistically significant increase in both parameters of hSLC2A9a- but not hSLC2A9b-mediated urate uptake (kinetic constants in absence and presence of PMA – K_m (mM): 0.79 \pm 0.40 vs. 1.97 \pm 0.43; V_{max} (pmol/ oocyte.20 min $^{-1}$): 555 \pm 5.10 vs. 940 \pm 2.17; **Figure 5.7**). Furthermore, the change in K_m and V_{max} of hSLC2A9a isoform in response to the drug yielded a concomitant increase in the ratio of K_m / V_{max} from 0.0035 \pm 0.0004 to 0.0059 \pm 0.0004, further supporting the notion that PKC activity alters the affinity of the full-length carrier for urate. Given that no functional changes in hSLC2A9a abundance were observed (**Figure 5.5**), it appears that the protein undergoes an intrinsic modification, possibly phosphorylation of Ser residues, to modulate its

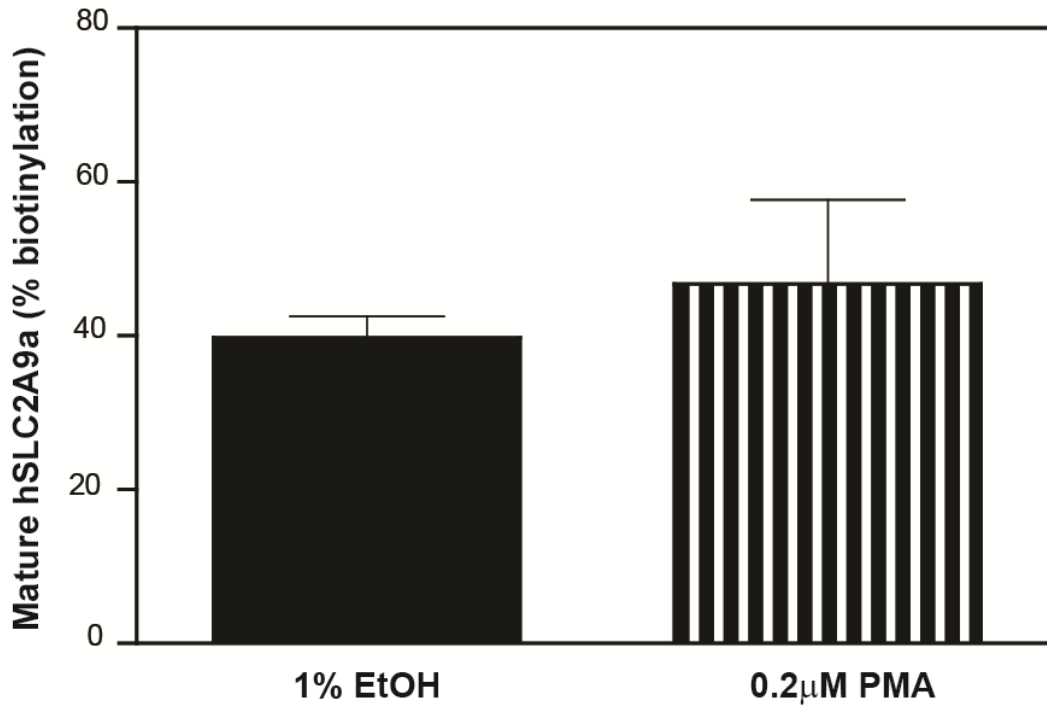


Figure 5.5. Cell-surface biotinylation of hSLC2A9a-expressing *Xenopus* oocytes. Oocytes were injected with hSLC2A9a cRNA 4 days prior to the experiments, which were carried out at room temperature (22°C). The drug or the solvent control (3ml) were applied for 20 min with gentle mixing to batches of 100 oocytes per condition, followed by biotinylation. Three lanes per condition were ran per condition: total biotinylated membrane protein (total), protein not bound by streptavidin (unbound), and biotinylated, streptavidin bound fractions (bound). Densitometry was performed on the mature (glycosylated) band. Amount of mature hSLC2A9a was calculated as percent of total protein by either subtracting unbound from total or by using the bound reading only. The two were averaged to give representative reading for each experiment; Mean densitometry for hSLC2A9a-expressing oocytes preincubated with solvent control (■) or with 0.2µM PMA (▨); Vertical bars represent standard deviation. n = 3.

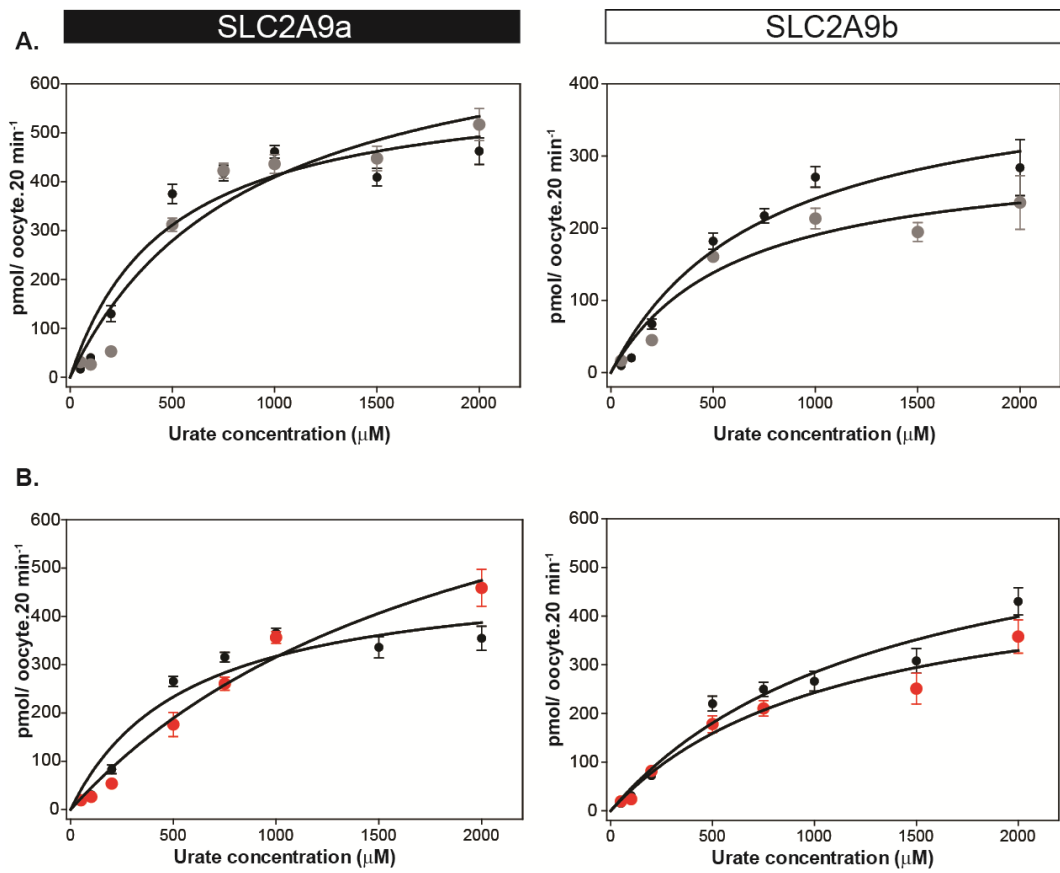


Figure 5.6. Representative Michaelis-Menten fits of hSLC2A9a- and hSLC2A9b-mediated ^{14}C -urate uptake into *Xenopus* oocytes in presence of kinase modulators. Oocytes were injected with corresponding cRNA 4 days prior to uptake experiments, which were carried out at room temperature (22°C). Drugs were applied only for the duration of uptake (20 min). Filled circles represent net ^{14}C -urate uptake over the indicated range of concentrations. (●) – respective hSLC2A9 isoform’s urate uptake in solvent control (1% EtOH); **A.** hSLC2A9a and hSLC2A9b-mediated urate uptake in presence of 200 μM IBMX + 200 μM Forskolin (●); **B.** hSLC2A9a and hSLC2A9b-mediated urate uptake in presence of 0.2 μM PMA (●); Averaged for 10 - 12 oocytes; Vertical bars represent \pm S.E.M.

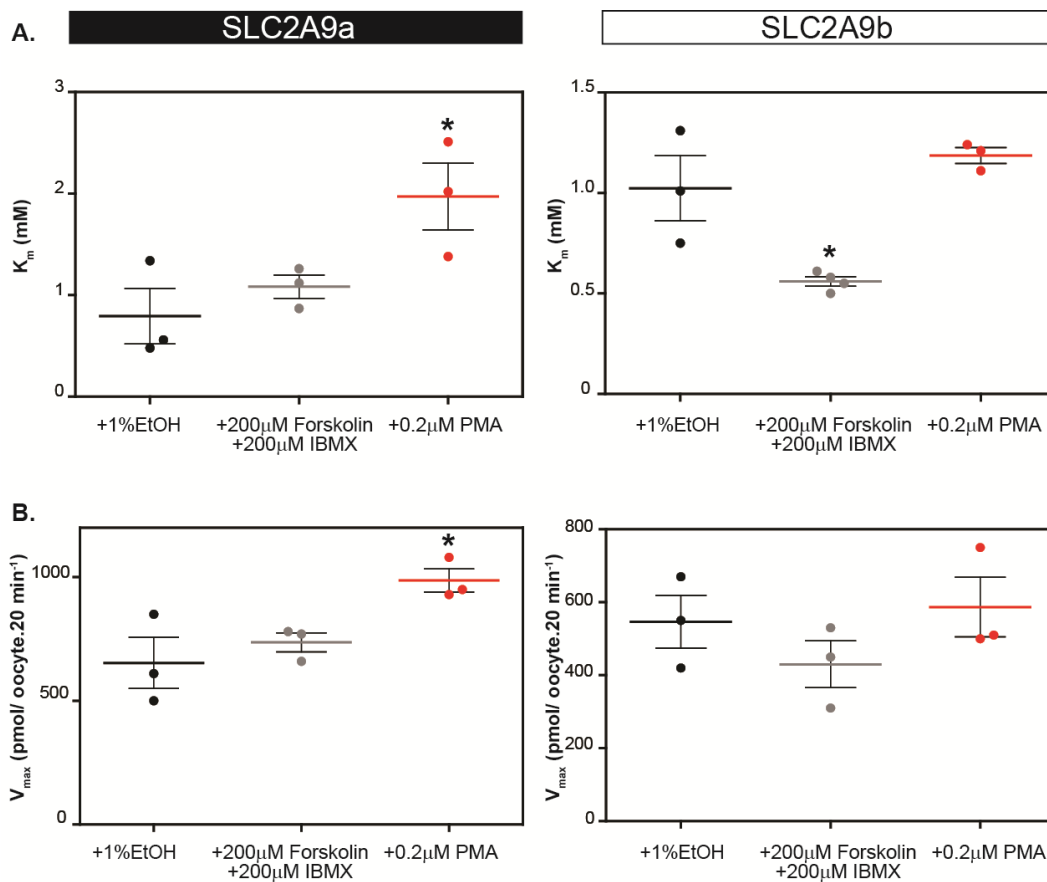


Figure 5.7. Mean values of kinetic constants for hSLC2A9a- and hSLC2A9b-mediated ^{14}C -urate uptake into *Xenopus* oocytes in presence of kinase modulators. Oocytes were injected with corresponding cRNA 4 days prior to uptake experiments, which were carried out at room temperature (22°C). Drugs were applied only for the duration of uptake (20 min). Filled circles represent individual values for K_m (A) and V_{max} (B). (●) – respective hSLC2A9 isoform's urate uptake in solvent control (1% EtOH); (●) – respective hSLC2A9 isoform's urate uptake in presence of 200µM IBMX + 200µM Forskolin; (●) – respective isoform's urate uptake in presence of 0.2µM PMA. Vertical bars represent \pm S.E.M. $n = 3 - 4$. (*) – $P \leq 0.05$, significance from control.

capacity to handle urate. The effect of IBMX / Forskolin on hSLC2A9a seen at 500 μ M but not at 100 μ M concentration (**Figure 5.4** vs. **Figure 5.2**) did not reach statistical significance when investigated over a range of urate concentrations, although hSLC2A9a's V_{max} had the tendency to increase in value upon intracellular cAMP elevation. It is unclear as to how that correlates with decreased urate uptake observed at 500 μ M.

In contrast, elevation of intracellular cAMP levels affected hSLC2A9b- but not hSLC2A9a-mediated urate uptake. More specifically, the K_m value decreased significantly (K_m (mM): 1.02 \pm 0.31 vs. 0.55 \pm 0.14) after application of equivalent concentrations of IBMX and Forskolin into the extracellular medium (**Figure 5.6**). Since V_{max} was unaffected by the drug, the K_m / V_{max} ratios also decreased (0.0047 \pm 0.0008 vs. 0.0031 \pm 0.0006), supporting the notion that activation of the cAMP-dependent pathway increased the apparent affinity of hSLC2A9b for urate. It is unclear as to why the drug panel at 100 μ M urate concentration showed significant decrease in hSLC2A9b-mediated urate uptake at low urate concentrations (**Figure 5.2**).

5.3.3 Kinase modulators affect hSLC2A9 isoforms' catalytic properties of urate efflux

As shown in Chapter 4, both isoforms of hSLC2A9 mediate electrogenic transport of urate which does not appear to be accompanied by the movement of ions such as Na⁺ or Cl⁻. Thus, in combination with the existing electrochemical gradient should favour hSLC2A9 function as an

efflux pump under physiological conditions. To test the observation of differential regulation of urate flux by cAMP- and PKC-dependent pathways, we have applied the aforementioned drugs to the extracellular medium while measuring ^{14}C -urate efflux from the oocytes (described in detail in Chapters 2 – 4). In this case, the cells were in contact with the drugs for 14 minutes, equivalent to the duration of efflux measurements.

As seen in **Figure 5.8**, efflux data fits well with the detailed analysis obtained for hSLC2A9a- and hSLC2A9b-mediated urate uptake. hSLC2A9a isoform responded to 0.2 μM PMA resulting in significant increase in rate of ^{14}C -urate efflux, which in all cases was corrected for the variations in the intracellular urate concentrations. cAMP elevation inside the oocytes did not evoke significant changes in ^{14}C -urate efflux mediated by either isoform. A plausible explanation may be that the incubation time of 14 minutes (versus 20 minutes used for uptake studies) may be too short to elicit a response by the latter drugs.

5.3.4 Ser9 and Ser22 may serve as sites for modulation of hSLC2A9a urate handling by PKC

As indicated in **Figure 5.1**, the N-terminus of the two splice variants of hSLC2A9 offers alternative putative phosphorylation sites for the two proteins. Given the very reproducible response of the basolateral hSLC2A9a isoform to PKC activation seen for both urate uptake and efflux, we have focused our investigation on the longer N-terminus. In particular, we chose to investigate the serine residues, since neither

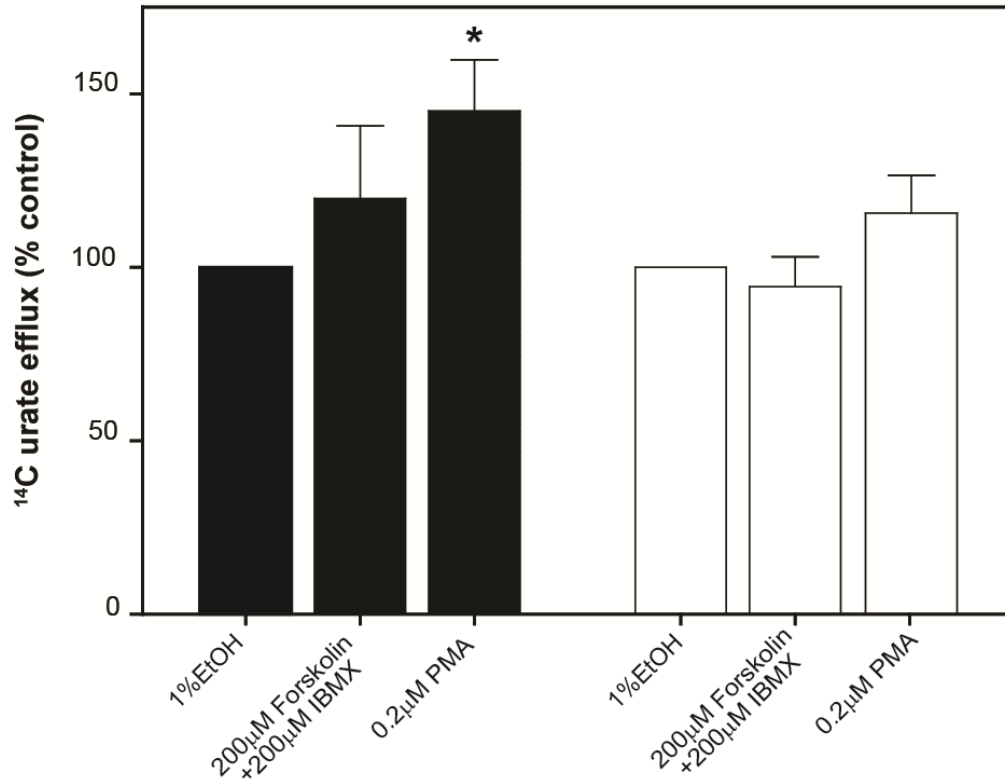


Figure 5.8. hSLC2A9a- and hSLC2A9b-expressing *Xenopus* oocytes show different ¹⁴C-urate efflux profiles in response to PKA and PKC modulation. Oocytes were injected with corresponding cRNA 4 days prior to uptake experiments, which were carried out at room temperature (22°C). Immediately prior to the experiment oocytes were injected with ~50nl of ¹⁴C-urate to achieve an intracellular [urate] ranging from 50 - 175μM. 20nl of extracellular media was sampled and replaced per time point over 14 min efflux period. Drugs were applied only for the duration of efflux (14 min). Bars represent mean initial rates of efflux corrected for variations in intracellular [urate] from hSLC2A9a-expressing oocytes (■) or from hSLC2A9b-expressing oocytes (□) expressed as % of solvent control; 20 - 25 oocytes per condition; Vertical bars represent ± S.E.M. n = 4. (*) – P ≤ 0.05, significance from control.

tyrosine nor tryptophan residues were predicted to be phosphorylated in the amino terminus of the two proteins. Furthermore, only serines have displayed a differential pattern of modification.

Out of the three serines available in the N-terminus of hSLC2A9a, two (Ser9 and Ser22) were predicted to be phosphorylated with a prediction value $P \geq 0.5$ (<http://www.cbs.dtu.dk/services/NetPhos/>; (31)) and only one was predicted to be targeted by a kinase (PKA) with the same degree of confidence (Ser9; <http://www.cbs.dtu.dk/services/NetPhosK/>; (31)). Since the prediction software is only a guiding tool, we have mutated both of these residues individually to an alanine using site-directed mutagenesis. As evident in **Figure 5.9**, only serine 9 mutation to alanine in hSLC2A9a did not produce the PMA-induced response seen with the WT 'a' isoform, suggesting that this residue may be important in modulating urate flux by this isoform. Fully responsive S22A mutant suggests that this residue is not important in functional regulation, as predicted by the software. However, it is interesting to note that Ser9 is predicted to be targeted by PKA, but it is the PKC-agonist that affected uptake and efflux profile of the basolateral transporter, while elevation of intracellular cAMP bears no consequence on the transport function in this system. This suggests that the modulating functions of kinases may be more complex than the simple modification of the N-terminus, initially postulated.

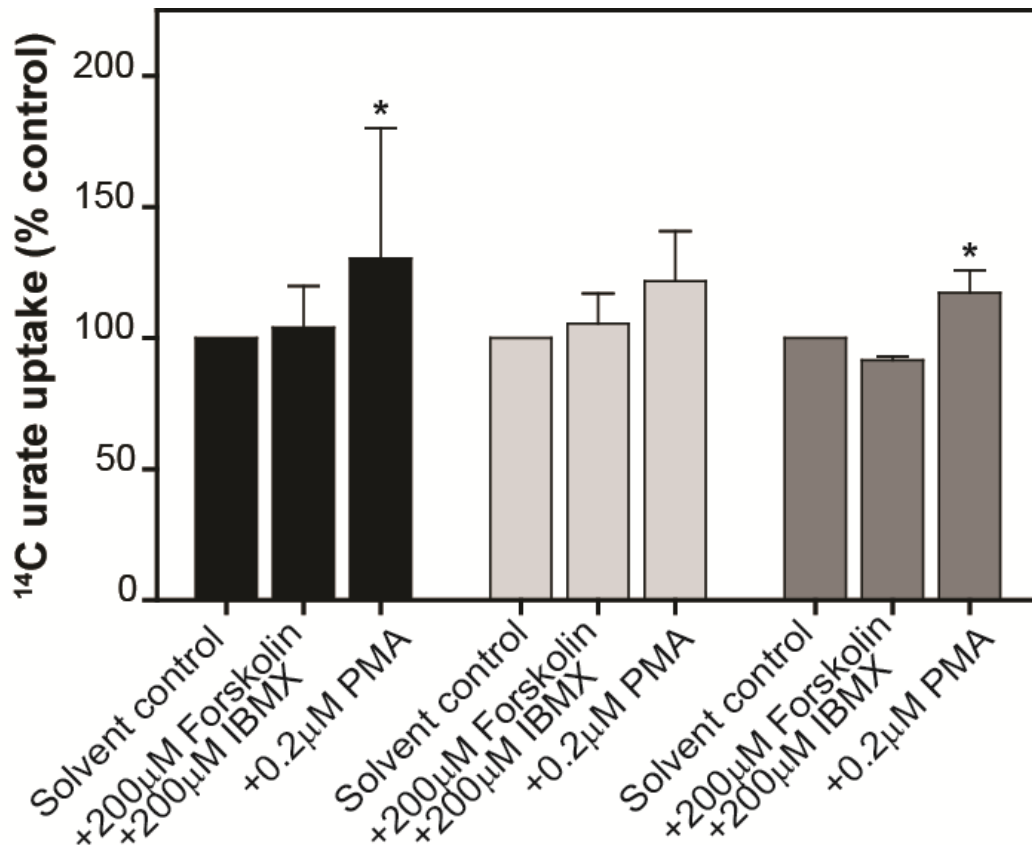


Figure 5.9. Serine 9 may be involved in modulating hSLC2A9a ¹⁴C-urate transport in *Xenopus* oocytes. Oocytes were injected with corresponding cRNA 4 days prior to uptake experiments, which were carried out at room temperature (22°C). Drugs were applied only for the duration of uptake (20 min). Bars represent net 100µM ¹⁴C-urate uptake into hSLC2A9aWT- or mutant-expressing oocytes; (■) – hSLC2A9a-expressing oocytes; (□) – hSLC2A9a-S9A- expressing oocytes; (▒) – hSLC2A9a-S22A- expressing oocytes; Uptake expressed as % of solvent control; 10 - 12 oocytes per condition; Vertical bars represent ± S.E.M. n = 2 – 4. (*) – P ≤ 0.05, significance from control

5.4 Discussion

Up till now, the existence of the two SLC2A9 isoforms (discussed in Chapter 1) was attributed to differential tissue distribution and alternative membrane trafficking (9, 32). In this study, we have furthered the functional comparison of the two splice variants of hSLC2A9 using *Xenopus* oocyte heterologous expression system. It appears that the two isoforms, despite their identical kinetics of urate flux ((5) and Chapter4), can react differentially to extracellular and intracellular stimuli.

Although far-reaching human physiological applications of this study should be made with caution, it can be safely said that significant differences in regulation of the basolateral (a) and apical (b) isoform of hSLC2A9 exist. In this study, two mechanisms of putative transmembrane protein modification were investigated based on *in silico* analysis of phosphorylation and kinase-target sites (PKA- and PKC-dependent mechanisms) and previous observations of differential urate-transport profiles in response to high intra- or extra-cellular hexose concentrations. Taken together, it appears that hSLC2A9a, in conjunction with hURAT1, is mediating the basolateral component of the proposed *trans*-cellular reabsorptive pathway of urate in the PCT, and is highly responsive to changes in intracellular and extracellular *milieu*. Evidence of regulation of this splice variant implies the importance of this transporter in the process of urate reabsorption and maintenance of steady-plasma urate levels.

Of all the experiments demonstrated, it is important to note that PKC agonists have induced consistent effects on hSLC2A9a, but not on hSLC2A9b, urate flux. Furthermore, given the growing body of experimental evidence (31, 32, *Chapter 4*) that hSLC2A9 represents the molecular identity of the human voltage-driven urate efflux pathway initially proposed by Roch-Ramel and colleagues (22–24, 27), the PKC activation effect on hSLC2A9a-mediated urate efflux seems physiologically relevant. At the moment, no studies have investigated regulatory processes of GLUTs in kidney epithelium. However, it is widely documented that the absorptive and secretory functions of the PCT polarized epithelium are governed by a network of highly coordinated signaling pathways (35). Of particular interest to this study is the Na⁺/P_i type II (SLC34) transporter, which is highly abundant in the PCT, is responsible for over 80% phosphate reabsorption, and exists in two isoforms, a and c, which target alternatively to the opposite sides of the epithelium (36). The two isoforms are differentially responsive to kinases, in that the ‘a’ isoform, expressed apically, has been shown to respond to PKA-, PKC- and PKG-induced signals, while the basolateral ‘c’ isoform seems unresponsive (36). The agonist responsible for inducing the signaling cascades is the parathyroid hormone (PTH). Interestingly, depending on whether PTH activates receptors located apically or basolaterally different set of signaling cascades are elicited. Presumably, a similar network of signals may govern hSLC2A9-mediated urate fluxes.

At the moment, it is difficult to comment whether regulation of the process in question aims to upregulate or downregulate urate absorption. Our observations indicate that the basolateral hSLC2A9a, upon PKC activation, increases its capacity to handle urate by both increasing its K_m (apparent affinity) and V_{max} (carrying capacity) for urate. Furthermore, in

contrast to Na⁺/P_i type IIa transporter, hSLC2A9a-mediated increase in urate transport was not matched by increase in the protein's functional expression, as evidenced by the biotinylation. This suggests that unlike other transporters which increase their transport capacity by increasing membrane retention and / or decreasing sub-membrane recycling, hSLC2A9a's catalytic activity is modified through direct or down-stream effects of PKC activation. These, given the complexity and specificity of cell signaling pathways from cell to cell type and from species to species (35, 37–40), have to be investigated in a mammalian renal cell-line models, like MDCK cells.

Less clear-cut are the results of kinase activation on the apical isoform of hSLC2A9b. Elevation of cytosolic cAMP in *Xenopus* oocytes showed down-regulation of hSLC2A9b-mediated urate uptake at a single urate concentration followed by a decrease in K_m value, implicating increase in apparent affinity of the carrier for substrate in a wide-range urate concentration analysis. Furthermore, no effect of the cAMP-stimulating signal was observed on the physiologically-important efflux of urate mediated by this isoform. It is difficult to reconcile these discrepancies. However, the most likely explanation is that cAMP level changes are linked to many signaling cascades, which target a multitude of effectors. More specific drugs should probably be applied in a mammalian expression system to further investigate potential roles of PKA and PKG on the putative mechanism of urate secretion.

As to the agonists that may be involved in mediating the extracellular-to-intracellular signal for urate transport-regulating kinase activation, the hormones of the rennin-angiotensin system (RAS), which are involved in strict salt-water balance homeostasis, seem to be the likely

candidate. Many studies have documented hypertension and hyperuricemia being a coincident occurrence in populations under 50 years of age (41, 42), however the converse, that managing hyperuricemia reduces hypertension, has not been demonstrated unequivocally (43). Regardless, much evidence points to a link between plasma urate levels and plasma volume. With hURAT1 capable of mediating urate-Cl⁻ exchange, and the intimate link between Cl⁻, Na⁺, and water movement across epithelia, the causation is not surprising. Furthermore, all diuretic therapy, regardless of the drug target, results in upregulated urate reabsorption (44). These observations could be mechanistically explained by a tertiary dependence of urate movement on Na⁺, which was first documented in the human epithelium in 1994 (23), and later supported by a model by Anzai *et al.*, proposing an PDZK1-mediated physical link between hURAT1 and SMT1C1 (28). To date, this model has not been functionally tested in face of the known molecular identities involved. As such, indirect links between urate and the hormones of the RAS are plausible. Finally, plasma urate has been shown to directly influence RAS, by stimulation of expression of Angiotensinogen and Angiotensin II mRNA in vascular smooth muscle cells (45).

These proposed mechanisms, although bearing limitations of the *Xenopus* oocytes heterologous expression system, provide a starting framework for investigation of hSLC2A9-mediated urate fluxes in the renal epithelium. Important questions of hSLC2A9 targeting, abundance and recycling, phosphorylation states as well as its potential interaction with other cytoskeletal components, have to be addressed in a mammalian, polarized cell expression system, and ultimately, demonstrated in the human tissue.

5.5 Bibliography

1. Döring, A., Gieger, C., Mehta, D., Gohlke, H., Prokisch, H., Coassin, S., Fischer, G., Henke, K., Klopp, N., Kronenberg, F., Paulweber, B., Pfeufer, A., Roszkopf, D., Völzke, H., Illig, T., Meitinger, T., Wichmann, H.-E., and Meisinger, C. (2008) SLC2A9 influences uric acid concentrations with pronounced sex-specific effects., *Nature genetics* 40, 430-6.
2. Stark, K., Reinhard, W., Neureuther, K., Wiedmann, S., Sedlacek, K., Baessler, A., Fischer, M., Weber, S., Kaess, B., Erdmann, J., Schunkert, H., and Hengstenberg, C. (2008) Association of common polymorphisms in GLUT9 gene with gout but not with coronary artery disease in a large case-control study., *PLoS one* 3, e1948.
3. Bannasch, D., Safra, N., Young, A., Karmi, N., Schaible, R. S., and Ling, G. V. (2008) Mutations in the SLC2A9 gene cause hyperuricosuria and hyperuricemia in the dog., *PLoS genetics* 4, e1000246.
4. Vitart, V., Rudan, I., Hayward, C., Gray, N. K., Floyd, J., Palmer, C. N. a, Knott, S. a, Kolcic, I., Polasek, O., Graessler, J., Wilson, J. F., Marinaki, A., Riches, P. L., Shu, X., Janicijevic, B., Smolej-Narancic, N., Gorgoni, B., Morgan, J., Campbell, S., Biloglav, Z., Barac-Lauc, L., Pericic, M., Klaric, I. M., Zgaga, L., Skaric-Juric, T., Wild, S. H., Richardson, W. a, Hohenstein, P., Kimber, C. H., Tenesa, A., Donnelly, L. A., Fairbanks, L. D., Aringer, M., McKeigue, P. M., Ralston, S. H., Morris, A. D., Rudan, P., Hastie, N. D., Campbell, H., and Wright, A. F. (2008) SLC2A9 is a newly identified urate transporter influencing serum urate concentration, urate excretion and gout., *Nature genetics* 40, 437-42.
5. Caulfield, M. J., Munroe, P. B., O'Neill, D., Witkowska, K., Charchar, F. J., Doblado, M., Evans, S., Eyheramendy, S., Onipinla, A., Howard, P., Shaw-Hawkins, S., Dobson, R. J., Wallace, C., Newhouse, S. J., Brown, M., Connell, J. M., Dominiczak, A., Farrall, M., Lathrop, G. M., Samani, N. J., Kumari, M., Marmot, M., Brunner, E., Chambers, J., Elliott, P., Kooner, J., Laan, M., Org, E., Veldre,

- G., Viigimaa, M., Cappuccio, F. P., Ji, C., Iacone, R., Strazzullo, P., Moley, K. H., and Cheeseman, C. (2008) SLC2A9 is a high-capacity urate transporter in humans., *PLoS medicine* 5, e197.
6. Dehghan, A., Köttgen, A., Yang, Q., Hwang, S.-J., Kao, W. L., Rivadeneira, F., Boerwinkle, E., Levy, D., Hofman, A., Astor, B. C., Benjamin, E. J., Duijn, C. M. van, Witteman, J. C., Coresh, J., and Fox, C. S. (2008) Association of three genetic loci with uric acid concentration and risk of gout: a genome-wide association study., *Lancet* 372, 1953-61.
 7. Brandstätter, A., Kiechl, S., Kollerits, B., Hunt, S. C., Heid, I. M., Coassin, S., Willeit, J., Adams, T. D., Illig, T., Hopkins, P. N., and Kronenberg, F. (2008) Sex-specific association of the putative fructose transporter SLC2A9 variants with uric acid levels is modified by BMI., *Diabetes care* 31, 1662-7.
 8. Keembiyehetty, C., Augustin, R., Carayannopoulos, M. O., Steer, S., Manolescu, A., Cheeseman, C. I., and Moley, K. H. (2006) Mouse glucose transporter 9 splice variants are expressed in adult liver and kidney and are up-regulated in diabetes., *Molecular endocrinology (Baltimore, Md.)* 20, 686-97.
 9. Augustin, R., Carayannopoulos, M. O., Dowd, L. O., Phay, J. E., Moley, J. F., and Moley, K. H. (2004) Identification and characterization of human glucose transporter-like protein-9 (GLUT9): alternative splicing alters trafficking., *The Journal of biological chemistry* 279, 16229-36.
 10. Dinour, D., Gray, N. K., Ganon, L., Knox, A. J. S., Shalev, H., Sela, B.-A., Campbell, S., Sawyer, L., Shu, X., Valsamidou, E., Landau, D., Wright, A. F., and Holtzman, E. J. (2011) Two novel homozygous SLC2A9 mutations cause renal hypouricemia type 2., *Nephrology, dialysis, transplantation : official publication of the European Dialysis and Transplant Association - European Renal Association* 1-7.
 11. Matsuo, H., Chiba, T., Nagamori, S., Nakayama, A., Domoto, H., Phetdee, K., Wiriyaermkul, P., Kikuchi, Y., Oda, T., Nishiyama, J., Nakamura, T., Morimoto, Y., Kamakura, K., Sakurai, Y., Nonoyama, S., Kanai, Y., and Shinomiya, N. (2008) Mutations in glucose transporter 9 gene SLC2A9 cause renal hypouricemia., *American journal of human genetics* 83, 744-51.

12. Phay, J. E., Hussain, H. B., and Moley, J. F. (2000) Cloning and expression analysis of a novel member of the facilitative glucose transporter family, SLC2A9 (GLUT9)., *Genomics* 66, 217-20.
13. Wright, A. F., Rudan, I., Hastie, N. D., and Campbell, H. (2010) A “complexity” of urate transporters., *Kidney international* 78, 446-52.
14. So, A., and Thorens, B. (2010) Uric acid transport and disease., *The Journal of clinical investigation* 120, 1791-9.
15. Johnson, R. J., Sautin, Y. Y., Oliver, W. J., Roncal, C., Mu, W., Gabriela Sanchez-Lozada, L., Rodriguez-Iturbe, B., Nakagawa, T., and Benner, S. A. (2009) Lessons from comparative physiology: could uric acid represent a physiologic alarm signal gone awry in western society?, *Journal of comparative physiology. B, Biochemical, systemic, and environmental physiology* 179, 67-76.
16. Sautin, Y. Y., and Johnson, R. J. (2008) Uric acid: the oxidant-antioxidant paradox., *Nucleosides, nucleotides & nucleic acids* 27, 608-19.
17. Folin, O., Berglund, H., and Derick, C. (1924) The uric acid problem. An experimental study on animals and man, including gouty subjects., *Journal of Biological Chemistry* 60, 361 - 471.
18. Levinson, D. J., and Sorensen, L. B. (1980) Renal handling of uric acid in normal and gouty subject: evidence for a 4-component system., *Annals of the Rheumatic Diseases* 39, 173-179.
19. Balinsky, J. B. (1972) Phylogenetic aspects of purine metabolism., *South African Medical Journal* 46, 993-7.
20. Hediger, M. A. (2002) Gateway to a long life ?, *Nature* 417.
21. Rathmann, W., Haastert, B., Icks, A., Giani, G., and Roseman, J. M. (2007) Ten-year change in serum uric acid and its relation to changes in other metabolic risk factors in young black and white adults: the CARDIA study., *European journal of epidemiology* 22, 439-45.

22. Roch-Ramel, F., Werner, D., and Guisan, B. (1994) Urate transport in brush-border membrane of human kidney., *The American journal of physiology* 266, F797-805.
23. Roch-Ramel, F., Guisan, B., and Schild, L. (1996) Indirect coupling of urate and p-aminohippurate transport to sodium in human brush-border membrane vesicles., *The American journal of physiology* 270, F61-8.
24. Roch-Ramel, F., Guisan, B., and Diezi, J. (1997) Effects of uricosuric and antiuricosuric agents on urate transport in human brush-border membrane vesicles., *The Journal of pharmacology and experimental therapeutics* 280, 839-45.
25. Hediger, M. A., Johnson, R. J., Miyazaki, H., and Endou, H. (2005) Molecular physiology of urate transport., *Physiology (Bethesda, Md.)* 20, 125-33.
26. Enomoto, A., Kimura, H., Chairoungdua, A., Shigeta, Y., Jutabha, P., Cha, S. H., Hosoyamada, M., Takeda, M., Sekine, T., Igarashi, T., Matsuo, H., Kikuchi, Y., Oda, T., Ichida, K., Hosoya, T., Shimokata, K., Niwa, T., Kanai, Y., and Endou, H. (2002) Molecular identification of a renal urate anion exchanger that regulates blood urate levels., *Nature* 417, 447-52.
27. Roch-Ramel, F., and Guisan, B. (1999) Renal Transport of Urate in Humans., *News in physiological sciences : an international journal of physiology produced jointly by the International Union of Physiological Sciences and the American Physiological Society* 14, 80-84.
28. Anzai, N., Kanai, Y., and Endou, H. (2007) New insights into renal transport of urate., *Current opinion in rheumatology* 19, 151-7.
29. Aubel, R. A. M. H. Van, Smeets, P. H. E., Heuvel, J. J. M. W. van den, and Russel, F. G. M. (2005) Human organic anion transporter MRP4 (ABCC4) is an efflux pump for the purine end metabolite urate with multiple allosteric substrate binding sites., *American journal of physiology. Renal physiology* 288, F327-33.
30. Woodward, O. M., Köttgen, A., Coresh, J., Boerwinkle, E., Guggino, W. B., and Köttgen, M. (2009) Identification of a urate transporter,

ABCG2, with a common functional polymorphism causing gout., *Proceedings of the National Academy of Sciences of the United States of America* 106, 10338-42.

31. Blom, N., Sicheritz-Pontén, T., Gupta, R., Gammeltoft, S., and Brunak, S. (2004) Prediction of post-translational glycosylation and phosphorylation of proteins from the amino acid sequence., *Proteomics* 4, 1633-49.
32. Scheepers, A., Schmidt, S., Manolescu, A., Cheeseman, C. I., Bell, A., Zahn, C., Joost, H., and Schürmann, A. (2005) Characterization of the human SLC2A11 (GLUT11) gene: alternative promoter usage, function, expression, and subcellular distribution of three isoforms, and lack of mouse orthologue., *Molecular membrane biology* 22, 339-51.
33. Bibert, S., Hess, S. K., Firsov, D., Thorens, B., Geering, K., Horisberger, J.-D., and Bonny, O. (2009) Mouse GLUT9: evidences for a urate uniporter., *American journal of physiology. Renal physiology* 297, F612-9.
34. Anzai, N., Ichida, K., Jutabha, P., Kimura, T., Babu, E., Jin, C. J., Srivastava, S., Kitamura, K., Hisatome, I., Endou, H., and Sakurai, H. (2008) Plasma urate level is directly regulated by a voltage-driven urate efflux transporter URATv1 (SLC2A9) in humans., *The Journal of biological chemistry* 283, 26834-8.
35. Brown, D., Breton, S., Ausiello, D. a, and Marshansky, V. (2009) Sensing, signaling and sorting events in kidney epithelial cell physiology., *Traffic (Copenhagen, Denmark)* 10, 275-84.
36. Murer, H., Hernando, N., Forster, I., and Biber, J. (2003) Regulation of Na/Pi transporter in the proximal tubule., *Annual review of physiology* 65, 531-42.
37. Gurevich, V. V., and Gurevich, E. V. (2008) Rich tapestry of G protein-coupled receptor signaling and regulatory mechanisms., *Molecular pharmacology* 74, 312-6.
38. Hamm, L. L., Feng, Z., and Hering-Smith, K. S. (2010) Regulation of sodium transport by ENaC in the kidney., *Current opinion in nephrology and hypertension* 19, 98-105.

39. Donowitz, M., Mohan, S., Zhu, C. X., Chen, T.-E., Lin, R., Cha, B., Zachos, N. C., Murtazina, R., Sarker, R., and Li, X. (2009) NHE3 regulatory complexes., *The Journal of experimental biology* 212, 1638-46.
40. McDonough, A. a. (2010) Mechanisms of proximal tubule sodium transport regulation that link extracellular fluid volume and blood pressure., *American journal of physiology. Regulatory, integrative and comparative physiology* 298, R851-61.
41. Johnson, R. J., Kang, D.-H., Feig, D., Kivlighn, S., Kanellis, J., Watanabe, S., Tuttle, K. R., Rodriguez-Iturbe, B., Herrera-Acosta, J., and Mazzali, M. (2003) Is there a pathogenetic role for uric acid in hypertension and cardiovascular and renal disease?, *Hypertension* 41, 1183-90.
42. Johnson, R. J., Feig, D. I., Herrera-Acosta, J., and Kang, D.-H. (2005) Resurrection of uric acid as a causal risk factor in essential hypertension., *Hypertension* 45, 18-20.
43. Menè, P., and Punzo, G. (2008) Uric acid: bystander or culprit in hypertension and progressive renal disease?, *Journal of hypertension* 26, 2085-92.
44. Rafey, M. A., Lipkowitz, M. S., Leal-Pinto, E., and Abramson, R. G. (2003) Uric acid transport., *Current opinion in nephrology and hypertension* 12, 511-6.
45. Perlstein, T. S., Gumieniak, O., Hopkins, P. N., Murphey, L. J., Brown, N. J., Williams, G. H., Hollenberg, N. K., and Fisher, N. D. L. (2004) Uric acid and the state of the intrarenal renin-angiotensin system in humans., *Kidney international* 66, 1465-70.

Chapter 6

General discussion

6.1 Thesis' aims revisited

The aim of this work was to provide an in-depth functional characterization of the novel transport function of hSLC2A9 (hGLUT9) in parallel with recent findings from GWAS, that link SNPs within the *hSLC2A9* gene with elevated plasma urate levels. Urate-handling ability of this transmembrane protein was investigated by overexpressing it in the *Xenopus laevis* oocyte heterologous expression system. Ultimately, we wanted to answer the following questions:

1. What are the kinetic parameters of hSLC2A9-mediated urate transport?
2. What is the nature of transport of a negatively charged organic anion (urate) by hSLC2A9, which, to date, was characterized as a facilitator of electroneutral transport?
3. What are the substrate-carrier interactions between the three known transported molecules of hSLC2A9: urate, D-glucose and D-fructose?
4. What are the functional roles of the two splice variants of hSLC2A9?

6.2 Physiological relevance

6.2.1 hSLC2A9 as a urate transporter and a molecular identity of plasma urate regulating mechanism

In 2008, several independent research groups, including ours, have described a strong correlation between elevated plasma urate levels and SNPs within the *hSLC2A9* gene (1–6), formerly described as a high affinity, low capacity D-glucose and D-fructose transporter (7, 8). Despite the use of highly advanced meta-analysis methods correcting for confounding variables, it was still of utmost importance to correlate the genetic observations with functional data. Thus, hSLC2A9 cRNA was expressed in *Xenopus* oocytes, and simple radiolabelled urate uptake was measured.

To our surprise, uptake of this substrate was approximately tenfold higher than that of D-glucose or D-fructose, the previously described substrates for hSLC2A9, over a wide range of concentrations tested. With an apparent affinity (K_m) of hSLC2A9 for urate at ~1mM, which is above the circulating plasma urate levels (250 – 370 μ M), this transporter appeared to be a high capacity urate transporter under physiological conditions. The relatively high K_m in relation to physiological substrate levels suggests that any increases in plasma urate is matched by hSLC2A9's proportional increase in transport rate, making it an attractive candidate for maintenance of urate homeostasis. Furthermore, this protein was shown to be selectively expressed in tissues largely involved in purine metabolism and clearance, namely liver and the kidney (7).

These findings provided two exciting opportunities for further research. First, it opened an avenue for investigation of a molecular identity for a poorly understood mechanism of human plasma urate regulation. Secondly, it posed some very important questions with regards to the carrier's structure and its substrate binding site. The surprising lack of competitive inhibition between urate and the hexoses also suggested that the protein may bind these substrates in different locations, undermining the assumptions of the simple carrier model.

6.2.2 Electrogenic nature of hSLC2A9-mediated urate flux and the voltage-dependent urate pathways in the kidney epithelium

Under physiological conditions uric acid ($pK_a = 5.75$) exists in its dissociated form, usually as monosodium urate. As such, urate is fairly soluble (> 200 mg/dl), however even slight changes in pH affect urate's solubility (10 fold decrease per 1 pH unit acidification) (9, 10). Given that the substrate in question is an organic anion, we asked the question whether the flux of urate through hSLC2A9 generates current. We again overexpressed hSLC2A9 in *Xenopus* oocytes, this time carefully considering both splice variants (a – full length or basolateral; b – ΔN or apical).

Under voltage clamped conditions ($V_m = -30$ mV), addition of 1mM urate to the external medium evoked positive current, suggesting movement of net negative charge into the oocyte. Furthermore, clamping the oocyte's membrane at increasingly more positive potentials increased the magnitude of urate-induced currents, strengthening the argument that

net negative charge is moving into these cells. Interestingly, no Na^+ sensitivity was detected, and only harsh Cl^- depletion (50% or greater) produced small increases in urate-induced currents, suggesting that perhaps non-specific Cl^- - carrier interactions are at play. All in all, the studies showed that hSLC2A9a and hSLC2A9b mediate electrogenic transport of urate, which is most likely the only charged species contributing to the current observed.

In conjunction with the electrophysiological studies, we undertook efforts to carefully characterize the kinetics of hSLC2A9 isoforms'-mediated urate influx and efflux. As previously postulated (11), facilitative transport of urate appears to be symmetrical with apparent affinity of the carrier for extracellular or intracellular urate approximating 1mM for both isoforms, within range of technical capacity. As is the case for any facilitative transporter, direction of SLC2A9-mediated urate flux is determined solely by the electrochemical gradient. Given that the membrane potential is negative with respect to the outside of the cell, and assuming that no urate microdomains form in the extracellular space, both apical and basolateral hSC2A9 act as efflux pumps. Furthermore, as shown in Chapter 3, hSLC2A9 displays a very selective profile of drug sensitivity, with benzbromarone being the only uricosuric agent to inhibit hSLC2A9-mediated urate uptake significantly.

These findings fit remarkably well with a series of studies on human proximal tubule brush-border vesicles, which have described both apical and basolateral, voltage-dependent routes of urate efflux, with unique sensitivity to benzbromarone (12–15). Given the discordance between purine metabolism in rodents and humans (discussed at length in Chapter 1; (10, 15)) this may be the only direct piece of evidence supporting that both hSLC2A9a (basolateral) and hSLC2A9b (apical) mediate urate reabsorption and secretion, respectively. This model would also explain

why SNPs in *hSLC2A9* gene can cause both hyperuricemia and hypouricemia (see **Figure 6.1**).

6.2.3 Differential regulation of hSLC2A9-mediated urate fluxes by hexoses may provide a link between hyperuricemia and metabolic syndrome

Another point of interest for our group was to define the interactions between D-glucose, D-fructose, urate and the carrier protein. As mentioned above, no competition for the binding site between urate and hexoses was observed, respectively, suggesting separate substrate binding sites. This is quite possible, given the recently published crystal structure of the bacterial sodium-hydrantoin transporter (Mph1), which clearly shows two distinct sites of binding within the translocation pore for its two distinct permeants (*personal communication*). When hSLC2A9-expressing oocytes were pre-incubated with urate, however, D-glucose uptake was increased from the control group, suggesting that hSLC2A9 can exchange D-glucose for urate, a phenomenon termed *trans-stimulation*, *trans-acceleration* or *hetero-exchange* (11). Employing a method developed in our laboratory, we investigated the reverse paradigm, seeing whether rates of efflux of radiolabelled urate would change in presence of extracellular hexoses. Initially performing the experiment with hSLC2A9a-expressing oocytes, we saw increased urate efflux rates in presence of outside D-glucose, as compared with the control. We used this observation to argue that urate fluxes measured in

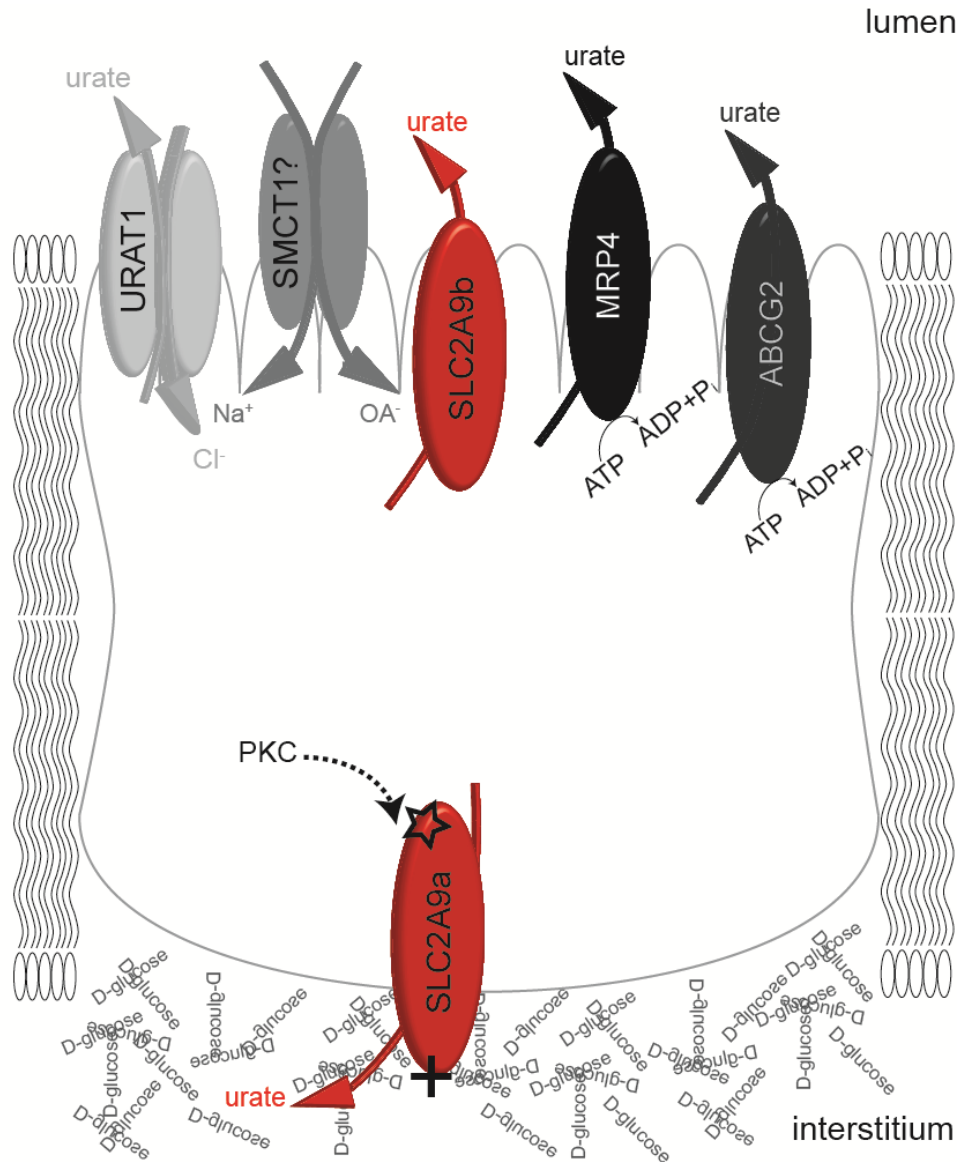


Figure 6.1. Proposed model for urate reabsorptive and secretory mechanisms in the human proximal convoluted tubule of the kidney. URAT1 – SLC2A9a represent the trans-cellular reabsorptive pathway, with tertiary Na⁺ dependence conferred possibly by SMCT1; SLC2A9b represents a putative secretory pathway for urate; ABCG2 and MRP4 provide proposed ATP-dependent efflux pumps for urate, which may serve transient regulatory roles; (···) – proposed targeting either direct or indirect; (☆) – unspecified protein modification; (+) – upregulation of transport activity in response to elevated interstitial D-glucose.

hSLC2A9-expressing oocytes are specific to the overexpressed protein and not due to upregulation of other endogenous transporters in these cells.

Despite these findings, the possible role of hexoses in urate transport was still to be answered. One hypothesis was to examine the attractive role of sugar-gated urate currents. Sugar-gated urate flux regulation has been proposed for the Galectin Family Transporter 9 (UAT1), which was thought to be a urate channel (17). However, no functional data exists to substantiate the proposed mechanism, along with scant evidence for the human Galectin-family urate channel. In our hands, the presence of extracellular D-glucose had no effect on the steady-state urate currents mediated by hSLC2A9a or hSLC2A9b-expressing oocytes, further substantiating the lack of *cis*-inhibition between D-glucose and urate observed in radiolabelled tracer assays (*unpublished observations*).

In contrast, radiolabelled urate efflux mediated by the two isoforms of hSLC2A9 showed distinct and unique responses to extracellular hexoses. Of particular importance is the observation that the basolaterally-expressed isoform was sensitive to extracellular *trans*-D-glucose while the apical isoform was not. This may be one of the underlying mechanisms linking diabetes, in some cases manifested by elevated blood glucose levels, with hyperuricemia (18). Presumably, the interstitial high D-glucose levels would promote an increase in urate reabsorption in the PCT, while the luminal elevated D-glucose in the glomerular filtrate would have no effect on urate secretion by the apical hSLC2A9a, driving net urate uptake into the tissues (see **Figure 6.1**). Another piece of evidence indicating that the link between D-glucose and urate may be of physiological importance comes from clinical studies testing an SGLT2-specific inhibitor which blocks D-glucose reabsorption in the gut, aiming to treat obesity. Lowering of blood sugar levels upon drug administration was paralleled with a

decrease in plasma urate levels in obese patients receiving the treatment (*personal communication*). Naturally, further investigation into these interactions in a mammalian system is necessary.

The reverse experiments looking at the effect of intracellular hexoses on urate uptake into hSLC2A9-expressing oocytes confirmed the aforementioned isoform differences in *trans*-hexose sensitivity. In this case, intracellular *trans*-D-glucose increased urate flux by the basolateral but not the apical isoform. Both isoforms responded to intracellular D-fructose, an effect that was not seen with either isoform when D-fructose was placed on the outside of the cells. It is hard to reconcile this finding with human physiology. Presumably D-fructose does not exist in its unmodified form in the cell's cytosol. However, this differential sensitivity of the exofacial and endofacial vestibules of the transporter to D-fructose points to differences in the structure of the carrier.

6.2.4 Differential regulation of hSLC2A9-mediated urate fluxes by cell signalling pathways may provide insight into renal control of urate secretion and reabsorption

Finally, the functional differences observed with the two isoforms in response to *trans*-hexoses, led us to investigate the only disparate region between these two membrane proteins, the N-terminus. As discussed in Chapter 5 of this thesis, hSLC2A9a and hSLC2A9b are true splice variants, in that the cytosolic N-terminus differs both in length and amino acid composition. Of note, the “full-length” hSLC2A9a isoform possesses the longest N-terminus of all SLC2A (GLUT) family members (18; *unpublished observation*), suggesting that this entity may have a functional

role. Modulating functions of cytosolic termini on transport function have been described for the renal epithelium, sodium-proton exchanger isoform 3 (NHE3) being one notable example (20).

Activating cAMP-dependent and PKC-dependent signalling pathways in *Xenopus* oocytes produced varied responses in urate transport profiles for the two hSLC2A9 isoforms. Of interest is the consistent response of the basolateral isoform 'a' to the PKC agonist, observed for uptake, and, more importantly, for efflux of the substrate. It suggests that the PCT's *trans*-cellular pathway for urate reabsorption mediated by URAT1 – hSLC2A9a apical to basolateral axis may be fine-tuned by intracellular signalling cascades. As mentioned previously, the putative agonists for those signals may involve the hormones of the RAS, which are involved in strict salt-water balance homeostasis (9). Many studies have documented hypertension and hyperuricemia being a coincident occurrence in populations under 50 years of age (21, 22), and that plasma volume changes are often paralleled by changes in plasma urate concentrations (eg. pregnancy) (9). Further studies are necessary to explore this attractive link between hormones and urate transport mechanisms.

It should be mentioned that although both hexoses and intracellular signaling messengers elicit differential urate-transport responses, we believe that these phenomena are not necessarily related. We have begun to investigate the putative target of PKC action, and identified Ser9 as a likely candidate. However, no such studies have been undertaken to understand the modulating role of hexoses in hSLC2A9-mediated urate transport.

6.2.5 Beyond the renal epithelium

This study focused on the possible mechanisms of facilitated movement of urate transport involved in regulating plasma urate levels, with specific application to the PCT kidney epithelium, which handles 70% of human body's uric acid load (10, 23). However, it is important to keep in mind that there exist at least two other organs which significantly contribute to the flux of uric acid in the human body: liver and gastrointestinal (GI) tract. Both of these can be thought of as urate "sources". Furthermore, both of these express a single isoform of hSLC2A9, the basolateral 'a' isoform (7; *unpublished observation*). To date, little focus has been placed on urate transport mechanisms in these tissues.

Liver is the central organ for all catabolic reactions, with purine breakdown being of no exception (10, 23). Xanthine oxidase (XO) is one of the last enzymes, which mediates the final steps of conversion of purines into the final breakdown product. It seems attractive to postulate that the interstitium-facing hSLC2A9a could be the efflux pump mediating delivery of urate into the circulating plasma, contributing to the maintenance of the elevated concentrations found in man (24). The findings presented in this thesis, suggesting that the basolateral isoform is much more susceptible to regulatory stimuli than the apical hSLC2A9b, lead to a hypothesis that the liver-expressed hSLC2A9a mediates urate efflux which could also be modulated. These signals, most likely, would be cell specific and distinct from those governing urate fluxes in the renal epithelium.

Urate transport in the GI epithelium is even less well understood. Presumably, dietary urate is not delivered in its direct form, but rather is

packaged as purines found in food sources like sweetmeats, red meat or anchovies (25), thus not requiring specific urate transporters to deliver the molecule into the bloodstream. The GI is implicated in processing the remaining 30% of the uric acid's secretory load not handled by the kidney (26). Thus, the net flux of urate across this epithelium and the molecular identity of its mediators deserve closer attention.

Finally, all cells within the human body undergo constant DNA breakdown, having to degrade the resultant purines. As such, they must possess means of ridding their contents of uric acid, to prevent its cytosolic accumulation, and states of chronic inflammation (9). With the volume of literature implicating many transporters in mediating urate movement across cell membranes (reviewed in Chapter 1), it seems likely that these multispecific transporters are expressed in the somatic cells, mediating this aforementioned process as a secondary function.

6.2.6 Reconciling human and rodent systems in face of urate homeostasis

This body of work has focused on proposing a regulatory mechanism for plasma urate homeostasis in humans. As discussed in previous chapters, the rodent animal model has a markedly different purine catabolic pathway, with uric acid being converted further into soluble allantoin, which is then excreted. As such, two clear differences in rodent *versus* man urate homeostasis should be highlighted:

1. Rodent liver acts as a urate “sink”, taking up the circulating substance for further degradation.

2. Rodent renal epithelium excretes allantoin and not urate as the final breakdown product of purines.

Mouse SLC2A9 has been cloned, and exists in multiple isoforms, with expression in the liver and the kidney (27, 28), and many studies aim at providing a mouse model to study human hyperuricemia (29). However, we believe that rodents solve plasma urate regulation in a very different manner from man. Consequently, caution should be used before drawing any conclusions from these models.

6.2.7 Validity of the simple carrier model in hSLC2A9-mediated urate transport analysis

Much of the discussion in the preceding chapters of this work pointed to the inconsistencies between experimental data obtained for hSLC2A9-mediated urate transport and the currently accepted model for explaining facilitative transport of solutes across semi-permeable cell membranes. One major assumption of this model is that within a given transport protein a single, specific binding site exists communicating the interaction between substrate and carrier. Two key experiments in this body of work suggest that hSLC2A9 has at least two, if not more, substrate binding sites. These include:

1. Lack of competitive inhibition between *cis* urate and hexoses when uptake of either is measured in hSLC2A9-expressing oocytes.
2. Maximal rates for urate uptake are at least tenfold greater than those for D-glucose or D-fructose when measured under the same conditions

Appendix 2 shows that when rates of hSLC2A9-mediated urate uptake are plotted against increasing urate concentrations, the Hill equation predicts the Hill coefficient (h) to be greater than 1, suggesting allosteric interactions between carrier and substrate.

6.3 Future directions

6.3.1 Determining the phosphorylation state of hSLC2A9 in the expression system

Research presented in Chapter 5 suggests that activation of PKC-dependent pathways modulates hSLC2A9a-mediated urate reabsorption in the renal epithelium. A putative serine residue is proposed as a site of possible protein phosphorylation, which would communicate the signals from the cellular *milieu* to the transporter. However, no studies have been undertaken to demonstrate the basal phosphorylation state of hSLC2A9. In order to argue that transport modulation involves phosphorylation, whether directly by PKC or by PKC-dependent kinases, one needs to show change in phosphorylation states in presence and absence of PKC agonists, like PMA. This should be done in the *Xenopus* oocyte expression system, as well as a mammalian expression system of choice by running phos-tag gels of appropriate protein preparations.

6.3.2 Alternative hSLC2A9 isoform targeting in the human tissue

The original publication reporting on the two splice variants of hSLC2A9 demonstrated alternative targeting of 'a' and 'b' isoforms in MDCK cells (7). Immunohistochemical staining of the human tissue detected basolateral staining of 'GLUT9 full-length'. However, no apical signal was detected with anti-GLUT9 antibody directed towards the C-terminal epitope. This inconsistency needs to be revisited, in order to move forward with modelling of hSLC2A9-mediated urate fluxes across the renal epithelium. Finally, co-staining human kidney tissue with URAT1 and hSLC2A9 antibodies would be beneficial to show that the two proteins coexist within the same cells, forming the *trans*-cellular pathway for urate.

6.3.3 Mammalian expression system for studies of urate flux

As mentioned in the past chapters, regulatory mechanisms governing the transport of urate are, most likely, cell specific. In this thesis we have attempted to outline functional and regulatory differences existing between the two transporter variants of hSLC2A9. However, we are not proposing specific mechanisms by which these changes are mediated.

Given the aforementioned findings, it is important to investigate the validity of our observations in a mammalian, polarized epithelium system, where the two isoforms can be simultaneously expressed in their appropriate membrane domains. The most obvious choice is the MDCK

cell line, since it is a polarized, renal epithelial cell line from dog. Two technical considerations should be highlighted before setting up appropriate culture conditions:

1. Validating the presence or absence of other, endogenously-expressed urate-carrying transporters, especially the apical URAT1.
2. Overcoming the difficulties of stable, dual transfection.

Point (2) can be overcome by creating stable cell lines expressing either isoform and using the transient transfection method to introduce the other hSLC2A9 isoform into the system. If MDCK cells do not express URAT1, presumably, precluding the study of the apical to basolateral urate flux, other expression systems will have to be considered. However, this is not anticipated to be the problem, given MDCK cells' origin.

6.3.4 Mechanism of benzbromarone action

Urate uptake studies under non-voltage clamped conditions in hSLC2A9-expressing oocytes revealed that this transporter is selectively sensitive to benzbromarone. This observation fits with the human BBMV studies (12), which characterized a voltage-sensitive pathway for urate efflux with specific affinity for this uricosuric. In attempt to provide a consistent functional profile for hSLC2A9-mediated urate handling, we attempted to test the effect of benzbromarone on the steady-state currents observed in response to addition of extracellular urate to the transporter-expressing oocytes. Surprisingly, benzbromarone appeared to affect current recordings in water-injected control oocytes, suggesting that its mode of action may not be hSLC2A9-specific (*unpublished observations*).

Thus, specific targets of this drug should be investigated using electrophysiological techniques.

6.3.5 Structure-function studies of hSLC2A9

Given the novel function of hSLC2A9 as a high capacity, electrogenic urate transporter, the key questions centre around the putative residues which interact with urate, forming the “specific substrate-binding site” postulated by the simple carrier model. Amino acid comparison across all GLUTs does not provide any clues as to which residues render isoform 9 suitable for urate transport. As indicated in **Figure 6.2**, many residues involved in D-glucose interactions in hGLUT1 are not present in hSLC2A9. Curiously, the amino acid substitutions in those positions do not provide hints of altered substrate specificity (residues circled in red in panel B). If any conclusion can be made from this analysis, it is that D-glucose and urate binding sites are distinct not only in their extracellular vestibules, but also within the translocation pore. Nonetheless, site directed mutagenesis should be performed to check the plausibility of this hypothesis.

Sequence alignments of hSLC2A9 and other human GLUT family members with the only other confirmed specific urate carrier, hURAT1, did not provide much insight either. A positively charged histidine residue within a region of high conservation between these two transporters was unique to hSLC2A9 and hGLUT12. However, other members of the GLUT family had an arginine or a lysine in that position, both of which are positively charged (**Figure 6.3**). Taken together, these observations

strengthen the notion that substrate specificity determinants are more subtle than previously thought.

Next, the intriguing interplay between the hexoses, urate and hSLC2A9 requires further investigation. First, the extracellular domain's properties should be tested by performing a dual-label experiment to determine the stoichiometry of exchange between urate and D-glucose or D-fructose. Secondly, the lack of competitive inhibition should be further investigated. It is possible that binding of the hexose may, within a specific concentration range, promote the transport of urate, a phenomenon termed *cis*-stimulation. Complex ligand binding phenomena have been observed with GLUT1 (30). Preliminary results of these proposed tests are presented in **Appendix 1**.

Finally, the *trans*-stimulating effect of intracellular D-fructose seen with hSLC2A9a- and hSLC2A9b-mediated urate uptake is of interest. The fact that extracellular D-fructose bears no such effect on either transporter suggests another point of difference between exofacial and endofacial vestibules. Measuring urate uptake over a range of intracellular D-fructose concentrations could provide useful insight into the binding dynamics of this sugar.

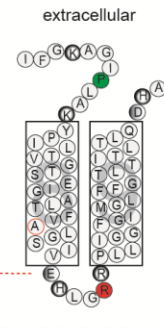


Figure 6.3. hURAT1 and hSLC2A9a sequence alignment. Amino acid residues of the two specific carriers were aligned using Clustal IW software (<http://www.ebi.ac.uk/Tools/msa/clustalw2/>); Grey outlines represent putative TM regions of hSLC2A9a determined using TMpred software (http://www.ch.embnet.org/software/TMPRED_form.html); Green outline represents PDZ-binding domain site; Red outline represents region of high conservation of residues between URAT1 and SLC2A9 which is unique among GLUTs. Inset represents a fragment of SLC2A9 topology showing the location of the conserved residues.

6.4 Bibliography

1. Brandstätter, A., Kiechl, S., Kollerits, B., Hunt, S. C., Heid, I. M., Coassin, S., Willeit, J., Adams, T. D., Illig, T., Hopkins, P. N., and Kronenberg, F. (2008) Sex-specific association of the putative fructose transporter SLC2A9 variants with uric acid levels is modified by BMI., *Diabetes care* 31, 1662-7.
2. Caulfield, M. J., Munroe, P. B., O'Neill, D., Witkowska, K., Charchar, F. J., Doblado, M., Evans, S., Eyheramendy, S., Onipinla, A., Howard, P., Shaw-Hawkins, S., Dobson, R. J., Wallace, C., Newhouse, S. J., Brown, M., Connell, J. M., Dominiczak, A., Farrall, M., Lathrop, G. M., Samani, N. J., Kumari, M., Marmot, M., Brunner, E., Chambers, J., Elliott, P., Kooner, J., Laan, M., Org, E., Veldre, G., Viigimaa, M., Cappuccio, F. P., Ji, C., Iacone, R., Strazzullo, P., Moley, K. H., and Cheeseman, C. (2008) SLC2A9 is a high-capacity urate transporter in humans., *PLoS medicine* 5, e197.
3. Dehghan, A., Köttgen, A., Yang, Q., Hwang, S.-J., Kao, W. L., Rivadeneira, F., Boerwinkle, E., Levy, D., Hofman, A., Astor, B. C., Benjamin, E. J., Duijn, C. M. van, Witteman, J. C., Coresh, J., and Fox, C. S. (2008) Association of three genetic loci with uric acid concentration and risk of gout: a genome-wide association study., *Lancet* 372, 1953-61.
4. Döring, A., Gieger, C., Mehta, D., Gohlke, H., Prokisch, H., Coassin, S., Fischer, G., Henke, K., Klopp, N., Kronenberg, F., Paulweber, B., Pfeufer, A., Roskopf, D., Völzke, H., Illig, T., Meitinger, T., Wichmann, H.-E., and Meisinger, C. (2008) SLC2A9 influences uric acid concentrations with pronounced sex-specific effects., *Nature genetics* 40, 430-6.
5. Stark, K., Reinhard, W., Neureuther, K., Wiedmann, S., Sedlacek, K., Baessler, A., Fischer, M., Weber, S., Kaess, B., Erdmann, J., Schunkert, H., and Hengstenberg, C. (2008) Association of common polymorphisms in GLUT9 gene with gout but not with coronary artery disease in a large case-control study., *PloS one* 3, e1948.
6. Vitart, V., Rudan, I., Hayward, C., Gray, N. K., Floyd, J., Palmer, C. N. a, Knott, S. a, Kolcic, I., Polasek, O., Graessler, J., Wilson, J. F.,

- Marinaki, A., Riches, P. L., Shu, X., Janicijevic, B., Smolej-Narancic, N., Gorgoni, B., Morgan, J., Campbell, S., Biloglav, Z., Barac-Lauc, L., Pericic, M., Klaric, I. M., Zgaga, L., Skaric-Juric, T., Wild, S. H., Richardson, W. a, Hohenstein, P., Kimber, C. H., Tenesa, A., Donnelly, L. A., Fairbanks, L. D., Aringer, M., McKeigue, P. M., Ralston, S. H., Morris, A. D., Rudan, P., Hastie, N. D., Campbell, H., and Wright, A. F. (2008) SLC2A9 is a newly identified urate transporter influencing serum urate concentration, urate excretion and gout., *Nature genetics* 40, 437-42.
7. Augustin, R., Carayannopoulos, M. O., Dowd, L. O., Phay, J. E., Moley, J. F., and Moley, K. H. (2004) Identification and characterization of human glucose transporter-like protein-9 (GLUT9): alternative splicing alters trafficking., *The Journal of biological chemistry* 279, 16229-36.
 8. Manolescu, A. R., Augustin, R., Moley, K., and Cheeseman, C. (2007) A highly conserved hydrophobic motif in the exofacial vestibule of fructose transporting SLC2A proteins acts as a critical determinant of their substrate selectivity., *Molecular membrane biology* 24, 455-63.
 9. Menè, P., and Punzo, G. (2008) Uric acid: bystander or culprit in hypertension and progressive renal disease?, *Journal of hypertension* 26, 2085-92.
 10. Hediger, M. A., Johnson, R. J., Miyazaki, H., and Endou, H. (2005) Molecular physiology of urate transport., *Physiology (Bethesda, Md.)* 20, 125-33.
 11. Neame, K. D., and Richards, T. G. (1972) Elementary kinetics of membrane carrier transport 1st ed. Blackwell Scientific Publications, Oxford, England.
 12. Roch-Ramel, F., Werner, D., and Guisan, B. (1994) Urate transport in brush-border membrane of human kidney., *The American journal of physiology* 266, F797-805.
 13. Roch-Ramel, F., Guisan, B., and Schild, L. (1996) Indirect coupling of urate and p-aminohippurate transport to sodium in human brush-border membrane vesicles., *The American journal of physiology* 270, F61-8.

14. Roch-Ramel, F., Guisan, B., and Diezi, J. (1997) Effects of uricosuric and antiuricosuric agents on urate transport in human brush-border membrane vesicles., *The Journal of pharmacology and experimental therapeutics* 280, 839-45.
15. Roch-Ramel, F., and Guisan, B. (1999) Renal Transport of Urate in Humans., *News in physiological sciences : an international journal of physiology produced jointly by the International Union of Physiological Sciences and the American Physiological Society* 14, 80-84.
16. Weyand, S., Shimamura, T., Beckstein, O., Sansom, M. S. P., Iwata, S., Henderson, P. J. F., and Cameron, A. D. (2011) The alternating access mechanism of transport as observed in the sodium-hydantoin transporter Mhp1., *Journal of synchrotron radiation. International Union of Crystallography* 18, 20-3.
17. Lipkowitz, M. S., Leal-Pinto, E., Cohen, B. E., and Abramson, R. G. (2004) Galectin 9 is the sugar-regulated urate transporter/channel UAT., *Glycoconjugate journal* 19, 491-8.
18. Bo, S., Cavallo-Perin, P., Gentile, L., Repetti, E., and Pagano, G. (2001) Hypouricemia and hyperuricemia in type 2 diabetes: two different phenotypes., *European journal of clinical investigation* 31, 318-21.
19. Phay, J. E., Hussain, H. B., and Moley, J. F. (2000) Cloning and expression analysis of a novel member of the facilitative glucose transporter family, SLC2A9 (GLUT9)., *Genomics* 66, 217-20.
20. Alexander, R. T., Jaumouillé, V., Yeung, T., Furuya, W., Peltekova, I., Boucher, A., Zasloff, M., Orłowski, J., and Grinstein, S. (2011) Membrane surface charge dictates the structure and function of the epithelial Na⁺/H⁺ exchanger., *The EMBO journal* 30, 679-91.
21. Johnson, R. J., Kang, D.-H., Feig, D., Kivlighn, S., Kanellis, J., Watanabe, S., Tuttle, K. R., Rodriguez-Iturbe, B., Herrera-Acosta, J., and Mazzali, M. (2003) Is there a pathogenetic role for uric acid in hypertension and cardiovascular and renal disease?, *Hypertension* 41, 1183-90.
22. Johnson, R. J., Feig, D. I., Herrera-Acosta, J., and Kang, D.-H. (2005) Resurrection of uric acid as a causal risk factor in essential hypertension., *Hypertension* 45, 18-20.

23. So, A., and Thorens, B. (2010) Uric acid transport and disease., *The Journal of clinical investigation* 120, 1791-9.
24. Hediger, M. A. (2002) Gateway to a long life ?, *Nature* 417.
25. Folin, O., Berglund, H., and Derick, C. (1924) The uric acid problem. An experimental study on animals and man, including gouty subjects., *Journal of Biological Chemistry* 60, 361 - 471.
26. Wright, A. F., Rudan, I., Hastie, N. D., and Campbell, H. (2010) A “complexity” of urate transporters., *Kidney international* 78, 446-52.
27. Keembiyehetty, C., Augustin, R., Carayannopoulos, M. O., Steer, S., Manolescu, A., Cheeseman, C. I., and Moley, K. H. (2006) Mouse glucose transporter 9 splice variants are expressed in adult liver and kidney and are up-regulated in diabetes., *Molecular endocrinology (Baltimore, Md.)* 20, 686-97.
28. Carayannopoulos, M. O., Schlein, A., Wyman, A., Chi, M., Keembiyehetty, C., and Moley, K. H. (2004) GLUT9 is differentially expressed and targeted in the preimplantation embryo., *Endocrinology* 145, 1435-43.
29. Preitner, F., Bonny, O., Laverrière, A., Rotman, S., Firsov, D., Costa, A. Da, Metref, S., and Thorens, B. (2009) Glut9 is a major regulator of urate homeostasis and its genetic inactivation induces hyperuricosuria and urate nephropathy., *Proceedings of the National Academy of Sciences of the United States of America* 106, 15501-6.
30. Robichaud, T., Appleyard, A. N., Herbert, R. B., Henderson, P. J. F., and Carruthers, A. (2011) Determinants of ligand binding affinity and cooperativity at the GLUT1 endofacial site., *Biochemistry* 50, 3137-48.

Appendix

1

cis-Stimulation and dual label experiments

A1.1 *cis*-Stimulation experiment

A1.1.1 Experimental design

These experiments were designed in light of the interesting hexose – urate interactions observed in *trans*-stimulation experiments with hSLC2A9-expressing oocytes. The principle behind this experiment is based on the radiolabelled uptake experiments described in Chapter 2. However, in this case, two distinct substrates of hSLC2A9 have been introduced simultaneously into the extracellular medium (*cis*-). It is believed that if the transporter does not obey simple carrier kinetics, uptake or efflux of the radiolabelled substrate can show upregulation in presence of another, non-labeled *cis* substrate. In this case, the non-labeled substrate (hexose) concentration was low (10 μ M), compared with the labeled permeant (urate).

A1.1.2. Results commentary

Two sets of *cis*-experiments have been performed, as shown in **Figure A1.1** and **Figure A1.2**. The first experiment was performed at a single time point, where uptake was measured for 20 minutes, just as with the regular flux experiment. hSLC2A9a- but not hSLC2A9b-expressing oocytes were affected by presence of 10 μ M *cis* D-glucose, showing approximately a 50% increase in net urate uptake under these conditions.

Extending the analysis over a range of time points yielded a slightly altered pattern of responses. hSLC2A9a showed sensitivity to 10 μ M *cis* D-glucose analog, 2-deoxy-D-glucose (2DOG) at the 15 minute time point only, while showing no response to D-glucose itself. Moreover, 2DOG also produced an increase in urate uptake in hSLC2A9b-expressing oocytes at the 20 minute time point. Although, no comparison between the two isoforms can be made at this stage, the fact that *cis*-stimulation is possible with hSLC2A9 is worth further investigation.

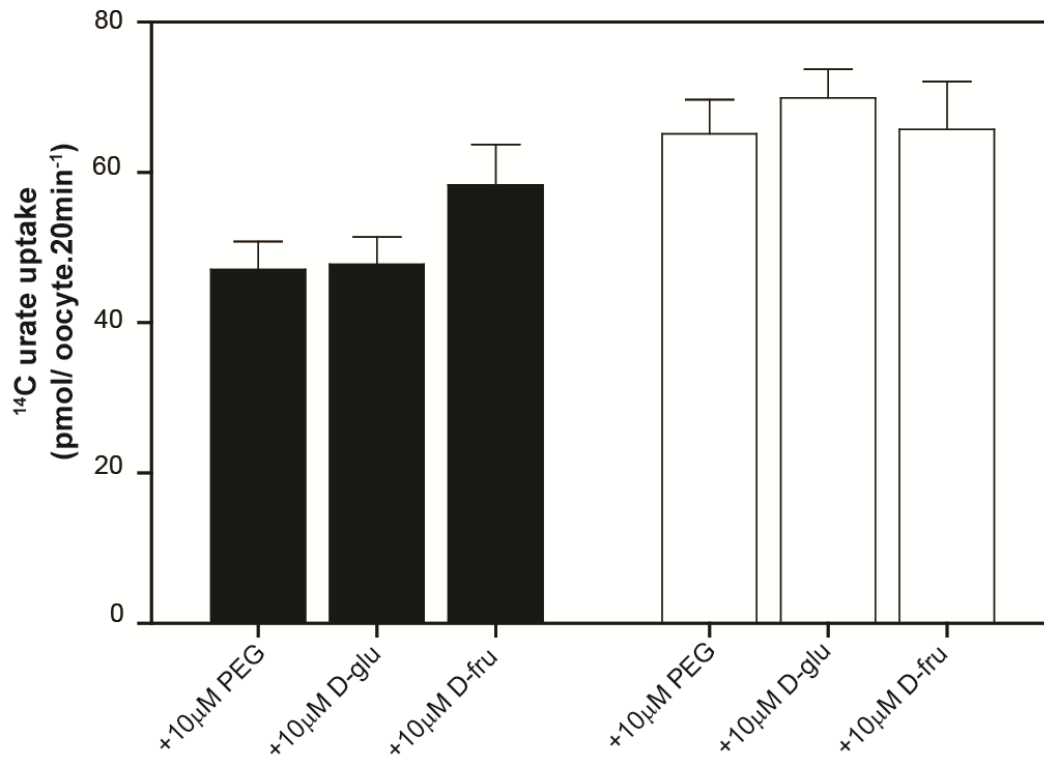


Figure A1.1. Effects of *cis* hexoses on hSLC2A9-mediated ¹⁴C-urate uptake in *Xenopus* oocytes: single time-point. Oocytes were injected with corresponding cRNA 4 days prior to uptake experiments, which were carried out at room temperature (22°C). 10µM non-labeled substance was added to the transport medium containing 100µM ¹⁴C-urate. Uptake of urate was measured over 20 minutes; Bars represent ¹⁴C-urate uptake into hSLC2A9a-expressing (■) or hSLC2A9b-expressing (□) oocytes, averaged for 10 – 12 cells; Vertical bars represent SEM.

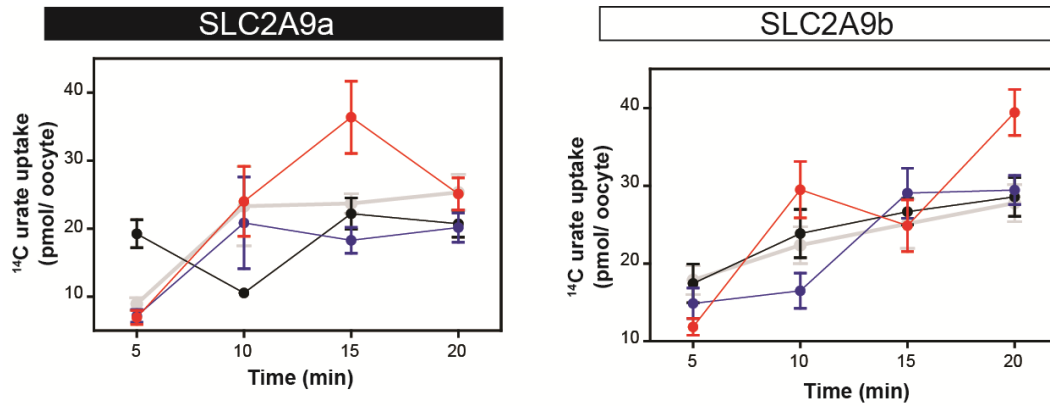


Figure A1.2. Effects of *cis* hexoses on hSLC2A9-mediated ^{14}C -urate uptake in *Xenopus* oocytes: time-course. Oocytes were injected with corresponding cRNA 4 days prior to uptake experiments, which were carried out at room temperature (22°C). Non-labeled substance was added to the transport medium containing $100\mu\text{M}$ ^{14}C -urate. Uptake of urate was recorded every 5 minutes over a 20 minute time period; Symbols represent ^{14}C -urate uptake into hSLC2A9a-expressing or hSLC2A9b-expressing oocytes under varied extracellular conditions: (○) – $10\mu\text{M}$ PEG, (●) – $10\mu\text{M}$ D-glucose, (●) – $10\mu\text{M}$ 2DOG, (●) – $10\mu\text{M}$ D-fructose, averaged for 10 – 12 cells; Vertical bars represent SEM.

A1.2 Dual-label experiment

A1.2.1 Experimental design

The dual label experiment aims at elucidating the stoichiometry of urate – hexose exchange. The procedure is a modified *trans*-stimulation experiment, where the only difference is that both the extracellular medium and the oocytes contain radiolabelled substances. In essence, we are measuring uptake of ^3H -labelled substances, which initially are present only in the oocytes' incubation medium and the efflux of ^{14}C -labelled urate, which initially is found only in the oocyte. This experiment was performed over a range of time points (5, 10, 15 minutes). As with the efflux experiments described in Chapter 2, oocytes were dissolved at the end of each respective time period. In contrast with the previously described efflux procedure, only one time point sampling of extracellular medium was performed, which was done in duplicate at the end of the flux-measurements. All samples obtained were counted in the scintillation counter, using a dual-label program.

A1.2.2 Results commentary

Figure A1.3 shows the results of a single dual label experiment. Extracellular ^3H 100 μM PEG served as an osmotic control, while ^3H 100 μM D-glucose and ^3H 1mM D-glucose aimed to test the sensitivity of

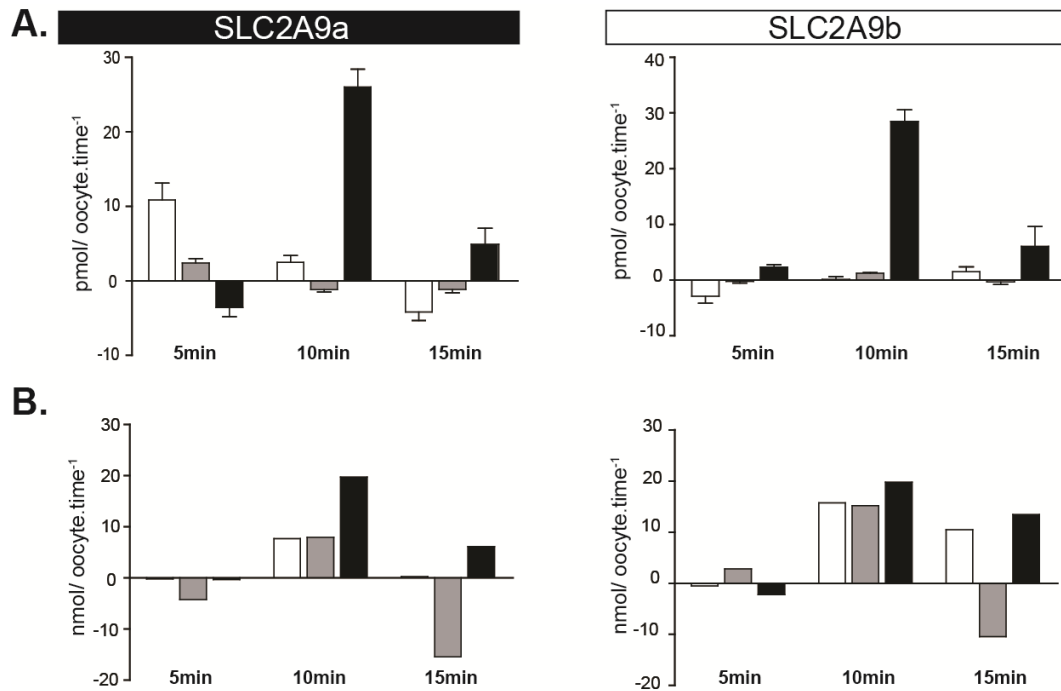


Figure A1.3. Measuring the stoichiometry of urate – hexose exchange in hSLC2A9-expression *Xenopus* oocytes: dual label experiment.

Oocytes were injected with corresponding cRNA 4 days prior to uptake experiments, which were carried out at room temperature (22°C). ³H-labeled substance was added to the incubation medium (100µM or 1mM). ¹⁴C-urate was micro-injected into batches of 10 oocytes per condition (43µM – 200µM [intracellular urate]). 500µl of incubation medium was used. Uptake of ³H-substances was recorded every 5 minutes by oocyte lysis. Efflux of ¹⁴C-urate was recorded by 50ul duplicate sampling of the incubation medium. **A.** Net uptake of ³H substances into hSLC2A9a- or hSLC2A9b- expressing oocytes; **B.** Total efflux of ¹⁴C-urate from hSLC2A9a- or hSLC2A9b- expressing oocytes; Bars represent corresponding uptake or efflux under varied extracellular conditions: (□) – 100µM ³H PEG, (■) – 100µM ³H D-glucose, (■) – 1mM ³H D-glucose. Vertical bars represent SEM.

the responses. **Panel A** of the figure represents net uptakes of the ^3H substances into the oocytes, while **Panel B** represents net efflux rates of ^{14}C -urate, normalized for variations in intracellular urate concentrations. 10 minute time point appears to yield the most reliable results for both uptake and efflux measurements. Furthermore, 1mM D-glucose appears to be the more suitable concentration than 100 μM D-glucose, in line with previously used extracellular substrate concentrations. These conditions should be used in subsequent experiments. There appears to be a 1000X difference in the amount of permeant effluxed and taken up. This disparity should be further investigated.

Appendix **2**

hSLC2A9 and multiple urate binding sites

A2.1 **F**itting kinetic data with Hill equation

A2.1.1 Experimental design

Kinetic data from chapter 5 (see **Figure 5.6**, page 169) was reanalyzed using Hill equation to determine whether the carrier may contain cooperative binding sites for urate. The following equation was used to fit the curve:

$$Y = V_{max} * \left(\frac{X^h}{K_{prime} + X^h} \right)$$

In this case the following constants are:

V_{max} - the maximum enzyme velocity in the same units as Y. It is the velocity of the enzyme extrapolated to very high concentrations of substrate, and therefore is almost always higher than any velocity measured in your experiment.

K_{prime} is related to the K_m, but is not equal the substrate concentration needed to achieve a half-maximum enzyme velocity (unless h=1). It is expressed in the same units as X.

h - the Hill slope. When n=1, this equation is identical to the standard Michaelis-Menten equation. When it is greater than 1, the curve is sigmoidal due to positive cooperativity, suggesting that

more than one substrate binding sites exists on the carrier. The variable n does not always equal the number of interacting binding sites, but its value cannot exceed the number of interacting sites. Think of n as an empirical measure of the steepness of the curve and the presence of cooperativity.

A2.1.2 Results commentary

Both control groups (ie. SLC2A9a- and SLC2A9b- expressing oocytes in presence of solvent control only) show sigmoidal curve fit when rates of urate uptake are plotted against increasing urate concentrations. In all cases, the Hill coefficient is greater than 1, suggesting that more than one urate binding site exists on either isoform of hSLC2A9 carrier. As such, simple carrier model is no longer sufficient to explain this transport behaviour.

Furthermore, application of drugs modulating intracellular kinase activity seems to be changing the Hill coefficient, although the exact nature of this change needs to be investigated further.

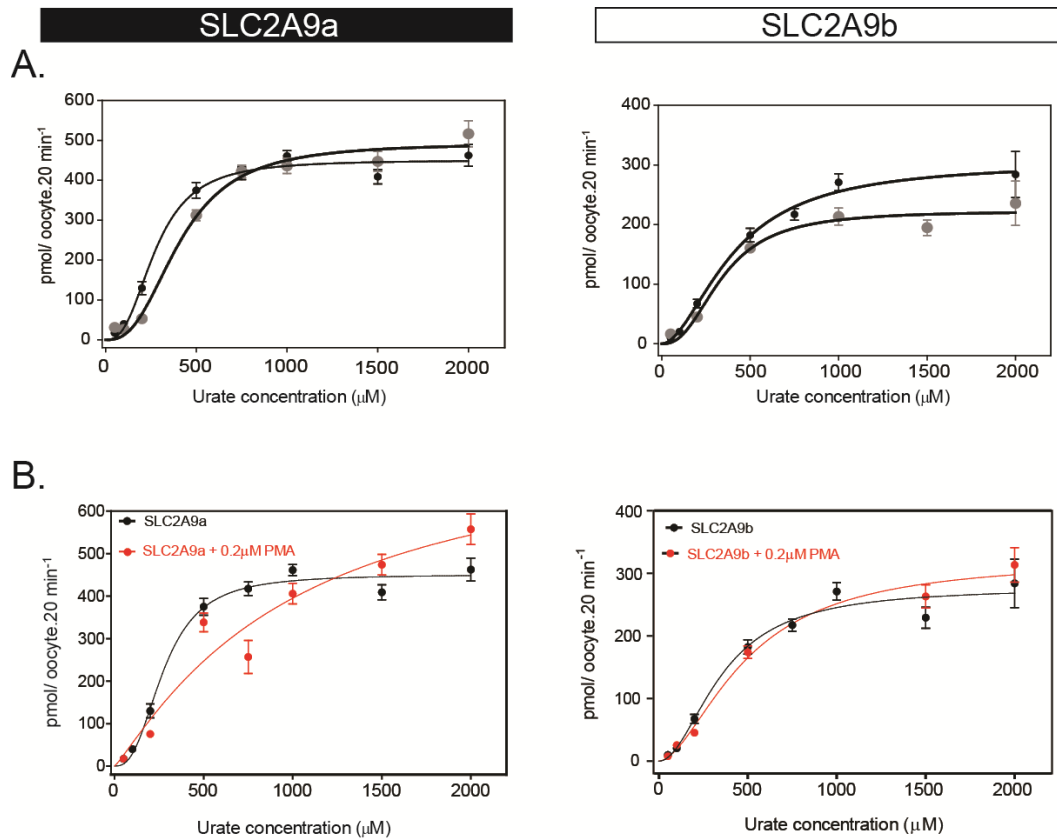


Figure A2.1. Reanalysis of kinetics of hSLC2A9-mediated ¹⁴C-urate uptake in *Xenopus* oocytes using allosteric sigmoidal curve fit.

Oocytes were injected with corresponding cRNA 4 days prior to uptake experiments, which were carried out at room temperature (22°C). Drugs were applied only for the duration of uptake (20 min). Filled circles represent net ¹⁴C-urate uptake over the indicated range of concentrations. (●) – respective hSLC2A9 isoform’s urate uptake in solvent control (1% EtOH); **A.** hSLC2A9a and hSLC2A9b-mediated urate uptake in presence of 200µM IBMX + 200µM Forskolin (●); **B.** hSLC2A9a and hSLC2A9b-mediated urate uptake in presence of 0.2µM PMA (●); Averaged for 10 - 12 oocytes; Vertical bars represent ± S.E.M

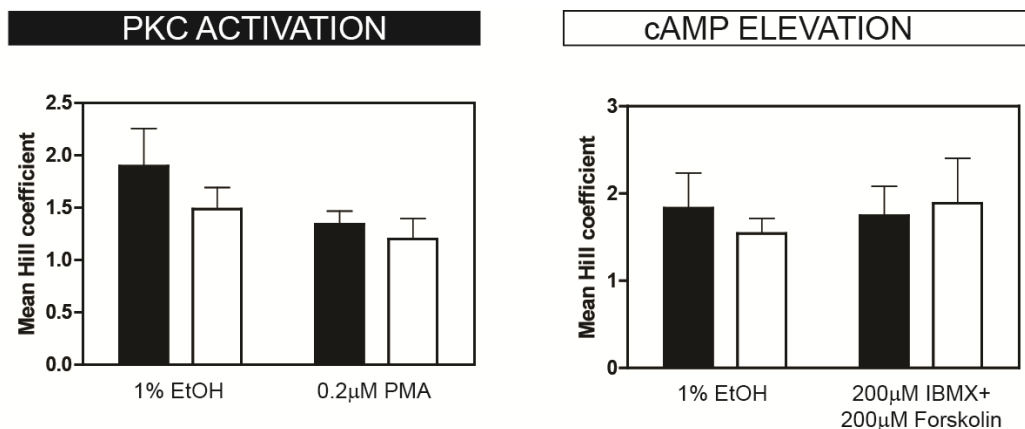


Figure A2.2. Mean Hill coefficients from alternative kinetic analysis of hSLC2A9a- and hSLC2A9b-mediated ¹⁴C-urate uptake in response to PKA and PKC modulating drugs. Oocytes were injected with corresponding cRNA 4 days prior to uptake experiments, which were carried out at room temperature (22°C). Drugs were applied only for the duration of uptake (20 min). Bars represent mean Hill coefficient obtained from four independent kinetic experiments analyzed as above. hSLC2A9a-expressing oocytes (■); hSLC2A9b-expressing oocytes (□); Vertical bars represent ± S.E.M. n = 4.